

132 **Topics in Current Chemistry**

Biomimetic and Bioorganic Chemistry II

Editors: F. Vögtle, E. Weber

With Contributions by
J. Franke, A. Gärtner, H. Nishide, F. P. Schmidtchen,
E. Tsuchida, F. Vögtle, U. Weser

With 32 Figures and 26 Tables



Springer-Verlag
Berlin Heidelberg New York Tokyo

This series presents critical reviews of the present position and future trends in modern chemical research. It is addressed to all research and industrial chemists who wish to keep abreast of advances in their subject.

As a rule, contributions are specially commissioned. The editors and publishers will, however, always be pleased to receive suggestions and supplementary information. Papers are accepted for "Topics in Current Chemistry" in English.

ISBN 3-540-16023-X Springer-Verlag Berlin Heidelberg New York Tokyo
ISBN 0-387-16023-X Springer-Verlag New York Heidelberg Berlin Tokyo

Library of Congress Cataloging-in-Publication Data.

(Revised for vol. 2) Main entry under title: Biomimetic and bioorganic chemistry.

(Topics in current chemistry = Fortschritte der Chemischen Forschung; 128)

Vol. 2 edited by F. Vögtle, E. Weber with contributions by J. Franke . . . [et al.].

Includes bibliographies and indexes.

1. Biological chemistry — Collected works. 2. Bioorganic chemistry — Collected works.

I. Cammann, Karl. II. Vögtle, F. (Fritz), 1939– . . . III. Weber, E. IV. Series. V. Series:

Topics in current chemistry; 128; etc.

QD1.F58 vol. 128 540s 574.19'2 85-2804

This work is subject to copyright. All rights are reserved, whether the whole or part of the material is concerned, specifically those of translation, reprinting, re-use of illustrations, broadcasting, reproduction by photocopying machine or similar means, and storage in data banks. Under § 54 of the German Copyright Law where copies are made for other than private use, a fee is payable to "Verwertungsgesellschaft Wort", Munich.

© by Springer-Verlag Berlin Heidelberg 1986

Printed in GDR

The use of registered names, trademarks, etc. in this publication does not imply, even in the absence of a specific statement, that such names are exempt from the relevant protective laws and regulations and therefore free for general use.

Typesetting and Offsetprinting: Th. Mützer, GDR;

Bookbinding: Lüderitz & Bauer, Berlin

2152/3020-543210

Editorial Board:

Prof. Dr. <i>Michael J. S. Dewar</i>	Department of Chemistry, The University of Texas Austin, TX 78712, USA
Prof. Dr. <i>Jack D. Dunitz</i>	Laboratorium für Organische Chemie der Eidgenössischen Hochschule Universitätsstraße 6/8, CH-8006 Zürich
Prof. Dr. <i>Klaus Hafner</i>	Institut für Organische Chemie der TH Petersenstraße 15, D-6100 Darmstadt
Prof. Dr. <i>Edgar Heilbronner</i>	Physikalisch-Chemisches Institut der Universität Klingelbergstraße 80, CH-4000 Basel
Prof. Dr. <i>Shô Itô</i>	Department of Chemistry, Tohoku University, Sendai, Japan 980
Prof. Dr. <i>Jean-Marie Lehn</i>	Institut de Chimie, Université de Strasbourg, 1, rue Blaise Pascal, B. P. Z 296/R8, F-67008 Strasbourg-Cedex
Prof. Dr. <i>Kurt Niedenzu</i>	University of Kentucky, College of Arts and Sciences Department of Chemistry, Lexington, KY 40506, USA
Prof. Dr. <i>Kenneth N. Raymond</i>	Department of Chemistry, University of California, Berkeley, California 94720, USA
Prof. Dr. <i>Charles W. Rees</i>	Hofmann Professor of Organic Chemistry, Department of Chemistry, Imperial College of Science and Technology, South Kensington, London SW7 2AY, England
Prof. Dr. <i>Fritz Vögtle</i>	Institut für Organische Chemie und Biochemie der Universität, Gerhard-Domagk-Str. 1, D-5300 Bonn 1
Prof. Dr. <i>Georg Wittig</i>	Institut für Organische Chemie der Universität Im Neuenheimer Feld 270, D-6900 Heidelberg 1

Table of Contents

Molecular and Functional Aspects of Superoxide Dismutases	
A. Gärtner, U. Weser	1
Hemoglobin Model — Artificial Oxygen Carrier Composed of Porphinatoiron Complexes	
E. Tsuchida, H. Nishide	63
Molecular Catalysis by Polyammonium Receptors	
F. P. Schmidtchen	101
Complexation of Organic Molecules in Water Solution	
J. Franke, F. Vögtle.	137
Author Index Volumes 101–132	171

Table of Contents of Volume 128

Biomimetic and Bioorganic Chemistry

Solvation and Ordered Structure in Colloidal Systems

G. Ebert

Active Transport of Ions Using Synthetic Ionophores Derived from Macrocyclic Polyethers and the Related Compounds

M. Okahara, Y. Nakatsuji

Quantitative Structure-Reactivity Analysis of the Inclusion Mechanism by Cyclodextrins

Y. Matsui, T. Nishioka, T. Fujita

The Role of Molecular Shape Similarity in Specific Molecular Recognition

T. Endo

Macrocyclic Polyamines as Biological Cation and Anion Complexones — An Application to Calculi Dissolution

E. Kimura

Micellar Models of Zinc Enzymes

W. Tagaki, K. Ogino

Chemical Basis of Ion Transport Specificity in Biological Membranes

D. W. Urry

Ion-Selective Bulk Membranes as Models for Biomembranes

K. Cammann

Molecular and Functional Aspects of Superoxide Dismutases

Alfred Gärtner and Ulrich Weser*

Anorganische Biochemie, Physiologisch-chemisches Institut der Universität Tübingen,
D-7400 Tübingen, FRG

Table of contents

Abbreviations	3
1 Introduction	3
2 Isolation of Erythrocyte Cu₂Zn₂Superoxide Dismutase	5
2.1 Precipitation with Organic Solvents	6
2.2 Aqueous Chromatography	6
2.3 Heating of the Haemolysate	8
2.4 Conclusion	8
3 Molecular Properties of Superoxide Dismutases	11
3.1 Molecular Aspects of the Cu ₂ Zn ₂ Enzyme	11
3.1.1 X-Ray Cristallographic Analysis	14
3.1.2 Newer Biophysical Investigations	16
3.1.3 Electromorphs of Cu ₂ Zn ₂ Superoxide Dismutase	17
3.1.4 Hydrogen Peroxide Treatment	20
3.2 Active Center of the Iron Enzymes	21
3.3 Molecular Properties of the Manganese Enzymes	23
3.4 The Apoproteins	24
4 Functional Aspects	26
4.1 Assays	26
4.1.1 Indirect Assays	27
4.1.2 Direct Assays	30
4.1.3 Immunochemical Methods	33
4.2 Mechanism of Action of the Cu ₂ Zn ₂ Superoxide Dismutase	35
4.2.1 Electrostatic Facilitation	36
4.2.2 Catalytic Activity of the Manganese and Iron Enzymes	39

* To whom all correspondence should be sent

- 4.3 Low Molecular Weight Compounds Mimicking Superoxide Dismutase Activity 40
- 5 Biochemical Function 46**
 - 5.1 Reactive Oxygen Species 47
 - 5.2 Biochemical Function and Distribution of Superoxide Dismutases . . . 49
- 6 Acknowledgements 53**
- 7 References 53**

Abbreviations

CD	— Circular dichroism
CM	— Carboxymethyl
Cmc	— S-carboxymethylcysteine
DDC	— Diethyldithiocarbamate
DEAE	— Diethylaminoethyl
EDTA	— Ethylenediamine tetraacetic acid
ENDOR	— Electron-nuclear double resonance
EPR	— Electron paramagnetic resonance
EXAFS	— Extended X-ray absorption fine structure
HEPES	— N-(2-hydroxyethyl)piperazin-N'-2-ethanesulphonic acid
NADH	— Reduced nicotinamide adenine dinucleotide
NBT	— Nitroblue tetrazolium chloride
NMR	— Nuclear magnetic resonance
SOD	— Superoxide dismutase
TEMED	— Tetramethylethylenediamine
XPS	— X-ray photoelectron spectroscopy

Superoxide dismutases are ubiquitously distributed in all biological systems including prokaryotic, eukaryotic and plant cells. These proteins contain either copper and zinc or manganese or iron in the active centre, respectively. During the catalytic activity, the superoxide anion is converted into dioxygen and hydrogen peroxide. Cu_2Zn_2 superoxide dismutase is one of the most intensively studied metalloproteins. The primary structure of many of these proteins has been elucidated. A convincing structure-function correlation was deduced from biophysical and chemical data. The influence of the protein backbone on the reactivity of the metal was thoroughly studied. Of special interest was the catalytic centre of Cu_2Zn_2 superoxide dismutase. The molecular architecture of the phylogenetically older iron and manganese enzymes is far less understood. At present, the clinical and biochemical aspects of reactive oxygen species enjoy a marked interest, as they are thought to be responsible for the oxygen derived cell-damage. This may reflect the overwhelming number of different assay systems described for the evaluation of superoxide dismutase activity. The most suitable and convenient assays are briefly discussed. The model chemistry for superoxide dismutases of low molecular mass complexes of transition metals is reviewed. Emphasis is placed on the biological significance of superoxide dismutase active copper ligands, frequently used as antiinflammatory drugs. The interaction of reactive oxygen species with superoxide dismutases and the biochemical and clinical relevance of this enzyme are critically summarized.

1 Introduction

Biochemically seen the periodic table of elements can be divided into four sections. Firstly, there are the group I and group II elements. They include typical metals of low ionization potentials for the first and the second electrons, respectively. Their polarizing power is low and they are known to participate neither in redox reactions nor in the formation of biopolymers. Together with the anions of group VII (halides), they are involved in maintaining the ionic strength in cellular and extracellular fluids. Electrophysiological reactions in nervous excitation are controlled. Magnesium and calcium form weakly stable complexes with nucleic acids and proteins, however, in general the tendency for complex formation of the group I and II elements is low.

Section two of the periodic table includes group IV up to group VI. The most prominent members are carbon, nitrogen, oxygen, sulphur and phosphorus. They contribute to the fundamental structural components of biopolymers. With regard to our aerobic atmosphere, oxygen plays a dual role in this event. Oxygen is incorporated into proteins, and, at the same time is required for energy supply. Due to its radical character and the possible formation of highly toxic intermediates ($\text{OH}\cdot$), some protective systems against reactive oxygen species had developed during evolution ¹⁾.

The third section of the periodic table comprises transition metals or the d-group elements, which are involved in many biological defence mechanisms against toxic radicals. As in chemical catalysis the same metals are active in biochemical systems. Surprisingly these redox mediators are involved in both, the generation and the removal of reactive oxygen species.

Zinc having a filled d shell and two 4 s electrons reacts like a Lewis acid of considerable polarizing power. Electrons are withdrawn from substrates with the consequence that a nucleophilic attack is facilitated. The elements with partially filled d shells and multiple oxidation states include Sc, Ti, V, Cr, Mn, Fe, Co, Ni and Cu. Hence, they are good candidates to actively participate in redox reactions. Attributable to d-d transitions most of the complexes of these species including many metalloproteins are coloured. This facilitates investigations of their properties by electron absorption spectrometry.

A fourth group in the periodic table of the elements can be assigned to the toxic elements Cd, Hg, Ag and Tl as well as the rare earths for which a biological function has not yet been detected. The radioactive actinides are not suitable for biological processes.

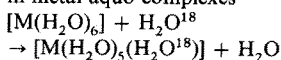
Nearly all metals mentioned before are found in the organism. The most prominent transition metals in biology include iron, zinc and copper. Manganese, cobalt and nickel are less abundant. In oxygen metabolism Fe, Cu and Mn are involved. Sometimes they act antagonistically or display co-operative effects. The antagonism is observed in inflammation. Iron proteins like cytochrome P-450 or myeloperoxidase aggravate the metabolic disorder by the generation of reactive oxygen species or hypochlorous acid. By way of contrast, copper proteins or low molecular weight copper chelates can be curative ^{2, 3)}. The co-operative effect of both, copper and iron is seen in cytochrome c oxidase ⁴⁾.

Iron forms very weak complexes with chelating agents, that produce no strong ligand fields. Amine complexes are very unstable. The porphyrin complexes are exempted where iron is coordinated to four nitrogens. The haem-iron can undergo a multiplicity of reactions including changes in valence and spin state. Haemoglobin is a typical example in which binding of oxygen results in changes of the spin state ⁵⁾. Of course, these changes can also be seen in other iron proteins like dioxygenases ⁶⁾ or iron-sulphur clusters ⁷⁾.

Copper is markedly different in its reactivity compared to iron. In porphyrins copper is totally buried. Due to the rigid structure of the porphyrins, where no twisting of the ligands is possible no reactivity with oxygen is seen. Hence, copper porphyrin-complexes display no superoxide dismutase activity ⁸⁾. In biological systems copper is essentially coordinated to nitrogen or sulphur. In octahedral Jahn-Teller distorted Cu(II) complexes a tetragonal distortion of the octahedron, usually an extension

corresponding to the lengthening of the two bonds on either moiety side of the equatorial plane coordination is seen. The rate of exchange of the two ligands on the perpendicular axis is enhanced⁹⁾. Therefore, it is not surprising that copper is an excellent reactant for fast exchange reactions. In comparing the exchange rates for water in the sixth coordination site of the aquo-complexes of different transition metals, it becomes clear, why iron, manganese and copper are exclusively bound in superoxide dismuting proteins^{9, 10)} (Table 1).

Table 1. Exchange rate of water in metal aquo-complexes¹⁰⁾



Aquo-complex	k_1 (s ⁻¹)
Cr ³⁺	5×10^{-7}
Al ³⁺	10^0
Fe ³⁺	3×10^3
Mg ²⁺	$> 10^4$
Ni ²⁺	3×10^4
Co ²⁺	10^6
Fe ²⁺	3×10^6
Mn ²⁺	3×10^7
Cu ²⁺	8×10^9

The Cu₂Zn₂superoxide dismutase has dismutation rates for the superoxide ion which are near the diffusion control ($2.0 \pm 0.5 \times 10^9$ M⁻¹s⁻¹) even at alkaline pH-values. The reaction catalyzed can be summarized as follows:



The properties of superoxide dismutases (SOD's) have been extensively reviewed¹¹⁻¹⁸⁾. Currently, it seems attractive to work on the biological activity of superoxide dismutases, whereas the chemical aspects are sometimes disregarded. However, devoid of a founded knowledge of the biophysical parameters of these enzymes, the catalytic action of the superoxide dismutases could never have been understood. Thus, a solid structure function correlation is essential.

2 Isolation of Erythrocyte Cu₂Zn₂Superoxide Dismutase

Apart from laboratory scale preparations bovine erythrocytes have become the most convenient source for Cu₂Zn₂superoxide dismutase for all kinds of applications including pharmaceutical, technical or routine purposes. Red blood cells are easily obtainable in large quantities and the costs are low or nearly nill. Special preparation techniques and mincing of cell particles can be omitted. Therefore, the isolation techniques are simple and convenient. It was the merit of Mann and Keilin who

successfully performed the first isolation of Cu_2Zn_2 superoxide dismutase from red blood cells of ox¹⁹⁾. They actually prepared a zinc-free protein and called it haemocuprein.

In the sixties an improvement was achieved by the introduction of new methods for precipitation of the haemoglobin including heavy metal or ethanol treatment^{20, 21)}. Some years later two preparation methods were established which are still currently used for routine isolations. The first was the aqueous isolation using batch absorption of nonhaemoglobin proteins to DEAE-cellulose gels²²⁾. The second was the precipitation of haemoglobin with chloroform/ethanol, the so called Tsuschihashi procedure²³⁾. Recently a new method was developed making use of the high thermal stability of vertebrate Cu_2Zn_2 superoxide dismutases²⁴⁾.

2.1 Precipitation with Organic Solvents

Cu_2Zn_2 superoxide dismutases are proteins which are of remarkable stability in the presence of organic solvents²⁵⁾. They survive concentrations of these chemicals where many other proteins are deteriorated. In the early days of biochemistry Tsuschihashi discovered that undesired haemoglobin can be readily precipitated from haemolysate by treatment with chloroform/ethanol, leaving some particular proteins dissolved²⁶⁾. Based on the resistance of Cu_2Zn_2 superoxide dismutase against organic solvents, McCord and Fridovich applied this method to the isolation of the former enzyme²³⁾. Some years later improved techniques with regard to gels and buffer systems were devised^{27, 28)}.

The procedure includes the precipitation of haemoglobin with a mixture of 0.25 volume of ethanol and 0.15 volume of chloroform. After centrifugation the superoxide dismutase is found in the supernatant. Further purification is accomplished upon precipitation of contaminating proteins by the addition of solid K_2HPO_4 (300 g per litre). After this treatment two liquid phases are obtained. Superoxide dismutase is present in the upper phase. It is precipitated by the addition of 0.75 volume of cold acetone and washed once with 0.75 % acetone. A final chromatography on DE-23 (DEAE cellulose) followed by gradient elution yields homogeneous Cu_2Zn_2 superoxide dismutase. Separation of minor contaminants and desalting is performed on Sephadex G-75 with distilled water.

Attributable to its fast performance and high convenience this procedure is usually employed for routine isolations. Unfortunately, the use of organic solvents bears some disadvantages because they are noxious. Moreover, by treatment of haemolysate with chloroform/ethanol a considerable coprecipitation and/or denaturation of superoxide dismutase is seen.

2.2 Aqueous Chromatography

The isolation technique based on sequential aqueous chromatography was introduced by Stansell and Deutsch²²⁾. They used batch absorption of the nonhaemoglobin proteins on DEAE cellulose for the removal of haemoglobin. The overall procedure was very laborious and time consuming. Therefore, a more convenient method shorter in time was developed²⁹⁾. The yield of purified SOD was the same as obtained with the Tsuschihashi method. Compared to the latter technique the different operation

procedures were much more susceptible to erroneous results. This may explain why the aqueous isolation is not frequently used. Recently, an improved aqueous isolation was devised and successfully employed^{30,31}. A significantly increased yield was obtained and in the last purification step, the charge isomers of Cu_2Zn_2 superoxide dismutase were separated on a preparative scale.

Crude haemolysate, obtained from citrated bovine blood (pH 6.8) is chromatographed on DEAE-Sephacel and the bound nonhaemoglobin proteins are eluted with a sharp NaCl gradient (0–1 M). The copper containing fractions are concentrated by membrane filtration under nitrogen pressure (1:10). Gel filtration on Sephadex G-75 yields one single copper containing protein band near $M_r \sim 32,000$. It can be exclusively assigned to Cu_2Zn_2 superoxide dismutase³⁰. It should be emphasized that neither high nor low molecular weight copper chelates can be detected after both, membrane filtration and gel filtration (Fig. 1).

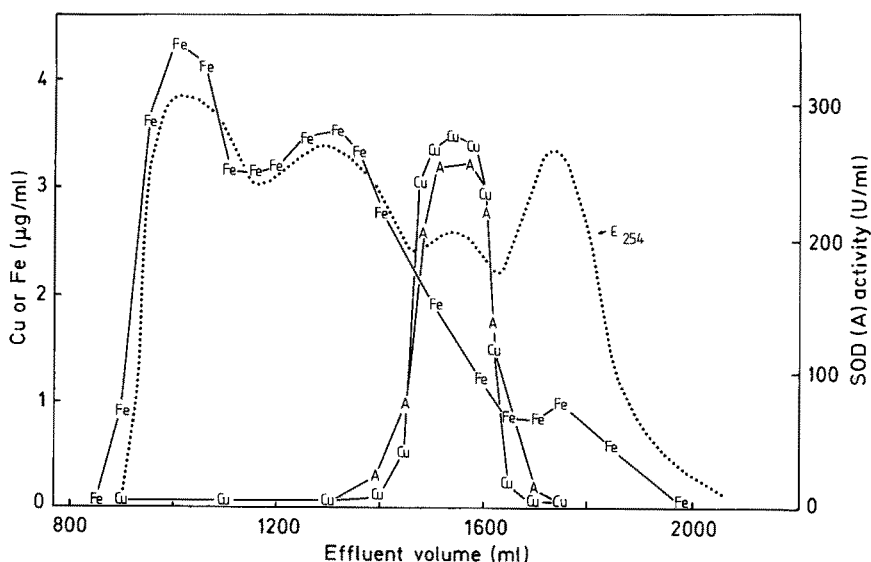


Fig. 1. Aqueous isolation of bovine erythrocyte Cu_2Zn_2 superoxide dismutase. Gelfiltration of the DEAE-eluate on Sephadex G-75. The fractions are assayed for Cu, Fe, superoxide dismutase activity (NBT-assay) and electronic absorption (A_{254}). The observed peaks are assigned to (from left to right): catalase, haemoglobin, Cu_2Zn_2 superoxide dismutase and cytochromes b/c

The crude superoxide dismutase is further purified using chromatography on DE-23 (DEAE-cellulose) and/or CM-Sephadex C-50 and/or phenylsepharose and/or hydroxyapatite. Usually one or two of the four possible chromatographic steps are sufficient. A final purification including the preparative separation of the charge isomers is accomplished by chromatofocusing. A linear gradient from pH 5.9 to pH 4.1 is applied (Polybuffer from Pharmacia 1:10 diluted). The two charge isomers are desalted on Sephadex G-75 in distilled water.

2.3 Heating of the Haemolysate

A completely different approach was made to modify the general isolation technique. Based on the thermal stability of Cu_2Zn_2 superoxide dismutase partial heat-deterioration of the haemolysate was employed²⁴⁾. Subsequent chromatography of the supernatant on DEAE-Sephacel and Sephadex G-75 yielded an electrophoretically homogeneous protein within less than five days.

Bovine red blood cells are diluted with two volumes of tap water and the lysate is dialyzed for 14 h to a conductivity of 2 mS. After heating to 70–80 °C for 10–15 min under rigorous stirring, the precipitate is separated by centrifugation. Roughly 90 % of the haemoglobin are removed by this procedure, whereas 60–70 % of the superoxide dismutase are recovered. Upon chromatography on DEAE-Sephacel the residual haemoglobin passes completely the ion exchanger. The bound nonhaemoglobin proteins are eluted with a linear NaCl gradient (0–200 mM) and freeze dried. Further separation of contaminant proteins as well as desalting is accomplished in one step after passage through a Sephadex G-75 column equilibrated with distilled water. A final yield of 50 % of the originally present enzyme is achieved.

Attributable to the enormous savings of time and financial efforts this highly efficient and simple method, probably, will prove to be the future technique for routine isolations. Furthermore, the translation from a laboratory-scale into technical-scale preparation appears to be easy.

2.4 Conclusion

In general Cu_2Zn_2 superoxide dismutase is isolated after treating the haemolysate with chloroform/ethanol²³⁾. Although this method is rather expedient, it has some major disadvantages. Roughly 25 % of the erythrocyte SOD are recovered, only. For routine work, handling of organic solvents can be hazardous. It is not unlikely that treatment of the protein with organic compounds results in minor conformational changes of the tertiary or quaternary protein structure. Previously it was demonstrated that essentially all of the erythrocyte copper is coordinated in Cu_2Zn_2 superoxide dismutase³⁰⁾. This enzyme is present in some vertebrate tissues in two forms of different isoelectric points^{32–34)}. At a final yield of only 25 % of the originally present enzyme, it is by no means clear, whether parts of form I or form II are lost or the loss of SOD is assigned to the statistical average of both forms during preparation.

Therefore, the aqueous isolation developed by Stansell and Deutsch²²⁾ was applied and improved, leading to a final yield of 50 % of originally present enzyme^{30, 31)}. It was demonstrated, that during the isolation either isoelectric variants are simultaneously lost. Although the aqueous isolation was substantially improved, it was still more time consuming than the method using organic solvents. Moreover, this procedure has another fundamental drawback. Haemoproteins and their degradation products are not readily removed by this technique.

Especially the latter species is known to act as a possible source of radical reactions. Thus, a gradual degradation of the protein in the course of the isolation process could not be fully excluded. However, the molecular properties of purified Cu_2Zn_2 superoxide dismutase obtained by the aqueous isolation are identical to those of the chloroform/ethanol treated protein^{30, 31)}.

In order to avoid the disadvantages of the above mentioned two different isolation methods a more simple, rapid and efficient method was devised ²⁴⁾. Based on the long known thermostability of Cu_2Zn_2 superoxide dismutase ²⁵⁾ undesired haemoglobin is readily removed. One important advantage of this method is, that nearly no chemicals are required to yield homogeneous SOD within five days.

The biophysical characterization of the differently prepared enzymes is summarized in Table 2 ^{29, 30)}.

Table 2. Physicochemical data of Cu_2Zn_2 superoxide dismutases obtained by different isolation techniques. Aqueously isolated charge isomers I and II are compared with the enzymes which were isolated from haemolysate previously treated with chloroform/ethanol or heating to 75 °C for 15 minutes

	Aqueously isolated		Cu_2Zn_2 SOD isolated by $\text{CHCl}_3/\text{EtOH}$ treatment	Heat treatment of haemolysate
	charge isomer I	charge isomer II		
Electron absorption				
$\epsilon_{259} \text{ [mol}^{-1}\text{cm}^{-1}\text{]}$	9840 ± 50	9820 ± 50	9840 ± 50	9870 ± 50
ϵ_{680}	313 ± 5	310 ± 5	315 ± 5	310 ± 5
Circular dichroism				
$\theta_{208} \left[\frac{\text{deg} \cdot \text{cm}^2}{\text{d mol}} \right]$	-6000	-5950	-6000	-6100
$\theta_{261} \left[\frac{\text{deg} \cdot \text{cm}^2}{\text{d mol}} \right]$	20000	10000	20000	19400
EPR spectroscopy				
$A_{ } \text{ cm}^{-1}$	0.014	0.013	0.014	0.013
$g_{ }$	2.062	2.060	2.062	2.063
g_{\perp}	2.263	2.262	2.263	2.261
X-ray photoelectron spectroscopy		No differences		
Amino acid analyses		No differences		
Electrophoreses	Two-bands	One-band	Three-bands	Three-bands
Isoelectric focusing	One-band	One-band	Two-bands	Two-bands
Specific SOD activity [U/mg] (Nitroblue tetrazoliumchloride assays)	1700	1600	1700	1700
Copper ($\mu\text{g}/\text{mg}$)protein	3.6	3.4	3.7	3.6
Zinc ($\mu\text{g}/\text{mg}$)protein	4.1	4.0	4.2	4.1

Essentially no profound changes are seen. Isolated superoxide dismutase employing chloroform/ethanol treatment had a slightly different electrophoretic pattern compared to the aqueously isolated enzyme. The quantity of charge isomer II was diminished to a minor extent.

When isolating superoxide dismutases from other tissues than erythrocytes the methods explained here are normally not suitable. For the purification from solid sources like liver a lot of other techniques are described ³⁵⁾. Moreover, Mn-SOD and Fe-SOD are neither resistant to organic solvents nor to heat treatment. Therefore, mild conditions are required for the isolation of these enzymes. The techniques used

for the purification of these SOD's are markedly different from those applied for the isolation of erythrocyte $\text{Cu}_2\text{Zn}_2\text{SOD}$'s^{35, 36)}.

An intriguing phenomenon was observed, when the purified bovine erythrocyte Cu_2Zn_2 superoxide dismutases, obtained by the different isolation techniques were compared. Thermal stability measurements revealed that the purified SOD's are much less heat resistant compared to the enzymes in the homogenates. Therefore, heat deterioration of the isolated protein must not be connected with the isolation technique described in Chapter 2.3. When freshly aqueously isolated Cu_2Zn_2 superoxide dismutase was heated to 77 °C a transient and marked increase of the specific enzymic activity is seen.

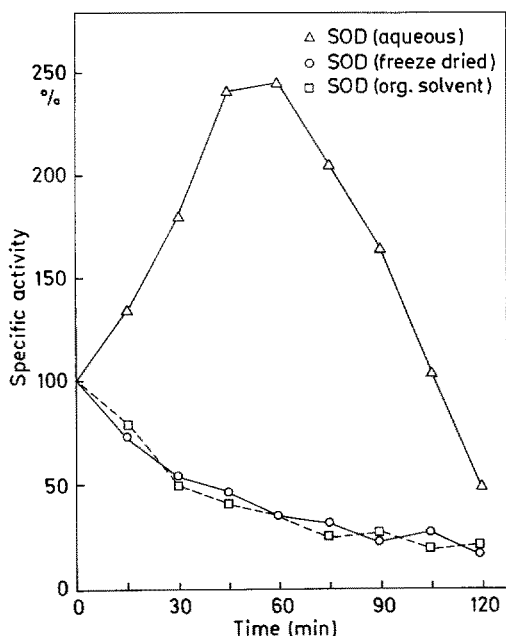


Fig. 2. Heat denaturation of purified bovine erythrocyte Cu_2Zn_2 superoxide dismutase. (○) SOD prepared by treatment with chloroform/ethanol, (Δ) aqueously isolated enzyme and (□) the same enzyme stored for three months as lyophilized powder at room temperature. When freshly prepared, all fractions of aqueously isolated superoxide dismutase showed the same behaviour as (Δ) regardless of the age of the animal and the isoelectric point. SOD-activity was estimated using the cytochrome c assay²³⁾

This phenomenon is not observed using SOD which was previously treated with organic solvents or lyophilized enzyme from either source stored for three months. It was suggested, that the molecular architecture of the active center of aqueously isolated enzyme differs from that of the other species³¹⁾.

The molecular properties of the SOD's summarized in the next chapter are essentially all derived from data collected from the enzyme which was isolated employing the chloroform/ethanol method. Data from Cu_2Zn_2 superoxide dismutases obtained by other isolation methods are awaited with great interest.

3 Molecular Properties of Superoxide Dismutases

Since the early work of Mann and Keilin a lot of structural investigations on superoxide dismutases were carried out. Little is known on the structural aspects of the phylogenetically older iron and manganese enzymes than on the properties of the Cu_2Zn_2 -SOD. Currently, the copper-zinc-protein is one of the best known metallo-proteins. Richardson and Richardson achieved the first breakthrough with the X-ray cristallographic analysis of bovine Cu_2Zn_2 superoxide dismutase³⁷⁾. Sequencing of the amino acid structure of Cu_2Zn_2 -SOD's from different sources and alternatively the iron and manganese enzymes revealed a high degree of sequence homology within the respective class of proteins¹⁾. It could be demonstrated that all amino acid residues involved in the catalytic reaction are conserved. Attributable to the founded knowlege on the structure and function of superoxide dismutases, they are excellent examples for understanding enzymatic catalysis. Moreover, the influence of the protein backbone on the catalytic effect of the metals can be comprehensively demonstrated.

3.1 Molecular Aspects of the Cu_2Zn_2 Enzyme

Cu_2Zn_2 superoxide dismutase is an enzyme of intriguingly high stability in vitro. It can be heated to 100 °C for one minute without any detectable loss of activity and it survives pH-ranges from 2–12²⁶⁾. Moreover, the enzymic activity survives the presence of ten molar urea and/or four per cent sodium dodecylsulphate. In a solution of six per cent guanidinium hydrochloride where most of the other proteins are deteriorated the denaturation of superoxide dismutase is reversible^{38, 39)}.

The Cu_2Zn_2 enzymes can be obtained from many sources. Apart from two exceptions^{40, 41)} they are exclusively found in eucaryotic organisms in nearly all tissues⁴²⁾. Only the enzymes from higher species have a blocked N-terminal group. These enzymes are generally more stable. Whether this phenomenon can be ascribed to the acetylation or not is still open to discussion. Iron SOD's are exclusively prokaryotic, whereas manganese superoxide dismutases are present in procaryotic cells as well as in mitochondria and the serum of vertebrates^{43–45)}. Their relative molecular mass is differing. Recently a high relative molecular mass copper containing enzyme of $M_r = 135,000$ was deduced to be present in human lung⁴⁶⁾. Cu_2Zn_2 enzymes in general have a relative molecular mass around 32,000.

The Cu_2Zn_2 superoxide dismutase of bovine erythrocytes is a homodimer of 31,300 daltons and contains one g atom of both, copper and zinc per subunit. SOD's from fungi, plants and vertebrates have remarkable homologies in the amino acid sequence⁴⁷⁾. The sequence of the bovine erythrocyte enzyme is summarized in Table 3⁴⁸⁾.

The sequence of human erythrocyte superoxide dismutase has been elucidated some years later^{49, 50)}. Bovine superoxide dismutase contains no tryptophane and very few aromatic and heteroaromatic amino acid residues, respectively. Eight histidines, one tyrosine and one phenylalanine are detected. The main portion of the protein is formed by neutral amino acids. Four sulphur containing amino acids (three cysteins and one methionine) are also present. Cysteine residues 55 and 144 are disulphide bridged⁵¹⁾, whereas one cysteine sulphhydryl group remains unbound. These data are contrasted by the properties of the human enzyme where 153 amino

Table 3. Complete amino acid Sequence of bovine Erythrocyte Superoxide Dismutase ⁴⁸⁾

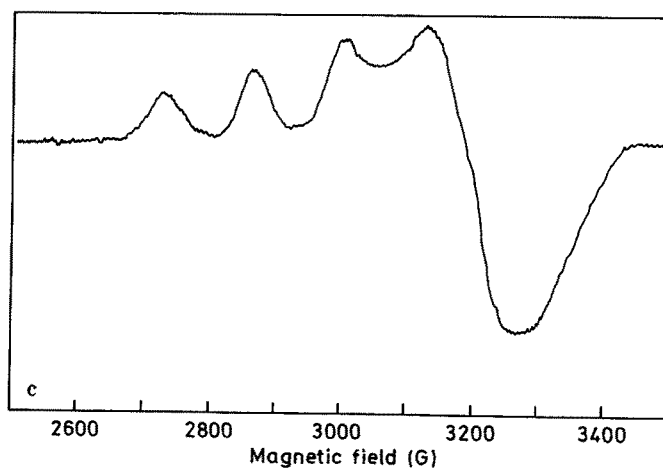
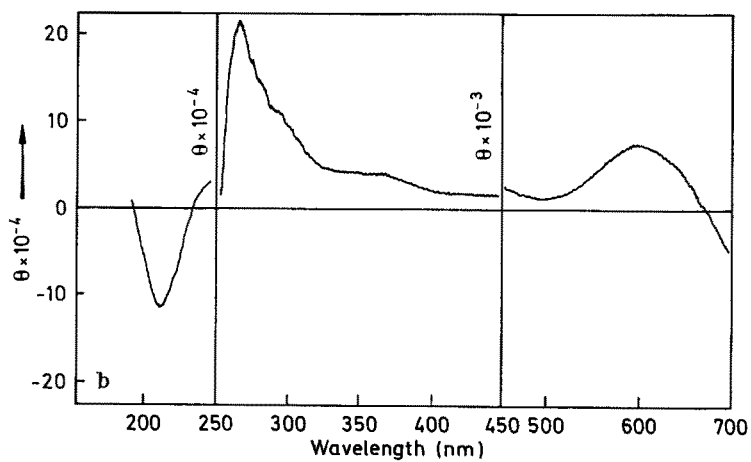
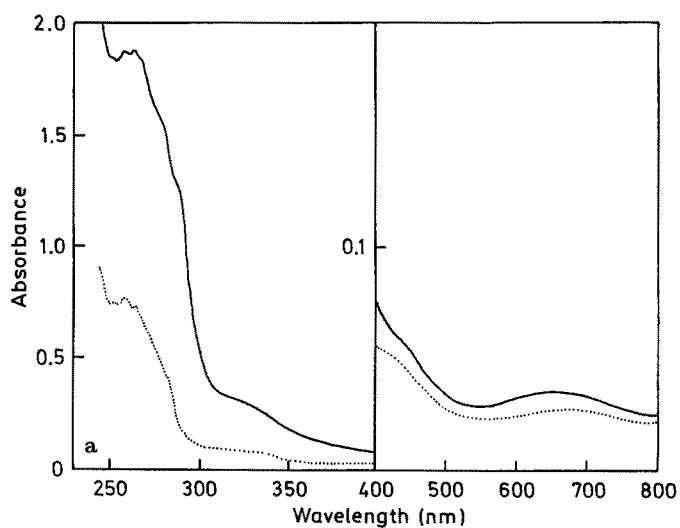
1	10
Ac — Ala — Thr — Lys — Ala — Val — Cmc — Val — Leu — Lys — Gly — Asp — Gly —	
20	
Pro — Val — Gln — Gly — Thr — Ile — His — Phe — Glu — Ala — Lys — Gly — Asp — Thr —	
30	40
Val — Val — Val — Thr — Gly — Ser — Ile — Thr — Gly — Leu — Thr — Glu — Gly — Asp —	
50	
His — Gly — Phe — His — Val — His — Gln — Phe — Gly — Asp — Asn — Thr — Gln —	
60	
Gly — Cmc — Thr — Ser — Ala — Gly — Pro — His — Phe — Asn — Pro — Leu — Ser —	
70	
Lys — Lys — His — Gly — Gly — Pro — Lys — Asp — Glu — Glu — Arg — His — Val —	
80	90
Gly — Asp — Leu — Gly — Asn — Val — Thr — Ala — Asp — Lys — Asn — Gly — Val —	
100	
Ala — Ile — Val — Asp — Ile — Val — Asp — Pro — Leu — Ile — Ser — Leu — Ser — Gly —	
110	120
Glu — Thr — Ser — Ile — Ile — Gly — Arg — Thr — Met — Val — Val — His — Glu — Lys —	
130	
Pro — Asp — Asp — Leu — Gly — Arg — Gly — Gly — Asn — Glu — Glu — Ser — Thr —	
140	
Lys — Thr — Gly — Asn — Ala — Gly — Ser — Arg — Leu — Ala — Cmc — Gly — Val —	
150	
Ile — Gly — Ile — Ala — Lys	

acid residues are found ^{49, 50)}. This phenomenon is also seen with the horse ⁵²⁾ and the yeast enzyme. Human Cu₂Zn₂-SOD contains tryptophane but no methionine. Horse liver SOD is devoid of tryptophane and tyrosine.

The spectral properties of Cu₂Zn₂superoxide dismutases are known since many years. Apart from the data obtained by classical methods and which are summarized in Fig. 3 ⁵³⁾ there are many investigations employing more sophisticated techniques.

The differences in the electron absorption spectrum between human and bovine SOD are attributed to the presence and absence of tryptophane, respectively ⁵⁴⁾.

Fig. 3a-c. Spectrometrical data of erythrocyte Cu₂Zn₂superoxide dismutase. *a* Electronic absorption of human (—) and bovine (·····) SOD. *b* Circular dichroism. *c* Electron paramagnetic resonance at 77 °K. Apart from electronic absorption spectrometry, no differences are seen between human and bovine SOD



No differences of chiroptical and EPR properties are detected. According to the definition given by Malkin and Malmström, Cu_2Zn_2 superoxide dismutase is classified as a non- blue copper protein ⁵⁵⁾.

3.1.1 X-Ray Cristallographic Analysis

Concomitant with the discovery of the complete amino acid sequence of bovine erythrocyte Cu_2Zn_2 superoxide dismutase work on X-ray cristallography of this enzyme was in progress. A preliminary study at 5.5 Å resolution revealed the approximate organisation of the quaternary structure ³⁷⁾. Further refinement of the data to a 2 Å solution was accomplished in 1982 ⁵⁶⁻⁵⁹⁾. The homodimer of two subunits each of which carries 151 amino acid residues cristallizes in space group C 2 with two dimeric enzyme molecules per asymmetric unit. Each subunit is composed of eight antiparrallel β strands containing 46 % of the residues that form a flattened cylinder, plus three external loops, involving 48 % of the residues. A schematic drawing of the subunit structure is provided in Fig. 4 ⁵⁹⁾.

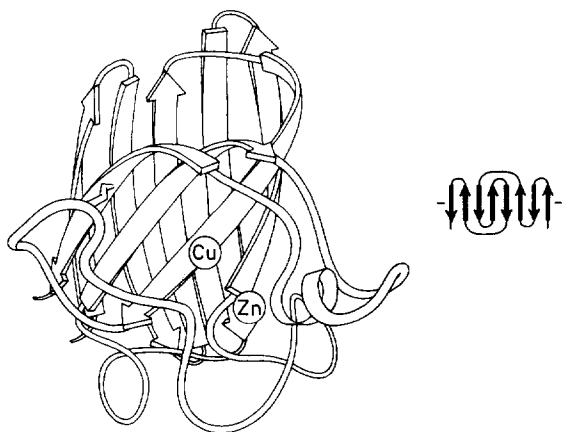


Fig. 4. Schematic drawing of the protein backbone of a Cu_2Zn_2 superoxide dismutase subunit. The arrows indicate the eight β-strands. The copper is solvent-accessible and lies at the bottom of the active-site channel which is mainly formed by two loops. (With permission from Ref. ⁵⁹⁾)

The main-chain hydrogen bonds primarily link β-strand residues, side-chain to main-chain hydrogen bonds are extensively involved in the formation of tight turns. The β-strands are numbered from 1–8. The loops are named for the β-strands at the beginning and the end of each loop i.e. 4.7, 6.5 and 7.8.

Loop 4.7 (Pro-100-Gly-112) is the smallest of the three SOD loops. The largest loop (loop 6.5) is complicated. It can be described as two distinct loop regions: a disulphide loop region (Gln-47-Pro-60) and a Zn ligand loop region (His-61-Leu-82). The single disulphide bridge, Cys-55 to Cys-144, forms a covalent bond between loop 6.5 and the base of loop 7.8. The zinc binding region contains all four Zn ligands.

Loop 7.8 (Glu-119-Leu-142) forms a lid of the active side, which lies 6.3 Å apart at the bottom of a long channel between loops 6.5 and 7.8 on the external surface of

β -barrel strands 5.6 and 7. The Zn is buried, while Cu is solvent-accessible. The side chain of His-61 forms a bridge between Cu and Zn and is almost planar to the metals.

The Cu ligands of His-44, -46, -61 and -118 show an uneven tetrahedral distortion from a square plane. Zn ligands of His-61, -69, -78 and Asp-81 are tetrahedrally arranged with a strong distortion toward a trigonal pyramid. The active site channel of Cu_2Zn_2 superoxide dismutase is demonstrated in Fig. 5⁶⁰⁾.

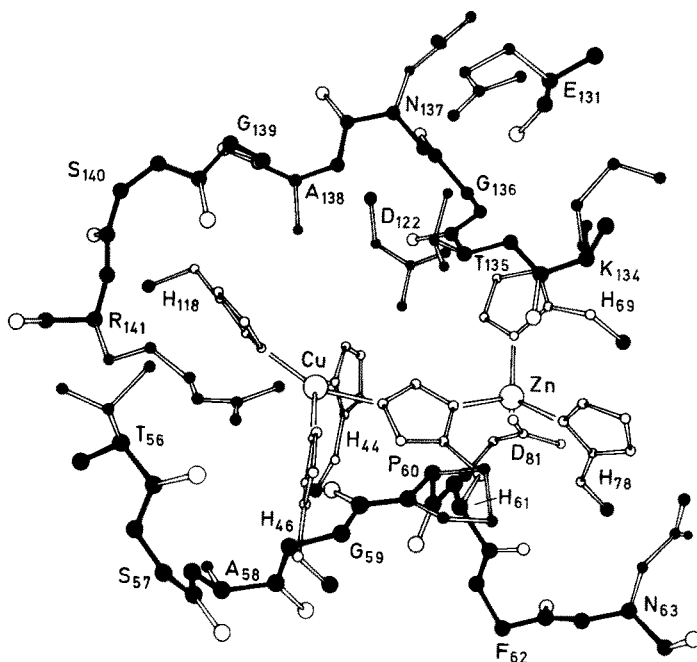


Fig. 5. The active-site of bovine erythrocyte Cu_2Zn_2 superoxide dismutase. View from the solvent. The copper is coordinated by His 44, 46, 61 and 118. The Zn is buried. The geometry of its ligands is tetrahedral. The imidazole ring of His 61 is the bridging ligand between Cu and Zn. (With permission from Ref. ⁶⁰⁾)

The SOD molecule exerts an extensive surface topography of sequence-conserved residues, suggesting that this invariance is critical to the enzymatic function⁶⁰⁾. Two pits are seen, forming specific binding sides in the narrowest part of the active-site channel floor. One pit (the Cu-site) is formed by the exposed surface of the Cu(II) and parts of His-61, His-118, Thr-135 and Arg-141. The adjacent pit (the water-site) is formed by parts of the exposed surface of Thr-135, Gly-136, Ala-138, Gly-139 and Cu-ligands His-44 and His-118. O_2^- fit the Cu-site surface with one oxygen bound to the Cu and the other H-bonded to Arg-141. Both active-site channel pits contain highly ordered water molecules.

The overall amino acid structure of Cu_2Zn_2 superoxide dismutase contains repeated folding patterns⁶¹⁾. The active-site face is formed by two similar paired subdomains which interlock and enclose the catalytically essential copper ion. This phenomenon was attributed to a gene duplication in the evolution of Cu_2Zn_2 superoxide dismutase.

3.1.2 Newer Biophysical Investigations

The large number of histidine residues associated with the active site of bovine SOD facilitates the study of its chemical and structural properties by nuclear magnetic resonance (NMR) spectroscopy. Mainly the downfield histidine imidazole N-proton resonances were subject of a large quantity of investigations⁶²⁻⁶⁴). The deuteration of histidine residues is dependent only on the absence of co-ordinated metal ions and not changes in the protein structure^{66,67}). Therefore, in apo-, zinc- and holo-superoxide dismutase, only those histidine residues not co-ordinated to metal ions will be deuterated at the C-2 position. This can be used as a simple method for the identification of co-ordinated histidine residues in metalloproteins employing only minimal chemical modifications.

The NMR-spectra of the human and the bovine enzymes are very similar. This is consistent with the significant homology in the amino acid sequences⁶⁶). The similarity is such, that it was predicted by NMR-spectroscopists, that all six histidine residues are conserved. Furthermore, Cu₂Zn₂-SOD from baker's yeast⁶⁷) and from wheat germs⁶⁹) also have conserved histidine residues, revealing considerable active-site structural homology between mammalian SOD's and the former two species.

Cadmium-113 nuclear magnetic resonance studies of the cadmium substituted bovine superoxide dismutase were carried out⁷⁰). Only a very small chemical-shift difference between the 2 Cd(II) protein (Cd(II) is bound to the zinc site and the copper site is unoccupied) and the 2 Cd(II)—2 Cu(I) enzyme (analogous to the reduced form of the native protein) was found. This was interpreted in that the imidazolate bridge is protonated at the Cu site after reduction.

Cu(II) with its d⁹ electron configuration can be easily visualized by electron spin resonance (EPR) in the oxidized Cu₂Zn₂superoxide dismutase. From the super-hyperfine splittings seen at alkaline pH, it was concluded that the copper in SOD is bound to four nitrogens²⁷). The copper is fully detectable⁵⁵). The two equivalent copper centers have been shown to be rhombic with a high degree of distortion⁷¹). Recently more ingenious EPR techniques were applied in studying the properties of the Cu sites of Cu₂Zn₂-SOD's. The local environment of Cu(II) in the bovine enzyme was examined using the nuclear modulation effect in pulsed EPR spectroscopy (Electron spin echo spectroscopy)⁷²). The echo envelope spectrum contains lines arising from the interaction of the spin of the Cu(II) with the remote ¹⁴N-atoms of the ligated imidazoles. At neutral or elevated pH, the lines are split, indicating that the interaction of the nitrogens with the copper has been altered by the zinc linked by the imidazolate bridge to Cu(II). This is not observed at low pH, suggesting that zinc (II) is no longer bound to the bridging imidazole. Contrary to azide, addition of cyanide to the Zn-free 2 Cu-protein does not change the echo envelope spectrum, whereas addition of cyanide to the holoprotein does. It was therefore deduced, that cyanide binding alters the bonding of Cu(II) to imidazole ¹⁴N in the holoprotein.

Electron-nuclear double resonance (ENDOR) is able to recover hyperfine and quadrupole information from incompletely resolved EPR-spectra. It was applied to native, azido- and cyano-derivatives of bovine Cu₂Zn₂superoxide dismutase⁷³). The ENDOR response of azido-SOD has led to the suggestion, that four nearly equivalent nitrogens surround the copper. The response of the native form was too complex for interpretation. The ENDOR response of the cyano form revealed that

two of the three EPR-observable nitrogens are magnetically equivalent. They have hyperfine and quadrupole interactions, that are larger than the third nitrogen. A square-planar arrangement of the three imidazole nitrogens and one cyanide carbon around the copper was therefore proposed. The CN^- is trans to the more weakly coupled nitrogen. The extremely low NMR relaxivity of the monocyano derivative suggests that water molecules cannot bind directly to the Cu(II) . Employing electron paramagnetic resonance investigations of single monoclinical crystals of SOD, the change in the coordination of the metal is also seen when CN^- binds to the copper ⁷⁴⁾.

Extended X-ray-absorption fine structures (EXAFS) on copper and zinc K-edge were measured in aqueous solution ⁷⁵⁾. After reduction of copper, it is co-ordinated to three imidazole residues at a shorter distance (0.194 nm) compared with the coordination of all four imidazole groups and an oxygen atom from solvent water in the oxidized form 0.199 nm. The changes at copper that accompany reduction introduce minimal perturbation on the stereochemistry at the zinc site. These results are in good accordance with the results obtained by the above mentioned biophysical methods. Together with the data collected from the chemistry of the apoproteins (Chapt. 3.4) and the investigations on the functional site (Chapt. 4.2), fragmentary informations could be put together like a jigsaw puzzle, yielding a unique picture of the chemical and biochemical reactivity of a metalloprotein.

3.1.3 Electromorphs of Cu_2Zn_2 Superoxide Dismutase

For many years it seemed to be an obscure phenomenon that purified SOD has a two-band pattern on gel electrophoresis ⁷⁶⁻⁷⁸⁾. This disadvantage has been overcome with the discovery of the isoelectric variance of two distinct SOD species by Crosti ³²⁾. The isomerism has been confirmed by other authors ⁷⁹⁾. Isoelectric variants, also called charge isomers, are found in human, bovine and rat erythrocytes. Although in thymus, lung, spleen, skeletal muscle, heart and brain Cu_2Zn_2 superoxide dismutase is present in considerable amounts, in those tissues charge isomerism could not be detected. Firstly, the isoelectric variance was attributed to posttranslational changes and not simple interactions of the enzyme with tissue specific components ⁸⁰⁾. This report was challenged by an investigation of the isoenzymes in inbred mice ⁸¹⁾. Three electrophoretic variants were found. Since the mice were highly inbred, it was concluded that this pattern is due to unequal rates of transcription of two linked nonallelic structural genes encoding SOD.

Both charge isomers have a relative molecular mass of 32,000 daltons. The isomerism is attributed to the different isoelectric points of the proteins ³³⁾. No differences were found in metal content, antigenicity, electron paramagnetic resonance and electron absorption spectroscopy ³⁴⁾. Holo- and apo-superoxide dismutase, which have electrophoretic mobilities similar to those of charge isomers I and II, respectively, show significant different antigenicity. However, the different electrophoretic mobility of the charge isomers was mainly ascribed to conformational changes. Charge isomer I with a p.I. of 5.2 is faster inactivated by heat treatment, than charge isomer II with a p.I. of 4.9.

Previously, the charge isomers of aqueously isolated bovine erythrocyte superoxide dismutase were separated and subjected to many biophysical investigations including the comparison with the enzymes isolated by the Tsushihashi-procedure ³¹⁾. Amino

acid analyses, XPS-spectroscopy of the $S_{2p1/2,3/2}$ -levels, EPR-, CD-, and electron absorption spectroscopy were carried out. Apart from CD-spectroscopy, no differences were found in the molecular properties of the charge isomers (Fig. 6).

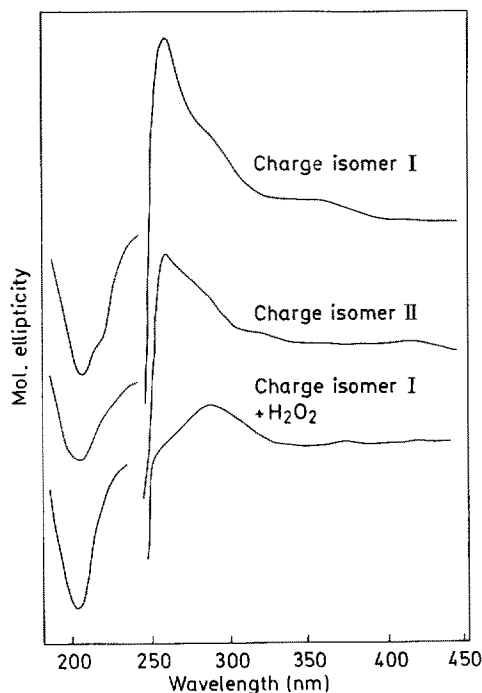


Fig. 6. Circular dichroism of the charge-isomers from aqueously isolated Cu_2Zn_2 superoxide dismutase. The molecular ellipticity at 261 nm of charge isomer I is twice as high compared to that of charge isomer II. Treating charge isomer I with H_2O_2 the band at 261 nm is levelled off and a new Cotton band is seen at 295 nm

The θ -value of charge isomer II at 261 nm was only half to that of charge isomer I. The molar ellipticity at 208 nm, corresponding to the α -carbon skeleton of the protein, remained unchanged. H_2O_2 -treated charge isomer I had a completely different spectrum in circular dichroism. Charge isomer II, therefore, cannot be generated by an attack of charge isomer I with hydrogen peroxide in vivo, which was suggested by some authors⁸²⁾.

Comparing charge isomer I with the variant II no bleaching of the chromophore at 261 nm is seen in electron absorption spectroscopy. The decrease in the chiroptical absorbance of charge isomer II must not necessarily be caused by a change of the geometry at the active site. However, there is strong evidence, that the difference between charge isomer I and II is mainly conformation related and not genetically determined. This judgement confirms earlier reports^{34, 80)}.

The reactivity of erythrocyte Cu_2Zn_2 superoxide dismutase in gel electrophoresis or isoelectric focusing is rather confusing. Upon electrophoresis on starch or poly-

acrylamide gels a three band pattern is observed, containing one slow migrating band of high intensity and two weaker faster migrating bands. In isoelectric focusing or chromatofocusing, where the proteins are separated according to their isoelectric points, only two bands can be detected. This complex situation is demonstrated in Fig. 7.

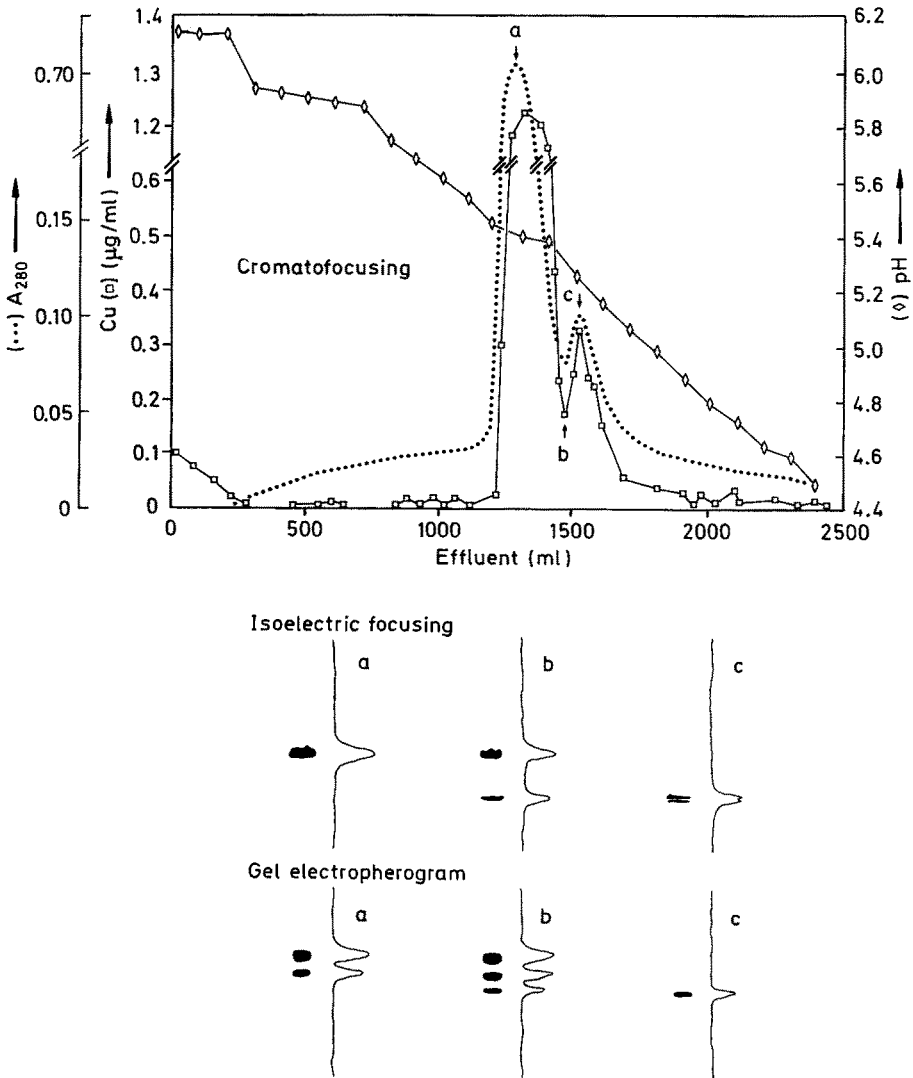
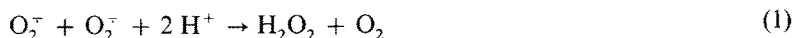


Fig. 7. Chromatofocusing, isoelectric focusing and polyacrylamide gel electrophoresis of aqueously isolated bovine erythrocyte Cu_2Zn_2 superoxide dismutase. In chromatofocusing and isoelectric focusing a two-band pattern is obtained, which are assigned to the two charge isomers of the enzyme. During electrophoresis charge isomer I is split in two bands, whereas charge isomer II remains single-band. Adjacent to photographs of the respective gels, the corresponding densitometrical scans are depicted. a), b) and c) refer to the different fractions obtained after chromatofocusing

The two bands after chromatofocusing are related to the above mentioned charge isomers I and II, carrying roughly 80 % and 20 % of the total erythrocyte copper, respectively. This pattern is reproduced after isoelectric focusing. Charge isomer I, if subjected to polyacrylamide gel electrophoresis shows a two-band pattern corresponding to the two SOD-bands seen in earlier studies⁷⁵⁻⁷⁸. Charge isomer II displays only one band during electrophoresis. According to more recent work this refers to the third band of the three band pattern³⁴. It is not clear which event is leading to such an unusual reactivity. Some authors suggested that the splitting of the SOD bands on gel electrophoresis may be attributed to a partial loss of copper, because the apoproteins have very similar mobilities⁸³. However, another aspect is, that the electrophoretic pattern of Cu₂Zn₂superoxide dismutase is strongly dependent on the experimental conditions applied during electrophoresis⁸⁴. At present it seems very attractive that a definitive solution to this problem will be given by X-ray diffraction studies of the two charge isomers or the electrophoretic variants, respectively.

3.1.4 Hydrogen Peroxide Treatment

The reaction catalyzed by superoxide dismutases is summarized in the following equation²³:



Shortly after the discovery of this enzymatic reaction the interaction of Cu₂Zn₂superoxide dismutase with its reaction product i.e. hydrogen peroxide was investigated⁸⁵⁻⁸⁷. It was found that the Cu(II) in the resting enzyme is reduced to Cu(I) by H₂O₂⁸⁸. It is a rapid process. Prolonged exposure to H₂O₂ results in the destruction of one histidine per subunit. In the electron absorption spectrum a bleaching of the chromophore in the UV-region and a new absorption band at 450 nm is seen⁸⁹. A Fenton's type reaction of Cu(I) with additional H₂O₂ was proposed generating ·OH-radicals which could then oxidatively attack an adjacent histidine.

The inactivation of the enzyme is pH-dependent. At alkaline pH the SOD is more readily inhibited than at pH 7.0. Therefore, most of the investigations were carried out at or above pH 10.0. At these pH-values the equilibrium of the reaction:



is pushed to the right side due to a pK_a of 11.6. The anion of peroxide is much less stable than the protonated form. Hence, it will strive for a stabilization, adding a proton or electrophils like histidine. The actual inactivating agent for superoxide dismutase at alkaline pH is therefore the HO₂⁻ anion^{90,91}. At these pH values arginine residues in the active funnel of the Cu₂Zn₂ enzymes are deprotonated. The binding of the HO₂⁻ anion to the active site is thus facilitated. The inactivation of the Cu₂Zn₂-SOD by hydrogen peroxide is seen with both, the yeast and the bovine enzymes. However, subtle differences in the kinetic parameters are noticed. It was suggested that the active sites of these Cu₂Zn₂superoxide dismutase are not entirely identical.

Sinet and Garber were first who investigated hydrogen peroxide treatment of human Cu₂Zn₂-SOD under physiological conditions⁹². Protection against hydrogen peroxide is observed with some OH-radical scavengers (formate, mannitol) but

not with all scavengers of this toxic intermediate (ethanol, t-butyl alcohol). Thus, free OH-radicals are not responsible for the inactivation. The reaction originally proposed by Hodgson and Fridovich ⁸⁹⁾:



poses thermodynamic and mechanistic problems because H_2O_2 is not a good one-electron reductant ⁹³⁾. The reduction of Cu(II) was therefore thought to be carried out by the superoxide anion ⁹²⁾. It was assumed that both, superoxide and hydrogen peroxide are necessary for the inactivation of Cu_2Zn_2 superoxide dismutase.

The treatment of superoxide dismutase with H_2O_2 is also interesting from another point of view. Hydrogen peroxide generates distinct electrophoretic variants which are comparable to those of the native enzyme ⁸²⁾ (see Chapt. 3.1.3). Increasing ratios of hydrogen peroxide result in an increase in the heterogeneity during electrophoresis. The reaction of SOD with hydrogen peroxide *in vivo* was said to be the source of the electrophoretic heterogeneity of native purified Cu_2Zn_2 superoxide dismutase. In other words, charge isomer II may be generated from charge isomer I by H_2O_2 inactivation.

This hypothesis was contrasted by the biophysical investigation of the charge isomers ³¹⁾. It was demonstrated the parameters obtained from charge isomers I and II were completely different from those of hydrogen peroxide treated enzyme. Thus, the electrophoretic heterogeneity of purified SOD cannot be attributed to an *in vivo* inactivation by H_2O_2 . In addition, it seems very unlikely that significant concentrations of hydrogen peroxide are present in the red blood cells. They have extremely high concentrations of haemproteins. In general, nearly all haemproteins are able to destroy hydrogen peroxide, although sometimes low rate constants are observed. Additional scavenging of H_2O_2 is provided by catalase and glutathione peroxidase which are present in erythrocytes in the same ratio as Cu_2Zn_2 -SOD ⁹⁴⁾. Although, liver cells are known to produce a higher fluxes of oxy radicals than erythrocytes, in this tissue charge isomerism of SOD could not be detected.

3.2 Active Center of the Iron Enzymes

Iron SOD's are found in prokaryotes ⁹⁵⁾ and plants ⁹⁶⁾. Manganese and iron enzymes are phylogenetically older and they show great sequence homologies which are different from those of the Cu_2Zn_2 superoxide dismutases ⁹⁷⁾. Compared to the latter species, iron and manganese containing SOD's have received much less attention.

Iron superoxide dismutase is commonly isolated as dimer or tetramer each subunit bearing a functional metal ion ⁹⁸⁾. There have been no reports of a strong interaction between the metal centers. The subunits display relative molecular masses around 22,000 daltons. The trivalent state of the metal atom seems to be the ground state.

The metal content has been a source of much controversy ⁹⁹⁾. Recently the iron content was determined directly from anomalous scattering measurements on crystals of the native enzyme ¹⁰⁰⁾. A symmetrical dimer with one iron per subunit was found. Since each subunit of the purified enzyme contained slightly more than half an iron atom, it was concluded, that the normal state of this enzyme would be two iron atoms per dimer and that some of the metal was lost during purification. Actually, the metal

binding constants for the iron-enzymes are much lower than those for the copper of the copper, zinc SOD's.

The optical spectrum of iron superoxide dismutase is characterized by a broad band near 350 nm that is attributed to a ligand-to-metal charge transfer band. The relatively high energy for this transition indicates that tyrosine is not a ligand to the Fe(III). The EPR-spectrum is characteristically rhombic ¹⁰¹⁾. Azide and fluoride are inhibitors of the enzymatic activity. Intriguingly, cyanide does not affect the catalytic action. As in the case with the Cu₂Zn₂ enzymes, hydrogen peroxide readily destroys the reactivity of iron SOD's, whereas manganese superoxide dismutases remain unaffected ¹⁰²⁾.

A hybrid superoxide dismutase, containing both functional iron and manganese was isolated from *Escherichia coli*. H₂O₂ treatment, leading to a selective inactivation of the iron enzyme resulted in a resegmentation of subunits with an active Mn enzyme and an inactive Fe enzyme ⁴⁴⁾. 10 % residual activity was still recovered with the H₂O₂ treated iron enzyme. Manganese was found in this protein in the same amount. Therefore, the iron enzyme seems to be a naturally occurring hybrid, containing both iron and 10 % manganese. More recently, another hybrid superoxide dismutase was isolated from *Nocardia asteroides* containing 1 to 2 g atoms each of Fe, Mn and Zn per mol ¹⁰³⁾. Its M_r is 100,000 and it is composed of four subunits which are not covalently joined. Azide at 1 and 20 mM inhibits the activity 10 and 40 %, respectively, and 5 mM H₂O₂ inhibits 40 %, whereas cyanide did not affect the enzyme.

Currently the X-ray cristallographic analyses of the iron superoxide dismutases from *Pseudomonas ovalis* and *Escherichia coli* have become available (Fig. 8) ^{41, 104)}.

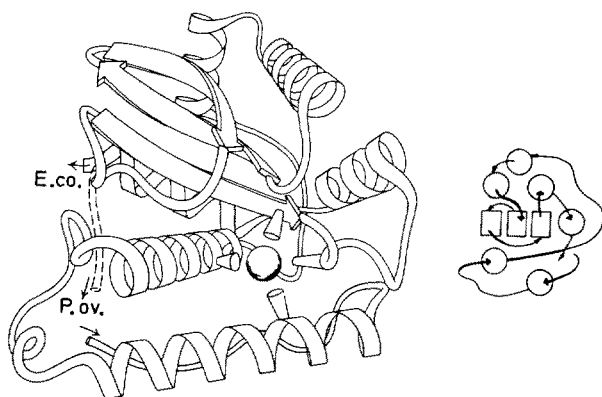


Fig. 8. Schematic drawing of the amino acid structure of iron superoxide dismutase subunits. The difference in the carboxyl terminal conformation between the enzymes from *E. coli* and *P. ovalis* is pointed out. (With permission from Ref. ¹⁰⁴⁾)

They are highly helical and have nearly identical foldings. The monomer is a two domain structure with six major helical segments and three strands of antiparallel β -sheet ¹⁰⁵⁾. The iron is ligated to four protein side chains, one from each of the two crossing helices in the N-terminal domain and the third and fourth from residues

near the end of the β -sheet in the C-terminal domain. The active center is exposed to the solvent. At present there are no data on the precise characterization of the iron coordination sphere.

3.3 Molecular Properties of the Manganese Enzymes

Much less information is available on the manganese superoxide dismutases. No crystal structure has been reported for such an enzyme, but similarities in the three-dimensional structures can be deduced from the Cd-spectra^{106, 107)} and comparisons of the amino acid sequences⁹⁷⁾. The manganese SOD's are widely distributed. In mammals they are found in liver, brain, renal cortex, heart, skeletal muscle, lymphatic node and extracellular fluids¹⁰⁸⁾. Cu_2Zn_2 enzymes are predominantly detected in the cytosol of the cells, the manganese form is present in the mitochondria¹⁰⁹⁾. Manganese enzymes could be also considered to be a prokaryotic enzyme. It is found in many protozoa¹¹⁰⁻¹¹⁵⁾.

Due to the relatively low metal-binding constants compared to the Cu_2Zn_2 -SOD's, the metal contents of isolated manganese superoxide dismutases are varying between 1.0 and 2.0 g atoms per dimer¹⁰⁹⁻¹¹⁵⁾. Remarkable differences are also found in the relative molecular mass. In the literature values ranging from 39,500 up to 94,00 daltons are reported¹⁰⁹⁻¹¹⁵⁾. The subunits have molecular weights of about 20,000. The manganese SOD's seem to form dimers as well as tetramers. In contrast to the Cu_2Zn_2 enzymes, the manganese superoxide dismutases are insensitive to cyanide. The manganese ion is found in the tervalent state. Unfortunately, apart from CD-spectra and the electron absorption spectrum, which is provided in Fig. 9, there are not much data obtainable on the biophysical properties of these enzymes^{116, 117)}.

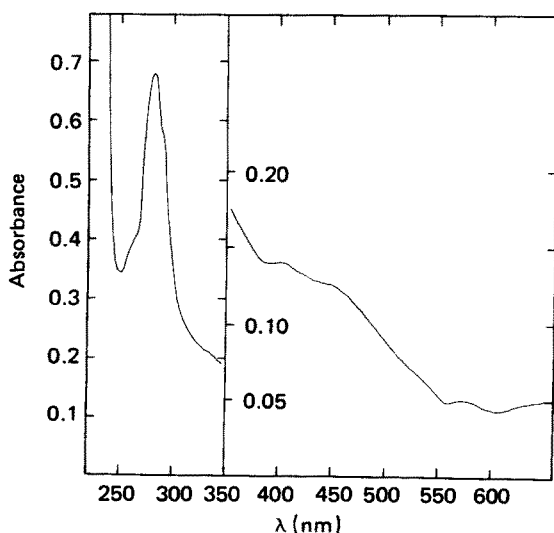


Fig. 9. Electronic absorption spectrum of manganese containing superoxide dismutase from *A. laidlawii*. (With permission from Ref. ¹¹⁶⁾)

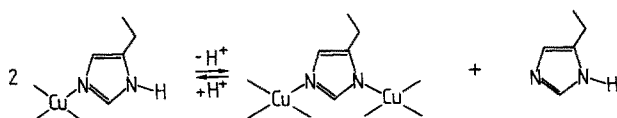
The amino acid sequences of mangano SOD's have been extensively studied ¹¹⁸⁻¹²⁰. The N-terminal residues indicate a high degree of sequence homology between iron and manganese enzymes. Prediction of the secondary structure of the manganese enzymes from the amino acid sequences and comparison with the secondary structure obtained for the iron enzyme reveals that the α -helices and β -strands align quite well.

Most of the current work on manganese superoxide dismutases is limited on purification studies of these unique class of enzymes ^{109-116, 121}. Recently the joint purification of manganese and Cu_2Zn_2 superoxide dismutase from human liver was described ⁴⁵. It would be highly desirable to learn more about the molecular properties of the metal binding sites of these enzymes since manganese proteins other than SOD are not very abundant. In addition, the influence of the chelating protein on the manganese ion leading to an equivalent reactivity compared to copper or iron would be of great interest.

3.4 The Apoproteins

Preliminary studies on the apoproteins of human and bovine erythrocyte Cu_2Zn_2 -superoxide dismutase showed that the purest species are obtained using a gelfiltration column previously equilibrated with EDTA ¹²². Other methods to remove the metal ions are dialysis against cyanide ^{123, 124} or diethyldithiocarbamate ¹²⁵. There are many reports on the preparation of various derivatives including half-apo, zinc free, zinc only, copper only and cobalt enzymes ¹²⁴⁻¹³¹.

Removal of the metals from the holoprotein result in a characteristic bleaching of the chromophore in the UV-absorption spectrum at 259 nm ^{27, 28}. Reconstitution experiments using either Zn(II) or Cu(II) or both disclosed that two different binding sites for copper and zinc are present in the protein moiety ¹³⁰. Furthermore, it was found that zinc neither contributes to the ultraviolet CD-absorption nor to the enzymatic activity. In derivatives in which the Cu-binding sites were occupied by two Cu(II) or both the Cu- and the Zn-binding sites were occupied by two Cu(II) a interaction between Cu(II) in the Zn site and Cu(II) in Cu site was seen, namely an anti-ferromagnetic coupling ¹³¹. A reversible pH-dependent migration of the copper ion from one subunit to the vacant zinc site of another subunit occurs, when the Cu_2E -superoxide dismutase (E = empty) is titrated to pH 10 (Scheme 1) ¹³².



Scheme 1. pH-dependent migration of copper to the vacant zinc-binding site of zinc free bovine erythrocyte superoxide dismutase ¹³²

Titration of $\text{Cu}_2\text{Zn}_2\text{SOD}$ to pH-values below 4.0 a breaking of the bond between the bridging histidine-61 and the zinc-atom is observed because the imidazolate is protonated ¹³³. At high pH-values (pH 8.0) the zinc binding site of Cu_2Zn_2 superoxide dismutase has a preference for binding Cu(II) as imidazole-bridged pair. This requires the deprotonation of histidine-61.

The enzymatic activity of the zinc-free protein is pH-dependent whereas native $\text{Cu}_2\text{Zn}_2\text{SOD}$ is active over a wide pH-range (pH 5.0–9.5)¹³⁴⁾. Cu(II) in the zinc binding site gives little superoxide dismutase activity. This conclusion arises from the observation that $\text{Ag}_2\text{Cu}_2\text{SOD}$ in which copper is in the zinc binding site, has almost no activity¹³⁵⁾ and that the Cu_2Cu_2 enzyme has nearly the same activity as the native protein¹³⁶⁾. Zn-free protein is much less resistant to thermal inactivation than the Cu_2Zn_2 enzyme. Therefore a structural role was assigned to zinc. Furthermore, it was concluded that zinc does not enhance the reactivity of copper.

At low pH the zinc is removed from the protein. $\text{Cu}_2\text{Zn}_2\text{SOD}$ and $\text{Cu}_2\text{E}_2\text{SOD}$ display nearly the same VIS/UV-absorption and EPR-properties at pH 4.0¹³⁶⁾. A similar result is obtained with $\text{Cu}_2\text{Cu}_2\text{SOD}$ and $\text{Cu}_2\text{Co}_2\text{SOD}$ ¹³³⁾. The transitions observed at acidic pH-values, which occur at a similar pH could not be a simple competition of the different metal ions for the protein ligand. A pH-dependent conformational change was therefore deduced. At pH-values below 4.0 the copper binding site is the only strong binding site. Attempts using Cd-113 NMR, electron spin echo spectroscopy and EXAFS of the native enzyme confirm the above mentioned results (see Chapt. 3.1.2)^{70, 72, 75)}.

The apparent binding constant of copper to the apoprotein were investigated with equilibrium dialysis¹³⁷⁾. Four different constants are found. They are pH-dependent. At low pH, two protons compete with copper in the native binding sites. This is not seen at pH 7.0 and above. At alkaline pH-values (pH 10.0) the binding constants are nearly similar. Simultaneous addition of equimolar copper and zinc at pH 5.0 to the apo enzyme results in the formation of an electrophoretically distinct metal-deficient protein species and in the incorporation of copper and zinc in a one-to-one ratio at various concentrations of added metal ions¹³⁸⁾. At low ratios of added equimolar metals, not all of the metal ions expected are bound. This may account for the low yields often obtained in reconstitution studies.

Recently the reaction of diethyldithiocarbamate (DDC) with Cu_2Zn_2 superoxide dismutase was scrutinized¹³⁹⁾. The formation of an enzyme bound Cu(II)-DDC complex was postulated after treatment of SOD with DDC. These results were challenged by a reexamination of the reaction of DDC with Cu_2Zn_2 superoxide dismutase¹⁴⁰⁾. A ternary Cu(II)-DDC-protein complex could not be detected spectroscopically. The copper was completely removed from the protein. Hence, diethyldithiocarbamate is now as ever a good reactant for the preparation of the apoprotein of $\text{Cu}_2\text{Zn}_2\text{SOD}$.

One reason for the poor knowledge on the apoproteins of iron and manganese enzymes are the low binding constants compared to Cu_2Zn_2 superoxide dismutase. Another disadvantage is that very little is known on either active center. One report is dealing with the preparation of a manganese apoenzyme from *B. stearothermophilus* by treatment with EDTA in acidic 8 M urea¹⁴¹⁾. Reconstitution was achieved with Mn, Fe, Co, Ni and Cu. The reconstituted enzymes were indistinguishable from the native enzyme with respect to gelfiltration and polyacrylamide-gel electrophoresis. Only the protein reconstituted with manganese retained its original specific activity.

Another study is available on the metal replacement in iron superoxide dismutase from *P. ovalis*. The apoprotein was prepared by titration to alkaline pH-values¹⁴²⁾. The enzyme was reconstituted using Cr, Cd and Mn-ions¹⁴³⁾. All substituted SOD's had no enzymatic activity. The chiroptical properties, however, were similar to those

of the native enzyme, indicating that the metals may bind to the same site as Fe in the native SOD.

4 Functional Aspects

Three decades elapsed between the first isolation of erythrocuprein and the discovery of a catalytic function for this protein. Attributable to the high interest in the biochemistry of reactive oxygen species, numerous enzymatic assays for superoxide dismutases were developed in the last years. Nevertheless, the original assay of McCord and Fridovich is still currently used for routine purposes²³⁾. The reactivity of superoxide dismutases, namely the reaction:



has been characterized by many biophysical methods. A reasonable structure function model was deduced.

4.1 Assays

In general the assays systems currently used for clinical, technical or laboratory purposes are based on coupled enzymic test systems. Attributable to the many possibilities of interference between the particular components, the results obtained by these assay systems are not always exactly reproducible. For qualitative or half-quantitative determinations they are well suited. Exact quantitative measurements should be carried out using direct assay techniques. The primary difficulty in evaluating SOD activity consists in the free radical nature of the substrate O_2^- . Apart from some exceptions, it can only be supplied by generation within the test medium. Another problem is the detection of the ongoing reaction by either physical methods or indicators.

Table 4. Indirect Assays for Superoxide Dismutases

Generation of Superoxide	Indicator Systems
Xanthine oxidase/xanthine ²³⁾	Reduction of cytochrome c ²³⁾
Electrolytic reduction of O_2 ²³⁾	Reduction of tetranitromethane ²³⁾
Photoreduction of riboflavin ¹⁴⁴⁾	Reduction of nitroblue tetrazoliumchloride ¹⁴⁴⁾
Autoxidation of pyrogallol ^{145, 146)}	Autoxidation of pyrogallol ^{145, 146)}
Autoxidation of catecholamines ^{147, 150)}	Autoxidation of catecholamines ¹⁴⁷⁻¹⁵⁰⁾
NADH oxidation by phenazine methosulfate ¹⁵¹⁾	Autoxidation of sulfite ¹⁵²⁾
	Oxidation of hydroxylamine ¹⁵³⁾
	Peroxidation of dianisidine ¹⁵⁴⁾
	Spin trapping (TMPO, DMPO) ¹⁵⁵⁾
	Oxidation of 2-ethyl-1-hydroxy-2,5,5-trimethyl-3-oxazolidine (Spin generation) ¹⁵⁶⁾
	Chemiluminescence of luminol ¹⁵⁷⁾
	Lactoperoxidase ^{158, 159)}

4.1.1 Indirect Assays

The indirect assays are divided in a system generating the superoxide anion and an indicator reaction. The many sources for O_2^- as well as the indicator systems are listed in Table 4:

Out of multifarious possible test systems three will be described in short. At present these assays are most frequently used.

Cytochrome c Reductase Test

The reduction of ferricytochrome c by superoxide was firstly described by McCord and Fridovich²³⁾. Upon reduction, the extinction of the α -band of cytochrome c at 550 nm is increased. Usually the xanthine oxidase/xanthine system is employed for producing the superoxide anion. Superoxide dismutases compete with cytochrome c for the substrate. The assay is executed in the following way:

The sample in 50 mM potassium phosphate buffer pH 7.8, containing 10^{-4} M EDTA is admixed with 5×10^{-5} M xanthine and 10^{-5} M ferricytochrome c. The reaction is started with 10^{-8} M xanthine oxidase (the values given are end concentrations in the cuvette). The increase of the absorbance at 550 nm is recorded. At minimum three values are necessary to extrapolate the value of 50% inhibition, which is defined as one unit of activity²³⁾. Different values are obtained by dilution of the sample. A/min is plotted versus the concentration of SOD. Alternatively another method can be used. The reagents are mixed and the reduction of cytochrome c is examined after a plateau is reached²⁵⁾. The plateau height is the measure for the enzymatic activity. In this assay system, the addition of catalase is required, because otherwise the reduced cytochrome c is reoxidized by hydrogen peroxide, causing an overestimation of the specific activity.

The range of sensitivity lies approximately between 10^{-10} and 10^{-9} M enzyme. One disadvantage is, that cytochrome c is susceptible to reduction by the many reducing agents in biological tissues (for example glutathione). Therefore cytochrome c reductase assays are only reproducible in purified samples or after dialysis of the homogenate. By the latter procedure low molecular weight reducing agents like ascorbate are removed. In addition, it is advisable to use acetylated or succinylated cytochrome c for the assay, because it is much less susceptible to reductases^{160, 161)}.

For routine work using different buffers or solvents, the cytochrome c assay has one advantage which is not present in other indirect assays. The activity of Cu_2Zn_2 -superoxide dismutase is dependent on the buffers used. For example, it decreases with increasing ionic strength¹⁶²⁾. Like SOD cytochrome c contains lysine residues which facilitate the reaction with anionic reductants¹⁶³⁾. Upon raising the ionic strength, the positive charge of both, the enzyme and the cosubstrate is reduced due to a blocking of the lysine residues by increasing buffer concentrations. Concomitantly, the activity is diminished. Thus, the lysines in both the enzyme and the cosubstrate are affected resulting in an unresponsiveness of the cytochrome c assay for SOD over a wide range of salt or miscible solvent concentrations¹⁶⁴⁾.

Recently, an ultrasensitive cytochrome c reductase test was described¹⁶⁵⁾. At high pH values (pH 10.0) the spontaneous dismutation of O_2^- is diminished. Hence, more superoxide is accumulated by the xanthine oxidase/xanthine reaction at alkaline pH.

If ferricytochrome c is added under these conditions a burst of reduction can be seen at 550 nm. In the presence of superoxide dismutase the burst is diminished. The assay is accomplished in the following manner: Ferricytochrome c is added at zero time and after ten minutes to the reaction mixture containing xanthine oxidase and xanthine. A_{550} (zerotime) is subtracted from A_{550} (10 minutes). Using this test system, SOD in the picomolar range of concentration can be detected.

Nitroblue Tetrazolium-Assay (NBT-Assay)

The reduction of nitroblue tetrazoliumchloride (NBT) by superoxide is a very specific indicator system for the determination of superoxide dismutases ¹⁴⁴⁾. The generation of superoxide may be provided either through the xanthine oxidase/xanthine system or the photoreduction of flavins. The NBT-test is predominantly used for activity staining after gel electrophoresis or isoelectric focusing. It is suitable for purified SOD's as well as crude homogenates. Colourless NBT is converted in the insoluble blue coloured dye formazan after the reduction with superoxide. Superoxide dismutases inhibit the dye formation and appear as colourless zones on the gels. Although a quantitative densitometer test has been described ⁷⁸⁾ the accuracy of this assay is usually not exact enough for precise quantification of SOD. The detection limit is around 2 ng ¹⁶⁶⁾. The insolubility of formazan made the utility for spectrophotometric assays in the cuvette rather limited. However, Fried has reported that gelatine prevents the precipitation of formazan ¹⁵¹⁾.

Activity staining for SOD is carried out in the following way: After electrophoresis the gels are immediately soaked in $2,45 \times 10^{-3}$ M nitroblue tetrazolium for 20 minutes, followed by an immersion for 15 minutes in a solution of 28 mM TEMED (tetramethylethylenediamine) and $2,8 \times 10^{-5}$ riboflavin in 36 mM potassium phosphate pH 7.8. Finally the gels are exposed to an UV-light source and illuminated for 15 minutes. Superoxide dismutase bands appear as colourless zones on the blue gels.

An alternative procedure is described in ^{151, 167)}. 100 mM HEPES (N-(2-hydroxyethyl)piperazine- N'_2 -2-ethanesulphonic acid) pH 7.8, containing 0.25 gelatine, catalase (0.3 U/ml) and 0.6 mg/ml nitroblue tetrazolium are mixed with one eighth of xanthine oxidase and sample, respectively. The reaction is started by the addition of a quarter of 1 mM xanthine solution. The absorption at 540 nm is followed spectrophotometrically until the reaction is completed (usually 5–7 minutes). The plateau height is a measure for the activity. It is plotted versus the concentration of SOD.

Using the photochemical flux of O_2^- for activity staining of gels, one interfering reaction is often overlooked. In the presence of hydrogen peroxide, catalase yields also achromatic bands. Owing to the reactivity of catalase (Eq. (4)) this phenomenon must be seen in the local rise of the pO_2 :



The reduction of NBT by superoxide proceeds via the tetrazoinyl radical ¹⁶⁸⁾:



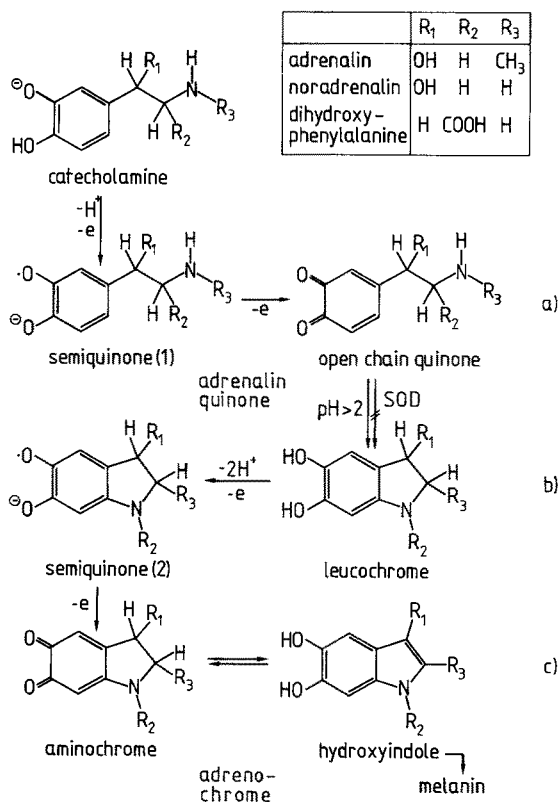
SOD reacts with O_2^- and shifts reaction (5) to the left. Catalase plus H_2O_2 raises pO_2 pushing reaction (5) even more to the left. This phenomenon can be used for a simultaneous activity stain of catalase and superoxide dismutases ¹⁶⁹⁾.

Oxidation of Catecholamines

The oxidation of catecholamines like epinephrine has been widely used as source for superoxide dismutase assays. Upon oxidation the catecholamines are transformed to the coloured product adrenochrome. The rate of oxidation by superoxide is inhibited in the presence of superoxide dismutases²³⁾. Likewise the autoxidation of catecholamines at alkaline pH-values is diminished¹⁴⁷⁾. Intriguingly, low molecular mass copper complexes which display superoxide dismutase activity accelerate the autoxidation¹⁷⁰⁾. Therefore, the interaction between superoxide and catecholamines and its inhibition by SOD is thought not to be a simple chemical reaction¹⁷¹⁾. Recently, this reaction was investigated in more detail¹⁵⁰⁾.

Whilst adrenalin autoxidation is very specifically inhibited by SOD, the reaction with other catecholamines like noradrenalin or dihydroxyphenylalanine, having no free amino group, is much less specific. Only 20 % inhibition by Cu_2Zn_2 superoxide dismutase are observed. The autoxidation reaction itself is very complex (Scheme 2) and still not fully understood.

The catecholamines are oxidized to a semiquinone (a) and cyclized to an indole compound (b). In the case of adrenalin, the reaction is directed by the reduction potentials¹⁷²⁾. It was demonstrated by X-ray photoelectron spectroscopy-, circular dichroism- and EPR-spectroscopy that the cyclization of adrenalinequinone to leuco-



Scheme 2. Autoxidation of Catecholamines

adrenochrome is prevented by the formation of an oxygen-adrenalin-protein-adduct ¹⁵⁰⁾. Concomitantly the active site copper is reduced. The formation of a ternary complex of SOD and adrenaline would plausibly explain why the free amino-group in catecholamines is essential for the assay-system. Thus, this test is not an indirect indicator system for superoxide. It may be seen as a direct measure for the SOD-concentration.

The detection limit of the autoxidation assay is 0.5 nM superoxide dismutase ¹⁵⁰⁾. The oxidation of adrenalin is followed at 480 nm spectrometrically. 850 µl 100 mM carbonate buffer, pH 10 and 100 µl water or sample are mixed. The reaction is started with 50 µl catecholamine stabilized at pH 2. ΔA/min is followed. Due to its convenience, this method can be employed in homogenates and other biological samples ^{149, 173)}. However, the assay can interfere with reduced glutathione, causing an overestimation of SOD ¹⁷⁴⁾. Therefore dialysis prior to determination of enzymatic activity seems appropriate in tissues rich in glutathione.

In general, all these indirect assays are well suited for qualitative or half quantitative measurements. Exact evaluations of the enzymatic activities of superoxide dismutases are better performed using direct assays, though, sometimes erroneous conclusions are possible. The strong point of the latter assays is, that velocity constants and reaction orders can be easily determined.

4.1.2 Direct Assays

The advantage of the very correct values obtained by direct assay systems is usually impaired by the enormous expenditure in the apparative techniques required for these methods. Moreover, a high degree of sample purity is often required. For routine examinations of superoxide dismutases in an ordinary equipped laboratory they are less practicable. A summary of direct assays is provided in Table 5: Many of the direct test systems for SOD are only of theoretical interest. The most frequent two assay systems are discussed below.

Pulse Radiolysis

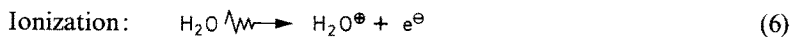
The direct evaluation of the catalytic activity of superoxide dismutases by pulse radiolysis was firstly developed in 1972 ^{181, 182)}. A recent overview is provided by

Table 5. Direct Assays for Superoxide Dismutase

Technique	Specification
EPR	Rapid-freeze EPR ¹⁷⁵⁾ O ₂ ⁻ production with iron-sulfur proteins ¹⁷⁶⁾ Steady state EPR ¹⁷⁷⁾
Potassium superoxide in aprotic solvents	Stopped flow spectrometry ¹⁷⁸⁾ Alkaline solution ¹⁷⁹⁾
NMR	¹⁹ F-NMR spectrometry ¹⁸⁰⁾
Simultaneous generation and determination of superoxide	Pulse radiolysis ^{181, 182)} Flash photolysis ¹⁸³⁾
Electrochemical methods	Opsonised graphite electrode ¹⁸⁴⁾ Polarography ¹⁸⁵⁾

Asmus¹⁸⁶⁾. This method is applicable for the determination of rate constants as well as exact measurements of the kinetic reaction orders. The major disadvantages of this method are, that highly purified samples and solvents (triply distilled water from KMnO_4) are required. In addition, the instrumentation employed is overwhelming.

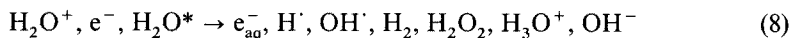
The irradiation of oxygenated aqueous solutions result in the following reactions:



or



The initial products are converted within 10^{-12} sec to the primary radicals¹⁸⁷⁾:



From the O_2 molecule, $\text{O}_2^{\cdot-}$ and HO_2 are formed according to the equations:



In the presence of formate buffers, OH-radicals and H-radicals are converted to $\text{O}_2^{\cdot-}$:



At last, the HO_2 radical is able to dissociate in H^+ and $\text{O}_2^{\cdot-}$. Thus, in formate buffers exclusively $\text{O}_2^{\cdot-}$ is formed¹⁸⁸⁾. Alternatively, OH-radical scavengers like ethanol or other alcohols including t-butanol can be used instead of formate¹⁸²⁾. Usually, this method is less employed because of the lower yield of superoxide.

Irradiation is accomplished by chasing a pulse of high energy electrons (2–4 MeV) through a oxygen saturated aqueous solution. It can be generated by Van de Graaff, linear accelerator or discharge (Febetron) machines. The resulting spectral changes at 245 nm, the absorption maximum of superoxide, are monitored with an oscilloscope. 10^{-6} – 10^{-5} M initial concentrations of $\text{O}_2^{\cdot-}$ are usually produced. From the superoxide decay curves, the reaction order as well as the reaction velocity is estimated.

Pulse radiolysis has met many advantages. The reaction constant can be determined directly and the enzymic activity is linear dependent on the enzyme concentration. The yield of superoxide is extremely high and the method is highly sensitive. The distinction between catalytic and non-catalytic reactions is possible. For example, the reactivity of superoxide dismutase was found to be catalytically and of second order. Rate constants between 1.5 and $2.6 \times 10^9 \text{ M}^{-1}\text{s}^{-1}$ at neutral pH are reported, thus being near the diffusion control^{88, 181, 182, 188–190)}. By way of contrast, caeruloplasmin the copper protein of the blood serum was demonstrated to react only stoichiometrically with superoxide¹⁹¹⁾.

Another advantage of pulse radiolysis lies in the evaluation of the catalytic scavenging of superoxide by low molecular mass complexes. Unlike the polarographic method, another direct superoxide dismutase assay, the reaction parameters of such compounds can be easily obtained.

Polarography

This method has proven to be a powerful tool for routine determinations of superoxide dismutases in nonpurified samples. The dropping mercury electrode acts in an O_2 -saturated aqueous solution as a source of superoxide and a detector of its dismutation as well¹⁸⁵⁾. The electroreduction of molecular oxygen in aqueous solutions is a bielectronic process. In the presence of protons the O_2^- generated in the first step is immediately reduced¹⁹²⁾.



Hydrophobic surfactants such as triphenylphosphinoxide (TPO) are able to cover the electrode surface. The proton transfer to superoxide on the surface is inhibited. This fact is demonstrated in Fig. 10 in which the cell current is plotted versus the potential for reduction of O_2^- :

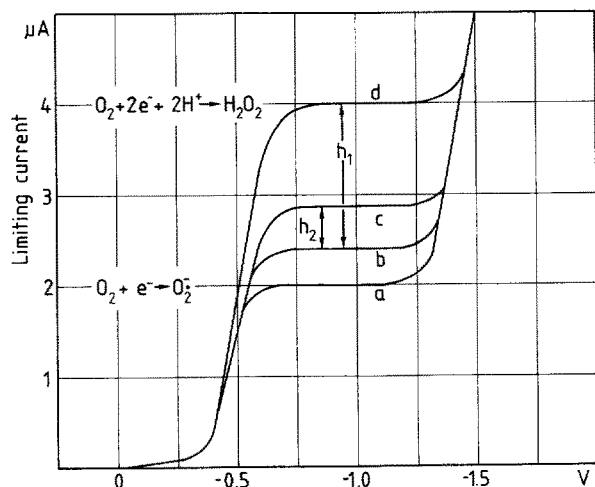


Fig. 10. Polarographic determination of oxygen and its derivatives. The cell current is plotted versus the potential for reduction of O_2 . Curve a) pH 12.5, triphenylphosphinoxide (TPO), 9×10^{-4} M; b) pH 9.9, TPO, 9×10^{-4} M; c) pH 9.9, TPO, 9×10^{-4} M, superoxide dismutase, 1.5×10^{-9} M; d) pH 9.9, the same curve is obtained in the presence of TPO and superoxide dismutase at 10^{-7} M. The value of the limiting current at -1.0 V is proportional to the concentration of dioxygen in the solution. (With permission from Ref. ¹⁸⁵⁾)

Curve a) shows the reduction to O_2^- in the presence of triphenylphosphinoxide, whereas curve d) corresponds to the reduction to H_2O_2 . The addition of superoxide dismutase converts part of the O_2^- to dioxygen which increases the limiting current. By that means, the dropping mercury electrode is at the same time both a source of O_2^- and a detector of its dismutation rate according to:



At pH 9–10 a very high flux of O_2^- is produced (millimolar concentrations). The limiting currents are measured at alkaline pH in the presence and absence of SOD. The calculation of the catalytic constants is simple. Using a rotating disk electrode coated with mercury even at physiological pH -values significant O_2^- fluxes can be generated¹⁹³⁾. Therefore, this method is frequently employed. Polarography is also suitable for the simultaneous determination of superoxide dismutase and catalase in biological tissues¹⁹⁴⁾. For SOD, the detection limit is 2×10^{-11} M.

With nearly all the assay systems described above SOD's carrying different metal ions can be easily discriminated. To distinguish the Cu_2Zn_2 superoxide dismutase from manganese and iron enzymes, cyanide can be added, which selectively inhibits the former enzyme¹⁹⁵⁾. Owing to the fact that iron enzymes are inhibited by H_2O_2 , whereas manganese SOD's are not, these superoxide dismutases can be distinguished from each other¹⁹⁶⁾.

4.1.3 Immunochemical Methods

There are numerous reports on immunochemical reactions of superoxide dismutases with their respective antibodies^{197–199)}. The immunochemical evaluation of SOD is not based on the determination of the enzymic activity. This does, however, not mean that there are no possibilities of interference. For example, quantification studies of erythrocyte Cu_2Zn_2 superoxide dismutase were mainly performed employing immunochemical methods^{20, 22, 42)}. The very early proposal of Mann and Keilin in 1938, that nearly all of the erythrocyte copper is coordinated in "haemocuprein" was later confirmed by immunochemical quantification²⁰⁾. Some years later, only 37% of erythrocyte copper were found in Cu_2Zn_2 superoxide dismutase employing again immunochemical methods^{22, 42)}. Previously in another approach, using chemical and biophysical methods it could be demonstrated that the conclusions drawn in the earlier work were correct³⁰⁾.

This example shows that immunochemical methods are not necessarily highly specific. Cross reactions with immunoprecipitable material or solubilization of antigen complexes can falsify the assay to a considerable extent. Currently more sophisticated techniques bearing a higher specificity than the older methods are employed^{200–204)}. They are used in many laboratories for routine purposes^{34, 204, 205)}. The most reliable and convenient techniques are the radioimmunoassay (RIA)^{200–202, 204)} and the electroimmunoassay (EIA)¹⁶⁶⁾.

Radioimmunoassay

Antibodies against Cu_2Zn_2 superoxide dismutase are prepared from rabbit antiserum. Purified Cu_2Zn_2 SOD is radioiodinated with ^{125}I -labeled p-hydroxyiodophenyl-

propionic acid ²⁰⁶). The principle of the assay is the competition of unlabeled antigen with ¹²⁵I-labeled SOD for a limiting amount of antibody. The displacement of ¹²⁵I-labeled superoxide dismutase by the unlabeled enzyme from the sample is compared with that of known amounts of purified SOD. The different fractions are counted in a gamma counter. Percentage precipitation is calculated based upon maximum and minimum counts per minute (cpm) with controls containing either no competitor and no antibody. The calculation is performed according to the equation:

$$\% \text{ precipitate} = \frac{{}^{125}\text{I} - {}^{125}\text{I} \text{ no antibody}}{{}^{125}\text{I} \text{ no competitor} - {}^{125}\text{I} \text{ no antibody}} \quad (19)$$

A standard curve can be constructed from dilutions of purified superoxide dismutase. The detection limit is 0.1 ng enzyme. The method is practicable in crude homogenates, like extracts of the red blood cell. The work with radioactive tracers, however, has some disadvantages. If the highly sensitive detection limit is not required, the classical electroimmunoassay can be used.

Electroimmunoassay

In an electric field SOD migrates on agarose gels because it has a net charge at physiological pH-values. If antibodies are added, an antigen-antibody complex is formed which precipitates under the appropriate conditions ¹⁶⁶). A rocket-shaped loop is obtained. The area of it is directly proportional to the amount of SOD. The gels can be stained with NBT, because the activity of superoxide dismutase is still present when the enzyme is bound to the antibody. The detection limit is 1 ng. After electrophoresis a calibration curve is produced by plotting the peak heights of the standard versus SOD concentration. A typical example is given in Fig. 11 ¹⁶⁶).

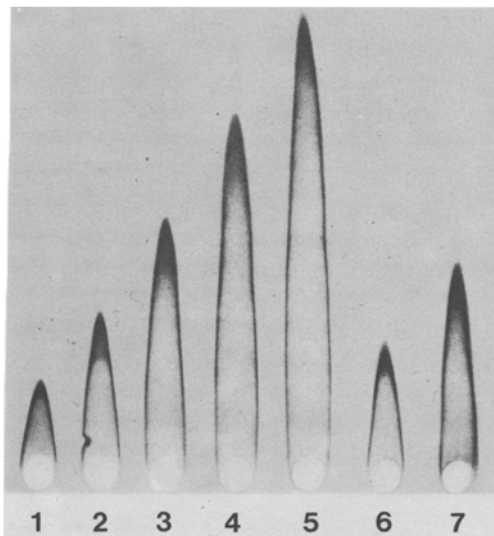
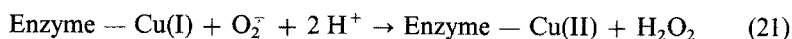
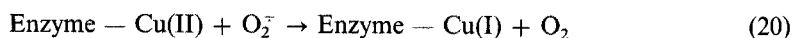


Fig. 11. Electroimmunoassay for human Cu₂Zn₂superoxide dismutase. Electrophoresis was carried out in the presence of antibodies against SOD. Loops 1 to 5: standards; loops 6 and 7 unknown samples. (With permission from Ref. ¹⁶⁶)

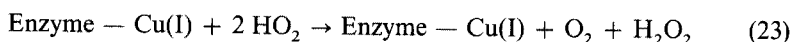
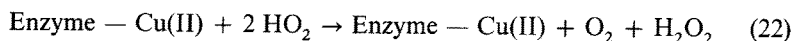
4.2 Mechanism of Action of the Cu₂Zn₂Superoxide Dismutase

The copper ions of Cu₂Zn₂superoxide dismutase display a redox potential of 420 mV²⁰⁷⁾. It is a long known phenomenon that during the catalytic cycle of SOD the copper is alternatively reduced and reoxidated^{188, 190, 208)}. Mainly pulse radiolysis was a powerful tool to elucidate the reactivity of the metals in superoxide dismutase. A pulse of superoxide diminishes the absorption at 680 nm which parallels the decrease of the Cu(II) concentration. If the copper is previously reduced with H₂O₂ a pulse of superoxide increases the absorption at 680 nm, corresponding to a reoxidation of Cu(I) to Cu(II). The overall reaction is a ping-pong mechanism of second order with a velocity-constant of about $2 \times 10^9 \text{ M}^{-1}\text{s}^{-1}$. Rising the viscosity of the solvent results in a decrease of the velocity constant. The reaction is around 10 % of the maximum diffusion controlled limit, calculated from the collision theory, neglecting steric and orientation factors²⁰⁹⁾. This is remarkable, as the catalytic Cu-ion forms only 0.1 % of the enzyme's molecular surface. The superoxide dismutase reaction can be summarized as follows:



The proton involved in the transition state must come from a source near the active site, because ²H₂O does not reduce the rate constant⁸⁹⁾. However, there are contradicting reports concerning the proton source. In one report it was suggested, that the proton stems from coordinated water molecules near the active site²¹⁰⁾. Other authors favoured the bridging imidazolate as proton source^{89, 211)}. This judgement seems to be very likely, as the Cu-facing nitrogen of the imidazolate bridge is rapidly protonated and deprotonated during catalysis.

In another approach using γ -irradiation as O₂⁻ source and EPR as its detector a loose complex Enzyme-Cu(II) \cdots HO₂ was postulated²¹²⁾. The O₂⁻ radical is relatively stable below 250 °K in aqueous solution or ice, respectively. Therefore, employing low temperature EPR (77 °K) superoxide can easily be detected after γ -irradiation. Subsequent annealing to 200 °K results in a slow decay of the superoxide anion. The decay of the loose complex was postulated to proceed without changes in the oxidation state of copper. The observed delay in the changes of the oxidation state of copper was attributed to a reaction of copper with the reaction products of the dismutation. A reaction mechanism different from that obtained by pulse radiolysis was proposed²¹³⁾. A transient state reaction of two HO₂ with the native enzyme (eq. 22) and the reduced enzyme (eq. 23) was thought to be responsible for the dismutation of the superoxide anion:



The reduced enzyme is not generated by the reaction cycle, but by a late reduction of copper with hydrogen peroxide, one of the reaction products.

In the current literature the pulse radiolytic oxidation-reduction cycle is preferred. As a consequence, a steady state level of 50 % reduced copper should be present during catalysis. Intriguingly, only 25 % of the copper was found to be reduced during steady state. Recently it was demonstrated, that the steady state level of oxidized copper is actually 50 % but can change to 75 % in previously lyophilized samples ²¹⁴⁾.

Another source of controversy has been the interaction of copper and zinc through the bridging imidazolate. In an older report, the interaction of the metals was disputed using ¹¹³Cadmium NMR ²¹⁵⁾. In more recent work, however, the interaction was regarded as to be necessary for the catalytic action ⁷⁰⁾. This conforms the currently accepted opinion, that the protonation of the imidazolate nitrogen is an important step in the catalytic cycle.

4.2.1 Electrostatic Facilitation

Cu₂Zn₂superoxide dismutase has approximately 150 times the surface area of aquated Cu(II). Random collisions of superoxide with the protein would be mostly fruitless, if not dangerous. Koppenol has suggested, that an overall negative charge on the surface of the protein, coupled with a cluster of cationic groups at the active site, may provide electrostatic guidance to the incoming O₂⁻, maximizing the percentage of fruitful collisions at the active site ²¹⁶⁾. Actually the isoelectric point of bovine SOD lies between pH 4.9 and 5.1 ^{31, 34)}. Therefore at physiologic pH-values Cu₂Zn₂superoxide dismutase has a net negative charge.

From this fact, it might be predicted that the reactivity with a negatively charged substrate such as superoxide would be enhanced by an increase in the ionic strength due to a screening of the charges on the protein. In fact, precisely the opposite is observed. It is a long known phenomenon that Cu₂Zn₂SOD is very susceptible to anion binding ^{71, 128, 217, 218)}. Binding of small anions to positively charged groups in or near the active center of the enzyme was very helpful in elucidating the catalytic mechanism of Cu₂Zn₂superoxide dismutase (see also Chapt. 3.1.2).

Azide and cyanide, which are inhibitors coordinate to the catalytically active copper, replacing the bound water molecule ²¹⁸⁾. The bridging imidazolate group remains unaffected ⁷²⁾. In contrast thiocyanate binds to the copper without inhibiting the enzyme ²¹⁹⁾. It is thought to displace a histidine ligand from the copper. Using Cu₂Cu₂-SOD containing copper in both, the copper and the zinc site, a cleavage of the imidazolate bridge between the copper is seen after addition of thiocyanate ²²⁰⁾. Furthermore, the aspartic acid ligand in the zinc site is replaced. As the SCN⁻ complex of the Cu₂Cu₂ enzyme is catalytically active, there is some evidence that the imidazolate bridge is not necessarily essential to the catalytic cycle of the native Cu₂Zn₂SOD.

After prolonged exposure of cyanate with Cu₂Zn₂superoxide dismutase a time dependent carbamylation of the lysine residues is observed ²²¹⁾. Carbamoylated SOD is less active than the native enzyme, but the extent of this inactivation is much less in buffers of low ionic strength ²²²⁾. This corroborates the electrostatic interactions between superoxide and the active center. However, surface charges on the enzyme are also thought to play a role in the catalytic activity. Some metals bind to Cu₂Zn₂superoxide dismutase leaving the enzymic activity unaffected. Ca(II) and Tb(III) bind to specific binding sites producing slight conformational changes of the protein ²²³⁾.

As the activity of $\text{Cu}_2\text{Zn}_2\text{SOD}$ decreases with increasing ionic strength it was attempted to modify the charges in the active site by covalent blocking of the amino acid residues involved in this interaction. Modification of lysine residues by acetylation or succinylation invert the ionic strength effect, whereas modification of arginine with phenylglyoxal does not¹⁶²⁾. However, it should be kept in mind that blocking of both, arginine and lysine causes a 90 % loss of activity. The responsiveness of lysine-modified Cu_2Zn_2 superoxide dismutase to ionic strength effects allows the conclusion, that the interaction of O_2^- with the anionic enzyme is assisted by a electrostatic guidance of positively charged lysine residues near the active center. Arginine at the active site seems to be much less affected by high anion concentrations, but raising the pH, which results in an elimination of the charge on the ϵ -amino group suppresses the catalytic activity. Chemical modification with phenylglyoxal of both, arg-141 of the bovine²²⁴⁾ and arg-143 of the yeast enzyme²²⁵⁾ which are in close proximity to the copper-site but not intimately associated with the metal, results in a nearly total loss of activity. After modification the anion binding capacity of arginine is drastically reduced²²⁶⁾. Visible absorption and EPR spectra are consistent with a shift toward a more axial coordination geometry. This may reflect the displacement of one of the histidyl imidazoles.

In contrast, modification of lysines by either succinylation or carbamoylation, leave the native rhombic geometry of the copper site unaffected. It was, therefore, concluded, that "pure" electrostatic interactions i.e. a decreased positive charge are responsible for the enzyme inactivation after blocking lysine residues²²⁷⁾. Similar effects are observed treating bovine or yeast Cu_2Zn_2 superoxide dismutases with hydrogen peroxide (see also Chapt. 3.1.4 and⁸⁸⁻⁹⁰⁾. It was found with yeast Cu_2Zn_2 -superoxide dismutase that the rate constant for inactivation decreases progressively raising the pH from 9.0 to 11.5. The reactive species is thought to be not H_2O_2 , but rather the HO_2^- anion. The essential arginine residue with a pK_a of approx. 12 is partially deprotonated at these pH-values. Therefore, the affinity for the HO_2^- anion is decreased at elevated pH.

Phosphate anions too can influence the properties of Cu_2Zn_2 superoxide dismutases^{71, 162, 220, 228, 229)}. The activity of bovine SOD in HEPES-buffer is decreased by 50 % when 10 mM phosphate is added²³⁰⁾. If arg-141 was modified with phenylglyoxal only a small decrease of the residual activity is seen after addition of phosphate. Phosphate also causes a reduced affinity of binding of azide and cyanide ions to the native superoxide dismutase. It was assumed that phosphate neutralizes the positive charge on the side chain of arg-141.

Contrary to porcine Cu_2Zn_2 superoxide dismutase the bovine enzyme is pH-independent over a wide pH-range¹⁸²⁾. Porcine SOD has an unusually high isoelectric point (6.8)²³¹⁾. Upon titration from pH 7.5 to pH 12.0 an almost linear decrease of activity is seen with increasing pH, while EPR- and NMR-parameters do not parallel this phenomenon²³²⁾. Using EPR- and NMR-spectroscopy only a pH-dependence above pH 9.5 was detected with the native enzyme. Elimination of lysine charges by succinylation abolishes the pH-dependence of activity and overlap the parameters of spectroscopy. Unlike the bovine enzyme, porcine SOD contains two more lysines per monomer. Thus, some additional positive charges may play a critical role in the rate determining step of the mechanism of that species of Cu_2Zn_2 superoxide dismutase.

These more chemical investigations were complemented by the biophysical studies and X-ray cristallographic analyses^{60, 233)}. A precise knowledge on the catalytic activity of the metal ions as well as the environment near the active site mainly of the bovine enzyme is now available.

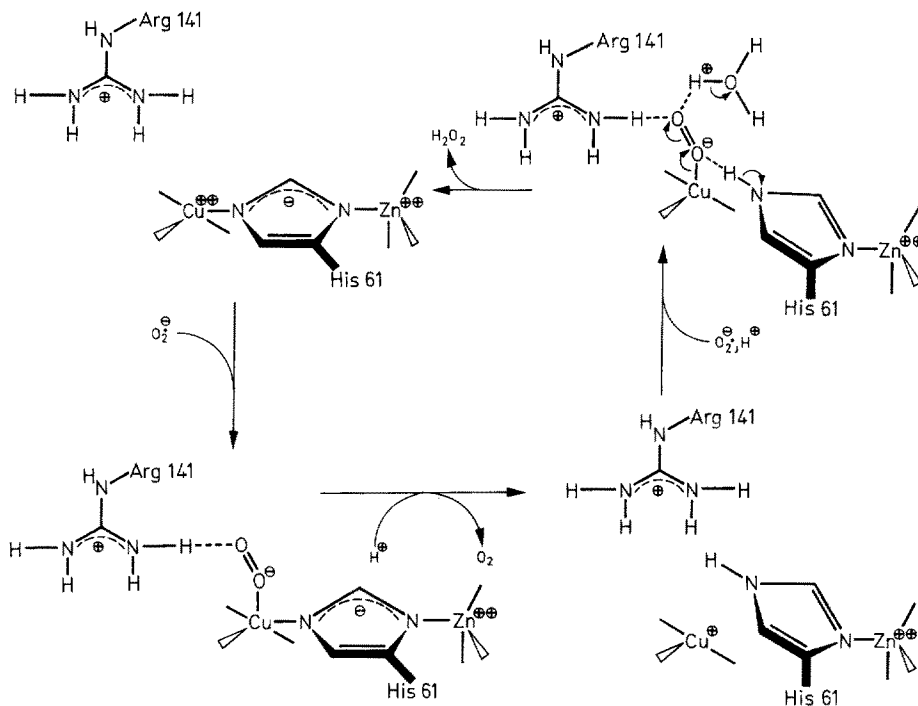


Fig. 12. Schematic drawing of the catalytic mechanism of Cu₂Zn₂superoxide dismutase. The superoxide displaces the axial water molecule at the Cu(II) and reduces the copper to Cu(I). Concomitantly the bond from Cu to His 61 is broken and O₂ is released. The Cu-facing nitrogen of His 61 becomes protonated and a second O₂⁻ becomes bound. An electron is transferred from Cu(I), coupled with a proton transfer from His 61. After addition of a second proton from an active-site water, the uncharged hydrogen peroxide is released. (With permission from Ref. ²³³⁾)

The catalytic cycle starts with the replacement of a water molecule at the axial position by superoxide (Fig. 12).

One oxygen binds to Cu(II), the other one is hydrogen bonded to the guanidinium group of arginine-141. Cu(II) is thereby reduced to Cu(I), breaking the bond to histidine-61. Oxygen is released and the imidazolate of histidine-61 is protonated. The hydrogen atom is delivered by the solvent. Zinc, which is bound to the other nitrogen of the bridging imidazolate, raises the pK_a of the unligated nitrogen to 13. Hence, at pH 7.0 it is protonated.

Although zinc seems to enhance the reactivity by this mechanism it is not essential for the reactivity of SOD, because at pH 7 the imidazolate nitrogen without zinc will be at least partially protonated. This would comprehensively explain, why in contrast

to the native $\text{Cu}_2\text{Zn}_2\text{SOD}$ the activity of $\text{Cu}_2\text{E}_2\text{SOD}$ is much more susceptible to varying pH-ranges^{134, 182)}.

When oxygen has been released from the copper, the second superoxide anion binds to Cu(I) . One oxygen atom forms a hydrogen bond to the protonated imidazolate of histidine-61. As in the first reaction cycle the other oxygen is hydrogen bonded to the guanidinium of arginine residue-141. One electron from copper is transferred to O_2^- and the proton from histidine-61 is bound to oxygen. An intermediate copper-hydroperoxide complex is formed which is protonated by a water molecule bound in the active site. Then the uncharged hydrogen peroxide molecule is released. The overall catalytic cycle is accompanied by shifts and rotations in the coordination sphere of both metals. The movements are less than 1 \AA ²³³⁾.

The active funnel of superoxide dismutases contains at least three positively charged amino acid residues (lys-120, lys-134 and arg-141) which are in close proximity to Cu(II) . They are essential for the enzyme's function and provide a guidance of the negatively charged superoxide anion to the Cu(II) . This is the reason why the overall negatively charged superoxide dismutase molecule with its positively charged substrate funnel is as active as low molecular mass copper complexes. This fact is remarkable as the surface of the enzyme is 150 times larger than that of the aquated copper ion. The question remains why the organism spares no efforts to remove the superoxide anion and why it does not use simple low molecular mass copper complexes for this purpose. A separate discussion is included in the last chapters.

It was of further interest, whether or not cooperative interactions occur between the two subunits of Cu_2Zn_2 superoxide dismutase during catalysis. Contrary to all other SOD's, the enzyme of wheat germ is dissociated in the presence of 4% sodium dodecylsulphate²³⁴⁾. This reagent does not affect the activity of $\text{Cu}_2\text{Zn}_2\text{SOD}$'s of dimeric structure, however, the wheat germ enzyme is reversibly inactivated. Until recently, no conditions were found to dissociate the bovine enzyme, and, at the same time maintaining the native state. Previously, it was reported that extensive succinylation of bovine Cu_2Zn_2 superoxide dismutase leads to the dissociation of the dimeric protein²³⁵⁾. Unfortunately the catalytic activity is lost by 90% after succinylation. Although, the active site as probed by EPR seems to be unaffected, the question whether there are subunit interactions or not is still open to discussion.

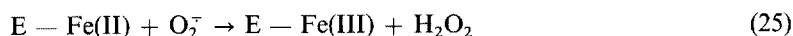
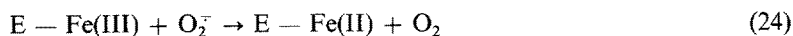
Replacement of the catalytically active copper by other metals results in an inactive enzyme^{135, 236)}. There is, however, strong evidence from a newer pulse radiolytic study of Co(II) derivatives of bovine SOD, that this opinion must be repudiated. Co, Zn and Co,Co-proteins display considerable enzymic activity having turnover rate constants of $4.8 \times 10^6 \text{ dm}^3 \times \text{s}^{-1} \times \text{mol}^{-1}$ and $3.1 \times 10^6 \text{ dm}^3 \times \text{s}^{-1} \times \text{mol}^{-1}$, respectively²³⁷⁾. Although these values are three orders of magnitude lower than those of native SOD a similar pH-independence in the range from pH 7.4–9.4 was seen. It was proposed, that the reaction may proceed through a ping pong mechanism as in the Cu_2Zn_2 superoxide dismutase (see above) or by a Co(II) -superoxy or Co(III) -peroxy intermediate. Further data are required for a definite solution of this problem.

4.2.2 Catalytic Activity of the Manganese and Iron Enzymes

Due to the uncomplete knowledge of the active centers of iron and manganese superoxide dismutases, only limited informations of the catalytic activities are available. It was demonstrated with nuclear magnetic relaxation techniques that the iron

containing SOD from *E. coli* contains at least one water molecule associated with the Fe(III)^{238, 239}. Anion binding studies revealed a discrepancy between the affinity of the iron for F⁻ and N₃⁻ and the inhibition of the catalytic activity by these anions^{101, 240}. Examination of the pH-dependence showed that the dissoziation constant of azide is influenced by a ionizing group near the iron having a pK_a of 8.7. The coordination of this anion to Fe(III) is thought to be preceded by an association with a non-chromophoric site on the protein which was termed "anion binding pocket".

In contrast to bovine Cu₂Zn₂- and iron superoxide dismutase from *P. leiognathi*, the iron enzyme from *E. coli* exhibits saturation kinetics during catalytic action²⁴¹. A group which ionizes with a pK_a = 8.8 was found to be responsible for this phenomenon. For the dismutation of superoxide by iron SOD's a reaction scheme is proposed which includes alternate reduction-oxidation of the metal:



This catalytic scheme is very similar to that of Cu₂Zn₂superoxide dismutases. The iron enzymes from *E. coli*, *A. vinelandii* and *P. ovalis* display redox potentials of 0.27 V²⁴⁷. In contrast to the other SOD's, the reduction potentials of Fe-proteins decrease when the pH is raised from pH 6.0 to 9.0. It was assumed that the reduction of Fe(III) causes a proton to be bound below pH 9.0, which is not observed above this pH-value.

Both, iron-containing and mangano superoxide dismutases bear a net negative charge at physiological pH-values. The enzymes from *E. coli* are less active with increasing ionic strength²⁴³. Acetylation of the lysine residues invert these effects. Therefore, a cationic group near the active site must be involved in the electrostatically facilitated catalysis. This observation parallels the ionic strength effects seen with Cu₂Zn₂superoxide dismutases (see Chapt. 4.2.1).

As the iron enzyme from *E. coli*, the manganese containing SOD from *P. denitrificans* shows saturation kinetics above O₂⁻-concentrations of 10⁻⁴ M²⁴⁴. It seems very likely that charge effects may play a role in an electrostatic guidance of the superoxide. The dismutation of superoxide to oxygen and hydrogen peroxide is not exclusively provided by superoxide dismutases. Although there is no direct catalysis, a very high rate of self-dismutation is observed in biological systems (approx. 10⁷ Mol⁻¹ × sec⁻¹). Furthermore, there are a lot of low molecular mass transition metal complexes which are described in the next section and which are highly SOD active.

4.3 Low Molecular Weight Compounds Mimicking Superoxide Dismutase Activity

It was intriguing to note significant higher rate constants of the catalytic dismutation of superoxide when native SOD was replaced by simple inorganic copper salts^{181, 189}. However, this phenomenon is only observed in acidic media and in the absence of perturbing chelating agents. At neutral pH-values, considerable superoxide dismutase activities of some low molecular weight Cu(II)-amino acid complexes were

demonstrated using the cytochrome c assay²⁴⁵). Subsequent pulse radiolytic measurements revealed, that the rate constants were half to those of the native $\text{Cu}_2\text{Zn}_2\text{SOD}$. $\text{Cu}(\text{Tyr})_2$ displays nearly the same reaction rate as superoxide dismutase^{3, 246}). Similar results are obtained using $\text{Cu}(\text{II})$ salicylates^{247, 248}). The highest rate constant is measured for $\text{Cu}(\text{II})$ formate ($2.7 \times 10^9 \text{ Mol}^{-1} \times \text{sec}^{-1}$). This compound is formed in formate buffers normally used in pulse radiolysis.

Using the nitroblue tetrazolium assay, $\text{Cu}(\text{tyr})_2$ and $\text{Cu}(\text{lys})_2$ also show a remarkable SOD-activity¹⁶⁷). However, the rate constants are three orders of magnitude lower than those calculated from the data of pulse radiolytic measurements. Intriguingly, adrenochrome formation, which is used as an indicator of superoxide is accelerated by low molecular mass copper chelates^{23, 147, 170}). The inhibition of adrenochrome formation by SOD was therefore ascribed to a complexation of catecholamines with Cu_2Zn_2 superoxide dismutase (see¹⁵⁰) and Chapt. 4.1.1).

The antiinflammatory drugs indomethacin (1-(p-chlorobenzoyl)-5-methoxy-2-methyl-indole acetate) and lonazolac (3-p-chlorophenyl)-1-phenyl-pyrazole-4-acetate) form thermodynamically stable copper complexes in aprotic solutions, which are highly superoxide dismutase active^{249, 250}). An example for the structure of these acetate like copper complexes is given in Fig. 13:

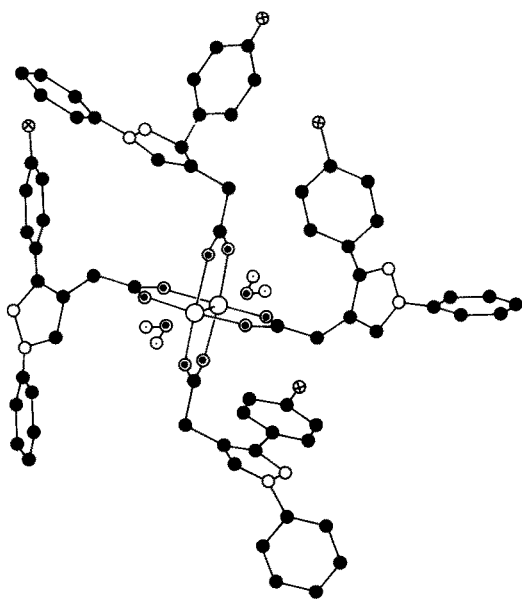


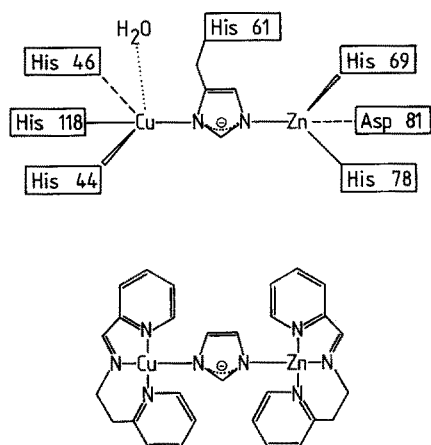
Fig. 13. Structure of $\text{Cu}_2(\text{lonazolac})_4$. The hydrogen atoms are deleted. The copper-copper distance is very close to that of metallic copper

Surprisingly, in such complexes, the copper-copper distance (263 pm) is very close to that of metallic copper¹⁴⁹). A spin-spin interaction, namely an antiferromagnetic coupling of the copper is observed. Two coordination sites in the copper-copper axis can be readily replaced by superoxide. For $\text{Cu}_2(\text{indomethacin})_4$ a second-order rate

constant of $6.0 \times 10^9 \text{ Mol}^{-1} \times \text{sec}^{-1}$ was found in lipophilic media (DMSO/water). This is the fastest constant ever observed for a copper-dependent dismutation of superoxide.

In aqueous systems proteins compete with the lipophilic complex ligands for the copper. Bovine serum albumin forms ternary complexes with $\text{Cu}_2(\text{lonazolac})_4$ ²⁵⁰⁾. An EPR-signal of the biuret-type is observed. Therefore in blood serum these complexes are only existing in very low concentrations. Many acetate-like copper chelators like salicylate are used as non-steroidal antiinflammatory drugs (for a review see²⁵¹⁾). They are potent inhibitors of lipid peroxidation^{249, 250)}. In biological tissues, these lipophilic ligands are able to coordinate copper in the aprotic regions of the cell (membranes), being lipophilic superoxide dismutases.

Macrocyclic polyamine complexes of Cu(II) and Ni(II) too can eliminate the superoxide anion catalytically²⁵²⁾. They are 10^7 -times more stable than Cu(II)-glycine at neutral pH-values²⁵³⁾. Unfortunately, they do not survive EDTA treatment, but they are very useful for Cu_2Zn_2 superoxide dismutase model chemistry. Thio-cyanate disrupts the magnetic coupling between the copper-pairs in the copperhexaazacyclotetracosane-complex, resulting in a cleavage of the imidazolate bridge²⁵⁴⁾. A similar behaviour is seen with the $\text{Cu}_2\text{Cu}_2\text{SOD}$ ²¹⁹⁾. Another approach was the synthesis of binuclear imidazole-bridged copper and zinc complexes (Scheme 3)²⁵⁵⁾:



Scheme 3. Active site of Cu_2Zn_2 superoxide dismutase and $[\text{Cu}(\text{pip})(\text{im})\text{Zn}(\text{pip})](\text{NO}_3)_3 \cdot 2 \text{H}_2\text{O}$ as a model for $\text{Cu}_2\text{Zn}_2\text{SOD}$ ²⁵¹⁾

The electron absorption profiles and the EPR properties were of striking similarity with those of the copper chromophore of the native enzyme. X-ray photoelectron spectroscopy of the oxidized or the reduced model complex revealed the existence of 3 d^9 Cu(II) and 3 d^{10} Cu(I). By way of contrast, the $2p_{3/2}$ binding energy of copper in $\text{Cu}_2\text{Zn}_2\text{SOD}$ remained constant. A rate constant of $3.8 \times 10^8 \text{ Mol}^{-1} \times \text{sec}^{-1}$ is obtained for the model complex using radiolysis. Four coordinated copper in bis cyclo(histidylhistidine) copper(II) complexes have catalytic activities in the same range²⁵⁶⁾. The catalytic activity of copper-histidyl complexes is, however, strongly dependent on the nature of the ligand. Dipeptide complexes of His-X-Cu(II), where X is phenylalanine, alanine, valine or tyrosine display relatively high superoxide dismutase activity, whereas X-His-Cu(II) complexes are relatively inactive²⁵⁷⁾.

Penicillamine is apotent chelator for copper which forms even *in vivo* very stable copper complexes²⁵⁸⁾. In contrast to all other complexes described above, copper penicillamine is resistant to EDTA and cyanide treatment. A considerable superoxide dismutase activity of the $(\text{Cu(II)}_6\text{Cu(I)}_8\text{-(D-penicillamine)}_{12}\text{Cl})^{-5}$ -complex was found employing indirect and direct assay systems²⁵⁹⁻²⁶¹⁾. These observations were challenged as no activity was found employing freshly prepared Cu-penicillamine²⁶²⁾. After aging of the complex the activity reappeared. In detailed reexamination a time dependent disintegration of the complex, especially in the light, could be demonstrated, resulting in a marked increase of EDTA-sensitive activity²⁶³⁾. Upon gel chromatography of aged samples, the original low inhibitory activity was restored. All EDTA-sensitive inhibitory activity was found in a clearly separated low M_r copper containing fraction. Concomitantly all chiroptical properties of the native complex are completely leveled off. The disintegration is markedly enhanced during irradiation with photons. Wavelengths between 420 and 435 nm in the region of the broad absorption band of the native Cu-penicillamine were most active. Due to the identical electronic absorption profile of both, the decomposition product and Cu(II)-D-penicillamine disulphide, the latter complex was assigned to be the unknown low superoxide dismutase active M_r copper-compound.

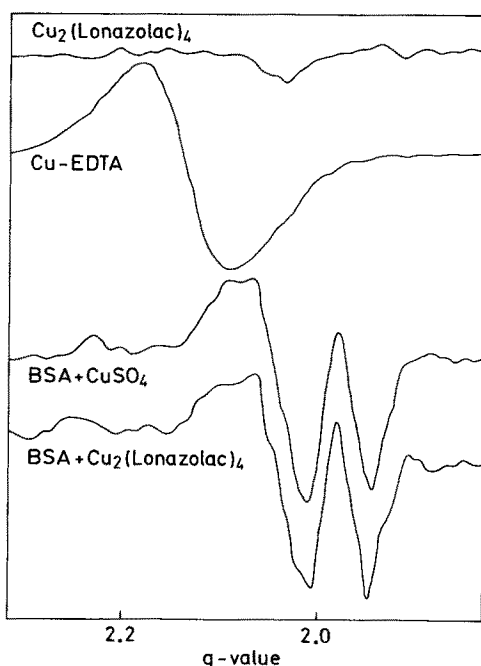


Fig. 14. Electron paramagnetic resonance spectra of low molecular mass copper complexes in the presence and in the absence of bovine serum albumin (BSA). All four copper concentrations are identical. Cu-EDTA served as standard. $\text{Cu}_2(\text{lonazolac})_4$ displays no EPR-signal due the antiferromagnetic coupling of the two copper-centers. After addition of BSA, a signal of the biuret-type is obtained, indicating that the original complex was disrupted. A similar signal is seen after addition of CuSO_4 to BSA

Concerning the catalytic superoxide dismutase activity of low molecular mass copper complexes, some general comments are necessary. Firstly, it should be emphasized, that apart from the inactive Cu-penicillamine, all complexes described above do not survive high concentrations of biological chelators in aqueous solutions. For example, bovine serum albumine is able to remove most of the copper from these complexes (Fig. 14).

However, it should be kept in mind, that these reactions are dependent on the equilibrium constants and thus, on the respective concentrations of either ligands. The coordinated copper is known to remain kinetically labile even in naturally occurring Cu-proteins. Although it may be below the usual detection limit, it could not be excluded, that a pool of low M_r copper complexes do exist in living organisms.

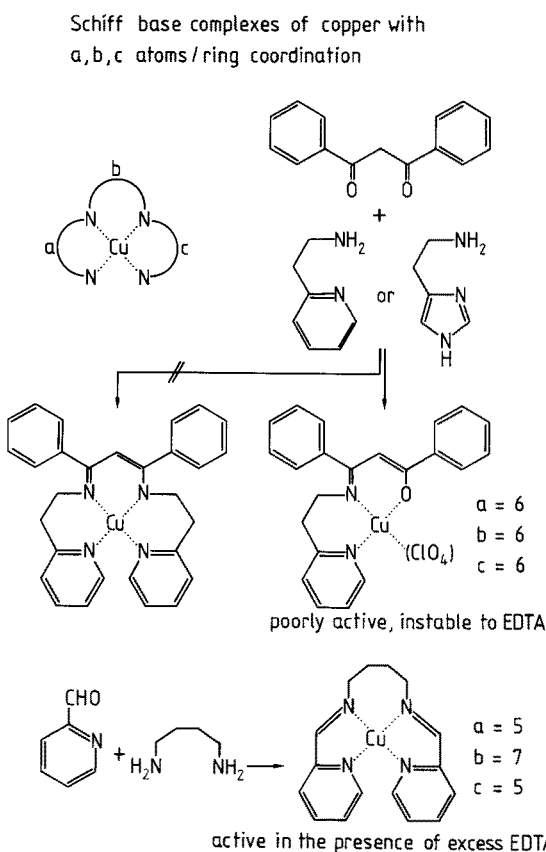
Secondly, nearly all complexes described above are highly lipophilic. In aqueous solutions they are very poorly soluble. In such aqueous compartments of the cells, scavenging of superoxide is provided by the cytosolic manganese, iron and Cu_2Zn_2 -enzymes, which are hydrophilic. As superoxide is a radical species, its dismutation requires little or no activation energy. Thus, it is not surprising that a large biopolymer is not required for this process. The spontaneous dismutation rate of O_2^- in biological fluids is assumed to be $10^7 \text{ Mol}^{-1} \times \text{sec}^{-1}$. Regardless of which copper chelator is employed, SOD-active low molecular mass copper complexes display rate constants of about $10^9 \text{ Mol}^{-1} \times \text{sec}^{-1}$ and even higher in aprotic solvents. No significant reports on membrane bound superoxide dismutases are known. Lipophilic membranes are extremely good solvents for both, superoxide and the highly lipophilic acetate like antiinflammatory drugs like salicylate. If there would be no possibility for scavenging superoxide in the membrane, it would be predominantly found in these regions of the cell, due to its dramatically enhanced half life in aprotic solvents and its lipophilic character. It was, therefore, proposed, that the antiinflammatory drugs trap the "free" copper mentioned before, forming artificial superoxide dismutases in the membranes and preventing the lipids from damaging effects of reactive oxygen species.

Recently, the superoxide dismutase activity of low molecular mass copper chelates in the indirect coupled assay systems has been disputed²⁶⁴⁾. It was demonstrated that copper in CuSO_4 and Cu(II)(gly)_2 prevents the ferricytochrome c and nitroblue tetrazolium reduction. This is not virtually new, as it is a well known phenomenon that Cu(II)-salts lead to a reoxidation of ferrocytochrome c and that they are potent inhibitors of xanthine oxidase²⁶⁵⁾, which is often used as O_2^- -generator in indirect SOD assay systems²³⁾. Although the indirect assays may be sometimes inadequate for the measurement of the SOD-activity, there are no doubts that low molecular mass copper chelates have their superoxide dismutase during pulse radiolysis.

The therapeutical use of Cu_2Zn_2 superoxide dismutase as scavenger for the potentially toxic superoxide anion is limited on very special events²⁶⁶⁾. The half-time of circulation in the organism is very short and it is unable to pass cellular membranes. As a consequence it was attempted to search for lipophilic substances, able to catalyze the dismutation of superoxide, but resistant to biological chelators. One approach was the use of different metalloporphyrins. Some iron and manganese prophyrins catalyze the dismutation of superoxide with about 3 % efficiency of native Cu_2Zn_2 -SOD^{267, 268)}. Apart from copper porphyrins, which are inactive as superoxide dismutases, no copper complexes have been described which are at the same time scavengers of superoxide and stable to proteins or EDTA.

In a completely different theoretical approach, it was attempted to construct a complex ligand for copper, ideally suited as an *in vivo* superoxide dismutase model. Three conditions had to be fulfilled. Firstly, the copper had to be four coordinate with a square planar arrangement, because a free fifth or sixth coordination site is essential for SOD activity. Secondly, during the catalytic cycle the twisting of the ligands should be possible due to a change from planar to tetrahedral coordination of Cu(I). Finally, the complex must survive biological chelators. Schiff-bases seemed to meet all these requirements and indeed, one Schiff-base complex was synthesized forming 5,7,5-rings with copper, which was active in the presence of EDTA (Linß, M., Weser, U.: to be published) (Scheme 4):

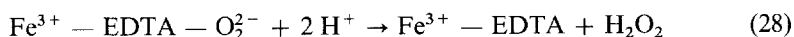
It should be pointed out, that Cu-EDTA alone has no SOD-activity. As mentioned before, copper porphyrins and $\text{Cu(II)}_6\text{Cu(I)}_8(\text{D-penicillamine})_{12}\text{Cl}^{5-}$ which are also stable to EDTA are inactive. Provided that they are not toxic, the Schiff-base-copper



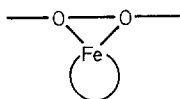
Scheme 4. Schiff-base superoxide dismutase models surviving biological chelators. Upper section: Dibenzoylmethane does not readily react with 2-(2-aminoethyl)-pyridine due to a keto-enol tautomerism. Therefore only poorly active and instable complexes are obtained. In contrast, 2-pyridine-aldehyde and putrescine yield a highly active and stable copper-complex

complexes could possibly act as lipophilic superoxide dismutases in biological tissues, thus preventing lipids from peroxidation.

Ferric ions and Fe(III)-EDTA generate toxic radicals ²⁶⁹⁾. Intriguingly, iron-EDTA is at the same time active as superoxide dismutase with a 0.01 % efficiency as SOD, as judged from the NBT or cytochrome c assay ²⁷⁰⁾. In subsequent reports, the decay of O_2^- was directly observed in a stopped flow instrument and it was concluded, that iron-EDTA catalyzes the dismutation of O_2^- as 0.1 % efficient as superoxide dismutase ^{271, 272)}. Some years later, the SOD-activity of iron-EDTA was emphasized to be a putative one ²⁷³⁾. The activity was attributed to an interference of iron-EDTA with the assay mixture. More recently, the SOD-activity of iron-EDTA was confirmed, using pulse radiolysis ²⁷⁴⁾. Fe(III)-EDTA chelates react with the superoxide radical at physiological pH-values, but the reaction constant is lower at alkaline pH. The reaction proceeds according to the following equations:



The formation of a peroxo complex (Eq. 27) was firstly described by Ilan and Czapski ²⁷²⁾ and confirmed by other authors ²⁷¹⁾. This reaction is very fast and largely independent of the pH. In contrast, the reduction step (Eq. 26) is much slower. However, at sufficiently high O_2^- -concentrations, the breakdown of the peroxo complex becomes rate limiting ²⁷⁵⁾. The structure of the complex is thought to be cyclic:



This structure is also proposed for the peroxide compounds of diperoxy molybdenum-(VI)- porphyrins ²⁷⁶⁾, titanium(IV)porphyrins ²⁷⁷⁾ and Fe(II)-tetraphenylporphyrins ²⁷⁸⁾.

Iron salts and iron-EDTA also catalyze the generation of highly reactive radicals from superoxide ²⁶⁹⁾. Thus, low M_r ferric iron and superoxide are often termed to be deleterious to the cell. This problem is leading to the last section of this article, namely the biological significance of the dismutation of superoxide.

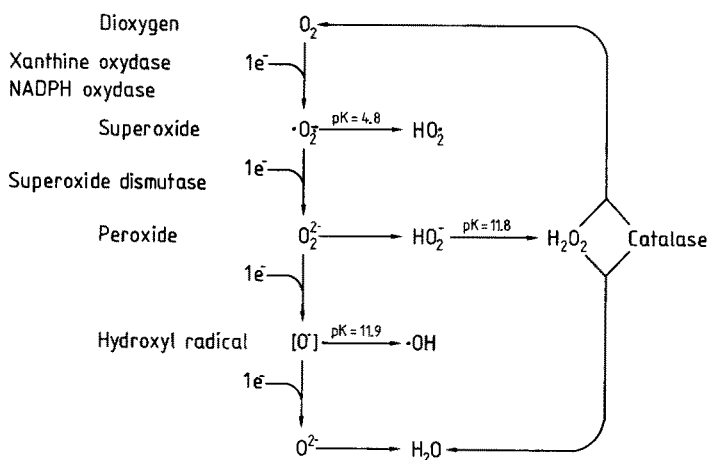
5 Biochemical Function

In the last ten years, there has been no research area, in which the biochemical function of an enzyme was discussed so controversially and emotionally than with superoxide dismutase. There is a polarization between one group which debates the biological importance of the dismutation of superoxide and another one which is convinced that this reaction is required in aerobic metabolism, preventing the organism from an attack of reactive oxygen species. The current knowledge does not allow a definite

solution to this problem. The present aim will be a brief discussion of the arguments of either group.

5.1 Reactive Oxygen Species

A hundred years after its discovery, oxygen was recognized as toxic to living organisms²⁷⁹⁾. O_2 supplied at concentrations higher than those in normal air causes damage to plants, animals and aerobic bacteria²⁸⁰⁾. There is considerable evidence that oxygen at concentration of 21 % has a detectable damaging effect. The toxicity is attributed to oxygen derived free radicals. O_2 has two unpaired electrons, each located in a π^* antibonding orbital. Due to the spin restriction, its reactivity with a reductant is most effective provided single electrons are transferred²⁸¹⁾. Assuming the latter case, the stepwise reduction of oxygen to water will generate four distinct species (Scheme 5):



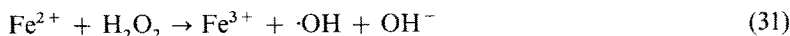
Scheme 5. Proposed mechanism for the stepwise reduction of dioxygen, including the enzymes, which are involved in the removal of reactive oxygen species

The transfer of one electron to dioxygen leads to superoxide. Addition of further electrons and in the presence of protons hydrogen peroxide, eventually OH-radicals and water are formed. Convincing proof of the existence of superoxide and $\cdot OH$ in intact biological tissues is still pending.

Another way of increasing the reactivity of oxygen is to dislocate one of the unpaired electrons into the other half-occupied orbital. A new excited species namely singlet $O_2^1\Delta_g$ oxygen is formed. The chemistry and biochemistry of reactive oxygen species has been extensively reviewed^{268, 282–285)}. Many authors favour the opinion, that the hydroxyl radical belongs to the most toxic species²⁸⁶⁾. In general it is obtained by the homolytic cleavage of the O—O bond in H_2O_2 . The reaction summarized in the following equation:



was firstly postulated by Haber and Weiss ²⁸⁷⁾. In aqueous solutions, the rate constant is very low if not zero. However, if the reaction is catalyzed by traces of transition metal ions including Fe(II) or Cu(I), a fast decomposition of hydrogen peroxide is seen. The following mechanism was proposed ²⁶⁸⁾. After the reduction of Fe(III) by superoxide, the so called Fenton reaction (Eq. 31) is observed ²⁸⁸⁾. The net reaction results in a generation of $\cdot\text{OH}$ radicals from H_2O_2 and O_2^- :



Attributable to the insolubility of $\text{Fe}_{\text{aq}}^{3+}$ ions at neutral pH-values, usually the model reactions of the Fenton type were carried out in acidic solutions. Recently, this reaction was reexamined at physiological pH-values ²⁸⁹⁾. The occurrence of such a reaction at pH 7.0 was confirmed. A similar result is obtained when Cu(I) salts are added to H_2O_2 solutions.

Three types of the destructive effects of OH-radicals with biopolymers can be distinguished: hydrogen atom abstraction, addition and electron transfer. Owing to the radical character, nearly no activation energy is required. Thus, extremely high rate constants are observed. On the condition that O_2^- , H_2O_2 , Fe(II) and Cu(I) are present in vivo, a possible damage of the organism by toxic oxygen radicals was proposed.

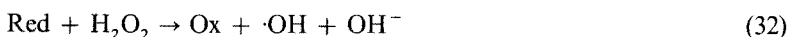
There are overwhelming reports on superoxide anion generation in defined biological systems including redox reactions of small molecules, autoxidable proteins and oxidative enzymes ²⁹⁰⁾. The most prominent enzyme is xanthine oxidase. However, some precautions are necessary, because the single electron reduction of dioxygen is considered to be an unnatural reactivity of this enzyme, which, under in vivo conditions acts like a dehydrogenase ²⁸⁵⁾.

In biological tissues H_2O_2 is present in considerable amounts ²⁹¹⁾. For example, it is a reaction product of amino oxidases, uricases and last not least superoxide dismutases. There remains an important question, dealing with the occurrence of "free" metal ions in biological tissues. The adult human contains about 4 g of iron, located in haemoglobin, myoglobin, cytochromes, catalase, iron transport and iron storage proteins, like transferrin and ferritin. Under normal physiological conditions the transferrins are only partially loaded with iron. Due to its extremely high iron binding constants, the concentration of "free" iron is virtually zero in the blood stream ²⁹²⁾. The iron not required in the cells is bound by ferritin. Although the organism spares no efforts to remove low M_r iron compounds, there may be a possible pool of non-protein bound iron, moving between transferrins, ferritin and haemoproteins.

The availability of copper in the body is somewhat different from that of iron. Copper in the blood serum is bound in caeruloplasmin. Excessive dietary copper is predominately carried by serum albumin. Serum albumin copper is in the equilibrium with low molecular mass complexes of amino acids or small peptides. Unfortunately, the concentration of such complexes is below the detection limit. Regardless of the

ligand, all these complexes are known to display superoxide dismutase activity (see Chapt. 4.3). Some authors have reported, that nontoxic concentrations of cell-bound or low M_r copper may cause damaging effects to bacteria and proteins^{293, 294}. The reaction was thought to proceed via a modified copper-driven Haber-Weiss reaction. The cellular damage by activated oxygen generated with Cu(I) is prevented after the addition of histidine or albumin²⁹⁵. It is currently accepted, that low M_r copper is not available for a Fenton's type reaction²⁶⁹. Moreover, it was demonstrated, that small copper compounds can be curative in some diseases²⁹⁶.

The completely different redox properties of reactive oxygen species in aprotic media or membranes lead to other routes of interaction of superoxide with hydrogen peroxide²⁹⁸. Another mechanism independent to the Haber-Weiss reaction was found. In addition, there are stoichiometrically acting molecules like ascorbate or NADPH, which were thought to be involved in the generation of hydroxyl radicals via the equation^{299, 300}:



Proof for this reaction under in vivo conditions is lacking. Nevertheless, the oxidation of ascorbate generates superoxide ions at rates, which are in the range of $10^{-9} - 10^{-8} \text{ Mol}^{-1} \times \text{sec}^{-1}$ under physiological conditions³⁰¹.

5.2 Biochemical Function and Distribution of Superoxide Dismutases

In the preceding chapter, it was pointed out that potentially toxic oxygen radicals can be generated in living organisms. As a consequence, there was an evolutionary pressure for the development of defense mechanisms against oxy radicals. Taking into account the widely distributed superoxide dismutases, the crucial point remains, whether or not the dismutation of superoxide is an important step in the detoxification of oxygen radicals and whether this reaction is the natural reactivity of SOD's in the organism.

There are some reports of the induction of superoxide dismutases by increased oxygen pressures. For example, *E. coli* contains an iron SOD which is found in the presence and absence of oxygen. After transfer of anaerobically grown cells to aerobic conditions, the manganese superoxide dismutase is induced³⁰². Another strong evidence for the necessity of superoxide dismutase comes from the increased rate of synthesis of manganese-SOD after the administration of paraquat in the presence of oxygen³⁰³. In the absence of paraquat no increase of the enzyme's concentration is seen. Paraquat (methyl viologen) is known to be reduced inside the cell, forming a semiquinone which successively generates superoxide radicals from dioxygen.

There are also a great deal of studies concerning the metal dependent synthesis of iron — or manganese superoxide dismutases. Unlike cells grown in iron-deficient medium, iron supplement to *E. coli* results in a higher resistance to survive phagocytosis⁹⁵. Phagocytosing cells are known to produce superoxide during the attack of bacteria. The fungus *D. dendroides* which contains both $\text{Cu}_2\text{Zn}_2\text{SOD}$ and the manganese enzyme produces more manganese superoxide dismutase provided the copper level

in the growth-medium is decreased ³⁰⁴). The loss of activity attributable to the drop of $\text{Cu}_2\text{Zn}_2\text{SOD}$ -concentration during copper deficiency is fully compensated by an increase of the manganese containing enzyme.

Intriguingly, there are aerotolerant bacteria, which were completely deficient of superoxide dismutases. In the case of *L. plantarum* it could be demonstrated, that the absence of a superoxide dismutase is fully compensated by significantly higher concentrations of a low molecular mass compound which is able to scavenge superoxide as effective as the manganese enzyme ³⁰⁵). The substitution of millimolar levels of Mn(II) for micromolar levels of Mn-SOD was thought to be a common principle in lactic acid bacteria, like *L. plantarum*. However, the question arises, why the organism produces the superfluid SOD's if low molecular mass complexes could fulfil the same task?

The anaerobic *P. shermanii* contains iron superoxide dismutase and synthesizes a manganese SOD, when grown under iron free conditions ³⁰⁶). Surprisingly, apart from the metal, this protein is practically indistinguishable from the originally present iron enzyme, including amino acid analyses. The catalytic activities of the apoproteins can either be restored using manganese or iron. In the last five years it was demonstrated that the synthesis of superoxide is influenced or induced by changes in the metal contents of the growth media ³⁰⁷⁻³¹²). The correlation between the metal supplied and the synthesis of the respective superoxide dismutase could not always be deduced ³¹¹). Moreover, taking into account the numerous iron containing enzymes, and, which are involved in oxygen metabolism, it is by no means clear, that a simple rise of iron SOD concentration should be responsible for the accelerated growth of microorganisms under the respective growth conditions.

In the red blood cells of patients suffering from diminished glucose-6-phosphate dehydrogenase levels, an enzyme involved in the supply of reductive equivalents in the oxy-radical shuttle, decrease of superoxide dismutase activity was shown ³¹³). This phenomenon was attributed to an increase of damaging oxygen radicals which cause the destruction of SOD and hemolysis. Likewise, ageing of the erythrocyte is mainly ascribed to the ageing of erythrocyte Cu_2Zn_2 superoxide dismutase (see also chapter 3.1.3 and ^{314, 315}). In species with a long life span a higher specific SOD-activity was found in the red blood cells compared to those species of a shorter life span ³¹⁶). Moreover, erythrocytes from old rats have lower SOD activities than those of young rats. Concomitantly, an increase in immunoprecipitable material, defective of enzymatic activity was found in old animals ^{205, 317}). However, in another report, no specific age related modifications in Cu_2Zn_2 superoxide dismutase from erythrocytes of old and young cows could be detected ³¹).

Superoxide dismutases are able to protect cells from damaging effects caused by radiation ³¹⁸⁻³²⁰). A reaction was proposed, in which SOD removes reactive oxygen species, generated by the irradiation and thus preventing the organisms from an attack by primary radicals or their reaction products, respectively ³²¹). Other reports on the radioprotective effect include the induction of superoxide dismutase in irradiated whole organs ³²²⁻³²⁴). However, a radiation-induced SOD synthesis was not confirmed ³²⁵). Further experiments are needed to elucidate whether or not superoxide dismutase is a physiological radioprotector.

Undoubtedly, there are many possible sources for the superoxide anion generation in biological systems ²⁹⁰). In a newer approach ¹⁹F-NMR spectroscopy was used

as a detector for O_2^- . The molecular spin of $^{19}F^-$, a very weak inhibitor of Cu_2Zn_2 -superoxide dismutase is specifically relaxed by the $Cu(II)$ at the active site of the enzyme³²⁶⁾. Therefore, the $Cu(II)/Cu(I)$ ratio can be estimated with much greater sensitivity than by EPR-techniques²¹⁴⁾. Approximately half of the catalytically active Cu_2Zn_2 -superoxide dismutase was found in the reduced state compared to the resting enzyme. The half reduction of SOD is a basic requirement for the catalytic action during superoxide dismutation, involving alternate reduction and reoxidation¹⁹⁰⁾. The ^{19}F -relaxation system can be employed to haemolysates or even intact erythrocytes³²⁷⁾. It is also applicable for the detection of the flux of superoxide, if SOD is used as redox standard³²⁸⁾.

Naturally occurring reducing agents such as glutathione or ascorbate reduce the oxidized enzyme much slower than O_2^- . Hence, even low fluxes of the superoxide anion are seen in biological tissues with ^{19}F -NMR. Haemoglobin does not contribute significantly to the relaxation of $^{19}F^-$. Moreover, the reoxidation of reduced $Cu(I)$ -SOD by dioxygen is a very slow process. Therefore, the high relaxation rate, observed in haemolysates can be exclusively attributed to reduced Cu_2Zn_2 -superoxide dismutase. The observed steady state (half reduction) gives strong evidence for a flux of superoxide in intact erythrocytes. Even though, artificial effects, for example reduction by the strongly reducing medium in the red blood cell are not fully excluded. Another source for interference may be the relatively high F^- -concentrations (up to 1 M), required for the NMR-spectroscopy, and which may perturb the biological system.

EPR-spectroscopy of the steady state level of Cu_2Zn_2 -superoxide dismutase is a less perturbative method. It was applied to crude haemolysates. If SOD is added in a concentration of about 10^{-5} M, a superoxide flux of 2.0×10^{-8} Mol \times sec $^{-1}$ was detected¹⁷⁷⁾. Increasing the pO_2 caused a saturation of O_2^- -production. The autooxidation of oxyhaemoglobin, which is thought to be a source of superoxide³²⁹⁾ did not significantly contribute to the superoxide production.

Superoxide chemistry differs greatly according to whether or not reactions occur in aqueous or in aprotic media. In aqueous solution, O_2^- reacts predominantly as a reducing agent. By way of contrast, the superoxide anion is more stable in lipophilic environments. Nevertheless, it can act as a powerful base, nucleophile and reductant^{330, 331)}. The lipophilic O_2^- -anion is often found inside the biological membranes, because it is the product of many membrane bound proteins^{332, 333)}. It may damage phospholipids by a nucleophilic attack. Hence, the existence of intra-membrane superoxide dismutases should be demanded instead of the cytosolic enzymes normally found. In fact, a membrane-associated SOD was reported recently, occurring within the bovine erythrocyte membrane²⁰⁴⁾. Further studies in this field would be highly desirable.

Although many of the investigations mentioned before give strong evidence for the biological importance of the dismutation of superoxide, a final proof is still lacking. Another unresolved problem is, why nature has not chosen a more simple way for the removal of superoxide if at all, by the oxidation of superoxide to dioxygen, omitting the production of H_2O_2 . As a matter of fact, the reactivity of free metals (Fenton reaction) would create no further problems. An unsolved question remains whether or not superoxide migrates fast enough to the dismutase before any side reactions with other biomolecules can occur. An interesting phenomenon should be pointed out why are the cytosolic concentrations of SOD's so high? O_2^- is predominantly found

in lipophilic environments, especially in the membranes. However, only minor concentrations of superoxide dismutases are found in this cellular compartment to control the level of superoxide concentrations.

Apart from its catalytical function, Cu_2Zn_2 superoxide dismutases was suggested to play a role as copper-transport and/or storage protein³³⁴⁾. Copper depleted E_2Zn_2 -superoxide dismutase (E = Empty) can be reconstituted using Cu(I)-thiolate proteins (metallothioneins)³³⁵⁾.

Both proteins are existing in the same cellular compartment i.e. the cytosol. The copperthioneins are very resistant to enzymic breakdown. None of the known proteases are able to attack these proteins. Surprisingly, the copper from these proteins is released offering an appropriate apoprotein or by an oxidative breakdown³³⁵⁻³³⁸⁾. Therefore, copper-free superoxide dismutase could be seen as a transport vehicle for the intracellular copper stored in the Cu(I)-thioneins. Moreover, the release of "free" copper, which may be harmful by generating reactive oxygen species, is by-passed by this mechanism.

Some more clinical aspects do not support the biological necessity of superoxide dismutating reactions. In patients, suffering from Fanconi's anemia, which is characterized by a deficiency of superoxide dismutase²⁰³⁾, no effect in the autioxidant defence capability of erythrocytes could be detected³³⁹⁾. Even in conditions of augmented oxidative injury, there were no significant changes. This judgement was confirmed by studies of the enzymes involved in the defence of the cell against excited oxygen species³⁴⁰⁾. These enzymes include catalase and glutathione peroxidase. They are known to destroy hydrogen peroxide. No correlation between these proteins and superoxide dismutase could be found in rats. This phenomenon is also seen in a disease named acatalasia. Patients suffering from this disorder though having no catalase, are devoid of any symptoms³⁴¹⁾.

Since the superoxide anion is a radical, it should react in the cellular matrix with free-radical scavengers such as glutathione and other thiols³⁴²⁾. It seems very likely, that these sulphur containing compounds play a major role in controlling O_2^- concentrations within the cell. Although, they do not act catalytically, their concentration is a hundredfold higher in the organism compared to superoxide dismutases, making the thiol effect possible.

M. pneumoniae a prokaryote, which consumes oxygen contains neither catalase nor superoxide dismutase³⁴³⁾. Amazingly, a considerable production of both, superoxide and hydrogen peroxide was detected. Therefore, the rule that organisms, which consume dioxygen synthesize superoxide dismutases is exempted by this prokaryote. After the isolation of the manganese superoxide dismutase gene from *E. coli*, it was found, that the intracellular superoxide concentration does not regulate the oxygen dependent induction of this enzyme³⁴⁴⁾. This result was deduced from the fact, that cells with widely varying levels of iron superoxide dismutases, which is also present in this organism, independently produce the manganese enzyme as a function of the dioxygen concentration supplied.

It may be concluded, that the physiological role of superoxide dismutases still remains to be debated. Although, it belongs to one of the best characterized metallo-proteins it shares the fate with xanthine oxidase, one of the "oldest" metalloenzymes³⁴⁵⁾. Both enzymes are widely abundant, but their genuine biological function is yet not fully understood.

6 Acknowledgements

Some experimental portions of this article were supported by grants from the Deutsche Forschungsgemeinschaft (DFG We 401/16 and 17), the Ministerium für Ernährung, Landwirtschaft, Umwelt und Forsten des Landes Baden-Württemberg (AZ 62-7990.2) and by the Fonds der Chemischen Industrie. Thanks go to Dr. H.-J. Hartmann for helpful discussions. We are greatly indebted to Helga Heinemann, Dietmar Schell and Heidi Schneider for skilful technical assistance.

7 References

1. Parker, M. W., Schinina, M. E., Bossa, F., Bannister, J. V.: *Inorg. Chim. Acta* 91, 307 (1984)
2. Zimmermann, R., Flohé, L., Weser, U., Hartmann, H.-J.: *FEBS Lett.* 29, 117 (1973)
3. Richter, C., Azzi, A., Weser, U., Wendel, A.: *J. Biol. Chem.* 252, 5061 (1977)
4. Kadenbach, B.: *Angew. Chem.* 95, 273 (1983)
5. Perutz, M. F.: *Nature* 228, 726 (1970)
6. Que, L. jr.: *Coord. Chem. Rev.* 50, 73 (1983)
7. Xavier, A. V., Moura, J. J., Moura, I.: *Struct. Bonding* 43, 187 (1981)
8. Pasternack, R. F., Halliwell, B.: *J. Am. Chem. Soc.* 101, 1026 (1979)
9. Eigen, M.: *Pure Appl. Chem.* 6, 105 (1963)
10. Basolo, F., Pearson, R. G.: *Mechanisms of Inorganic Reactions*, 2nd edition, J. Wiley, New York 1967
11. Michelson, A. M., McCord, J. M., Fridovich, I. (eds.): *Superoxide and Superoxide Dismutases*, London, New York, San Francisco, Academic Press 1977
12. Weser, U. (ed.): *Metalloproteins*, Stuttgart, New York Georg Thieme Verlag 1979
13. Bannister, J. V., Hill, H. A. O. (eds.): *Chemical and Biochemical Aspects of Superoxide and Superoxide Dismutases*, *Developments in Biochemistry*, Vol 11A, Elsevier North-Holland 1980
14. Bannister, W. H., Bannister, J. V. (eds.): *Biological and Clinical Aspects of Superoxide and Superoxide Dismutases*, *Developments in Biochemistry*, Vol 11B, Elsevier North-Holland 1980
15. Oberley, L. W. (ed.): *Superoxide Dismutase*, Vol I + II, Boca Raton, Florida, CRC Press, Inc. 1982
16. Croatto, U. (ed.): *Inorganica Chimica Acta*, 1st International Conference on Bioinorganic Chemistry, Vol 79 (B7), Lausanne, Elsevier Sequoia S.A. 1983
17. Lontie, R. (ed.): *Copper Proteins and Copper Enzymes*, Vol. II, Boca Raton, Florida, CRC Press, Inc. 1984
18. Bors, W., Saran, M., Tait, D. (eds.): *Oxygen Radicals in Chemistry and Biology*, Berlin, New York, Walter de Gruyter, 1984
19. Mann, T., Keilin, D.: *Proc. R. Soc. London Ser. B* 126, 303 (1939)
20. Markowitz, H., Cartwright, G. E., Wintrobe, M. M.: *J. Biol. Chem.* 234, 40 (1959)
21. Shields, G. S., Markowitz, H., Klassen, W. H., Cartwright, G. E., Wintrobe, M. M.: *J. Clin. Invest.* 40, 2007 (1961)
22. Stansell, M. J., Deutsch, H. F.: *J. Biol. Chem.* 240, 4299 (1965)
23. McCord, J. M., Fridovich, I.: *J. Biol. Chem.* 244, 6049 (1969)
24. Gärtner, A., Hartmann, H.-J., Weser, U.: *Biochem. J.* 221, 549 (1984)
25. Weser, U., Bohnenkamp, W., Cammack, R., Hartmann, H.-J., Voelcker, G.: *Hoppe Seyler's Z. Physiol. Chem.* 353, 1059 (1972)
26. Tsuschihashi, M.: *Biochem. Z.* 140, 65 (1923)
27. Weser, U., Bunnenberg, E., Cammack, R., Djerassi, C., Flohé, L., Thomas, G., Voelter, W.: *Biochim. Biophys. Acta* 243, 203 (1971)
28. Bannister, J. V., Bannister, W. H., Wood, E.: *Europ. J. Biochem.* 18, 178 (1971)
29. Hartz, J. W., Deutsch, H. F.: *J. Biol. Chem.* 247, 7043 (1972)
30. Gärtner, A., Weser, U.: *FEBS Lett.* 155, 15 (1983)
31. Gärtner, A., Schroth-Pollmann, M., Weser, U.: *Inorg. Chim. Acta* 107, 117 (1985)

32. Crosti, N.: *Biochem. Genet.* **16**, 739 (1978)
33. Kovárová, H., Simsa, J., Krizala, J.: *Collect. Czechoslovak. Chem. Commun.* **46**, 2140 (1981)
34. Civalieri, L., Pini, C., Rigo, A., Federico, R., Calabrese, L., Rotilio, G.: *Mol. Cell. Biochem.* **47**, 3 (1982)
35. Bannister, J. V., Bannister, W. H.: Isolation and Characterization of Superoxide Dismutase, in: *Methods in Enzymology*, Vol. 105 (ed.) Packer, L., pp. 88, Orlando Florida, Academic Press, Inc. 1984
36. McCord, J., Boyle, J. A., Day, E. D., Rizzolo, L. J., Salin, M. L.: A Manganese-Containing Superoxide Dismutase from Human Liver, in: *Superoxide and Superoxide Dismutases*, (eds.) Michelson, A. M., McCord, J. M., Fridovich, I., pp. 129, London, New York, San Francisco, Academic Press 1977
37. Thomas, K. A., Rubin, B. H., Bier, C. J., Richardson, J. S., Richardson, D. C.: *J. Biol. Chem.* **249**, 5677 (1974)
38. Forman, H. J., Fridovich, I.: *J. Biol. Chem.* **248**, 2645 (1973)
39. Bannister, J. V., Anastasi, A., Bannister, W. H.: *Biochem. Biophys. Res. Commun.* **81**, 469 (1978)
40. Flohé, L., Bannister, J. V., Bannister, W. H., Günzler, W. A., Kim, S. M., Ötting, F., Steffens, G. J.: *Hoppe-Seyler's Z. Physiol. Chem.* **364**, 319 (1983)
41. Steinman, H. M.: *J. Biol. Chem.* **257**, 10283 (1982)
42. Hartz, J. W., Funakoshi, S., Deutsch, H. F.: *Clin. Chim. Acta* **46**, 125 (1973)
43. Stallings, W. C., Powers, T. B., Patridge, K. A., Fee, J. A., Ludwig, M. L.: *Proc. Natl. Acad. Sci. USA* **80**, 3884 (1983)
44. Clare, D. A., Blum, J., Fridovich, I.: *J. Biol. Chem.* **259**, 5932 (1984)
45. Asayama, K., Burr, I. M.: *Anal. Biochem.* **136**, 336 (1984)
46. Marklund, S. L.: *Proc. Natl. Acad. Sci. USA* **79**, 7634 (1982)
47. Hassan, H. M.: Superoxide Dismutases, in: *Ciba Foundation Symposium 79, Biological Roles of Copper*, pp. 125, Amsterdam, Excerpta Medical 1980
48. Steinmann, H. M., Naik, V. R., Abernethy, J. L., Hill, R. L.: *J. Biol. Chem.* **249**, 7326 (1974)
49. Jabusch, J. R., Farb, D. L., Kerschensteiner, D. A., Deutsch, H. F.: *Biochemistry* **19**, 2310 (1980)
50. Barra, D., Martini, F., Bannister, J. V., Schinina, M. E., Rotilio, G., Bannister, W. H., Bossa, F.: *FEBS Lett.* **120**, 53 (1980)
51. Abernethy, J. L., Steinman, H. M., Hill, R. L.: *J. Biol. Chem.* **249**, 7339 (1974)
52. Lerch, K., Ammer, D.: *J. Biol. Chem.* **256**, 11 545 (1981)
53. Weser, U.: *Struct. Bonding* **17**, 1 (1973)
54. Keele, B. B., McCord, J. M., Fridovich, I.: *J. Biol. Chem.* **246**, 2875 (1971)
55. Malkin, R., Malmström, B. G.: *Advan. Enzymol.* **33**, 177 (1970)
56. Richardson, J. S., Thomas, K. A., Richardson, D. C.: *Biochem. Biophys. Res. Commun.* **63**, 986 (1975)
57. Richardson, J. S., Thomas, K. A., Rubin, B. H., Richardson, D. C.: *Proc. Natl. Acad. Sci. USA* **72**, 1349 (1975)
58. Richardson, J. S., Richardson, D. C., Thomas, K. A., Silverton, E. W., Davies, D. R.: *J. Mol. Biol.* **102**, 221 (1976)
59. Tainer, J. A., Getzoff, E. D., Beem, K. M., Richardson, J. S., Richardson, D. C.: *J. Mol. Biol.* **160**, 181 (1982)
60. Tainer, J. A., Getzoff, E. D., Richardson, J. S., Richardson, D. C.: *Nature* **306**, 284 (1983)
61. McLachlan, A. D.: *Nature* **285**, 267 (1980)
62. Lippard, S. J., Burger, A. R., Ugurbil, K., Pantoliano, M. W., Valentine, J. S.: *Biochemistry* **16**, 1136 (1977)
63. Cass, A. E. G., Hill, H. A. O., Smith, B. E., Bannister, J. V., Bannister, W. H.: *Biochemistry* **16**, 3061 (1977)
64. Cass, A. E. G., Hill, H. A. O., Smith, B. E., Bannister, J. V., Bannister, W. H.: *Biochem. J.* **165**, 587 (1977)
65. Stoerz, J. D., Malinowski, D. P., Redfield, A. G.: *Biochemistry* **18**, 4669 (1979)
66. Cass, A. E. G., Hill, H. A. O., Bannister, W. H., Bannister, J. V.: *Biochem. Soc. Trans.* **7**, 716 (1976)
67. Cass, A. E. G., Hill, H. A. O., Bannister, J. V., Bannister, W. H., Hasemann, V., Johansen, J. T.: *Biochem. J.* **183**, 127 (1979)

68. Hill, H. A. O., Lee, W.-K., Bannister, J. V., Bannister, W. H.: *Biochem. J.* **185**, 245 (1980)
69. Burger, A. R., Lippard, S. J., Pantoliano, M. W., Valentine, J. S.: *Biochemistry* **19**, 4139 (1980)
70. Bailey, D. B., Ellis, P. D., Fee, J. A.: *Biochemistry* **19**, 591 (1980)
71. Rotilio, G., Morpurgo, L., Giovagnoli, C., Calabrese, L., Mondovi, B.: *Biochemistry* **11**, 2187 (1972)
72. Fee, J. A., Peisach, J., Mims, W. B.: *J. Biol. Chem.* **256**, 1919 (1981)
73. Van Camp, H. L., Sands, R. H., Fee, J. A.: *Biochim. Biophys. Acta* **704**, 75 (1982)
74. Lieberman, R. A., Sands, R. H., Fee, J. A.: *J. Biol. Chem.* **257**, 336 (1982)
75. Blackburn, N. J., Hasnain, S. S., Binsted, N., Diakun, G. P., Garner, C. D., Knowles, P. F.: *Biochem. J.* **219**, 985 (1984)
76. Stansell, M. J., Deutsch, H. F.: *J. Biol. Chem.* **240**, 4306 (1965)
77. Hartz, J. W., Deutsch, H. F.: *J. Biol. Chem.* **244**, 4565 (1969)
78. Bohnenkamp, W., Weser, U.: *Hoppe-Seyler's Z. Physiol. Chem.* **356**, 747 (1975)
79. Malinowski, D. P., Fridovich, I.: *Biochemistry* **18**, 237 (1979)
80. Crosti, N., Sausa, P.: *Biochem. Genet.* **18**, 693 (1980)
81. Bloor, J. H., Holtz, D., Kaars, J., Kosman, D. J.: *Biochem. Genet.* **21**, 349 (1983)
82. Jewett, S. L.: *Inorg. Chim. Acta* **79** (B7), 144 (1983)
83. Henry, L. E. A., Palmer, J. M., Hall, D. O.: *FEBS Lett.* **93**, 327 (1978)
84. Zepp, R. A., Chelack, W. S., Pettkau, A.: Bovine Superoxide Dismutase Preparations: Comparison of their Biochemical and Biophysical Characteristics, in: *Chemical and Biochemical Aspects of Superoxide and Superoxide Dismutase*, (eds.) Bannister, J. W., Hill, H. A. O., pp. 201, New York, Amsterdam, Elsevier/North Holland 1980
85. Weser, U., Voelcker, G.: *FEBS Lett.* **22**, 15 (1972)
86. Symonjan, M. A., Nalbandyan, R. M.: *FEBS Lett.* **28**, 22 (1972)
87. Rotilio, G., Morpurgo, L., Calabrese, L., Mondovi, B.: *Biochim. Biophys. Acta* **302**, 229 (1973)
88. Bray, R. C., Cockle, S. A., Fielden, E. M., Roberts, P. B., Rotilio, G., Calabrese, L.: *Biochem. J.* **139**, 43 (1974)
89. Hodgson, E. K., Fridovich, I.: *Biochemistry* **14**, 5294 (1975)
90. Blech, D. M., Borders, C. L., Jr.: *Arch. Biochem. Biophys.* **224**, (1983)
91. Fuchs, H. J. R., Borders, C. L., Jr.: *Biochem. Biophys. Res. Commun.* **116**, 1107 (1983)
92. Sinet, P.-M., Garber, P.: *Arch. Biochem. Biophys.* **212**, 411 (1981)
93. Lawrence, G. D., Sawyer, D. T.: *Biochemistry* **18**, 3045 (1979)
94. Rapoport, S. M., Müller, M.: Catalase and Glutathione Peroxidase, in: *Cellular and Molecular Biology of Erythrocytes*, (eds.) Yoshikawa, M., Rapoport, S. M., pp. 167, München, Berlin, Wien Urban und Schwarzenberg 1974
95. Yost, F. J., Jr., Fridovich, I.: *J. Biol. Chem.* **248**, 4905 (1973)
96. Salin, M. L., Bridges, S. M.: *Arch. Biochem. Biophys.* **201**, 369 (1980)
97. Walker, J. E., Auffret, A. D., Brock, C. J., Steinman, H. M.: Structural Comparisons of Superoxide Dismutases, in: *Chemical and Biochemical Aspects of Superoxide and Superoxide Dismutases*, (eds.) Bannister, J. V., Hill, H. A. O., pp. 212, New York, Amsterdam Elsevier/North-Holland 1980
98. Muno, D., Isobe, T., Okuyama, T., Tchiara, K., Noda, Y., Kusunose, E., Kusunose, M.: *Biochem. Int.* **2**, 33 (1981)
99. Yamakura, F.: *Biochim. Biophys. Acta* **422**, 280 (1976)
100. Ringe, D., Petsko, G. A., Yamakura, F., Suzuki, K., Ohmori, D.: *Proc. R. Soc. Lond. B* **218**, 119 (1983)
101. Fee, J. A., McClune, G. J., Lees, A. C., Zidovetzki, R., Pecht, I.: *Isr. J. Chem.* **21**, 54 (1981)
102. Okado, S., Kanematsu, S., Asada, K.: *FEBS Lett.* **103**, 106 (1979)
103. Beaman, B. L., Scates, S. M., Moring, S. E., Deem, R., Misra, H. P.: *J. Biol. Chem.* **258**, 91 (1983)
104. Ringe, D., Petsko, G. A., Yamakura, F., Suzuki, K., Ohmori, D.: *Proc. Natl. Acad. Sci. USA* **80**, 3879 (1983)
105. Stallings, W. C., Bull, C., Patridge, K. A., Powers, T. B., Fee, J. A., Ludwig, M. L., Ringe, D., Petsko, G. A.: The Three-Dimensional Structure of Iron Superoxide Dismutase: Kinetic and Structural Comparisons with Cu/Zn and Mn Dismutases, in: *Oxygen Radicals in Chemistry and Biology*, (eds.) Bors, W., Saran, M., Tait, D., pp. 779, Berlin, New York, Walter de Gruyter & Co 1984

106. Anastasi, A., Bannister, J. V., Bannister, W. H.: *Int. Biochem.* 7, 541 (1976)
107. Sato, S., Nakazawa, K. J.: *Biochem. (Tokyo)* 83, 1165 (1978)
108. Marklund, S.: Mammalian Superoxide Dismutases, in: *Oxygen Radicals in Chemistry and Biology*, (eds.) Bors, W., Saran, M., Tait, D., pp. 765, Berlin, New York, Walter de Gruyter & Co 1984
109. Weisiger, R. A., Fridovich, I.: *J. Biol. Chem.* 248, 3582 (1973)
110. Keele, B. B., McCord, J. M., Fridovich, I.: *J. Biol. Chem.* 245, 6176 (1970)
111. Sato, S., Harris, J. I.: *Eur. J. Biochem.* 73, 373 (1977)
112. Ravindranath, S. V., Fridovich, I.: *J. Biol. Chem.* 250, 6107 (1975)
113. Vance, P. G., Keele, B. B., Rajagopalan, K. V.: *J. Biol. Chem.* 247, 4782 (1972)
114. Lavelle, F., Michelson, A. M.: *Biochimica* 57, 375 (1975)
115. Salin, M. L., Day, E. D., Crapo, J. D.: *Arch. Biochem. Biophys.* 187, 223 (1978)
116. Reinhardt, R., Altdorf, R., Ohlenbusch, H.-D.: *Hoppe-Seyler's Z. Physiol. Chem.* 365, 577 (1984)
117. Sevilla, F., Lopez Gorge, J., Del Rio, L. A.: Preliminary Characterization of a Mn-Containing Superoxide Dismutase from Higher Plant (*Pisum Sativum* L.) in: *Chemical and Biochemical Aspects of Superoxide and Superoxide Dismutase*, (eds.) Bannister, J. V., Hill, H. A. O., pp. 185, New York, Amsterdam, Elsevier/North-Holland 1980
118. Steinman, H. M.: *J. Biol. Chem.* 253, 8708 (1978)
119. Brock, C. J., Walker, J. E.: *Biochemistry* 19, 8708 (1978)
120. Ditlow, C., Johansen, J. T., Martin, B. M., Ivendsen, I. B.: *Carlsberg Res. Commun.* 47, 81 (1982)
121. Terech, A., Vignais, P. M.: *Biochim. Biophys. Acta* 657, 411 (1981)
122. Weser, U., Hartmann, H.-J.: *FEBS Lett.* 17, 78 (1971)
123. Carrico, R. J., Deutsch, H. F.: *J. Biol. Chem.* 245, 723 (1970)
124. Rotilio, G., Calabrese, L., Bossa, F., Barra, D., Finazzi-Agro, A., Mondovi, B.: *Biochemistry* 11, 2182 (1972)
125. Rigo, A., Viglino, P., Calabrese, L., Cocco, D., Rotilio, G.: *Biochem. J.* 161, 27 (1977)
126. Fee, J. A.: *Biochim. Biophys. Acta* 295, 107 (1973)
127. Fee, J. A.: *J. Biol. Chem.* 248, 4229 (1973)
128. Beem, K. M., Rich, W. E., Rajagopalan, K. V.: *J. Biol. Chem.* 249, 7298 (1974)
129. Fee, J. A., Gaber, B. P.: *J. Biol. Chem.* 247, 60 (1972)
130. Fee, J. A., Briggs, R. G.: *Biochim. Biophys. Acta* 400, 439 (1975)
131. Cocco, D., Calabrese, L., Rigo, A., Marmocchi, F., Rotilio, G.: *Biochem. J.* 199, 675 (1982)
132. Valentine, J. S., Pantoliano, M. W., McDonnell, P. J., Burger, A. R., Lippard, S. J.: *Proc. Natl. Acad. Sci. USA* 76, 4245 (1979)
133. Calabrese, L., Cocco, D., Morpurgo, L., Mondovi, B., Rotilio, G.: *FEBS Lett.* 59, 29 (1975)
134. Pantoliano, M. W., Valentine, J. S., Burger, A. R., Lippard, S. J.: *J. Inorg. Biochem.* 17, 325 (1982)
135. Beem, K. M., Richardson, D. C., Rajogopalan, K. V.: *Biochemistry* 16, 1930 (1977)
136. Pantoliano, M. W., McDonnell, P. J., Valentine, J. S.: *J. Am. Chem. Soc.* 101, 6454 (1979)
137. Hirose, J., Ohhira, T., Hirata, H., Kidani, Y.: *Arch. Biochem. Biophys.* 218, 179 (1982)
138. Jewett, S., Latrenta, G. S., Beck, C. M.: *Arch. Biochem. Biophys.* 215, 116 (1982)
139. Misra, H. P.: *J. Biol. Chem.* 254, 11623 (1979)
140. Cocco, D., Calabrese, L., Rigo, A., Argese, E., Rotilio, G.: *J. Biol. Chem.* 256, 8983 (1981)
141. Brock, C. J., Walker, J. E.: Superoxide Dismutase from *Bacillus Stearothermophilus*: Metal Binding and Complete Amino Acid Analysis, in: *Chemical and Biochemical Aspects of Superoxide and Superoxide Dismutase*, (eds.) Bannister, J. V., Hill, H. A. O., pp. 237, New York, Amsterdam, Elsevier/North-Holland 1980
142. Yamakura, F.: *J. Biochem. (Tokyo)* 83, 849 (1978)
143. Yamakura, F., Suzuki, K., Petsko, G., Tsernoglou, D.: Metal Replacement Studies and Crystallographic Data on Iron-Superoxide Dismutase from *Pseudomonas Ovalis*, in: *Chemical and Biochemical Aspects of Superoxide and Superoxide Dismutase*, (eds.) Bannister, J. V., Hill, H. A. O., pp. 242, New York, Amsterdam, Elsevier/North-Holland 1980
144. Beauchamp, C., Fridovich, I.: *Anal. Biochem.* 44, 276 (1971)
145. Puget, K., Michelson, A. M.: *Biochimie* 56, 1255 (1974)
146. Marklund, S., Marklund, G.: *Eur. J. Biochem.* 47, 469 (1974)

147. Misra, H. P., Fridovich, I.: *J. Biol. Chem.* **247**, 3170 (1972)
148. Sun, M., Zigman, S.: *Anal. Biochem.* **90**, 81 (1978)
149. Heikkilä, R. E., Cabbat, F.: *Anal. Biochem.* **75**, 356 (1976)
150. Schubotz, L. M., Weser, U.: *Inorg. Chim. Acta* **46**, 113 (1980)
151. Fried, R.: *Biochimie* **57**, 657 (1975)
152. McCord, J. M., Fridovich, I.: *J. Biol. Chem.* **244**, 6056 (1969)
153. Elstner, E. F., Heupel, A.: *Anal. Biochem.* **70**, 616 (1976)
154. Misra, H. P., Fridovich, I.: *Anal. Biochem.* **79**, 553 (1977)
155. Finkelstein, E., Rosen, G. M., Rauckman, E. J., Paxton, J.: *Mol. Pharmacol.* **16**, 676 (1979)
156. Rosen, G. M., Finkelstein, E., Rauckman, E. J.: *Arch. Biochem. Biophys.* **215**, 367 (1981)
157. Bensinger, R. E., Johnson, C. M.: *Anal. Biochem.* **116**, 142 (1981)
158. Bors, W., Saran, M., Lengfelder, E., Michel, C., Fuchs, C., Frenzel, C.: *Photochem. Photobiol.* **28**, 629 (1978)
159. Kuthan, H., Tsuji, H., Graf, H., Ullrich, V., Werrigloer, J., Estabrook, R. W.: *FEBS Lett.* **91**, 343 (1978)
160. Azzi, A., Montecucco, C., Richter, C.: *Biochem. Biophys. Res. Commun.* **65**, 597 (1975)
161. Finkelstein, E., Rosen, G. M., Patton, S. E., Cohen, M. S., Rauckman, E. J.: *Biochem. Biophys. Res. Commun.* **102**, 1008 (1981)
162. Cudd, A., Fridovich, I.: *J. Biol. Chem.* **257**, 11443 (1982)
163. Petersen, L. C., Cox, R. P.: *Biochem. J.* **192**, 687 (1980)
164. Cudd, A., Fridovich, I.: *FEBS Lett.* **144**, 181, (1982)
165. Kirby, T. W., Fridovich, I.: *Anal. Biochem.* **127**, 435 (1982)
166. Flohé, L., Ötting, F.: Superoxide Dismutase Assays, in: *Methods in Enzymology*, Vol. 105, (ed.) Packer, L., pp. 93, Orlando Florida, Academic Press, Inc. 1984
167. Younes, M., Weser, U.: *FEBS Lett.* **61**, 209 (1976)
168. Bielski, B. H. J., Shive, G. G., Bajuk, S.: *J. Phys. Chem.* **84**, 830 (1980)
169. Clare, D. A., Duong, M. N., Darr, D., Archibald, F., Fridovich, I.: *Anal. Biochem.* **140**, 532 (1984)
170. Younes, M., Weser, U.: *FEBS Lett.* **71**, 87 (1976)
171. Bors, W., Saran, M., Michel, C., Lengfelder, E., Fuchs, C., Spöttl, R.: *Int. J. Radiat. Biol.* **28**, 353 (1975)
172. Trautner, E. M., Bradley, T. R.: *Austr. J. Sci. Res. Ser. B* **4**, 303 (1951)
173. Mavelli, I., Mondovi, R., Federico, R., Rotilio, G.: *J. Neurochem.* **31**, 363 (1978)
174. McNeil, C. J., Banford, J. C., Brown, D. H., Smith, W. E.: *FEBS Lett.* **133**, 175 (1981)
175. Ballou, D., Palmer, G., Massey, V.: *Biochem. Biophys. Res. Commun.* **36**, 898 (1969)
176. Orme-Johnson, W. H., Beinert, H.: *Biochem. Biophys. Res. Commun.* **36**, 905 (1969)
177. Scarpa, M., Viglino, P., Contri, D., Rigo, A.: *J. Biol. Chem.* **259**, 10657 (1984)
178. McClune, G. J., Fee, J. A.: *FEBS Lett.* **67**, 294 (1976)
179. Marklund, S.: *J. Biol. Chem.* **251**, 7504 (1976)
180. Rigo, A., Viglino, P., Argese, E., Terenzi, M., Rotilio, G.: *J. Biol. Chem.* **254**, 1759 (1979)
181. Klug, D., Rabani, J., Fridovich, I.: *J. Biol. Chem.* **247**, 4839 (1972)
182. Rotilio, G., Bray, R. C., Fielden, E. M.: *Biochim. Biophys. Acta* **268**, 605 (1972)
183. Takahashi, M.-A., Asada, K.: *J. Biochem.* **91**, 889 (1982)
184. Green, M. J., Hill, H. A. O., Tew, D. G., Walton, N. J.: *FEBS Lett.* **170**, 69 (1984)
185. Rigo, A., Viglino, P., Rotilio, G.: *Anal. Biochem.* **68**, 1 (1975)
186. Asmus, K.-D.: Pulse Radiolysis Methodology, in: *Methods in Enzymology*, Vol. 105, (ed.) Packer, L., pp. 167, Orlando Florida, Academic Press Inc. 1984
187. Behar, D., Czapski, G., Rabani, J., Dorfman, L. M., Schwarz, H. A.: *J. Phys. Chem.* **74**, 3209 (1970)
188. Klug-Roth, D., Fridovich, I., Rabani, J.: *J. Am. Chem. Soc.* **95**, 2786 (1973)
189. Brigelius, R., Spöttl, R., Bors, W., Lengfelder, E., Saran, M., Weser, U.: *FEBS Lett.* **47**, 72 (1974)
190. Fielden, E. M., Roberts, P. B., Bray, R. C., Lowe, D. J., Mautner, G. N., Rotilio, G., Calabrese, L.: *Biochem. J.* **139**, 49 (1974)
191. Bannister, J. V., Bannister, W. H., Hill, H. A. O., Mahood, J. F., Willson, R. L., Wolfenden, B. S.: *FEBS Lett.* **118**, 127 (1980)
192. Kuta, J., Kovita, J.: *Collect. Czech. Chem. Commun.* **30**, 4095 (1965)

193. Argese, E., De Carli, B., Orsega, E., Rigo, A., Rotilio, G.: *Anal. Biochem.* **132**, 110 (1983)
194. Rigo, A., Rotilio, G.: *Anal. Biochem.* **81**, 157 (1977)
195. Beauchamp, C., Fridovich, I.: *Biochim. Biophys. Acta* **317**, 50 (1973)
196. Asada, K., Yoshikawa, K., Takahashi, M., Maeda, Y., Enmanji, K.: *J. Biol. Chem.* **250**, 2801 (1975)
197. Reiss, U., Gershon, D.: *Biochem. Biophys. Res. Commun.* **73**, 255 (1976)
198. Eriksson, A. W., Frants, R. R., Jongbloet, P. H., Bijlsma, J. B.: *Clin. Genet.* **10**, 355 (1976)
199. Crapo, J. D., McCord, J. M.: *Am. J. Physiol.* **231**, 1196 (1976)
200. Kelly, K., Barefoot, C., Sehon, A., Petkau, A.: *Arch. Biochem. Biophys.* **190**, 531 (1978)
201. Del Villano, B. C., Tischfield, J. A.: *J. Immunol. Methods* **29**, 253 (1979)
202. Baret, A., Michel, P., Imbert, M. R., Morcellet, J. L., Michelson, A. M.: *Biochem. Biophys. Res. Commun.* **88**, 337 (1979)
203. Joenje, H., Frants, R. R., Arwert, F., de Bruin, G. J., Kostense, P. J., van den Kamp, J. J., de Koning, J., Eriksson, A. W.: *Scand. J. Clin. Lab. Invest.* **39**, 759 (1979)
204. Petkau, A., Copps, T. P., Kelly, K.: *Biochem. Biophys. Acta* **645**, 71 (1981)
205. Bartosz, G., Soszynski, M., Retelewska, W.: *Mech. Ageing Dev.* **17**, 237 (1981)
206. Del Villano, B. C., Tischfield, J. A.: Quantitation of Human Cuprozinc Superoxide Dismutase (SOD-1) by Radioimmunoassay and Its Possible Significance in Disease, in: *Methods in Enzymology*, Vol. 74, (eds.) Langone, J. J., Van Vunakis, H., pp. 359, Orlando Florida, Academic Press, Inc. 1981
207. Fee, J. A., Di Corleto, P. E.: *Biochemistry* **12**, 4893 (1973)
208. Blumberg, W. E., Peisach, J., Eisenberger, P., Fee, J. A.: *Biochemistry* **17**, 1842 (1978)
209. Margerum, D. W., Cayley, G. R., Weatherburn, D. C., Pagenkopf, G. K., in: *Coordination Chemistry*, (ed.) Martell, A. E., pp. 1, Washington DC, American Chemical Society 1978
210. Fee, J. A., Ward, R. L.: *Biochem. Biophys. Res. Commun.* **71**, 427 (1976)
211. Mc Adam, M. E., Fielden, E. M., Lavelle, F., Calabrese, L., Cocco, D., Rotilio, G.: *Biochem. J.* **167**, 271 (1977)
212. Plonka, A., Metodiewa, D., Jeziorowska, A.: *Biochem. Biophys. Res. Commun.* **81**, 1344 (1978)
213. Plonka, A., Metodiewa, D., Gasyna, Z.: *Biochim. Biophys. Acta* **612**, 299 (1980)
214. Viglino, P., Rigo, A., Argese, E., Calabrese, L., Cocco, D., Rotilio, G.: *Biochem. Biophys. Res. Commun.* **100**, 125 (1981)
215. Armitage, I. M., Shoot-Uiterkamp, A. J. M., Chlebowski, J. F., Coleman, J. E.: *J. Mag. Res.* **29**, 375 (1978)
216. Koppenol, W. H., in: *Oxygen and Oxy-Radicals in Chemistry and Biology*, (eds.) Rogers, M. A. J., Powers, E. L., pp. 671, New York, Academic Press, Inc. 1981
217. Haffner, P. H., Coleman, J. E.: *J. Biol. Chem.* **248**, 6626 (1973)
218. Rotilio, G., Rigo, A., Calabrese, L., in: *Frontiers in Physicochemical Biology*, (ed.) Pullman, B., pp. 357, New York, Academic Press Inc. 1978
219. Rigo, A., Stevanato, R., Viglino, P., Rotilio, G.: *Biochem. Biophys. Res. Commun.* **79**, 776 (1977)
220. Strothcamp, K. G., Lippard, S. J.: *Biochemistry* **20**, 7488 (1981)
221. Bertini, I., Borghi, E., Luchinat, C., Scozzafava, A.: *J. Am. Chem. Soc.* **103**, 7779 (1981)
222. Cocco, D., Rossi, L., Barra, D., Bossa, F., Rotilio, G.: *FEBS Lett.* **150**, 303 (1982)
223. Cocco, D., Calabrese, L., Finazzi-Agrò, A., Rotilio, G.: *Biochim. Biophys. Acta* **746**, 61 (1983)
224. Malinowski, D. P., Fridovich, I.: *Biochemistry* **18**, 5909 (1979)
225. Borders, C. L., Jr., Johansen, J. T.: *Biochem. Biophys. Res. Commun.* **96**, 1071 (1980)
226. Bermingham-Mc Donogh, O., de Freitas, D. M., Kumamoto, A., Saunders, J. E., Blech, D. M., Borders, C. L., Jr., Valentine, J. S.: *Biochem. Biophys. Res. Commun.* **108**, 1376 (1982)
227. Cocco, D., Mavelli, I., Rossi, L., Rotilio, G.: *Biochem. Biophys. Res. Commun.* **111**, 860 (1983)
228. Rigo, A., Viglino, P., Rotilio, G., Tomat, R.: *FEBS Lett.* **50**, 86 (1975)
229. Calabrese, L., Cocco, D., Desideri, A.: *FEBS Lett.* **106**, 142 (1979)
230. de Freitas, D. M., Valentine, J. S.: *Biochemistry* **23**, 2079 (1984)
231. Salin, M. L., Wilson, W. W.: *Mol. Cell. Biochem.* **36**, 157 (1981)
232. Argese, E., Rigo, A., Viglino, P., Orsega, E., Marmocchi, F., Cocco, D., Rotilio, G.: *Biochim. Biophys. Acta* **787**, 205 (1984)
233. Getzoff, E. D., Tainer, J. A., Weiner, P. K., Kollman, P. A., Richardson, J. S., Richardson, D. C.: *Nature* **306**, 287 (1983)

234. Rigo, A., Marmocchi, F., Cocco, D., Viglino, P., Rotilio, G.: *Biochemistry* 17, 534 (1978)
235. Marmocchi, F., Mavelli, I., Rigo, A., Stevanato, R., Bossa, F., Rotilio, G.: *Biochemistry* 21, 2853 (1982)
236. Ose, D. E., Fridovich, I.: *J. Biol. Chem.* 251, 1217 (1976)
237. O'Neill, P., Fielden, E. M., Cocco, D., Rotilio, G., Calabrese, L.: *Biochem. J.* 205, 181 (1982)
238. Villafranca, J. J., Yost, F. J., Fridovich, I.: *J. Biol. Chem.* 249, 3532 (1974)
239. Villafranca, J. J.: *FEBS Lett.* 62, 230 (1976)
240. Slykhouse, T. O., Fee, J. A.: *J. Biol. Chem.* 251, 5472 (1976)
241. Fee, J. A., McClune, G. J., O'Neill, P., Fielden, E. M.: *Biochem. Biophys. Res. Commun.* 100, 377 (1981)
242. Barette, W. C., Jr., Sawyer, D. T., Fee, J. A., Asada, K.: *Biochemistry* 22, 624 (1983)
243. Benovic, J., Tillman, T., Cudd, A., Fridovich, I.: *Arch. Biochem. Biophys.* 221, 329 (1983)
244. Terech, A., Pucheault, J., Ferradini, C.: *Biochem. Biophys. Res. Commun.* 113, 114 (1983)
245. Joester, K. E., Jung, G., Weber, U., Weser, U.: *FEBS Lett.* 25, 25 (1972)
246. Brigelius, R., Hartmann, H.-J., Bors, W., Saran, M., Lengfelder, E., Weser, U.: *Hoppe-Seyler's Z. Physiol. Chem.* 356, 739 (1975)
247. Weser, U., Richter, C., Wendel, A., Younes, M.: *Bioinorg. Chem.* 8, 201 (1978)
248. Younes, M., Lengfelder, E., Zienau, S., Weser, U.: *Biochem. Biophys. Res. Commun.* 81, 576 (1978)
249. Weser, U., Sellinger, K.-H., Lengfelder, E., Werner, W., Strähle, J.: *Biochim. Biophys. Acta* 631, 232 (1980)
250. Deuschle, U., Weser, U.: *Inorg. Chim. Acta* 91, 237 (1984)
251. Weser, U., Lengfelder, E., Sellinger, K.-H., Schubotz, L. M.: Reactivity of Chelated Copper with Superoxide, in: *Inflammatory Diseases and Copper*, (ed.) Sorenson, J. R. J., pp. 513, Clifton, N. J., Humana Press 1982
252. Kimura, E., Sakonaka, A., Nakamoto, M.: *Biochim. Biophys. Acta* 678, 172 (1981)
253. Kimura, E., Yatsunami, A., Watanabe, A., Machida, R., Koike, T., Fujioka, H., Kuramoto, Y., Sumomogi, M., Kunimitsu, K., Yamashita, A.: *Biochim. Biophys. Acta* 745, 37 (1983)
254. Martin, A. E., Lippard, S. J.: *J. Am. Chem. Soc.* 106, 2579 (1984)
255. Weser, U., Schubotz, L. M., Lengfelder, E.: *J. Mol. Catal.* 13, 249 (1981)
256. Kubota, S., Yang, J. T.: *Proc. Natl. Acad. Sci. USA* 81, 3283 (1984)
257. Amar, C., Vilkas, E., Foos, J.: *J. Inorg. Biochem.* 17, 313 (1982)
258. Walshe, J. M.: Wilson's Disease, a Review, in: *The Biochemistry of Copper*, (eds.) Peisach, J., Aisen, P., Blumberg, W. E., pp. 475, New York, Academic Press 1966
259. Younes, M., Weser, U.: *FEBS Lett.* 78, 1247 (1977)
260. Lengfelder, E., Elstner, E. F.: *Hoppe Seyler's Z. Physiol. Chem.* 359, 751 (1978)
261. Lengfelder, E., Fuchs, C., Younes, M., Weser, U.: *Biochim. Biophys. Acta* 567, 492 (1979)
262. Robertson, P., Jr., Fridovich, I.: *Arch. Biochem. Biophys.* 203, 830 (1980)
263. Deuschle, U., Weser, U.: *Inorg. Chim. Acta* in the press.
264. Russanov, E. M., Ljutakova, S. G., Leutchev, S. I.: *Arch. Biochem. Biophys.* 215, 222 (1982)
265. Bergel, F., Bray, R. C.: *Biochem. J.* 73, 182 (1959)
266. Flohé, L., Loschen, G.: *Eur. J. Rheumatol. Inflamm.* 4, 183 (1982)
267. Pasternack, R. F., Skowronek, W. R., Jr.: *J. Inorg. Biochem.* 11, 261 (1979)
268. Pasternack, R. F., Bauth, A., Pasternack, J. M., Johnson, C. S.: *J. Inorg. Biochem.* 15, 261 (1981)
269. Halliwell, B., Gutteridge, J. M. C.: *Biochem. J.* 219, 1 (1984)
270. Halliwell, B.: *FEBS Lett.* 56, 34 (1975)
271. McClune, G. J., Fee, J. A., McCluskey, G. A., Groves, J. T.: *J. Am. Chem. Soc.* 99, 5220 (1977)
272. Ilan, Y. A., Czapski, G.: *Biochim. Biophys. Acta* 498, 386 (1977)
273. Diguiseppi, J., Fridovich, I.: *Arch. Biochem. Biophys.* 203, 145 (1980)
274. Butler, J., Halliwell, B.: *Arch. Biochem. Biophys.* 218, 174 (1982)
275. Bull, C., McClune, G. J., Fee, J. A.: *J. Am. Chem. Soc.* 105, 5290 (1983)
276. Cherrier, B., Dibold, Th., Weiss, R.: *Inorg. Chim. Acta* 19, 157 (1976)
277. Guillard, R., Latour, J.-M., Lecomte, C., Marchon, J.-C., Protas, J., Ripoll, D.: *Inorg. Chem.* 17, 1228 (1978)
278. McCandlish, E., Miksztal, A. R., Nappa, M., Sprenger, A. Q., Valentine, J. S., Stong, J. D., Spiro, T. G.: *J. Am. Chem. Soc.* 102, 4268 (1980)

279. Gilbert, D. L., in: *Oxygen and Living Processes*, (ed.) Gilbert, D. L., pp. 1, New York, Heidelberg, Springer Verlag 1981
280. Balentine, J. D.: *Pathology of Oxygen Toxicity*, New York, Academic Press 1982
281. Collman, J. P.: *Acc. Chem. Res.* **1**, 136 (1968)
282. Walling, C., in: *Oxidases and Related Redox Systems*, (eds.) King, T. E., Mason, H. S., Morrison, M., pp. 85, Oxford, Pergamon Press 1982
283. Lynch, R. E.: The Metabolism of Superoxide Anion and Its Progeny in Blood Cells, in: *Topics in Current Chemistry*, Vol. 108, (ed.) Boschke, F. L., pp. 35, Berlin, Heidelberg, New York, Springer Verlag 1984
284. Green, M. J., Hill, H. A. O.: *Chemistry of Dioxygen*, in: *Methods in Enzymology*, Vol. 105, (ed.) Packer, L., pp. 3, Orlando Florida, Academic Press, Inc. 1984
285. Brunori, M., Rotilio, G.: *Biochemistry of Oxygen Radical Species*, in: *Methods in Enzymology*, Vol. 105, (ed.) Packer, L., pp. 22, Orlando Florida, Academic Press, Inc. 1984
286. Fridovich, I.: *Oxygen Radicals, Hydrogen Peroxide, and Oxygen Toxicity*, in: *Free Radicals in Biology*, Vol. 1, (ed.) Pryor, W., pp. 239, New York, Academic Press 1976
287. Haber, F., Weiss, J.: *Proc. R. Soc. London Ser. A* **147**, 332 (1934)
288. Fenton, H. J. H.: *J. Chem. Soc.* **65**, 899 (1894)
289. Cohen, G., Sinet, P. M.: Fenton's Reagent — Once more Revisited, in: *Chemical and Biochemical Aspects of Superoxide and Superoxide Dismutase*, (eds.) Bannister, J. V., Hill, H. A. O., pp. 27, New York, Amsterdam, Elsevier/North-Holland 1980
290. Fridovich, I.: Overview: Biological Sources of O_2^- , in: *Methods in Enzymology*, Vol. 105, (ed.) Packer, L., pp. 59, Orlando Florida, Academic Press Inc. 1984
291. Chance, B., Sies, H., Boveris, A.: *Physiol. Rev.* **59**, 527 (1979)
292. Gutteridge, J. M. C., Rowley, D. A., Halliwell, B.: *Biochem. J.* **199**, 263 (1981)
293. Gutteridge, J. M. C., Wilkins, S. J.: *Biochim. Biophys. Acta* **759**, 38 (1983)
294. Aronovitch, J., Godinger, D., Samuni, A., Czapski, G.: The Effect of Cell-Bound Copper on the Toxicity of Superoxide and Vitamin C, in: *Oxygen Radicals in Chemistry and Biology*, (eds.) Bors, W., Saran, M., Tait, D., pp. 219, Berlin, New York, Walter de Gruyter & Co 1984
295. Rowley, D. A., Halliwell, B.: *Arch. Biochem. Biophys.* **225**, 279 (1983)
296. Sorenson, J. R. J.: Copper Complexes as the Active Metabolites of the Antiinflammatory Agents, in: *Inflammatory Diseases and Copper*, (ed.) Sorenson, J. R. J., pp. 289, Clifton, New Jersey, Humana Press 1982
297. Deuschle, U., Weser, U.: Copper and Inflammation, in: *Progress in Clinical Biochemistry and Medicine*, Vol. 2, in the press, Berlin, Heidelberg, New York, Springer Verlag 1985
298. Afanas'ev, I. B., Kuprianova, N. S., Letuchaia, A. V.: New Mechanism of the Reaction of O_2^- with H_2O_2 : Significance for Biology, in: *Oxygen Radicals in Chemistry and Biology*, (eds.) Bors, W., Saran, M., Tait, D., pp. 17, Berlin, New York, Walter de Gruyter & Co 1984
299. Halliwell, B.: *Biochem. J.* **205**, 461 (1982)
300. Winterbourn, C. C.: *Biochem. J.* **205**, 463 (1982)
301. Rigo, A., Scarpa, M., Argese, E., Ugo, P., Viglino, P.: Generation of Superoxide in the Autoxidation of Ascorbate and Glutathione, in: *Oxygen Radicals in Chemistry and Biology*, (eds.) Bors, W., Saran, M., Tait, D., pp. 171, Berlin, New York, Walter de Gruyter & Co 1984
302. Hassan, H. M., Fridovich, I.: *J. Bacteriol.* **129**, 1574 (1977)
303. Hassan, H. M., Fridovich, I.: *J. Biol. Chem.* **252**, 7667 (1977)
304. Shatzman, A. R., Kosman, D. J.: *J. Bacteriol.* **137**, 313 (1979)
305. Archibald, F. S., Fridovich, I.: *J. Bacteriol.* **146**, 928 (1981)
306. Meier, B., Barra, D., Bossa, F., Calabrese, L., Rotilio, G.: *J. Biol. Chem.* **257**, 13977 (1982)
307. Yamakura, F.: *Biochim. Biophys. Acta* **422**, 280 (1976)
308. Yamo, K., Nishie, H.: *J. Gen. Appl. Microbiol.* **24**, 333 (1978)
309. Gregory, E. M., Dapper, C. H.: *Arch. Biochem. Biophys.* **220**, 293 (1983)
310. Moody, C. S., Hassan, H. M.: *J. Biol. Chem.* **259**, 12821 (1984)
311. Martin, M. E., Strachan, R. C., Aranha, H., Evans, S. L., Salin, M. L., Welsch, B., Arceneaux, E. L., Byers, B. R.: *J. Bacteriol.* **159**, 745 (1984)
312. Pugh, S. Y. R., Diguseppi, J. L., Fridovich, I.: *J. Bacteriol.* **160**, 137 (1984)
313. Grieger, M., Schulz, S.: *Folia Haematol. (Leipz.)* **110**, 427 (1983)
314. Reiss, U., Gershon, D.: *Eur. J. Biochem.* **63**, 617 (1976)
315. Bartosz, G., Tannert, Ch., Fried, R., Leyko, W.: *Experientia* **34**, 1464 (1978)

316. Tolmasoff, J. M., Ono, T., Cutler, R. G.: *Proc. Natl. Acad. Sci. USA* 77, 2777 (1980)
317. Glass, G. A., Gershon, D.: *Biochem. Biophys. Res. Commun.* 103, 1245 (1981)
318. Goscin, S. A., Fridovich, I.: *Radiat. Res.* 56, 565 (1973)
319. Michelson, A. M., Buckingham, M. E.: *Biochem. Biophys. Res. Commun.* 58, 1079 (1974)
320. Petkau, A., Chelack, W. S., Pleskach, S. D., Meeker, B. E., Brady, C. M.: *Biochem. Biophys. Res. Commun.* 65, 886 (1975)
321. Misra, H. P., Fridovich, I.: *Arch. Biochem. Biophys.* 176, 577 (1976)
322. Petkau, A., Chelack, W. S., Pleskach, S. D.: *Int. J. Radiat. Biol.* 29, 297 (1976)
323. Krizala, J., Stoklasová, A., Kovárová, H., Ledvina, M.: *Radiat. Res.* 91, 507 (1982)
324. Kovárová, H., Krizala, J., Dostal, M.: *Stud. Biophys.* 87, 41 (1982)
325. Bartosz, G., Leyko, W., Fried, R.: *Experientia* 35, 1194 (1979)
326. Rigo, A., Viglino, P., Argese, E., Terenzi, M., Rotilio, G.: *J. Biol. Chem.* 254, 1729 (1979)
327. Scarpa, M., Viglino, P., Rigo, A.: *Biochem. Biophys. Res. Commun.* 122, 1276 (1984)
328. Rigo, A., Ugo, P., Viglino, P., Rotilio, G.: *FEBS Lett.* 132, 78 (1981)
329. Misra, H. P., Fridovich, I.: *J. Biol. Chem.* 247, 6990 (1972)
330. Sawyer, D. T., Valentine, J. S.: *Acc. Chem. Res.* 14, 393 (1981)
331. Roberts, J. L., Sawyer, D. T.: *J. Am. Chem. Soc.* 103, 712 (1981)
332. Babior, B. M.: *New Engl. J. Med.* 298, 659 (1978)
333. Johnston, R. B., Jr., Godzik, C. A., Cohn, Z. A.: *J. Exp. Med.* 148, 115 (1978)
334. Valentine, J. S., Pantoliano, M. W.: *Protein-Metal Ion Interactions in Cuprozin Protein (Superoxide Dismutase)*, in: *Copper Proteins*, (ed.) Spiro, T. G., pp. 291, New York, John Wiley 1981
335. Cocco, D., Mavelli, I., Rotilio, G., Hartmann, H.-J., Weser, U.: submitted
336. Hartmann, H.-J., Morpurgo, L., Desideri, A., Rotilio, G., Weser, U.: *FEBS Lett.* 152, 94 (1983)
337. Morpurgo, L., Hartmann, H.-J., Desideri, A., Weser, U., Rotilio, G.: *Biochem. J.* 211, 515 (1983)
338. Hartmann, H.-J., Gärtner, A., Weser, U.: *Hoppe Seyler's Z. Physiol. Chem.* 365, 1355 (1984)
339. Mavelli, I., Ciriolo, M. R., Rotilio, G., De Sole, P., Castorino, M., Stabile, A.: *Biochem. Biophys. Res. Commun.* 106, 286 (1982)
340. Mavelli, I., Rigo, A., Federico, R., Ciriolo, M. R., Rotilio, G.: *Biochem. J.* 204, 535 (1982)
341. Aebi, H., Suter, H.: *Advan. Hum. Genet.* 2, 143 (1971)
342. Mc Neil, C. J., Banford, J. C., Brown, D. H., Smith, W. E.: *FEBS Lett.* 133, 175 (1981)
343. Lynch, R. E., Cole, B. C.: *Biochem. Biophys. Res. Commun.* 96, 98 (1980)
344. Nettleton, C. J., Bull, C., Baldwin, T. O., Fee, J. A.: *Proc. Natl. Acad. Sci. USA* 81, 4970 (1984)
345. Fried, R.: *Metabolic Role of Xanthine Oxidase as Source of Superoxide Radicals and Hydrogen Peroxide*, in: *Chemical and Biochemical Aspects of Superoxide and Superoxide Dismutase*, (eds.) Bannister, J. V., Hill, H. A. O., pp. 65, New York, Amsterdam, Oxford, Elsevier/North-Holland 1980

Hemoglobin Model — Artificial Oxygen Carrier Composed of Porphinatoiron Complexes

Eishun Tsuchida and Hiroyuki Nishide

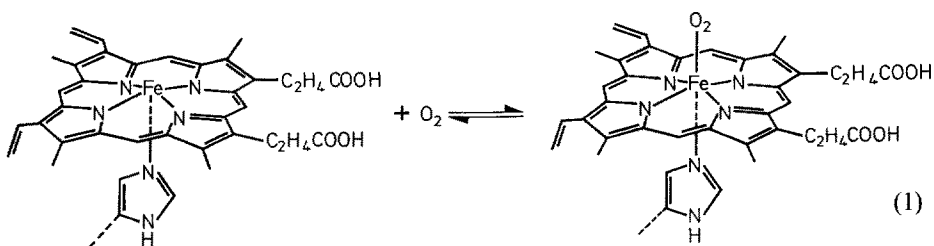
Department of Polymer Chemistry, Waseda University, Tokyo 160, Japan

Table of Contents

1 Introduction	64
2 Modified Porphinatoirons as Oxygen Carriers	66
3 Oxygen-Binding to Polymer-Bound Porphinatoirons	72
4 Structure of Liposome-Embedded Porphinatoirons	79
5 Oxygen Transporting Profile	88
6 Approach to a Blood Substitute	92
7 Conclusion and Further Studies	95
8 References	96

1 Introduction

The respiratory proteins, hemoglobin (Hb) and myoglobin (Mb), serve to transport and to store molecular oxygen in a living body. Hb is a conjugated protein with molecular weight 64,450 and consists of four polypeptide chains (globin proteins), each of which has a protoporphinatoiron IX group (protoheme). Mb consists of a single globin protein and a protoheme which are very similar to the single chain of Hb. Hb and Mb are the proteins which are easily and purely isolated from a living body, and their primary, secondary and tertiary structures are early and accurately investigated. A clear view of the structures of Hb and Mb is now shown ^{1, 2)}. The globin chain has a globular and compact conformation, and the heme group is embedded in the 'pocket' of the globular protein. The heme coordinately bonds to the imidazole of the histidine residue of the pocket-forming segment of globin and becomes the oxygen binding site, as shown in Eq. (1). The hydrophobic character of the space inside of the heme pocket, caused by the surrounding hydrophobic amino acid residues, seems to relate to the oxygen-binding function of Hb and Mb, as will be discussed later ^{3, 4)}.



On exposure of the Hb solution to oxygen, the heme complex (deoxy type) forms its oxygen adduct (oxy type) [Eq. (1)] and turns brilliant red. 1 mol Hb binds 4 mol oxygen, i.e. 1 g of Hb adsorbs 1.34 ml of oxygen at 37 °C under oxygen atmosphere. 100 ml of the blood of human adults uptakes 23 ml of oxygen, which is about 10 times of the volume physically uptaken by water and serum ⁵⁾.

Typical curves of oxygen-binding vs the partial pressure of oxygen (P_{O_2}) under physiological conditions are shown in Fig. 1 for Hb and Mb. The oxygen binding affinity of Hb is remarkably reduced at low P_{O_2} . However, once oxygen begins to bind, the oxygen binding affinity increases successively, and the binding curve becomes sigmoidal (i.e. cooperative binding). On the other hand, the oxygen reservoir Mb has a greater oxygen affinity than Hb at any P_{O_2} and its curve is of a hyperbolic type. Hb adsorbs oxygen with 95% of the binding saturation in the lungs (P_{O_2} = ca. 100 mmHg), and desorbs oxygen (the binding is reduced to 72%) in the terminal tissue (P_{O_2} = ca. 40 mmHg), and gives it to Mb in the tissue. Thus Hb effectively transports molecular oxygen from the lungs to the terminal tissue although there is only a small difference in P_{O_2} .

If the oxygen-binding site, the heme complex, is isolated from Hb and Mb and exposed to oxygen in a solution, the heme complex is immediately and irreversibly oxidized to its ferric [iron (III)] complex and it does not act as an oxygen carrier.

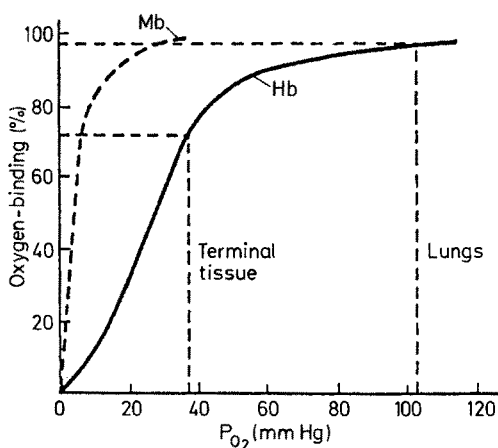


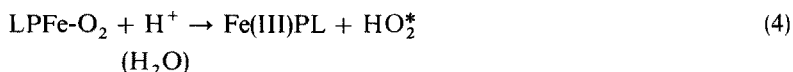
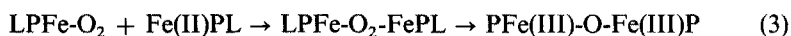
Fig. 1. Oxygen-binding curves of Hb and Mb

The reasons for the oxygen-binding by Hb and Mb are considered to be as follows⁶⁻⁸⁾:

- (i) The heme complex has a five-coordinate structure whose sixth coordination site is vacant to bind molecular oxygen [Eq. (2)].
- (ii) The heme complex is dispersed and diluted to suppress the irreversible oxidation via μ -dioxo dimer [Eq. (3)].
- (iii) The heme complex is surrounded by the hydrophobic environment causing the proton-driven oxidation [Eq. (4)] to be retarded.



Reversible Oxygen-binding



Irreversible Oxidation

In (2)–(4) FeP, Fe(II)P, and Fe(III)P represent porphinato-iron, -iron(II), and -iron(III), respectively, and L is an axial ligand such as an imidazole derivative.

Globin protein forms the five-coordinate heme complex and ‘tucks’ it separately, i.e. globin protein protects the heme complex from the oxidation [Eq. (3)] by embedding it separately in the macromolecule, and the hydrophobic domain of the globular protein excludes water molecules and suppresses the protein-driven oxidation [Eq. (4)].

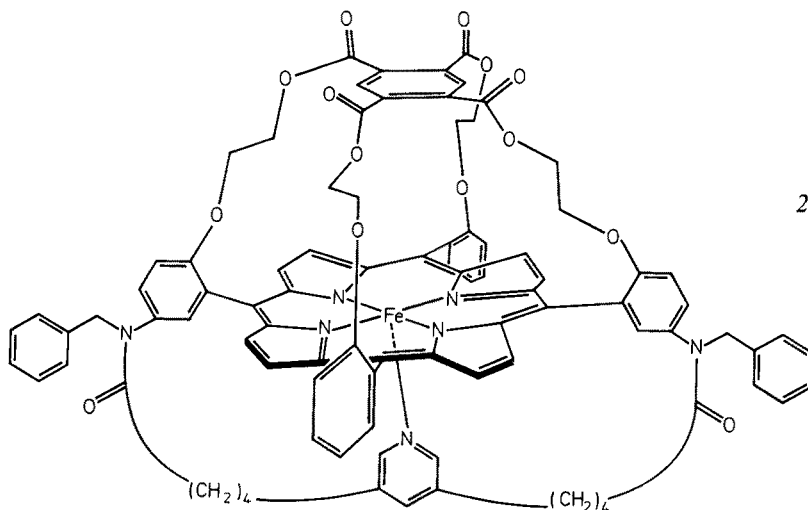
Since a decade ago, much research has been directed to mimic the oxygen carrier like Hb by synthesizing various modified porphinatoiron derivatives⁹⁻¹¹⁾. These synthetic porphinatoirons have been successful in oxygen-binding reversibly in organic solvents and solid states, but in aqueous media they have been irreversibly oxidized. Till recently, only Hb and Mb are known as oxygen carriers in aqueous media.

The purpose of this article is the discussion how to mimic the oxygen transporting function of Hb by using a porphinatoiron complex in "aqueous media", because various extensive investigations on porphinatoiron complexes as an oxygen carrier have been reported but most of these were restricted to the oxygen-binding reaction in non-aqueous media⁹⁻¹¹). Thus the discussion here will be centered not only on the study of the active site (porphinatoiron complexes) but also on effects of the environment (globin proteins) surrounding the active site. We describe in this article first briefly the advance in modified porphinatoirons as oxygen carriers and then mainly our attempt to replace the roles of the globin protein with a synthetic macromolecule or a macromolecular assembly, including our approaching study to a blood substitute.

2 Modified Porphinatoirons as Oxygen Carriers

Much recent work has been aimed at overcoming the requisites for the reversible oxygen-binding to a porphinatoiron complex (i)–(iii) and has been partially successful in aprotic solvents. In aprotic solvents the proton-driven oxidation [(iii), Eq. (4)] is excluded, so that the problems of reversible oxygen-binding are how to form the five-coordinate complex as deoxy state (i) and how to inhibit the irreversible oxidation via dimerization [(ii), Eq. (3)]. The successful approach was an elegant steric modification of porphyrins: Porphyrins have been substituted in a fashion that satisfies (i) and (ii). Some interesting porphinatoirons have been produced by clever synthetic techniques: capped porphinatoirons¹²), bridged porphinatoirons¹³⁻¹⁶), fenced porphinatoirons^{17,18}), imidazole-chelated porphinatoirons¹⁹), etc. A typical example is Collman's 'picket-fence' porphinatoiron: tetra($\alpha,\alpha,\alpha,\alpha$ -o-pivalamidophenyl)porphinatoiron (*1*)^{17,20}). *1* has steric bulkiness constructed with the pivalamido groups on one side of the porphyrin plane and leaves the other side unencumbered. The imidazole ligand is allowed to coordinate to the unhindered side of the porphinatoiron, with the other side of the porphinatoiron remaining as a pocket for oxygen-binding. Moreover the fence would discourage the dimerization of a μ -dioxo complex. The *1* imidazole complex could bind molecular oxygen reversibly in dry benzene at room temperature over a week. This result means that a skelton structure and a special environment around the oxygen-binding site are important to form the reversible oxygen adduct. As several reviews of the oxygen-binding to modified porphinatoirons have appeared^{9-11,21-24}), only a brief discription on the advance in it in these few years is appropriate here.

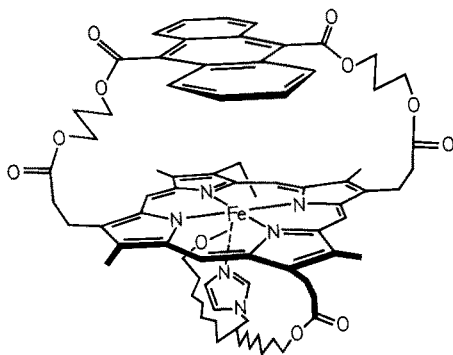
Modification at the porphyrin plane becomes recently more skilful and complicated. Starting from tetraphenylporphinatoiron, Baldwin et al.²⁵) built up 'capped strapped' porphinatoiron *2* which underwent reversible oxygen-binding in toluene. The irreversible oxidation product of *2* was not a μ -oxo dimer but was an iron(III) species, which indicates perfect inhibition of the irreversible oxidation step via dimerization [Eq. (3)]. Although the oxygen adduct of *2* has an extremely long life-time compared with other porphinatoiron complexes, the oxygen-binding affinity was too much reduced and only a small amount of the oxygen adduct existed at room temperature. The latter result was considered to be ascribed to locking or unfavourable steric interactions of the parent porphinatoiron in the 'domed' configuration (see the structure of *2*).



Momenteau et al.²⁶⁾ synthesized 'hanging imidazole' porphinatoiron where one strapping group contained an imidazole group as the axial ligand of the parent porphinatoiron and the other strapping group was a simple alkyl chain bridging over the oxygen-binding site. This porphinatoiron has a relatively high affinity for oxygen-binding and the life-time of the oxygen adduct was about one day in dry toluene. The kinetic constants for the oxygen and carbon monoxide (CO)-binding indicated the importance of the coordinated hanging imidazole in stabilization.

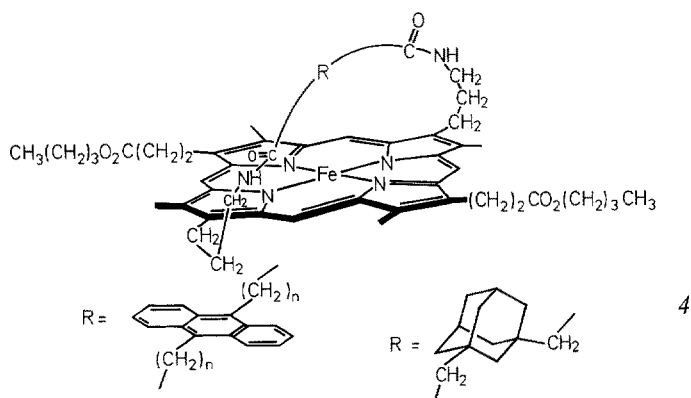
Oxygen-binding to tetra(2',4',6'-triphenyl)porphinatoiron was reported by Suslick et al.²⁷⁾. This porphinatoiron has two 'pockets' formed by phenyl substitutes on both faces of the porphyrin. The gaseous molecule-binding affinity was studied in benzene solution: The pocket structure minimized the solvation of the coordinated oxygen and of CO and influenced the affinity ratio of oxygen/CO. But the life-time of the oxygen adduct was not enhanced in comparison with that of *I*.

The use of the porphinatoirons having meso-hydrogens is important for a more accurate model of the active site of Hb, because it leads to the visible absorption spectral features and porphyrin-cleavage reactions very similar to those of natural protoporphinatoiron IX (protoheme) isolated from Hb and Mb. However, the



synthesis and chemical modification of these porphinatoirons are more difficult than those of tetraphenylporphinatoirons and resistivity of their oxygen adducts against irreversible oxidation is not good due to the smaller reduction potential of these porphinatoirons in comparison with that of tetraphenylporphinatoirons. Starting from the porphinatoiron having 4 meso-hydrogens, Battersby et al.²⁸⁾ synthesized doubly bridged porphinatoiron **3**, which has a cavity formed on one face by an 'anthracene-containing bridge and an imidazole group strapped across the other face. **3** was reported to bind oxygen stable for almost 2 days in DMF at room temperature.

Traylor et al. kinetically studied the oxygen- and CO-binding to the porphinatoirons when they are solubilized both in organic solvents and suspended in a micellar medium^{11, 19, 29)}. The kinetic study for the oxygen-binding in the aqueous medium was carried out with a flash photolysis technique in the coexistence of CO which protects the porphinatoirons against rapid irreversible oxidation and makes a moment observation of the unstable oxygen adduct possible in the aqueous medium. They pointed out that the simple imidazole-chelated meso- and proto-porphinatoiron, which maintain preferentially the five-coordinate structure, are already a kinetically good model of the oxygen-binding to Hb and that the globin protein is not absolutely necessary, in principle. Subsequently, they synthesized a series of 'cyclophane porphinatoiron' derivatives **4**, containing an anthracene or an adamantane group strapped symmetrically over the porphyrin, to provide hindrance toward the oxygen- and CO-binding and to discriminate the binding of oxygen/CO. Recently, they summarized steric effects in the binding to these hindered porphinatoirons³⁰⁾. The oxygen- and CO-binding affinity, especially the latter, were certainly reduced and closed to those of Hb for **4** in comparison with unhindered porphinatoirons. But they concluded that steric effects are manifested primarily in the binding step of gaseous molecules and that the reported bending or tilting of the coordinated CO in Hb is of minor chemical significance for the synthetically hindered **4** composed of conformationally mobile caps.



Diporphinatometal derivatives **5** were first synthesized by Chang et al.³¹⁾. They reported that the imidazole complex of diporphinatocopper-iron **5a** ($M_1 = \text{Cu(II)}$, $M_2 = \text{Fe(II)}$ in **5**) reversibly forms its oxygen adduct and the life-time of the oxygen adduct is fairly long and comparable to that of the **1** complex in dry benzene at room temperature³²⁾. Molecular oxygen binds to the porphinatoiron through opening of

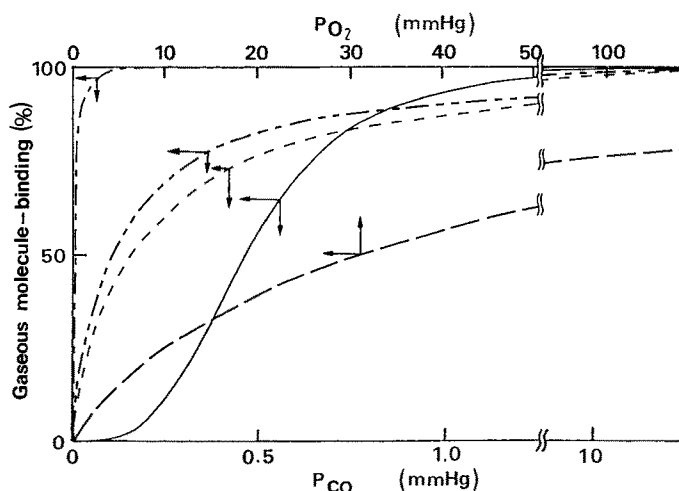
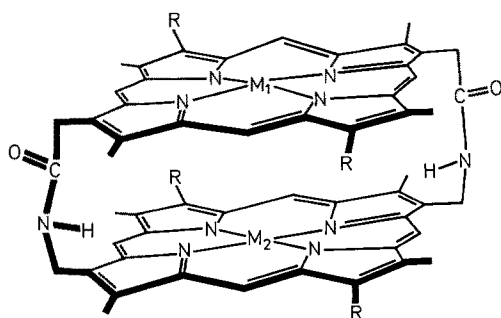


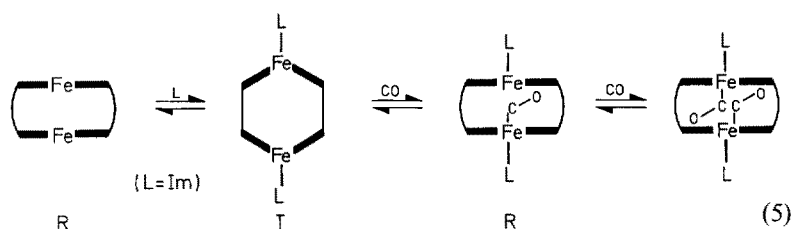
Fig. 2. Oxygen- and carbon monoxide-binding curves of the 5 complexes in benzene (—) *5b*, (---) *5c*, (·····) *9a*, (-·-·-) *5a*, (—) *5a*

the face-to-face structure of diporphyrin. It was considered that the inert prophinato-copper, tightly linked to the porphinatoiron, protects the porphinatoiron-oxygen adduct. The CO-binding affinity of the *5a* complex was much reduced and similar to that of Hb compared to those of unmodified, planar porphinatoiron complexes, as shown in Fig. 2^{32,33}), also due to the sterically hindering effect of the porphinato-copper cap effectively covering the gaseous molecule-binding site.



Diporphinatodiiron *5b* ($M_1 = M_2 = \text{Fe(II)}$ in 5) showed the same reduced affinity to CO, whereas it bound two CO molecules due to the diiron structure³⁴). The CO-binding equilibrium curve for the *5b*-imidazole complex appears sigmoidal, while the curves for the *5a*-imidazole complex and the imidazole complex of diporphinatoiron *5c* ($M_1 = \text{Fe(II)}$, $M_2 = 2 \text{ H}$ in 5) are hyperbolic³⁵). The cooperative parameter (n)³⁶) was estimated for the CO-binding to *5b* to be 3.4 which meant a strong cooperativity in the binding reaction, while those for *5a* and *5c* were unity (n for Hb = 2.8, n for Mb = 1.0).

To explain this pseudo-cooperative CO-binding phenomenon, the following porphinatoiron-porphinatoiron interaction was proposed by a binding-kinetic and X-ray crystallographic study³⁴⁾. For *5b*, planar porphinatoirons linked covalently in a parallel and stable face-to-face structure [probably corresponding to 'relaxed (R)' state of Hb³⁷⁾, see Scheme (5)]. For the *5b*-imidazole complex, two imidazole ligands coordinate to the porphinatoiron only from the outward-facing side: This leads to the five-coordinate and high-spin porphinatoiron complex where the iron ions lie slightly out of the plane and the porphyrin planes are distorted [probably corresponding to 'tense (T)' state of Hb³⁷⁾]. When one of the porphinatoiron-imidazole complexes of *5b* combines with CO, the T structure changes to that of the six-coordinate and the low-spin CO complex and the porphyrin plane combined with CO becomes strictly planar. This structural change of the first reacted porphinatoiron induces the faced and distorted porphyrin to return the planar R state, which facilitates the CO binding to this second porphinatoiron.

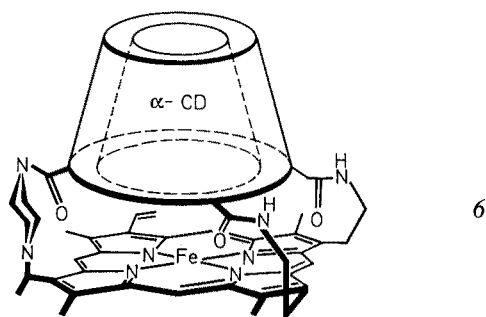


The similar cooperative binding of the *5b*-imidazole complex was observed with oxygen in cooled toluene but a quantitative result was not given due to the short lifetime of the *5b*-oxygen adduct. Anyhow, the cooperative binding of the synthetic *5b* with gaseous molecules was produced by trigger of a structural change of the coupling binding-sites (porphinatoirons) and was a good model of the cooperative binding of Hb where conformational change of the globin protein induces the reactivity change of heme.

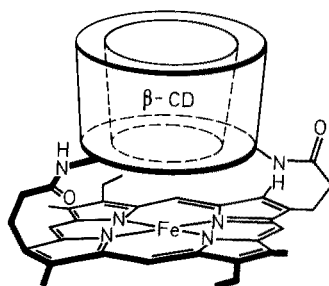
The above mentioned studies on the modified porphinatoirons are of great significance because they have demonstrated steric and environmental effects on the oxygen-binding reaction. But in these studies the discussions were restricted to mimic the secondary functions in oxygen-transporting Hb and Mb such as the resistivity to endogenous CO poisoning and the cooperative binding profile, i.e. steric influences of the modifying groups on the binding affinity ratio of O₂/CO or on the cooperativity in gaseous molecule-binding, and the oxygen-binding ability itself for these compounds in aqueous media was unfortunately not described.

A water-soluble and modified porphinatoiron was recently reported³⁸⁾. Cyclodextrin was used as the sterically protective group covering one face of the porphyrin plane. Protoporphinatoiron IX or porphinatoiron derivatives were coupled with α - or β -cyclodextrin with 2–4 covalent bonds to lead to a series of cyclodextrin-capped porphinatoirons. Examples are 6, where the secondary hydroxy groups (larger bottom) of the α -cyclodextrin were combined with protoporphinatoiron IX with three urethane bonds, and 7, where the primary hydroxy groups (smaller bottom) of β -cyclodextrin were coupled with porphinatoiron dicarboxylic acid with two amido bonds. The ¹³C-NMR spectral data for the corresponding iron-free porphyrin deriva-

tives supported their cyclodextrin-capping structure: The carbon signals of the cyclodextrin were shifted to upper field by diamagnetic ring current of the suspended porphyrin. A hydrophobic effect of the capping cyclodextrin was also confirmed by a fluorescence spectrum of the corresponding porphinatozinc derivatives in aqueous media. These compounds formed five-coordinate deoxy complexes with a sterically bulky and water-soluble imidazole ligand, due to the one face-hindering structure provided by the capping cyclodextrin³⁹⁾. Some of these imidazole complexes of the cyclodextrin-capped porphinatoirons, e.g. 6 and 7, formed semi-stable oxygen adducts



6



7

in an aqueous medium cooled at -10 to -30 °C (water/ethylene glycol as an anti-freeze agent = 1/1 v/v), whereas non-modified porphinatoiron-imidazole complexes were rapidly and irreversibly oxidized under the same conditions. The spectrum of the oxygen adduct changed to that of the CO adduct upon bubbling CO gas through the solution and returned to the deoxy complex after careful bubbling of nitrogen gas. This indicates that the ferrous state of the central iron ion was not changed during the exposure to oxygen and also the reversible oxygen-binding in the aqueous medium. It was considered that a toroidal shape structure with a hydrophobic inside moiety of the capping cyclodextrin keeps the sixth coordination site vacant for oxygen-binding, prevents the irreversible oxidation via dimerization, and provides a hydrophobic cavity for the bound oxygen to retard the proton-driven oxidation.

The effect of the hydrophobic cyclodextrin cavity of 7 was enhanced and the life-time of the 7-oxygen adduct was prolonged to about 1 hr in the aqueous medium at -10 °C when a drop of benzene was dispersed in the aqueous medium of the deoxy-7 imidazole complex. The benzene was probably occluded in the cavity of the capping cyclodextrin⁴⁰⁾. However, the life-time decreased with temperature of the aqueous medium and the oxygen adduct was scarcely observed above 0 °C. The steric and

hydrophobic effects of the modifying group on the porphyrin plane were limited ones in aqueous media.

As described above, the modification of porphinatoiron becomes more skilful and complicated in these few years. But often, the visible absorption spectra of these highly modified porphinatoirons were not similar to those of the parent porphinatoirons and the central iron ion was eliminated from the porphyrin planes even under mild conditions. This means that a strain is introduced to the porphyrin plane by the strapping or capping structure over the plane and by substitution with too excessively bulky groups on the plane. There is a limitation for the approach to give a porphinatoiron oxygen-binding ability under severe conditions such as in aqueous media by modifying porphyrin itself.

3 Oxygen-Binding to Polymer-Bound Porphinatoirons

In Hb and Mb the globin protein protects the porphinatoiron complexes which are tucked separately into a hydrophobic domain of the protein. A "syntetic" polymer might be expected to protect the oxygen adduct against irreversible oxidation in much the same way as the globin protein does. In a classic experiment Wang⁴¹ reported the first synthetic oxygen carrier of porphinatoiron based on the use of a solid polymer. He embedded the phenylethylimidazole complex of the diethyl ester of protoporphinatoiron IX in a polystyrene film which combined slowly but reversibly with molecular oxygen and remained stable for a few days without irreversible oxidation. He considered that the hydrophobic polystyrene matrix excluded water molecules and the isolation of the porphinatoiron complex from each other by the matrix prevented the oxidation via dimerization.

Oxygen-binding to porphinatoiron complexes attached to polymers in the solid state was successively reported. For example, tetraphenylporphinatoiron was coordinated to silica gel which contained an imidazolyl group⁴¹, and protoporphinatoiron was complexed with poly(vinylpyridine) in the solid state^{42,43}. Protoporphinatoiron IX was also covalently introduced to a polymer chain by using the polymerizability of the 2,4-vinyl groups of protoporphyrin. It could be copolymerized with vinyl monomers such as styrene, methyl methacrylate, and vinylimidazole combining at one end of the polymer chain by use of a radical initiator⁴⁴ or γ -ray irradiation⁴⁵. The obtained films or beads containing the porphinatoiron complex adsorbe oxygen and cyanide ions in the solid state. But in general, the oxygen-binding occurred very slowly in the solid state and its rate depended upon the surface condition or gas permeability of the polymer matrix. Thus, the attempt should be made to synthesize a polymer-bound porphinatoiron which will form a stable oxygen adduct in a homogeneous solution.

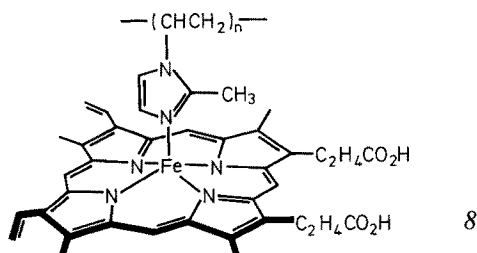
We have already studied the chemical properties of the synthetic polymer-metal complexes in homogeneous solution and have found that the chemical reactivity of a metal complex is often affected by a polymer that exists outside the coordination sphere and surrounds the metal complex⁴⁶⁻⁴⁸. The effects of polymers have been summarized under the following two terms:

- (i) the steric effect, which is determined by the conformation and density of the polymer chain, and
- (ii) the special environment constituted by a polymer chain.

From this point of view, we synthesized oxygen carriers in aqueous solution by combining porphinatoiron complexes with water-soluble synthetic polymers.

The most simple example is the water-soluble complex of poly(1-vinyl-2-methylimidazole) (PMI) and protoporphinatoiron IX (protoheme) **8**. PMI with molecular weight $>10^4$ predominantly forms a five-coordinate complex **8** with protoheme in aqueous media, of which stability was shown by the following result ⁴⁹⁾. It is known that protoheme simultaneously combines two nitrogeneous ligands in aqueous media, e.g. bis(imidazole)-coordinated heme with an extra large formation constant. When a small amount of PMI was added to the six-coordinate heme-imidazole complex solution, PMI selectively transferred the stable six-coordinate low-spin imidazole complex into the five-coordinate and high-spin **8** complex. Excess addition of the low-molecular weight analogue 2-methylimidazole did not bring about the structure change of protoheme. The polymeric PMI ligand forms the five-coordinate deoxy heme complex even in the presence of a large amount of compounds with coordinating ability such as imidazole. A study on the shape of the polymer complex **8** indicated that the polymer chain markedly contracts upon complexation with protoheme. The polymer-heme complex adopts a very compact structure in aqueous media, protoheme being occluded within the contracted polymer chain.

The six-coordinate heme complexes of imidazoles are known to be immediately oxidized upon exposure to oxygen. Irreversible oxidation was also observed for the



five-coordinate heme complexes of 2-methylimidazoles and for the polymeric six-coordinate heme complex of poly(1-vinylimidazole) even at low temperature. However, the polymeric five-coordinate PMI-heme complex **8** showed a spectrum (410, 545, and 577 nm) of its oxygen adduct which perfectly agreed with that of oxyHb (414, 542, and 578 nm) when its aqueous solution (water/ethylene glycol) was cooled to -10 to -30 °C and exposed to oxygen ^{50,51)}. The oxy-spectrum returned to that of deoxy-heme on bubbling nitrogen through, and this oxy-deoxy cycle was repeated several times at -30 °C.

The deoxy **8** complex which was enzymatically reduced from the corresponding protohemin [Fe(III)] complex with a reductase system gave the oxygen adduct with the same spectrum and life-time ⁵²⁾. Oxygen-binding was also observed with the deuteroporphinatoiron complex of PMI. Reversible oxygen-binding in the cold aqueous medium was further supported by a flash-photolysis reaction of the oxygen-adduct ⁵¹⁾ and Mössbauer parameters of the complexes ⁵³⁾.

Only the five-coordinate heme complex with the polymeric ligand forms an oxygen adduct in the cold aqueous solution. This polymer complex contrasts with the low-molecular-weight heme complex of 2-methylimidazoles in that it binds oxygen

reversibly, whereas the latter ($[2\text{-methylimidazole}]/[\text{heme}] = 10^3\text{--}10^4$) which show the same spectra as the deoxy-heme and the heme-CO complexes, are irreversibly oxidized.

Figure 3 shows the effect of the molecular weight of the PMI ligand on the life-time of the oxygen adduct; the molecular weight has to be high ($> 10^4$) to give the oxygen adduct in aqueous solution⁵¹⁾. The composition of the polymeric ligand affected the oxygen-binding. The oxygen adduct was observed only for the heme complexes with the non-ionic polymers, PMI, and the copolymers of 1-vinyl-2-methylimidazole with 1-vinyl-2-pyrrolidone and with acrylamide, and not with the ionic copolymers of 1-vinyl-2-methylimidazole with methacrylic acid and with 1-vinyl-2-methyl-3-benzyl-imidazolium chloride. The ionic residues of the polymer, carboxylate and imidazolium, had undesirable effects on the oxygen-binding. The life-time of the oxygen adduct was also influenced by the composition of the copolymer ligand for the heme complexes with the copolymers of 1-vinyl-2-methylimidazole with 1-vinyl-2-pyrrolidone and with acrylamide. The life-time decreased with increasing content of comonomer, according to the hydrophilicity of the copolymer.

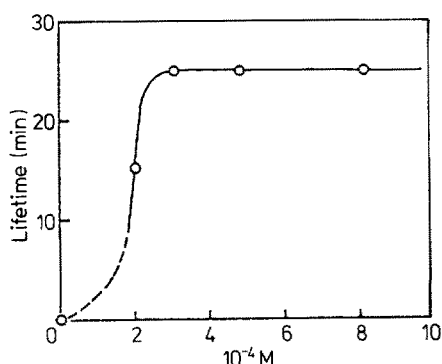


Fig. 3. Effect of the molecular weight of the PMI ligand on the life-time of the oxygen adduct in cold aqueous medium

The oxygen adduct of **8** was decayed to the corresponding protohemin [Fe(III)] complex with isosbestic points, and this decay obeyed first-order kinetics. The life-time of the **8**-oxygen adduct was increased with the pH of the aqueous solution. Its life-time was independent of the heme concentration. These results indicate that the irreversible oxidation [to Fe(III)] of the heme-oxygen adduct with the polymeric ligand proceeds mainly via a monomolecular process caused by the attack of a proton on the heme-coordinated oxygen (proton-driven oxidation) rather than via a μ -dioxo dimer.

The effect of additives on the oxygen-binding to **8** is interesting. The oxygen adduct was formed in aqueous ethylene glycol solution regardless of its ethylene glycol content, but it was destroyed by adding alcohol or urea, as was oxyHb⁵⁴⁾.

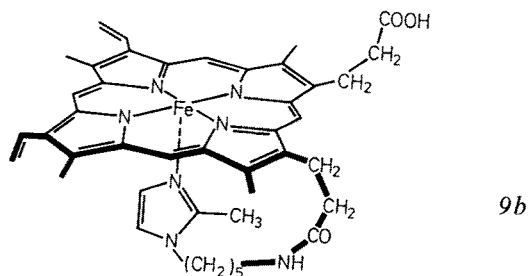
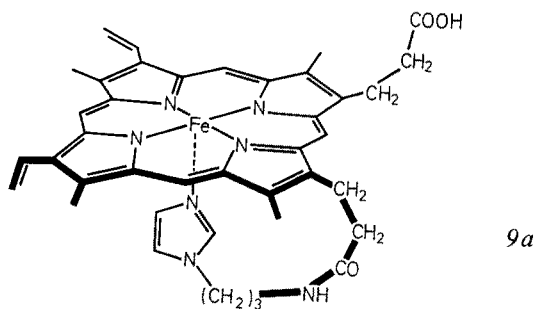
From these results, it is concluded that the proton-driven irreversible oxidation has to be suppressed to enable the oxygen-binding in aqueous media and that by combining the five-coordinate protoheme complex with a water-soluble but hydrophobic polymer the oxygen adduct can be observed in the cold aqueous medium due to the hydrophobic environment.

The life-time of the δ -oxygen adduct was much prolonged in the presence of poly(saccharide)s such as dextran and hyaluronic acid: e.g. > 5 hr at -30°C in the presence of 0.4 wt % hyaluronic acid⁵⁵. The poly(saccharide)s used did not act as reducing agents to protohemin. The stabilizing effect of the added poly(saccharide)s on the δ -oxygen adduct was considered to be due to the efficient suppressing of the irreversible oxidation via a μ -dioxo dimer in the viscous solution of the poly(saccharide) added system. On the other hand, addition of other synthetic polymers caused a decrease of the life-time accompanied by unstabilization of the δ complex itself.

A warmed agar solution containing δ was injected into cooled water giving finely a dispersed red agar gel. δ incorporated in agar gel formed the oxygen adduct at 0°C for a few minutes⁵⁵; the oxygen adduct was easily and clearly observed without the CO protection method although its life-time was not long. It is significant that the oxygen adduct of unmodified natural protoheme could be formed in aqueous media by binding to a polymeric water-soluble but hydrophobic ligand and by incorporating in a water-containing gel structure.

A coacervate is formed by mixing a pair of oppositely charged polyelectrolytes in aqueous media and the coacervate adsorbs dyes with a hydrophobic interaction⁵⁶. The protoheme derivative with a covalently bound imidazole-ligand, protoporphinatoiron-mono(imidazolylpropylamide) (*9a*), was incorporated in the coacervate; it formed the oxygen adduct at -30°C , while irreversible oxidation was observed for the *9a* solutions containing a component polyelectrolyte⁵⁷. A more hydrophobic coacervate gave the oxygen adduct with longer life-time. ESR spectra of the spin-labeled heme showed that the coacervate effectively immobilized the heme derivative.

Protoporphinatoiron mono(2-methylimidazolylpentylamide) (*9b*) was covalently bound to dextran, by reacting *9b* with the amino derivative of dextran derived from



dextran carbonate⁵⁸⁾. The dextran-bound heme *10* was water-soluble and formed the oxygen adduct at -30°C , whereas analogous compounds, dextran-bound heme-methylimidazole and dextran-bound methylimidazole-heme, were irreversibly oxidized under the same conditions⁵⁹⁾. A physiological salt solution containing 6% dextran is common as a plasma expander; *10* is expected to be a biocompatible compound because it is composed of metabolic non-failure dextran and protoheme.

9 was covalently bound with the water-soluble but hydrophobic polymer poly(1-vinyl-2-pyrrolidone) to give *11*: These polymers were soluble in water up to ca. 5 wt%⁶⁰⁾. The content of bound *9* was ca. 1 mol% per vinyl monomer residue and the molecular weight of the polymer was 35,000; one polymer molecule contained ca. one heme unit. *11* formed the oxygen adduct in the aqueous medium cooled at -10 to -30°C . The life-time was over 1 hr, which was longer than that of *8*. The oxygen adduct was

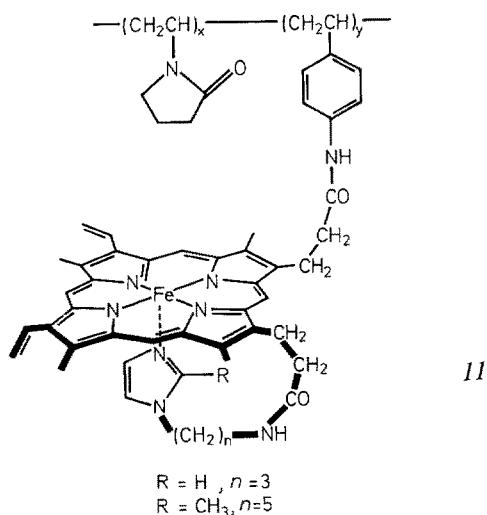
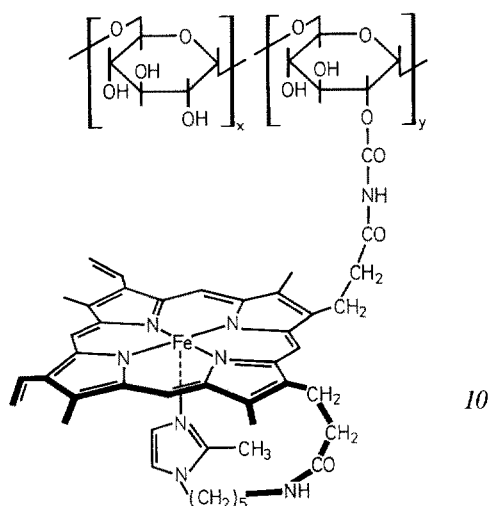


Table 1. Oxygen- and carbon monoxide-binding rate constants and affinities for the polymer-bound hemes in aqueous media

Hemes	$k_{on}(O_2)$ l/mol · sec	$k_{off}(O_2)$ l/sec	$P_{1/2}(O_2)$ mmHg	$k_{on}(CO)$ l/mol · sec	$k_{off}(CO)$ l/sec	$P_{1/2}(CO)$ mmHg
8	1.0×10^5	170	236	1.6×10^4	0.04	1.7
11a	7.9×10^4	10	35	1.2×10^4	8.3	0.027
9a	2.6×10^7	47	1.0	3.6×10^6	0.009	0.0018
Hb in blood	2.9×10^6	180	27	1.0×10^5	0.09	0.10
Mb	1.0×10^7	10	0.37	3.0×10^5	0.0015	0.004

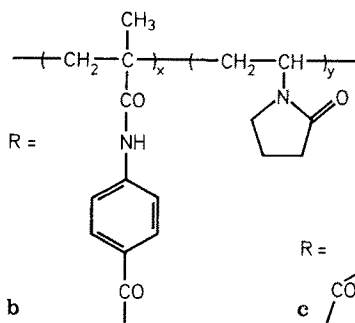
not observed for polymer-non-bound analogues 9 alone or with 2% poly(vinylpyrrolidone). Reversible oxygen-binding in aqueous medium is more efficient when heme is covalently bound to a hydrophobic polymer.

The oxygen-binding kinetic parameters for the polymer-bound hemes 8 and 11 were estimated by a stopped-flow method and are listed in Table 1⁶¹⁾ together with reference data. Because the oxygen adducts of 8 and 11 have a short life-time even at room temperature, the oxygen-binding ($k_{on}(O_2)$) and -dissociation ($k_{off}(O_2)$) rate constants can be estimated from the spectral change within ca. 1 sec. $k_{on}(O_2)$ and the carbon monoxide-binding rate constant ($k_{on}(CO)$) of the polymer-bound hemes are much smaller than those of the polymer-non-bound analogue. It was considered that the heme is occluded in the contracted polymer chain which protects the heme and its oxygen adduct in the aqueous medium and which, on the other hand, sterically retards the coordination of gaseous molecules. A gaseous molecule encounters the barrier of the contracted polymer chain when it approaches from the solvent phase to the internal heme.

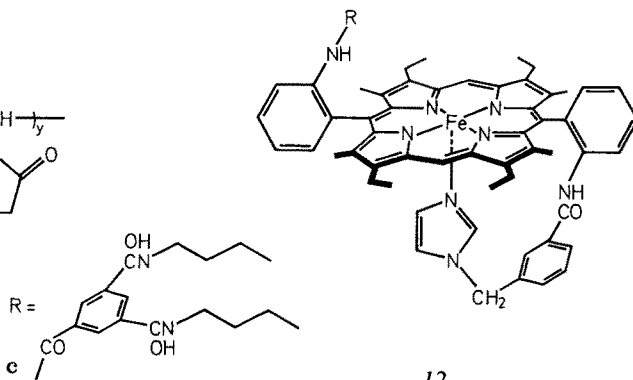
The oxygen-binding affinity, $P_{1/2}(O_2)$, i.e. the oxygen pressure at 50% oxygen-binding for porphinatoiron, was estimated from the midpoint of the oxygen-binding equilibrium curve for the polymer bound heme in the cold aqueous medium^{15, 61)}. The smaller $k_{on}(O_2)$ values of the polymer-bound heme brought about lower oxygen-binding affinity (larger $P_{1/2}(O_2)$ values) in comparison with those of the polymer-non-bound analogue, and the resultant oxygen-binding affinity of the polymer-bound hemes resembles that of Hb in a red blood cell.

R = H

a



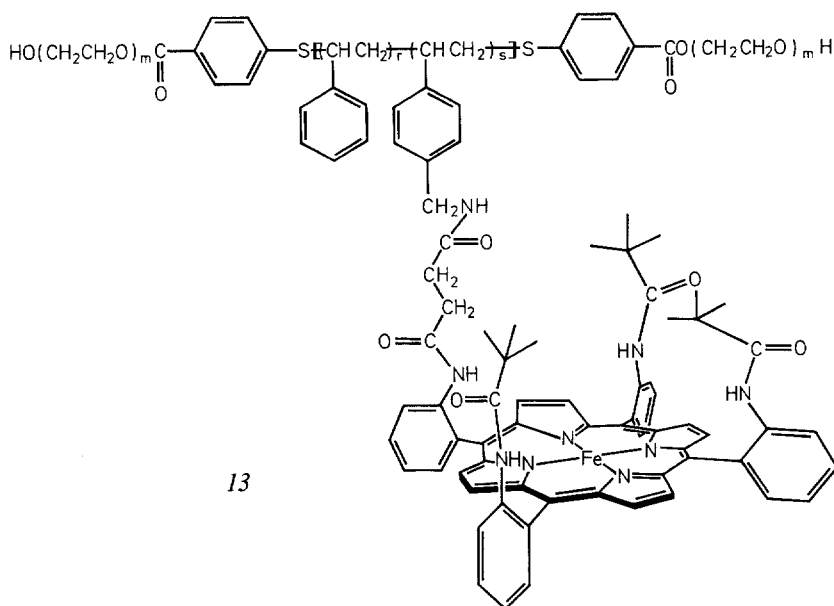
b



12

'Diphenylheme' **12**⁶²⁾ has two meso-phenyl groups of which rotation is restricted around the meso C-aryl C bond due to the tetramethyl substituents on the porphyrin. This should immobilize the imidazole ligand and strengthen the iron-imidazole bond. This also causes the restricted conformation of the group attached to the meso-phenyl group such as the trimesic acid residue in **12c**: These groups are expected to cover the sixth coordination site, i.e. the oxygen-binding site. Diphenylheme exhibits absorption spectral features very similar to protoheme. This diphenylheme was combined with poly(1-vinyl-2-pyrrolidone) to give **12b**⁶³⁾. In an aqueous medium, the life-time of the **12b**-oxygen adduct was more than 2 hr at -30°C and 3 min at 15°C . In contrast, **12a** and **12c** solubilized with surfactants in the same solvent was oxidized immediately even at -30°C . Reversible oxygen-binding in the aqueous medium is here also efficient when the diphenylheme is covalently bound to a water-soluble but hydrophobic polymer. The life-time of the **12b**-oxygen adduct was longer than that of the polymer-bound heme **11**. This indicates that the spacing-group, phenylmethacrylamide, and/or the polymer chain covers the sixth coordination site of diphenylheme and protects the oxygen adduct efficiently in the aqueous medium.

One way to minimize the irreversible oxidation is the inclusion of a porphinatoiron complex into stiff hydrophobic substances solubilized in water^{21, 64)}. Oxygen-binding in aqueous media was examined by using water-soluble hydrophilic-hydrophobic-hydrophilic triblock copolymers⁶⁵⁾. The derivative of **1**^{66, 67)} was covalently bound to the central hydrophobic block of the triblock copolymer: poly(ethylene oxide)/polystyrene/poly(ethylene oxide) yielding **13**. **13** with ethylimidazole was soluble in water by micelle-forming and gave the oxygen adduct with life-time of half a day at room temperature, although the oxygen-binding and -dissociation occurred slowly. This is the first success in oxygen-binding reversibly in aqueous medium at room temperature. The porphinatoiron complex is expected to be completely immobilized



into the polymeric micelle core and be surrounded by the styryl residues of the block copolymer even in the aqueous solution.

As described above, reversible oxygen-binding of a porphinatoiron complex was successfully observed in aqueous media by combining it with synthetic water-soluble polymers, but the following items still remained to develop it as an oxygen carrier under physiological condition.

- (i) Reversible oxygen-binding is to be realized at 37 °C with sufficient life-time.
- (ii) Oxygen is to be rapidly ad- and desorbed by a porphinatoiron complex.
- (iii) The carrying amount of oxygen is to be increased, i.e., a large amount of a porphinatoiron must be solubilized.
- (iv) The macromolecular porphinatoiron complex system is expected to be composed of biocompatible compounds.

4 Structure of Liposome-Embedded Porphinatoirons

In order to construct a hydrophobic environment in aqueous solution, it is a possibility to use the liposome of a phospholipid instead of the globin protein. Some attempts to achieve reversible oxygen-binding by solubilizing a porphinatoiron complex in water with a micelle or a liposome have been reported^{68,69}, but they resulted in a questionable oxygen-binding or irreversible oxidation.

Recently we found that the *I* complex of 1-lauryl-2-methylimidazole incorporated into the hydrophobic region of the bilayer of a phospholipid liposome [abbreviated as 'liposome-embedded heme' (lipid liposome/heme); Fig. 4 shows the lipid liposome/lipid-heme described later.] binds molecular oxygen reversible under semi-physiological conditions (at pH 7 in aqueous media at 37 °C)^{70,71}. The spectrum of the five-coordinate deoxy heme complex (535, 562 nm) changed to that of the oxygen adduct (546 nm), which agrees with the well-established spectra of the *I* complex in an organic solvent, on exposure to oxygen through isosbestic points. The oxy-deoxy cycle could be repeated more than dozens of times. The life-time of the oxygen adduct of the liposome-embedded heme was half a day at pH 7 in aqueous media at 37 °C.

The life-times of the oxygen adduct were measured for the lipid liposome/hemes composed of various imidazole ligands and phospholipids. Only the lipid liposome/heme complexes with a hydrophobic group-substituted imidazole, e.g. 1-lauryl-, 1-stearyl-, and 1-trityl-2-methyl-imidazole, gave a stable oxygen adduct. A stable oxygen adduct was observed for the heme complex solubilized with the liposome of phosphatidylcholine such as dimyristoylphosphatidylcholine (DMPC), dipalmitoylphosphatidylcholine (DPPC), and egg yolk lecithin (EYL) or its mixture with cholesterol. The only unstable oxygen adducts were observed for the heme complex solubilized with micelles of synthetic surfactants such as poly(ethyleneoxide) mono-nonanoylphenylether and cetyltrimethylammonium bromide; the heme complex solubilized with non-micelle forming surfactant such as the block copolymer of ethyleneoxide and propyleneoxide resulted in rapid irreversible oxidation of heme on exposure to oxygen. The heme complex solubilized with a mixture of EYL and lyso egg yolk lecithin, which can not form a liposome, did not produce the stable oxygen adduct. The use of a phospholipid and a hydrophobic imidazole was necessary to prepare the liposome-embedded heme with oxygen-binding ability.

Our idea is once more described as follows. First, a hydrophobic environment to retard the proton-driven oxidation [Eq. (4)] is constructed around porphinatoiron in aqueous media by embedding porphinatoiron in a phospholipid bilayer. Secondly, the porphinatoiron is molecularly dispersed in the phospholipid bilayer and the porphyrin plane of the porphinatoiron is oriented parallel to the bilayer, which prevents the oxidation via a μ -dioxo dimer [Eq. (3)] (see Fig. 4). We further synthesized novel, sterically modified and amphiphilic porphinatoiron derivatives, in order to improve the compatibility of the porphinatoiron with the phospholipid bilayer of the liposome.

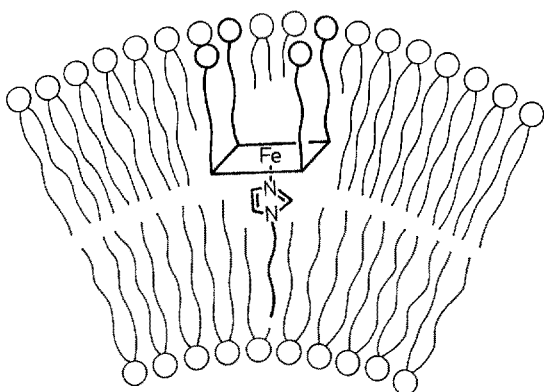


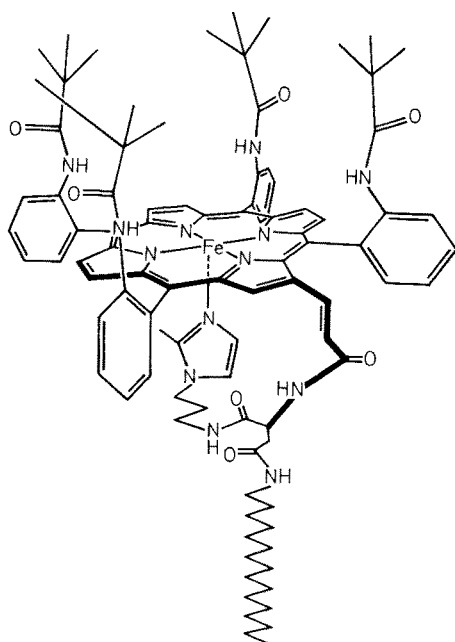
Fig. 4. Liposome-embedded heme (Lipid liposome/lipid-heme)

The first target was the synthesis of novel and finely modified porphinatoiron derivatives. Liposomes containing a porphinatometal have been often studied as models for the photochemical reactions of the photosynthesis and for the redox reactions of hemoproteins^{72, 73}. But these studies were partly limited by the unclear structure of the bilayers containing the porphinatometal. That is, the position and orientation of the porphyrins in bilayers have not been elucidated because of the relatively simple structure of the porphyrins. Viewing the geometry and the lipophilic and/or amphiphilic property of porphinatoiron to enhance both the oxygen-binding ability and the compatibility with a phospholipid bilayer, we synthesized the following derivatives of porphinatoiron.

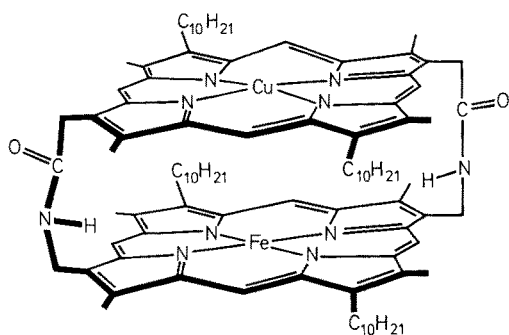
The lipophilic porphinatoiron derivative having both, a long alkyl group and an imidazole group was synthesized by coupling the β -amino derivative of **1** with the carboxylic acid derivative of the long alkyl imidazole to give **14**⁷⁴. It is expected that the compatibility of the porphinatoiron with a lipid bilayer is improved and that the coordination equilibrium of the porphinatoiron with imidazole is disregarded.

Tetradecyl-substituted diporphinatocopper-iron **15** was synthesized as a lipophilic derivative of **5** which increases the compatibility with the hydrophobic region of a liposome⁷⁵.

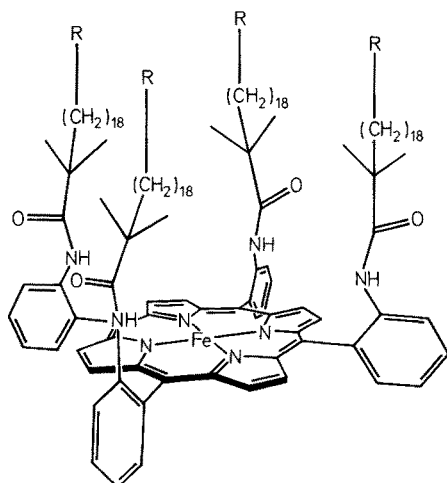
The porphinatoiron derivative having four carboxylalkaneamide groups on the porphyrin plane **16a** was synthesized⁷⁶. Here a good hydrophobic and hydrophilic balance of the porphinatoiron within a liposome is expected. Corresponding derivatives having oligoethylene oxide groups **16b** and saccharide groups **16c** as the hydrophilic part were also synthesized⁷⁷.

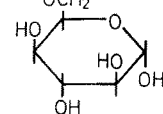


14



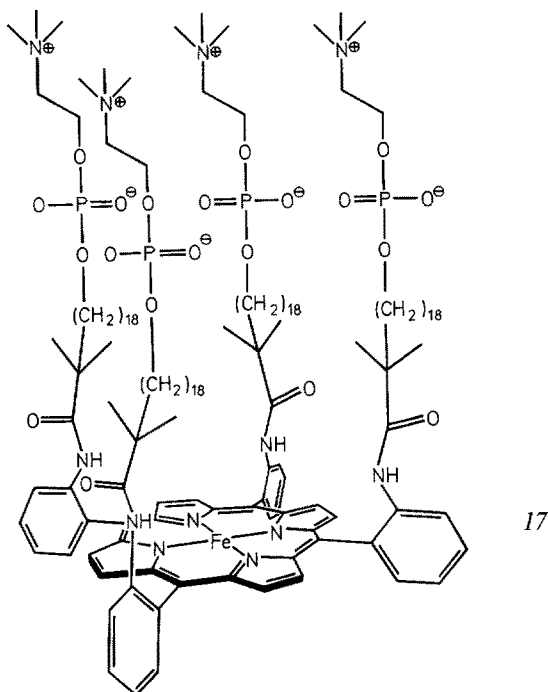
15



- a* ; R = —OCOOH
b ; R = —O(CH₂CH₂O)_n H
c ; R = —OCH₂


16

17 represents a lipid derivative of porphinatoiron: the porphinatoiron having four alkanephosphocholine groups on the porphyrin plane⁷⁸⁻⁸⁰. Tetra[(hydroxy dimethyleicosanamido)phenyl]porphine was derived from tetra(aminophenyl)porphine and its $\alpha,\alpha,\alpha,\alpha$ -structure was confirmed by NMR spectroscopy. This porphine was phosphorylated, and iron-inserted to give tetra[$\alpha,\alpha,\alpha,\alpha$ -o-(20-2'-trimethylammonioethoxy)phosphinatoxy-2,2-dimethyleicosanamidophenyl]porphinatoiron [17, abbre-



viated as 'lipid-heme']. Because not only the hydrophobic-hydrophilic balance but also the geometry are adjusted to a lipid bilayer, it is expected that the lipid-heme forms a stable bilayer with phospholipids.

The structure and property of the porphinatoiron complex in the lipid bilayer of a liposome was studied for the liposome-embedded heme composed of DMPC and lipid-heme (DMPC liposome/lipid-heme) as follows⁷¹⁻⁸¹.

The incorporation was first confirmed by ultracentrifugation; the supernatant did not contain both the phospholipid and the lipid-heme. This indicated that lipid-heme is included in the liposome. The liposome solution was also checked by gel permeation chromatography monitored by the absorption at 300 and 415 nm based on the phospholipid and the heme, respectively. The curve coincided with each other, which means that the heme is included in the liposome.

The electron microscopic photograph (TEM) is shown in Fig. 5. The liposome-embedded heme was able to be prepared as a single-walled, unilamellar liposome with the diameter of ca. 400 Å (Fig. 5a) or a multilamellar liposome with the diameter of ca. 700 Å (Fig. 5b). The lipid-heme is embedded in the lipid bilayer of the liposome, i.e., the white roop(s) of vesicle, and one liposome vesicle contains ca. 500 or 2,000 heme

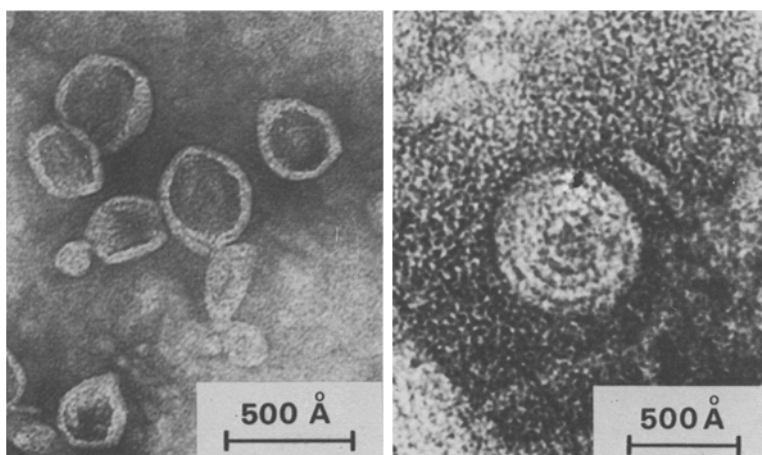


Fig. 5. Electron microscopic photographs for the liposome-embedded heme (DMPC liposome/lipid-heme): a) single-walled, b) multilamellar

molecules for Fig. 5a and 5b, respectively. The average particle size of the liposome-embedded hemes was also measured by a light scattering method; the most frequent diameters were determined to be ca. 400 Å and ca. 640 Å with the sharp distribution for Fig. 5a and 5b, respectively. Anyhow, the liposome-embedded heme can be prepared as fine particles (diameter < 0.1 μm) and expected to pass through small capillaries of the human body.

The formation of the liposome (single-walled type) was confirmed by NMR measurements. When europium ion (Eu^{3+}) is added to a liposome solution, Eu^{3+} interacts with the choline groups of the outward facing phospholipid and shifts the NMR signal of choline methyl groups upfield⁸²⁾. The same shift was observed for DMPC liposome/lipid-heme with the addition of Eu^{3+} . This result means the liposome formation for the liposome-embedded heme solution. The liposome formation was also supported by the sharp ^{31}P -NMR spectrum (0.8 ppm), which was caused by the spherical geometry of the phosphatidyl group.

The closed vesicle structure of the liposome-embedded heme was also confirmed by the following experiment⁸³⁾. A water-soluble fluorescent compound was encapsulated into the inside water phase of the single-walled liposome of the liposome-embedded heme. A fluorescence spectrum was not observed because the encapsulated and concentrated fluorescent compound within the liposome quenched each other: This supports the closed vesicle structure of the liposome-embedded heme. The leakage of the fluorescent compound across the phospholipid bilayer occurred slowly; rate of the leakage was DMPC liposome/lipid-heme \geq DMPC liposome \geq DMPC liposome/1. This means that the phospholipid forms a stable liposome with lipid-heme 17.

The Fourier-transform ^1H -NMR spectrum of DMPC liposome/lipid-heme at 37 °C showed the absorption signal at -0.1 ppm assigned to the β -dimethyl group of the heme beside the signals based on DMPC. This suggests that the heme complex is molecularly dispersed in the bilayer of the DMPC liposome.

The lipid-heme complex labeled with nitroxide was studied by ESR spectroscopy^{71, 81)}. The spin-labeled heme complex in homogeneous methanol solution gave a triplet

signal in the z-direction and weak signals in the x- and y-directions. On the other hand, the spin-labeled heme complex forced to be solubilized in water showed only the z-direction signal, which was often observed in the solid state. The spectrum of the spin-labeled heme complex solubilized in water by the liposome is similar to that in a homogeneous methanol solution. This result also suggests that the heme complex is molecularly dispersed and well solubilized in the bilayer of liposome.

The incorporation of lipid-heme in the liposome was studied by fluorescence spectral measurement using porphyrinatozinc as the fluorescent probe ^{71,81}). For homogeneous alcohol solutions of the porphyrinatozinc, the fluorescence intensity increased with the decrease of the solvent polarity (methyl, ethyl, and butyl alcohol), as expected. The intensity was much larger, more than twice, for the liposome-embedded porphyrinatozinc than those in alcohols, indicating that the porphyrinatozinc is incorporated into the hydrophobic region of the lipid bilayer and is molecularly dispersed in the liposome. This supports also the incorporation of the heme in the liposome.

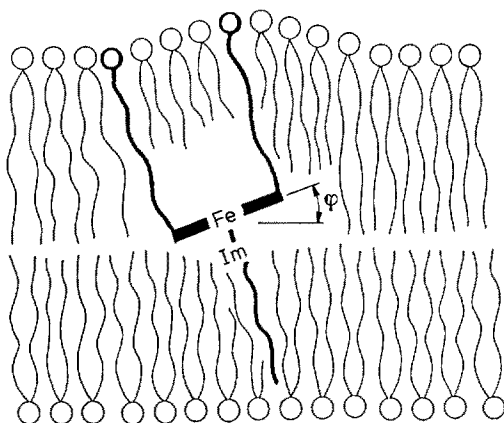


Fig. 6. Orientation of the lipid-heme in the phospholipid bilayer

The porphyrin plane of the lipid-heme is assumed to be oriented nearly parallel to the phospholipid bilayer (Fig. 6). This was confirmed by an electrooptical measurement ⁸⁴). At first electric birefringence of the liposome (diameter $> 800 \text{ \AA}$) solution was measured: The liposome has a larger refractive index in a perpendicular direction to the electric field, which means that the longer axis of the liposome (oval-shaped under electric field) is aligned parallel to the electric field. Dichroism of the heme embedded in the bilayer was monitored under an electric field. The transient absorbance change was much larger when the incident light is polarized parallel with the electric field. From these results, it was concluded that the angle (ϕ) between the porphyrin plane and the phospholipid bilayer is practically small (Fig. 6), probably based on the steric structure of the heme derivative.

There is a question whether the heme is outward or inward facing, as shown in Fig. 7. The binding-reaction of a bulky ligand such as nitrosobenzene to the liposome-embedded heme was studied by a stopped-flow method ⁸³). The time-curve for the ligand-binding of the single-walled, small liposome/lipid-heme (diameter ca. 400 \AA) was that of a mono-phase system, while the curve for the single-walled, large liposome/

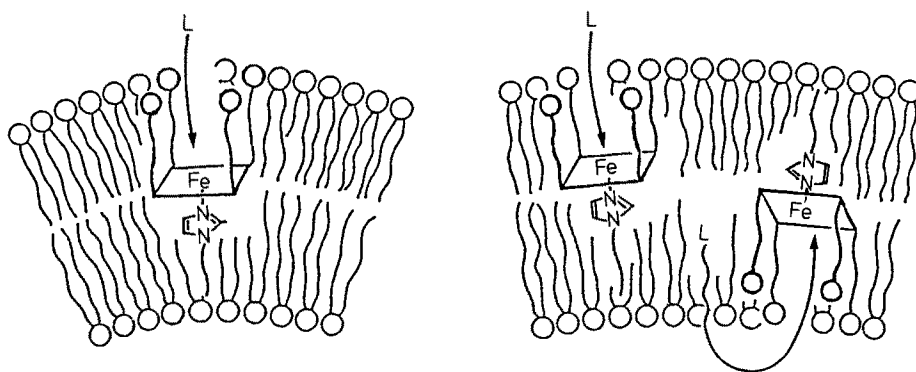


Fig. 7. Outward and inward facing lipid-heme in the liposome

lipid-heme (diameter ca. 800 Å) was that of a two-phase system; the rapid reaction agreed with that of the small liposome/heme, and the slower reaction corresponded to the ligand-binding where the bulky ligand at once crossed the lipid bilayer and bound to the heme from the inner water phase. The slower reaction component was estimated ca. 20% for the large liposome. The lipid-heme has no perfect cylindrical structure but a somewhat cone-like structure, so that the heme situates preferentially in outward facing orientation in the bilayer of the small liposome.

The DSC thermogram of the liposome-embedded heme was measured to estimate the phase transition of the lipid bilayer of the liposome-embedded heme^{71,81}. The DMPC-liposome showed the endothermic peak at 24 °C, which was corresponding to the gel-liquid crystal phase transition temperature (T_g) of the liposome⁸⁵. But for the liposome in which a simple heme such as *I* was embedded, the phase transition peak was broadened and shifted to lower temperature (22 °C). On the other hand, the peak was also observed at 24 °C for the DMPC liposome/lipid-heme. This suggests that the orientation of the phospholipid in the liposome is equivalent for the DMPC-liposome and the DMPC liposome/lipid-heme and that the compatibility of the lipid-heme with the phospholipid is large enough to form a stable liposome.

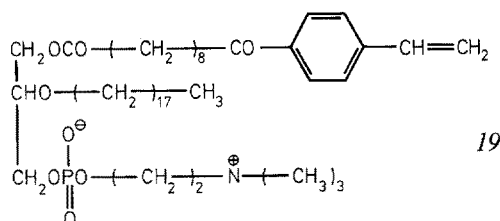
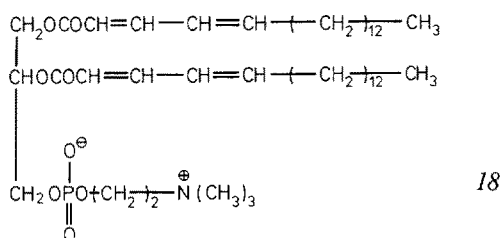
The stability and miscibility of lipid-heme with phospholipid could also be confirmed from surface pressure-surface area isotherms of the lipid monolayer on a water surface. For the heme *I*, the curve shifted to right hand of the curve of the phospholipid monolayer itself, which reveals no good packing of the lipid molecules in the monolayer film. Against this, the curve for the lipid-heme-embedded monolayer film coincided with that for the lipid film itself.

The results mentioned above lead to the following conclusion: The lipid-heme complex is included and molecularly dispersed in the hydrophobic environment of the liposome which protects the heme-oxygen adduct from the irreversible oxidations [Eqs. (3) and (4)]. The geometry of the lipid-heme derivative is assumed to emphasize the incorporation of the porphinatoiron into the phospholipid bilayer of the liposome. The following result also supports this conclusion. The lipid-heme complex was more efficiently taken into the DMPC liposome than the heme complex *I* of 1-lauryl-2-methylimidazole was; only 20 moles of DMPC were enough to solubilize one mole of the lipid-heme completely in water, while more than 100 moles were necessary for

the latter. This could be explained by the high compatibility of the lipid-heme with the phospholipid which is caused by the introduction of the alkanephosphocholine groups upon the porphyrin plane of the lipid-heme.

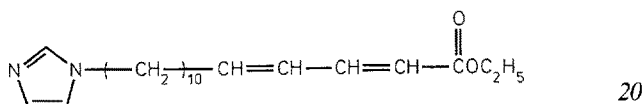
Next we intended to improve the stability of the liposome as the carrier of the porphinatoirons, which will bring about a highly concentrated, physically and mechanically stable and storageable solution of the porphinatoirons just like as or superior to blood. To accomplish this intention, we apply a new concept which makes liposomes stable by the polymerization of the lipid bilayer⁸⁶⁾. The double bond of the phospholipid derivative is rapidly polymerized under UV irradiation because of its assembled and oriented structure, to give a covalently bound and very stable lipid bilayer.

The lipid-heme **17** complex of 1-lauryl(-2-methyl-imidazole) was embedded in polymerized liposomes of di(octadecadienoyl)-glycerophosphatidylcholine (**18**)⁸⁷⁾ and



of (vinylbenzoyl)nonanoyl-octadecyl-glycerophosphatidylcholine (**19**)⁸⁸⁾ (abbreviated as 'poly-lipid liposome/lipid-heme'). The poly-lipid liposome/lipid-heme was prepared as follow⁸⁹⁾. The liposome of **17** and **18** was prepared with normal ultrasonication. The prepared liposome was allowed under nitrogen atmosphere to polymerize under UV irradiation to give poly-**18** liposome/**17**. The reduction of the Fe(III) derivative of **17** to the deoxy spontaneously occurred during the polymerization. Complete polymerization was confirmed by UV absorption and ¹³C-NMR spectroscopical measurement; disappearance of the absorption based on the vinyl group and of the characteristic signals based on the vinyl carbons of **17**. The poly-lipid liposome/lipid-heme was concentrated up to a ca. 20 wt% solution by an ultrafiltration method.

An alkylimidazole derivative having a vinyl bond was synthesized: 1-imidazolyl-dodecadienoylacid ester (**20**)⁹⁰⁾. The phospholipid derivative **18** or **19** was copolymerized with **20** in the presence of **17** to give a more advanced 'poly-lipid liposome/lipid-heme' (Fig. 8) where **17** was more strongly fixed into the poly-lipid liposome.



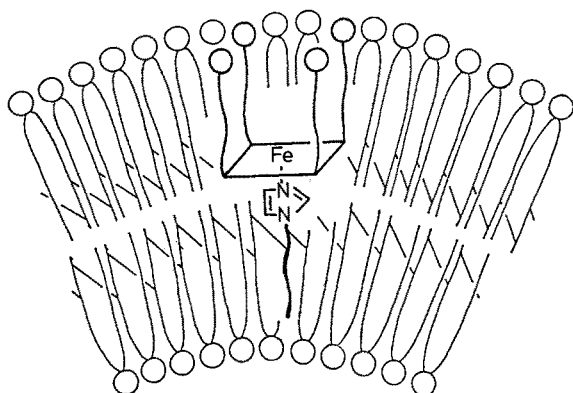


Fig. 8. Poly-lipid liposome/lipid-heme

By TEM of the poly-lipid liposome/lipid-heme the diameter was ca. 350 Å (Fig. 9) and it did not change before and after the polymerization. The gel permeation chromatography and the ultracentrifugation of the liposome/heme showed that all of 17 was entrapped within the liposome. Solution properties of the poly-lipid liposome/lipid-heme were almost the same as those of human blood: specific gravity 1.012, viscosity 3.75–4.12 cp, and osmotic pressure 334 mOsm. The solution of the poly-lipid liposome/lipid-heme was stable and could be stocked for months without precipitation and change of the particle size, i.e. without aggregation and fusion of the liposome, at ambient temperature.

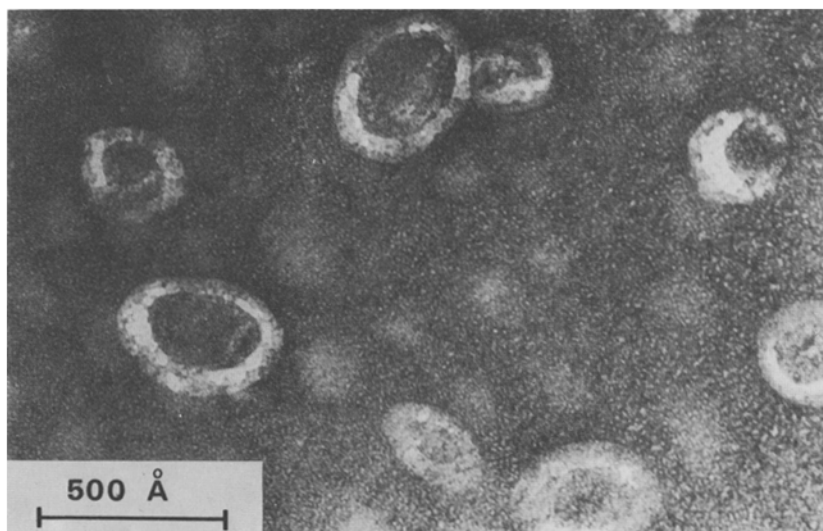


Fig. 9. Electron microscopic photograph for poly-lipid liposome/lipid-heme

5 Oxygen Transporting Profile

The red and transparent solution of the liposome-embedded heme (lipid liposome/lipid-heme and poly-lipid liposome/lipid-heme) was changed to its oxygen adduct solution on exposure to oxygen. The oxygen adduct of the liposome-embedded heme was stable, and the adduct formation was rapid and reversible under physiological conditions even at high concentration ([lipid-heme] = 10 mM, being equal to that of human blood). The oxy-deoxy cycle could be repeated more than a thousand times under physiological conditions^{81, 89)}.

The volume of the oxygen gas bound to the liposome-embedded heme was measured⁸⁹⁾. It was found to be 20 ml per 1 mmol of the heme (100 ml liposome-embedded heme solution: [heme] = 10 mM) at 37 °C corresponding to ca. 80% of the saturated value. The heme-free EYL-liposome solution (100 ml) physically uptook 2.2 ml of oxygen, i.e. 22.2 ml of oxygen was dissolved in the liposome-embedded heme solution at 37 °C. Table 2 shows the oxygen volume dissolved in various media, e.g. 100 ml Blood uptakes 23 ml oxygen. The 100 ml solution of the liposome-embedded heme uptook 22 ml of oxygen, which is corresponding to that of blood and is ca. 10 times of that physically uptaken by water. Raising the heme concentration, of course, increases the oxygen volume bound to the liposome-embedded heme up to ca. 32 ml per a 100 ml solution. An extraordinary high volume of the dissolved oxygen is one of the merits of the liposome-embedded heme as an artificial oxygen carrier.

An oxygen-15 radiotracer method was applied to the precise determination of chemically bound oxygen to the liposome-embedded heme⁹¹⁾. The ¹⁵O₂ gas produced with a cyclotron was passed through the liposome-embedded heme solution, and the volume of oxygen bound to the heme was evaluated with the annihilation radiation intensity within a 5% error of the value given above.

The kinetic profile of the oxygen-transporting by the liposome-embedded heme was studied by a stopped flow method as follows^{92, 93)}. Oxygen-binding and -dissociation occurred reversibly and were completed within sec: The oxygen-binding and -dissociation of the liposome-embedded heme are rapid enough to act as an oxygen carrier. $k_{on}(O_2)$ and $k_{off}(O_2)$ are summarized in Table 3 with references. The k_{on} values of the liposome-embedded heme were a little faster than or similar to those of the red blood cell suspension. The referred oxygen-binding rate parameters in homogeneous systems, i.e. 9a, Mb, and stripped Hb⁹⁴⁾, also listed in Table 3, were about 10³ times larger than those of the liposome-embedded heme and the red blood cell suspension. This

Table 2. Solubility of oxygen in various media (at 37 °C, P_{O₂} = 760 mmHg)

Media	Heme conc. mM	Oxygen solubility gas ml/medium 100 ml
Poly-lipid liposome/lipid-heme	10	22
Poly-lipid liposome/lipid-heme	15	32
Human blood	9.2	23
Water	—	2
Serum	—	2
Fluorocarbon emulsion	—	8

Table 3. Oxygen-binding rate constants for the liposome-embedded hemes

Heme	$10^{-4} \cdot k_{\text{on}}$ l/mol · sec	k_{off} l/sec	$10^{-4} \cdot K (= k_{\text{on}}/k_{\text{off}})$ l/mol
Poly-lipid liposome/lipid-heme	1.3	0.10	1.3
DMPC liposome/lipid-heme	3.7	2.2	1.6
DMPC liposome/heme	0.79	0.32	2.5
DPPC liposome/heme	0.24	0.11	2.2
Burst DMPC liposome/heme	1.2	0.29	4.2
Chelated heme 9a	2600	47	55
Hb in red blood cell	1.1	0.25	4.4
Stripped Hb	3300	12	270
Mb	1000	10	100

means that the oxygen-binding reactions for the liposome-embedded heme and the red blood cell suspension showed a similar feature. The oxygen-binding reaction is assumed to be largely retarded by the diffusion process of oxygen in and through the phospholipid membrane. The oxygen-binding rate was larger for the DMPC- than for the DPPC-liposome/heme. This may be explained as follows: The DPPC-liposome is below its T_c (41 °C) and the DMPC-liposome is above its T_c (23 °C) under these experimental conditions (at 25 °C), so that the membrane fluidity and probably also the oxygen permeability of the DMPC-liposome is larger than that of DPPC. The largest oxygen-binding rate was observed for the burst DMPC-liposome/heme. It is assumed that this liposome has a lamellar structure or a non-closed (non-vesicle) bilayer structure, and this is advantageous for the supply of oxygen to the heme.

The $k_{\text{on}}(\text{CO})$ value of the liposome-embedded heme is similar to that of the red blood cell suspension and far apart from those given in the literature for homogeneous systems. It seems also that the CO-binding reaction is also retarded by the diffusion process of CO in and through the phospholipid membrane.

The oxygen-binding profile of red blood cells has been well studied by Roughton et al.⁹⁵⁾ taking the diffusion process of oxygen into account. The overall oxygen-binding rate constant for red blood cells (k_h) is expressed by $k_h = (1/a) (k \cdot D \cdot c_0)^{1/2}$ where k is the true oxygen-binding rate constant of stripped Hb, D is the diffusion constant, c_0 is the concentration of Hb in the red blood cell, and a is the average diameter of the red blood cell. For the liposome-embedded heme each value could be estimated from the data mentioned above; a : 400 Å, k : $1.1 \times 10^8 \text{ l} \cdot \text{mol}^{-1} \cdot \text{s}^{-1}$, D : $1.8\text{--}1.5 \times 10^{-5} \text{ g} \cdot \text{m}^2 \cdot \text{s}^{-1}$, c_0 : 0.1 mM. Substituting these values in the Roughton's equation yielded the k_h value of the liposome-embedded heme; k_h : $4.0 \times 10^4 \text{ l} \cdot \text{mol}^{-1} \cdot \text{s}^{-1}$. This value is similar to the $k_{\text{on}}(\text{O}_2)$ value determined in this experiment (Table 3). The liposome-embedded heme is clearly a suitable model to study the mechanism of oxygen uptake and release by red blood cells.

The oxygen-binding equilibrium curve (Fig. 10) shows that the liposome-embedded heme binds molecular oxygen in response to the oxygen pressure. The oxygen-binding affinity ($P_{1/2}$) of the liposome-embedded heme was determined by the equilibrium curve and listed in Table 4. $P_{1/2}$ of the liposome-embedded hemes are ca. 50 mmHg at 37 °C, which are closed to that of Hb in blood, but situate fairly apart from that of Mb. This suggests that the liposome-embedded heme has a potential to act as an

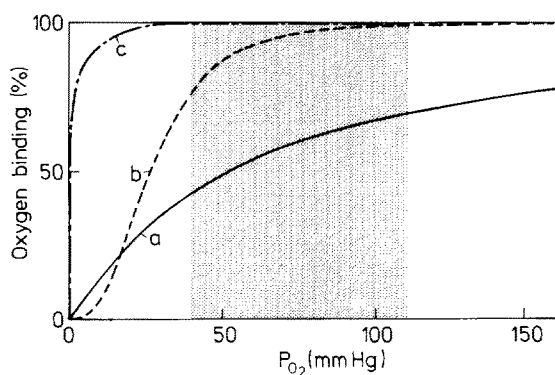


Fig. 10. Oxygen-binding curve of the liposome-embedded heme: **a)** poly-lipid liposome/lipid-heme, **b)** Hb in a red blood cell, **c)** Mb. The shaded area corresponds to the oxygen pressure at the lungs and muscle tissue

oxygen carrier under physiological conditions which transports oxygen from lungs (P_{O_2} : ca. 110 mmHg) to Mb in muscle tissue (P_{O_2} : ca. 40 mmHg), as Hb does. Table 4 also shows the thermodynamic parameters for the oxygen-binding. The enthalpy change (ΔH) and entropy change (ΔS) for the oxygen-binding of the liposome-embedded hemes were estimated to be ca. $-15 \text{ kcal mol}^{-1}$ and ca. -40 eu , respectively: These values are comparable to those of Hb and Mb. This result indicates that the oxygen-binding by the liposome-embedded heme proceeds in the same way as the binding by Hb and Mb. We once more emphasize by seeing Fig. 10 that the oxygen-transporting efficiency between the oxygen pressure at lungs and muscle tissue is ca. 30% which is superior to that of blood (25%).

Two phenomena in which environmental phospholipid bilayer affects the oxygen-binding affinity of heme are described below in comparison with the oxygen-binding behavior of Hb.

Figure 11 shows the temperature-dependence of the oxygen affinity, i.e. the reciprocal of the $P_{1/2}$ value and the reciprocal of the temperature⁹⁶⁾. The plots for the oxygen-binding of DMPC- and EYL-liposome/heme give linear relationship. On the other hand, the temperature dependence for DMPC-liposome/heme has a breaking point at about 24 °C. ΔH for the oxygenbinding of the EYL-system and the DMPC-system above 24 °C are ca. -15 kcal/mol and comparable to that of the corresponding heme complex in toluene and that of Hb. On the contrary, ΔH for the DPPC-system and the DMPC-system below 24 °C are much larger than those of the others. The phospholipid environment gives a large effect on the oxygen-binding

Table 4. Oxygen-binding affinity and thermodynamic parameters under physiological conditions

Heme	$P_{1/2}$ mmHg	ΔH kcal/mol	ΔS e.u.
Poly-lipid liposome/lipid-heme	43	-13	-38
Lipid liposome/lipid-heme	53	-15	-40
Lipid liposome/heme	51	-16	-46
Hb in red blood cell	27	-14	-42
Stripped Hb	0.22-0.36	-14--15	ca. -40
Mb	0.37-1.0	-14--21	ca. -40

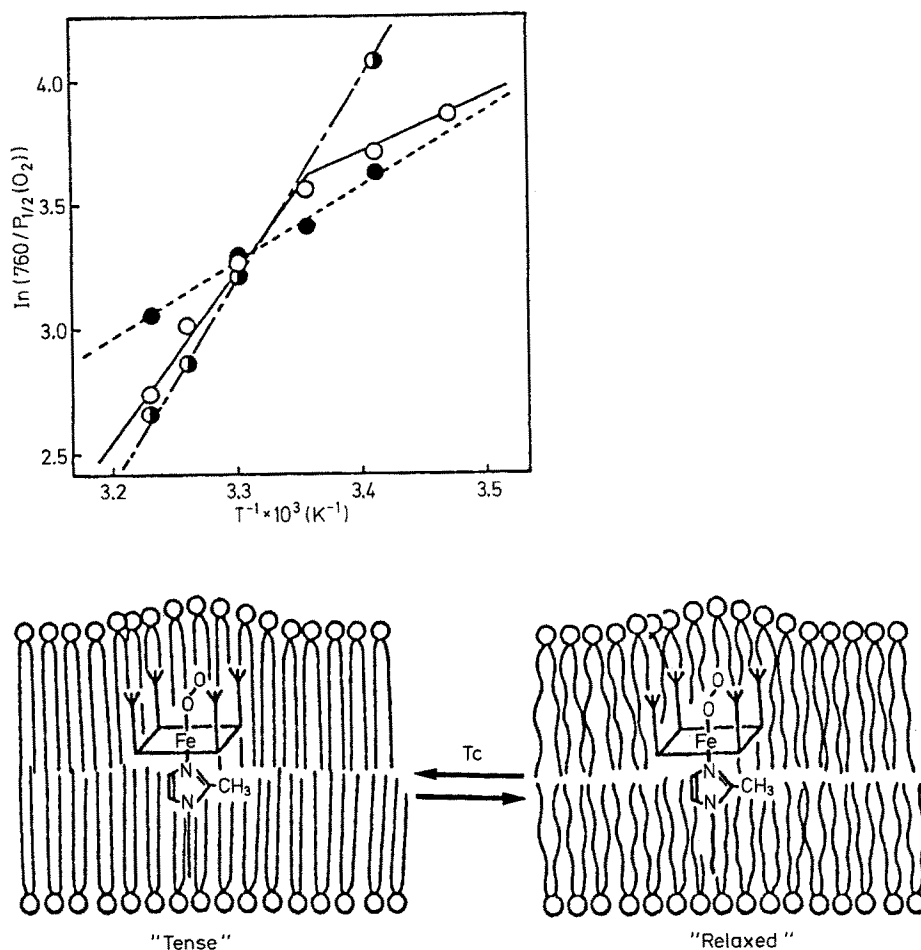


Fig. 11. Temperature-dependence of the oxygen-binding affinity of the liposome-embedded heme liposome/heme composed of (○) DMPC, (●) DPPC, (○) EYL

affinity through its enthalpy contribution. The breaking point of the temperature dependence of oxygen-binding by the DMPC-system agrees with T_c of the DMPC-liposome. This phenomenon may be explained as follows. Above T_c the phospholipid molecules are in the liquid crystalline state, which provides the environment just like organic solvents such as toluene around the complex; the heme complex is in a 'relaxed (R)' state³⁷⁾, and the gaseous molecule-binding affinity and the enthalpy values are comparable with those of the corresponding heme complex in toluene and with those of Hb. On the contrary, below T_c the phospholipid molecules are in the crystal state, which probably induces an orientation of the laurylimidazole ligand and a structural distortion of the heme complex because the bulky heme molecule is embedded in the phospholipid bilayer; the heme complex is in a 'tense (T)' state³⁷⁾, and this reduces the oxygen-binding affinity. The R and T states of the heme complex for the liposome-embedded heme are not the same ones as the R and T states for Hb;

the latter are caused by globin protein. But the gaseous molecule-binding phenomenon of the liposome-embedded heme resembles that of Hb.

The oxygen-binding affinity of Hb decreases ($P_{1/2}$ increases) with the decrease in pH of the medium. This phenomenon is called 'Bohr effect' of Hb: Hb releases oxygen more efficiently when the pH of the medium decreased in the presence of carbon dioxide. On the other hand, EYL-liposome/lipid-heme binds oxygen more strongly at lower pH⁹⁷⁾. This behaviour is in contrast to the Hb's Bohr effect and is explained as follows. The EYL-liposome/heme contains a small excess of laurylimidazole, and the non-coordinated imidazole situates in the bilayer directing the hydrophilic imidazole group outward. The outward directing imidazole is protonated at lower pH and destroys the packing structure of the bilayer, which lets the heme complex in a relaxed structure. This pH dependence of $p_{1/2}$ was cancelled for the EYL-liposome/heme with higher EYL concentration and for poly-lipid liposome/lipid-heme.

Of course, the same oxygen-transporting profile of the liposome embedded heme was also observed for other porphinatoiron derivatives embedded in liposomes. For example, non-tetraphenyl type-porphinatoiron *15* was embedded in a liposome⁷⁵⁾. This liposome-embedded heme solution turned brilliant red on exposure to oxygen. The oxygen and carbon monoxide-binding rate constants and the binding affinity are listed in Table 5. Both $k_{on}(O_2)$ and $k_{on}(CO)$ decreased for lipid liposome/*15* probably due to steric hindrance of the porphinatocopper cap, which brought about lower gas binding affinity in comparison with other synthetic porphinatoiron complexes. The M value [$P_{1/2}(O_2)/P_{1/2}(CO)$] resembles to that of Hb, and this liposome-embedded heme has a resistivity to CO poisoning.

Table 5. Oxygen and carbon monoxide-binding rate constants and affinities for the liposome-embedded heme *15* under physiological conditions

Heme	$10^{-5} \cdot k_{on}(O_2)$ l/mol · sec	$P_{1/2}(O_2)$ mmHg	$10^{-5} \cdot k_{on}(CO)$ l/mol · sec	$P_{1/2}(CO)$ mmHg	M $P_{1/2}(O_2)/P_{1/2}(CO)$
Liposome/ <i>15</i>	4.5	36	0.25	0.14	275
<i>9a</i>	260	1.0	36	0.0018	560
Hb in blood	29	27	1.0	0.10	270

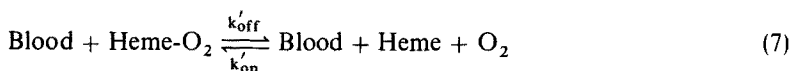
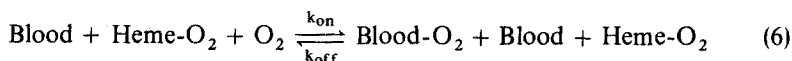
6 Approach to a Blood Substitute

The oxygen-binding reaction of the liposome-embedded heme was examined by using poly-lipid liposome/lipid-heme in a *pseudo vivo* and *ex vivo* system.

First the oxygen-exchanging reaction of the liposome-embedded heme with blood was tested, using an artificial lung apparatus⁹⁸⁾. Deoxy bovine blood was contacted with the oxy liposome/heme in counter-current flow through the hollow fibers composed of a cellulose membrane ($\varnothing 200 \mu$, membrane thickness 5μ , pore size $25 \sim 30 \text{ \AA}$). The liposome/heme was flowed with high space velocity, more than 100 ml per min. It was mechanically stable under strong share stress and acted as the oxygen carrier. Oxygen was effectively supplied from the oxy liposome/heme to deoxy blood, which turned to oxy blood at the outlet of the artificial lung apparatus.

The direct and rapid oxygen-exchanging reaction between the liposome-embedded heme with a red blood cell was observed by a rapid-scanning stopped flow method ⁹⁹⁾. Although both the liposome/heme and blood are red colored solutions, their visible absorption spectra were slightly different from each other and this small difference could be analyzed in a high sensitive and rapid scanning spectrophotometer with data processor. After rapid mixing deoxy blood with the oxy liposome/heme, the absorption change was monitored at the double wavelengths, which were selected from the deoxy-oxy isosbestic points for both media. The oxygen-exchanging reaction completed within 1 sec, and the oxygen-binding percentages for the liposome/heme and blood at the equilibrium were agreed with those estimated from the oxygen-binding equilibrium curves. For example, when a deoxy red blood cell suspension was mixed with the dilute oxy liposome/heme solution saturated with air, 1.5 ml oxygen surely transferred to the deoxy blood.

The oxygen-binding and -dissociation rate constants were also determined from the mixture system of blood and the liposome/heme. A three-stage reaction was observed; the first stage is the binding reaction of the oxygen dissolved physically in solution to deoxy-blood [Eq. (6), $k_{on} = 3.4 \times 10^4 \text{ M}^{-1} \text{ s}^{-1}$]. The second is the oxygen dissociation from the oxy liposome/heme in response to the oxygen pressure in solution, as shown in Eq. (7): $k'_{off} \cdot k''_{on} = 5.0 \times 10^3 \text{ M}^{-1} \text{ s}^{-1}$. The third is the binding reaction of the released oxygen with the remained deoxy blood [Eq. (8)]. The reverse of this three stage reaction was also observed for the oxygen-exchanging reaction between the deoxy liposome/heme and oxy blood. The kinetic constants determined were in accord with those determined previously for the individual oxygen-binding reactions.



The poly-lipid liposome/lipid-heme solution was also stable in a physiological salt solution, plasma expander, human serum, and whole blood even at high concentration, [heme] = 10 mM which is equal to that of human blood. In these media, it gave the same stable oxygen adduct with oxygen-binding affinity ($P_{1/2}(\text{O}_2) = \text{ca. } 50 \text{ mmHg}$) and life-time (ca. 1 day).

Oxy poly-lipid liposome/lipid-heme was flowed from the artery to the vein of a dog leg. In this experiment the injected fluid does not circulated through internal organs for a few hours, its toxicity can be neglected during the observation. The oxygen concentration was monitored at the muscle tissue of the leg with a needle-type oxygen electrode. After the artery-vein circulation was connected with the oxy liposome/heme solution, the oxygen concentration was kept at a higher level in comparison with the controlled experiment using a physiological salt solution. This result demonstrates the fact that the synthetic liposome-embedded heme transports and supplies oxygen to the muscle tissue.

The liposome-embedded hemes were composed of synthetic derivatives of porphinatoiron and phospholipids originated in nature. To improve the bio-compatible property of the liposome/heme some attempts have been reported.

The biomembrane of a red blood cell was isolated from a human red blood cell and taken into fragments by ultrasonication¹⁰⁰⁾. The heme complex was incorporated into the bilayer of a liposome reconstructed with the fragment: This spherical liposome had its average diameter at ca. 0.1 μ and was composed of phospholipids, membrane proteins, and the heme complex (Fig. 12). The membrane fluidity of this liposome was the same as that of the membrane of a red blood cell, which means the physical property of this liposome/heme is corresponding to that of a red blood cell. This liposome/heme showed reversible oxygen-binding under physiological conditions.

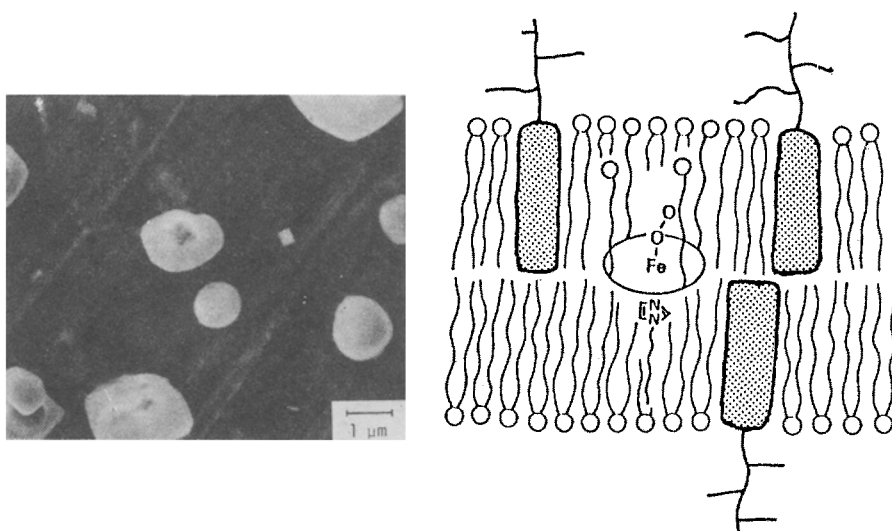


Fig. 12. Electron microscopic photograph for hybrid liposome/heme

Glycoprotein from bovine serum was incorporated into the bilayer of liposomes¹⁰¹⁾. It reduced the segmental motion of lipid molecules especially of the hydrocarbon chains of the lipid,² which brought about an increase in the hydrophobic property of the inner region of the liposome bilayer. This hybrid liposome/heme gave a stable oxygen adduct. The incorporation of natural membrane proteins not only physically reinforces the liposome/heme *in vitro* but also increases its bio-compatibility.

The combination of the liposome-embedded heme with catalase or tocopherol (Vitamin E) much prolonged the life-time of the liposome-embedded heme as the oxygen carrier¹⁰²⁾. On degradation of the heme-oxygen adduct under physiological conditions slight amounts of superoxide and hydrogen peroxide are formed, which oxidize phospholipids and weaken the liposome. The coexistence of the catalase with the liposome/heme removes hydrogen peroxide and thus prolonged the life-time of the oxygen adduct. Tocopherol was incorporated in the liposome bilayer: it acted as an anti-oxidizing agent of lipids in the bilayer. The poly-lipid liposome/lipid-heme

containing a small amount of tocopherol works as the oxygen carrier under physiological conditions for a few weeks.

Characteristics of the liposome-embedded heme as an artificial oxygen carrier are summarized as follows.

- (i) Oxygen-binding is reversible and very rapid.
- (ii) The oxygen volume dissolved in the solution is similar or superior to that of blood.
- (iii) The oxygen-binding affinity is close to that of blood.
- (iv) The particle size is smaller than 0.1 μ .
- (v) Physically and mechanically stable under shear stress and storage.

It is an important subject to develop an oxygen carrier as an artificial blood. There are several methods to construct artificial bloods. The first method is to utilize natural Hb by modifying it with a chemical reactions. The membrane of a red blood cell (storoma) has type compounds and causes unconformity of the blood groups and so on. On the other hand, the storoma-free Hb is common for normal human bodies. But when the storoma-free Hb is injected in a blood circular, it is cleared up within a few minutes. To avoid this problem, the storoma-free Hb is combined with a synthetic polymer such as dextran ¹⁰³⁾, the Hb is polymerized with glutaraldehyde ¹⁰⁴⁾, the Hb is encapsulated with a synthetic polymer such as nylon ¹⁰⁵⁾, and the Hb is encapsulated with the phospholipid liposome instead of the red blood cell membrane ¹⁰⁶⁾. But there still remain problems such as supply of ultra-pure human Hb.

The second method is to use fluorocarbons in which oxygen is physically dissolved about 10 times of water. Fluorocarbons are chemically stable and do not show any biological reaction. 20–35 vol% of fluorocarbons such as triperfluorobutylamine and perfluorodecalin are emulsified in the presence of a surfactant. The white emulsion stays in a blood circular over several days when the particle size of fluorocarbon is smaller than 0.1 μ . The fluorocarbon emulsion has been tried experimentally in hundreds of patients in Japan and the U.S. ¹⁰⁷⁾. But there also still remain problems. The emulsion carries only 5 ml oxygen per 100 ml medium and a patient is to be kept under an oxygen tent. Fluorocarbons are so much radically different in their chemical properties from natural Hb, that there is still a possibility to cause unknown problems in an *in vivo* system.

As mentioned above, the liposome-embedded hemes are promising as an artificial blood in many ways, but they are not yet usable as substitutes for the red blood cell in living animals. Tests conducted in rodents showed that the liposome/heme indeed transports oxygen *in vivo*, but only for several hours ¹⁰⁸⁾. After that, the animals died, presumably because of a severe immune system reaction in the animal. Further experiments are being carried out by our group to try to overcome that problem.

7 Conclusion and Further Studies

In this article we demonstrated our strategy to chemically mimic Hb and a red blood cell. As the model of a red blood cell, usually Hb has been separated from a red blood cell and this membrane-free Hb has been artificially encapsulated with a synthetic polymer or a phospholipid liposome. We also used a liposome as the carrier of the active site but payed attention on the skin layer of the closed vesicle and not on its inside water phase. That is, we utilized the hydrophobic region of the liposome bilayer

as the substitution of the hydrophobic domain of a globular protein and embedded a synthetic porphinatoiron, which is the analogous compound of the oxygen-binding site of Hb, into the liposome bilayer. This liposome-embedded heme transports oxygen under physiological conditions and even *in vivo* just as Hb or a red blood cell does. We would like to emphasize here that our attention has been focused on the environment around the active site; i.e., how to realize a hydrophobic environment around the molecularly dispersed active site in aqueous media and how to adjust the structure of the active site to the environment from the viewpoint of its configuration and hydrophobic-hydrophilic balance. Such a subject has been drawn little attention by researchers in bio(in)organic chemistry.

It seems to us that the applications of an oxygen carrier are not limited to artificial blood. For example, it will be developed for the purpose of isolating pure oxygen from the air, i.e. the oxygen enriching system (films on fluids) containing an oxygen carrier¹⁰⁹⁾. Other applications include its use as catalysts for reactions of molecular oxygen *in vitro* and *in vivo*. They become a model of oxygenase and a candidate of reagents for drug-metabolism and of anti-cancer agents. Although this article covers only porphinatoiron, of course there are many porphinatometals and other metal complexes having a possibility to be oxygen carriers¹¹⁰⁾ and many metal complexes with gaseous molecule-binding ability for nitrogen, carbon dioxide, etc.¹¹¹⁾ may exist. Macromolecular metal complexes have a potential as a carrier or an activator of gaseous molecules as metalloenzymes such as Hb and nitrogenase do.

Apart from the gaseous molecule-binding ability, the combination of a porphianto-metal with lipid layer films or highly ordered macromolecular films often offers possibilities not attainable in other ways. For example, electron-transfer from the porphinatozinc embedded in lipid layer to the outside of the layer is interesting¹¹²⁾. An electron is transferred across the lipid layer by a tunneling mechanism and its allowing distance was ca. 15 Å. Because porphinatometals are active centers of mediators for electron-transfer (redox), electro-magnetic activity, small molecule- and ion-binding etc., the porphinatometal containing ultra-thin films have a potential to apply as new devices of molecular level such as molecular switch, memory, and transducer.

As the science of Hb provided basic knowledges of biochemistry and biophysics, chemically mimicked models of Hb are expected to offer new unique fields to chemistry in the near future.

8 References

1. Dickerson, R. E., Geis, I.: *The Structure and Action of Proteins*, Harper & Row, London 1969
2. Lehninger, A. L.: *Biochemistry* (2nd Ed.), Worth Pub. New York 1975
3. Perutz, M. F., Muirhead, H., Cox, J. M., Goaman, L. C.: *Nature* 219, 131 (1968)
4. Wang, J. H.: *J. Am. Chem. Soc.* 80, 3168 (1958)
5. Jones, N. L.: *Blood Gases and Acid-Base Physiology*, Marcel Dekker, New York 1980
6. Cohen, I. A., Caughey, W. S.: *Biochem.* 7, 636 (1968)
7. Hammond, G. S., Wu, C. S.: *Chem. Ser.* 77, 186 (1968)
8. Kao, O. H., Wang, J. H.: *Biochem.* 4, 342 (1965)
9. Jones, R. D., Summerville, D. A., Basolo, F.: *Chem. Rev.* 79, 139 (1979)
10. Collman, J. P.: *Acc. Chem. Res.* 10, 265 (1977)
11. Traylor, T. G., Traylor, P. S.: *Annu. Rev. Biophys. Bioeng.* 11, 105 (1982)
12. Baldwin, F. E., Huff, J.: *Am. Chem. Soc.* 95, 5757 (1973)

13. Chang, C. K.: *ibid.* 99, 2819 (1977)
14. Traylor, T. G., Campbell, D., Tsuchiya, S.: *ibid.* 101, 4748 (1979)
15. Battersby, A. R., Hamilton, A. D.: *J. Chem. Soc., Chem. Commun.* 1980, 117
16. Momenteau, M., Loock, B.: *J. Mol. Catal.* 7, 315 (1980)
17. Collman, J. P., Gagne, R. R., Halbert, T. R., Marchon, J. C.: *J. Am. Chem. Soc.* 95, 7868 (1973)
18. Collman, J. P., Brauman, J. I., Collins, T. J., Pittman, R. B., Sessler, J. L.: *ibid.* 105, 3038 (1983)
19. Chang, C. K., Traylor, T. G.: *ibid.* 95, 8475 (1973)
20. Collman, J. P., Gagne, R. R., Reed, C. A., Halbert, T. R., Lang, G.: *ibid.* 97, 1427 (1975)
21. Tsuchida, E.: *J. Macromol. Sci. A13*, 545 (1979)
22. Traylor, T. G.: *Acc. Chem. Res.* 14, 102 (1981)
23. Collman, J. P., Hegedus, L. S.: *Principles and Applications of Organotransition Metal Chemistry*, University Sci. Books, Cal. 1980
24. Baldwin, J. E., Perlmutter, P.: *Top. Curr. Chem.* 121, 181 (1984)
25. Baldwin, J. E., Cameron, J. H., Crossley, M. J., Dagley, I. J., Klose, T.: *J. Chem. Soc., Dalton Trans.* 1984, 1739
26. Momenteau, M., Loock, B., Lavalette, D., Tetreau, C., Mispelter, J.: *J. Chem. Soc., Chem. Commun.* 1983, 962
27. Suslick, K. S., Fox, M. M., Reinert, T. J.: *J. Am. Chem. Soc.* 106, 4522 (1984)
28. Battersby, A. R., Bartholomew, S. A., Nitta, T.: *J. Chem. Soc., Chem. Commun.* 1983, 1291
29. Chang, C. K., Traylor, T. G.: *Proc. Nat. Acad. Sci. USA*, 70, 2646 (1973)
30. Traylor, T. G., Tsuchiya, S., Campbell, D., Mitchell, M., Koga, N.: *J. Am. Chem. Soc.* 107, 604 (1985)
31. Chang, C. K.: *ACS Adv. Chem. Ser.* 173, 162 (1979)
32. Ward, B., Wang, C. B., Chang, C. K.: *J. Am. Chem. Soc.* 103, 5236 (1981)
33. Tsuchida, E., Nishide, H., Takane, M., Yohsioka, H.: *J. Bioinorg. Chem.* 25, 43 (1985)
34. Tsuchida, E., Wang, S-g., Yuasa, M., Nishide, H.: *J. Chem. Soc., Chem. Commun.* 1986, 23
35. Wang, S-g., Nishide, H., Tsuchida, E.: *Nippon Kagaku Kaishi (J. Chem. Soc. Jpn.)* 1985, 182
36. The cooperative parameter n is estimated from Hill's equation [Hill, A. V.: *J. Physiol.* 40, 190 (1910); Wyman, J.: *Adv. Protein Chem.* 19, 223 (1964)]. The relationship between the partial pressure of a gaseous molecule and the degree of the binding with $n = 1$ corresponds to a hyperbolic binding-equilibrium curve, and that for $n > 1$ is sigmoidal. The binding with $n > 1$ is understood that the binding sites cooperatively interact with each other and the binding occurs at a stroke (cooperative binding). n Corresponds to the strength of the cooperative interaction between the sites.
37. The planar structure of porphinatoirons slightly differ from each other depending on their fifth and sixth coordinating ligands. In the low-spin porphinatoiron complexes, the central iron ion lies in the porphyrin plane and gives the plane a strictly planar structure. This is the case for oxyHb, carboxyHb, and deoxyHb with higher binding reactivity [relaxed (R) state of deoxyHb]. In contrast, the central iron ion of the high-spin porphinatoiron complexes is pulled up above the plane and the plane is slightly distorted, which occurs in the cases of met-[Fe(III)]Hb and deoxyHb with lower binding reactivity [tense (T) state of deoxyHb]. It is considered to be related to the cooperative binding by Hb that Hb contains deoxy-porphinatoirons which are in equilibrium between the T and R states that differ in their binding reactivity.
38. Eshima, E., Matsushita, Y., Hasegawa, E., Nishide, H., Tsuchida, E.: *Polym. Prepr. Jpn.* 31, 542 (1982)
39. Eshima, E., Matsushita, Y., Sekine, M., Nishide, H., Tsuchida, E.: *Nippon Kagaku Kaishi (J. Chem. Soc. Jpn.)* 1983, 214
40. Eshima, E., Nishide, H., Tsuchida, E.: *J. Chem. Soc., Chem. Commun.* to be submitted; *Jpn. Tokyo Koho JP* 59-55885 (1984)
41. Leal, O., Andorson, D. L., Bowman, R. G., Basolo, F.: *J. Am. Chem. Soc.* 97, 5125 (1975)
42. Tsuchida, E., Honda, K., Hata, S.: *Bull. Chem. Soc. Jpn.* 49, 868 (1976)
43. Fuhrhop, J. H., Besecke, S., Subramanian, J.: *Makromol. Chem.* 178, 1621 (1977)
44. Nishide, H., Shinohara, K., Tsuchida, E.: *J. Polymer Sci. Chem. Ed.* 19, 1109 (1981)
45. Nishide, H., Kato, M., Tsuchida, E.: *Eur. Polymer J.* 17, 579 (1981)
46. Tsuchida, E., Nishide, H.: *Adv. Polymer Sci.* 24, 1 (1977)
47. Kaneko, M., Tsuchida, E.: *J. Polymer Sci. Rev.* 16, 397 (1981)
48. Tsuchida, E., Nishide, H.: *ACS Sym. Ser.* 212, 49 (1983)

49. Tsuchida, E., Nishide, H., Ohno, H.: *J. Inorg. Biochem.* **17**, 283 (1982)
50. Nishide, H., Ohno, H., Tsuchida, E.: *Makromol. Chem., Rapid Commun.* **2**, 55 (1981)
51. Tsuchida, E., Nishide, H., Yokoyama, H.: *J. Chem. Soc., Dalton Trans.* **1984**, 2383 (1984)
52. Uotani, N., Hasegawa, E., Nishide, H., Tsuchida, E.: *J. Inorg. Biochem.* **22**, 85 (1984)
53. Tsuchida, E., Nishide, H., Yokoyama, H., Inoue, H.: *Polymer J.* **16**, 325 (1984)
54. Nishide, H., Sekine, M., Tsuchida, E.: *ibid.* **14**, 629 (1982)
55. Tsuchida, E., Nishide, H.: *Makromol. Chem., Rapid Commun.* **3**, 417 (1982)
56. Tsuchida, E., Abe, K.: *Adv. Polymer Sci.* **45**, 1 (1982)
57. Tsuchida, E., Nishide, H., Taguchi, K.: *Makromol. Chem., Rapid Commun.* **3**, 161 (1982)
58. Tsuchida, E., Nishide, H., Sato, Y.: *Bull. Chem. Soc., Jpn.* **55**, 1980 (1982)
59. Tsuchida, E.: *J. Pharm. Dyn.*, **6**, 9 (1983)
60. Tsuchida, E., Nishide, H., Sato, Y.: *J. Chem. Soc., Chem. Commun.* **1982**, 556
61. Tsuchida, E., Nishide, H.: *J. Chem. Soc., Dalton Trans.*, to be submitted
62. Young, R., Chang, C. K.: *J. Am. Chem. Soc.* **107**, 898 (1985)
63. Tsuchida, E., Nishide, H., Yokoyama, H., Young, R., Chang, C. K.: *Chem. Lett.* **1984**, 991
64. Nishide, H., Tsuchida, E.: *Makromol. Chem.* **183**, 1883 (1982)
65. Shigehara, K., Shinohara, K., Sato, Y., Tsuchida, E.: *Makromolecules* **14**, 1153 (1981)
66. Hasegawa, E., Tsuchida, E.: *J. Polymer Sci. Chem. Ed.* **15**, 3039 (1977)
67. Tsuchida, E., Hasegawa, E., Kanayama, T.: *Macromolecules* **11**, 947 (1978)
68. Vasilenko, I. A., Ushakova, I. P., Radyukhin, V. A.: *J. Gen. Chem. USSR*, **1979**, 126
69. Makino, N., Yokoya, M., Sugita, Y.: *Biochem. Biophys. Res. Commun.* **108**, 1010 (1982)
70. Hasegawa, E., Matsushita, Y., Eshima, K., Tsuchida, E.: *ibid.* **104**, 793 (1982); **105**, 1416 (1982)
71. Tsuchida, E., Nishide, H., Yuasa, M., Hasegawa, E., Matsushita, Y.: *J. Chem. Soc., Dalton Trans.* **1984**, 1147
72. Loach, P. A., Kong, J. L. Y.: *ACS Symp. Ser.* **201**, 515 (1982)
73. Fendler, J. H.: *Membrane Mimetic Chemistry*, John Wiley, New York 1982
74. Eshima, K., Yuasa, M., Nishide, H., Tsuchida, E.: *J. Chem. Soc., Chem. Commun.* **1985**, 130
75. Nishide, H., Maeda, H., Wang, S., Tsuchida, E.: *ibid.* **1985**, 260
76. Matsushita, Y., Hasegawa, E., Eshima, K., Tsuchida, E.: *Heterocycles* **22**, 1403 (1984)
77. Tsuchida, E.: to be published
78. Matsushita, Y., Hasegawa, E., Eshima, K., Tsuchida, E.: *Heterocycles* **22**, 2547 (1984)
79. Matsushita, Y., Hasegawa, E., Eshima, K., Tsuchida, E.: *Chem. Lett.* **1983**, 1387
80. Tsuchida, E., Hasegawa, E., Matsushita, Y.: *Inorg. Chim. Acta* **93**, 137 (1984)
81. Tsuchida, E., Nishide, H., Yuasa, M., Hasegawa, E., Matsushita, Y.: *J. Chem. Soc., Dalton Trans.* **1985**, 275
82. Ohno, H., Maeda, Y., Tsuchida, E.: *Biochim. Biophys. Acta* **642**, 27 (1981)
83. Ogata, Y., Nishide, H., Tsuchida, E.: *Polym. Prepr. Jpn.* **34**, 646 (1985)
84. Tsuchida, E., Nishide, H., Sekine, M., Yamagishi, A.: *Biochim. Biophys. Acta* **734**, 274 (1983)
85. Liposomes undergo distinct structural changes at a certain temperature, i.e. the phase transition temperature (T_c), when heated or cooled. These changes do not affect the gross structural features of liposomes, i.e. they remain as roughly spherical closed smectic mesophases of the phospholipid bilayer, and correspond to the orientation of the alkyl chains of the lipid. Below T_c , lipids in the bilayers are in highly ordered gel states, with their alkyl chains in all-trans conformations. Above T_c lipids become liquid crystal states as the consequence of gauche rotations and kink formations. For example, the T_c values of EYL, and DPPC liposomes are -15 to -7 , 23.5 and 41 °C, respectively (Ansell, G. B., Dmason, R. M., Hamthorne, J. N.: *Form and Function of Phospholipid*, Elsevier, Amsterdam 1973).
86. Ringsdorf, H., Gros, L., Schupp, H.: *Angew. Chem., Int. Ed. Eng.* **20**, 305 (1981)
87. Hupfer, B., Ringsdorf, H., Schupp, H.: *Makromol. Chem.* **182**, 247 (1981)
88. Hasegawa, E., Matsushita, Y., Eshima, K., Nishide, H., Tsuchida, E.: *Makromol. Chem., Rapid Commun.* **5**, 779 (1984)
89. Tsuchida, E., Hasegawa, E., Matsushita, Y., Eshima, K., Yuasa, M., Nishide, H.: *Chem. Lett.* **1985**, 1650
90. Tsuchida, E.: to be published
91. Yuasa, M., Ogata, Y., Nishide, H., Tsuchida, H., Nozaki, T.: *Chem. Lett.* **1984**, 1889
92. Tsuchida, E., Nishide, H., Yuasa, M.: *J. Chem. Soc., Chem. Commun.* **1984**, 96
93. Tsuchida, E., Yuasa, M., Nishide, H.: *J. Chem. Soc., Dalton Trans.* **1985**, 65

94. Antonini, E., Brunoi, M.: Hemoglobin and Myoglobin in their Reactions with Ligands, North-Holland Pub., Amsterdam 1971
95. Roughton, F. J. W.: Proc. R. Soc. London *111*, 1 (1932)
96. Tsuchida, E., Nishide, H., Yuasa, M., Sekine, M.: Bull. Chem. Soc. Jpn. *57*, 776 (1984)
97. Yuasa, M., Nishide, H., Tsuchida, E.: J. Pharm. Dyn. *8*, 17 (1985)
98. Tsuchida, E.: to be published
99. Tsuchida, E., Nishide, H., Yuasa, M.: Biochim. Biophys. Acta., to be submitted
100. Seki, N., Ohno, H., Tsuchida, E., Sasakawa, S.: Bull. Chem. Soc. Jpn. *57*, 2863 (1984)
101. Ohno, H., Seki, N., Tsuchida, E.: Makromol. Chem. *185*, 329 (1984)
102. Tsuchida, E.: to be published
103. Tam, S., Blumenstein, J., Wong, J. T.: Can. J. Biochem. *56*, 981 (1978)
104. Friedman, H. I., De Venuto, F., Schwavtz, B. D., Nemeth, T. J.: Surgery Gynecology Obstetrics, *159*, 429 (1984)
105. Chang, T. M. S.: Artificial Cells, Medical Inform. Ser., Montreal 1976
106. Djorjevich, L., Miller, I. F.: Exp. Hemat. *8*, 584 (1980)
107. Chem. Eng. News, May *3*, 31 (1982)
108. Chem. Eng. News, Jan. *14*, 42 (1985)
109. Tsuchida, E., Nishide, H.: Makromol. Chem., Rapid Commun. *3*, 693 (1982)
110. Martell, A. E., Calvin, M.: Chemistry of the Metal Chelate Compounds, Printice-Hall, Englewood 1952
111. Kurimura, Y., Tsuchida, E.: Makromol. Chem. *183*, 2889 (1982)
112. Tsuchida, E., Kaneko, M., Nishide, H.: J. Phys. Chem. *90*, in press (1986)

Molecular Catalysis by Polyammonium Receptors

Franz P. Schmidtchen

Lehrstuhl für Organische Chemie und Biochemie
der Technischen Universität München, 8046 Garching, FRG

Table of Contents

A Introduction	102
B Definitions	103
C On the Advantages of Polyammonium Molecular Catalysts	104
D Cyclophanes	105
D.I Cyclophane Hosts without Additional Catalytic Functions	105
D.II Functionalized Cyclophanes	109
E Macrotricyclic Ammonium Cage Compounds	111
E.I Conceptual Design and Host-Guest Interactions	111
E.II Rate Effects Shown by Macrotricyclic Quaternary Ammonium Salts	117
F Miscellaneous Polyammonium Catalysts	128
F.I Azacrown Ethers	128
F.II Steroid Based Catalysts	130
G Conclusion	131
H References	131

A Introduction

The continuing strive of chemists for selectivity in chemical reactions may be grouped into two general approaches: Selectivity in the sense of a discrimination between several possible reaction modes of an ensemble of reaction partners may be the result of a joint action of protection/activation procedures, use of sometimes very elaborate reagents and careful tuning of reaction conditions. Although there can be great art in assembling the individual steps into a successful strategy for obtaining a selective transformation, this approach appears wasteful from an economic standpoint on comparison to the alternative. This is the employment of catalysts to effect the selective reactions. By definition catalysts are not used up like the technical aids in the former approach and they are required in minute amounts only depending on their activity.

The shining examples of the potential of this approach are the natural enzymes, which represent the most selective reaction systems we presently know of. Thus, it is no surprise that the increasing knowledge about the biocatalysts initiates attempts to adopt enzymic working principles for the introduction of selectivity into abiotic systems. It is admittedly true that we have certainly not a quantitative understanding of biocatalysis ¹⁾ and even its molecular basis is still being disputed ²⁾.

However, a number of features have been discovered and unequivocally proven to contribute to the success of enzymes. If one accepts the view that selectivity (and rate enhancement) is *not* imperatively associated with the protein nature of enzymes, it is only rational to exploit these insights for the design of selective but artificial catalysts. The term "enzyme model" which was coined for catalysts possessing common design features with enzymes could mean, that studying these models might help in the elucidation of enzyme mechanisms. The inverse reasoning, however, that the adaptation of enzymic principles should lead to better catalysts even for non biological reactions appears far more promising.

The first lesson to learn from enzymes is that complex formation between the protein and the substrate(s) in the ground state is mandatory for enzyme action ³⁾. This feature is generally acknowledged and X-ray crystallography has supplied evidence for the dedicated interaction of the functionalities in the substrate structure with subsites of the enzyme macromolecule resulting in complexes having a well defined and unique structure. Part of the overall selectivity of the enzyme reaction is already recognized in the first association step prior to any bond breaking or forming event. This notion determines the use of artificial host-guest systems to mimic enzymic properties. In addition to ground state complex formation a variety of features related to structure or function and common to the majority of enzymes ⁴⁾ may be incorporated into synthetic catalysts: The enzyme-like catalyst itself should possess a well defined structure with a stoichiometric number of substrate binding ("active") sites. These active sites should generally be located in concave surfaces (cavities, pockets, clefts) offering a densely packed rather hydrophobic environment. Functions to perform chemical mechanisms (nucleophilic-, electrophilic-, covalent-, general acid-base-, electrostatic catalysis) can supplement the basic host structures.

The present review deals with the construction of polyammonium salts, the design of which was largely inspired and still owes much of its attraction by analogy to natural enzymes, and their effects on reaction rates. This is to define the frontline in our

efforts to cope with the underlying motivation for studying enzyme models: the enhancement of selectivity in chemical systems ⁵⁾.

B Definitions

Selectivity used as defined above is a kinetic phenomenon, because the *rates* of conversion of competing substrates are compared. Thus its magnitude may depend on the ability of a given molecular species to accelerate or decelerate one particular reaction to a greater extent than all the others. Rate accelerations are a consequence of catalysis, but regrettably the latter term has become blurred. Since clarity of terms is an obligatory requirement for any meaningful comparison catalysis as it relates to the natural enzymes and artificial model systems needs some assessment of its meaning ⁶⁾.

1) Catalysis is the rate acceleration observed in the presence of a molecular species (the catalyst) compared to the rate of the *same reaction* (defined by the initial and final states) in its absence. As trivial as this statement may seem, it frequently has been violated in particular when huge “catalytic rate accelerations of enzyme models” have been claimed based on the comparison of partial reactions to the overall process. Another example of a frequently used misleading term is “intramolecular catalysis”. Systems which are said to exhibit “intramolecular catalysis” violate the aforementioned condition, because they cannot provide the appropriate (same) uncatalyzed reaction to compare with.

2) Catalysts should not change the free energy of the reaction system (i.e. the equilibrium). This condition, however, appears to be less stringent, recognizing that any addition to the reaction system (addition of catalyst, too) *will* change the free energy. So this issue reduces to a matter of quantitative concern: Using the terminology of transition state theory a molecule can be named a catalyst if it affects the energy of the transition state of a given reaction to a much higher degree than the ground state. The observation of a rate enhancement in a reaction ($k_{\text{uncatalyzed}} \rightarrow k_{\text{observed}}$, $k_{\text{obs}} > k_{\text{un}}$) on addition of a substance by itself *does not* prove catalysis. The rate increase may well emerge from a change in the equilibrium constant from K_{eq} (uncatalyzed) = $k_{\text{uncat}}/k_{\text{reverse}} \rightarrow K'_{\text{eq}} = k_{\text{obs}}/k_{\text{reverse}}$ i.e. it may be attributable to a pure ground state effect.

The extrema in the range of possibilities are set by the enzymes on one side, which were shown first by Borsook et al. ⁷⁾ not to alter the position of the equilibrium within experimental accuracy and on the other side by synthetic macroions, the rate enhancement of which entirely could be traced back to changes in the equilibrium constant ⁸⁾. Clearly the assessment of rate augmentations to be catalytic, will present problems especially with those systems of poor activity, which require high concentrations of “catalyst” in order to display a rate effect.

By adding the attribute “molecular”, catalytic systems are defined which owe their activity to a complex formation step. Noncovalent forces serve to connect the catalyst (host) and the guest (substrate(s)) in a thermodynamically stable fashion prior to the rate-limiting conversion step. The aim is to correlate structural features of the host to the rate augmentation, so that a deliberate modification of structure will yield a predictable rate effect. Prerequisite to a rational structure variation is some

knowledge of the mode of host-guest association. Systems, which cannot furnish definit complex structures due to their dynamic and rapidly rearranging nature are therefore much less amenable to tailoring. Ammonium macroions and aggregating amphiphiles ^{9, 10)} will thus be excluded from the present discussion, although they may display substrate binding behaviour and show considerable rate enhancements in certain reactions. Incorporation of these systems into structures of higher order (membranes, monolayers, vesicles etc.) can boost selectivity and enjoys a promising perspective ¹¹⁾.

C On the Advantages of Polyammonium Molecular Catalysts

Artificial molecular catalysts comparable to the natural enzymes should be able to catalyze reactions in an aqueous environment. Although the underlying catalytic principles might as well be demonstrated in other solvents, this condition can be exploited to take advantage of the most powerful force for combining individual molecules into noncovalent complexes in water: the hydrophobic bond ¹²⁾. Associations predominantly based on hydrophobic effects cannot exhibit great selectivity, because the hydrophobic bond originates from a rearrangement of the aqueous surroundings rather than from direct interactions of the complex forming partners. Consequently, the guests could be exchanged within broad limits provided they possess hydrophobic surfaces, without harming the stability of the overall system. The situation compares planely to a marriage of convenience, which generally yields a very stable configuration by some external "pressure" rather than by "emotional ties" between the partners. In spite of the poor selectivity to be gained on complex formation, this concept may in fact pay off in bimolecular reactions, the rates of which are ruled by highly negative intrinsic activation entropies. Here the bringing together of the reactant groups in spatial vicinity in the host-guest complex may show up in rate accelerations, because an unfavourable component (e.g. part of the negative activation entropy) has been removed from the rate limiting step and has been transferred to the prior but kinetically incompetent association process. Thus, in this instance a moderate selectivity of host-guest complex formation via hydrophobic interaction in the ground state experiences multifold magnification through the interdependent rate process.

The exploitation of hydrophobic forces requires the molecular catalysts to supply hydrophobic molecular regions yet the structure must remain water soluble. This can be achieved through the attachment of sufficient hydrophilic functions to a more lipophilic hydrocarbon like core structure. The quantitative relationship between hydrophilic and hydrophobic functions determines the degree of self association, which has to be avoided in order to obtain interpretable results. The natural cyclic oligosaccharides (cyclodextrins) exhibit a similar construction pattern and have thus been widely used as enzyme models ¹³⁾. With the introduction of charged hydrophilic functions into the host molecule one can gain an extra bonus on the selectivity, because the superposition of an electrostatic field to the hydrophobic bond adds another condition to be met by the guest. This could be demonstrated for semisynthetic cyclodextrins ¹⁴⁾ as well as for totally artificial cyclophane hosts ¹⁵⁾. Judging from this aspect only anionic and cationic solubilizing functions should be equally convenient. However, the cationic ammonium function offers a number of additional advantages

over their anionic competitors, which makes it very appealing as a construction unit for molecular catalysts. Besides their hydrophilicity, the most attractive feature of amines and ammonium salts is their highly developed chemistry. Since a great multitude of high yield reactions is known for the build up and interconversion of amino functionality, the rational synthetic strategies for the construction of desired molecular frameworks can be designed rather readily. The capability of amino functions to form 3 to 4 covalent bonds may well serve to build rigid host molecules by virtue of a high connectivity. Rigidity, in turn, seems to be a prerequisite for steric discrimination of guests and certainly aids the interpretation of binding data in different solvents, because host-guest interaction should not be obscured by conformational equilibria of the host.

More practical advantages arise from the ready modifiability of amino groups, the most straightforward being protonation. So the properties of the host may be tuned through the setting of the pH-value. Alternatively the measurement of changes in pH-value on addition of guest species provides a very accurate and sensitive means to determine binding stoichiometries and complex formation constants¹⁶⁾. This can help with the purification of the host as can the variation of counterions which may ease crystallisation to obtain suitable crystals for X-ray structure determination.

So far the arguments in favour of ammonium functions to build molecular catalysts on referred to the set up of an host-guest relationship known to be a fundamental feature of biocatalysis. Supplementary to the ground state stabilisation of substrates in a noncovalent complex, the transition state of the reaction as well might be prone to stabilising effects or it can be changed entirely to furnish a more speedy reaction route in the presence of ammonium salts. Chemical mechanisms of catalysis like nucleophilic-, electrostatic-, and general acid-base catalysis^{6, 17)} can be incorporated into molecular catalysts via attachment of suitable ammonium groups. This opens a large field with countless degree of freedom to design artificial catalysts and test their efficiency while retaining an analogy to the natural counterparts which are known to profit from the properties of ammonium groups in their catalytic action, too¹⁸⁾.

D Cyclophanes

D.I Cyclophane Hosts without Additional Catalytic Functions

Among the first to exploit totally synthetic water soluble host compounds to catalyze chemical reactions were Tabushi et. al. who found an accelerating influence of their newly developed¹⁹⁾ polyammonium cyclophane **1** on the hydrolysis of aromatic chloroacetates²⁰⁾. These authors showed conclusively that a rapid association of substrate and **1** precedes the rate limiting attack of solvent on the ester group. This step is amenable to buffer catalysis, too. Some relevant rate data are given in Table 1.

The evaluation of these data now depends largely on definitions. Tabushi et al. chose to view their results in terms of a “kinetic substrate specificity” manifested in $k_{\text{cat}}/k_{\text{un}}$ ratios. As a corollary they state a “marked specificity” in the conversion of substrates **2–4**. This is formally correct but it bears the danger of misinterpretation and is certainly seductive to draw faulty conclusions.

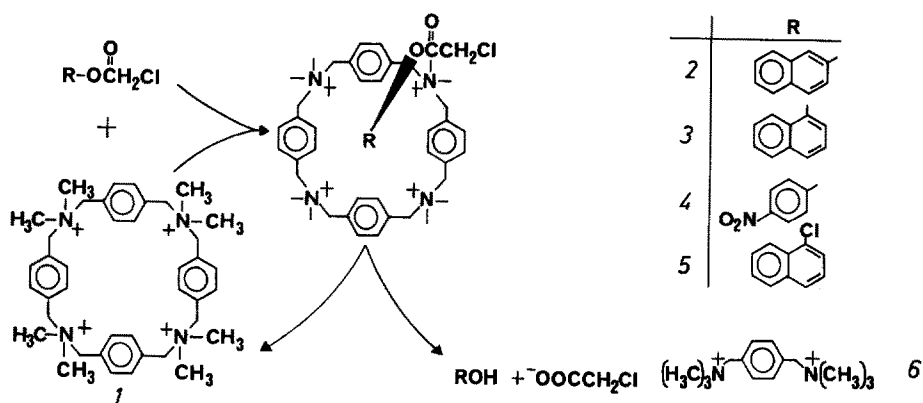


Table 1. Spontaneous and catalysed hydrolysis of aromatic esters in water; 20.2 °C, pH 8.10; 1/15 *M* phosphate buffer; selected illustrative examples from ²⁰⁾

catalyst	substrate	K_M [mM]	$k_{\text{cat}}/k_{\text{un}}$	k_{cat}/K_M [$\text{l} \cdot \text{mol}^{-1} \cdot \text{s}^{-1}$] ^{a)}
1	2	0.54	25	35.5
	3	0.18	6.0	27.2
	4	0.51	2.6	28.6
	5	0.20	0.085	1.1
	2	2.62	1.6	0.5
6	2	0.03	6.8	197

^{a)} recalculated from the data given in Ref. ²⁰⁾

If one accepts that in enzyme analogues substrate complex formation as well as transition state (TS) stabilisation contribute to the efficiency of the model, the parameter which takes both influences into account is k_{cat}/K_M . It reflects the free energy of the highest barrier along the reaction path relative to the initial state and thus determines the conversion rates of competing substrates ²¹⁾. Taking this measure there is virtually no selectivity (maximum factor $35.5/27.2 \sim 1.3$) in the positive catalysis of the ester cleavage by 1. The free energies of the TS — given the plausible assumption of identical ground state energies of hydrolysis at least for the naphthyl derivatives 2 and 3 — are very much alike. ($\Delta\Delta G^\ddagger < 0.72$ KJ/mol). Differences in the free energies of the noncovalent complexes in the ground state predominantly account for the differential rate effects observable at saturation ($k_{\text{cat}}/k_{\text{un}}$). Thus the conclusion that $\text{N}^+ \rightarrow \text{oxyanion}$ interaction at the TS for the tetrahedral intermediate formation remarkably depends on the substrate structure ²⁰⁾ does not seem to be justified. One substrate 5 shows inhibition rather than acceleration. From the alternatives of explanation offered — nonproductive binding and/or induced disfit — the former one which was favoured ²⁰⁾ is not likely to be the predominant factor, because nonproductive binding should not change the value of k_{cat}/K_M ²²⁾ the opposite being found experimentally.

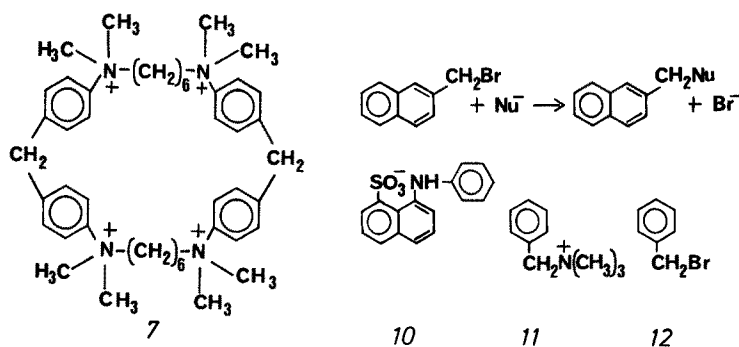
In order to put the efficiency of molecular catalysts into perspective one must compare it to their natural analogues wherever possible. The figure for comparison

again is given by the $k_{\text{cat}}/K_{\text{M}}$ -value, since this number appears to be under maximising evolutionary pressure in enzymes²³⁾. Natural broad specificity esterases^{24, 25)} exhibit a higher efficiency by 10^4 – 10^5 fold than *1*, which is even inferior to CTAB micelles according to this criterion (Table 2). However, in spite of the obvious paucity in catalytic efficiency of *1*, it was recognized that the general concept would hold and successive structural variation might improve the catalytic capabilities considerably.

Table 2. Comparison of esterolytic efficiencies of natural and abiotic molecular catalysts

catalyst	substrate	$k_{\text{cat}}/K_{\text{M}}$ [$\text{l} \cdot \text{mol}^{-1} \cdot \text{s}^{-1}$]
1	2	35.5
1	4	28.6
17	3	25
17	2,4-dinitrophenylchloroacetate	1220
pig liver esterase	p-nitrophenylbutyrate	$2.6 \cdot 10^6$
acetylcholine- esterase	acetylcholine	$1.6 \cdot 10^8$
	ethylacetate	$2 \cdot 10^5$
CTAB	2	197

Another attempt to use the host-guest complexation of simple cyclophanes has been reported by Schneider²⁶⁾. They take the easily accessible host **7**, an analogue of which had been demonstrated by Koga¹⁵⁾ to bind aromatic guest molecules by inclusion into its molecular cavity, and study its rate effects on nucleophilic aliphatic substitutions of ambident anions (NO_2^- , CN^- , SCN^-) on 2-bromomethylnaphthalene **8** and benzylbromide. Similar bimolecular reactions are well known in cyclodextrin chemistry²⁷⁾ and other artificial host systems²⁸⁾. In addition to the rather poor accelerations observed (see Table 3) the product ratio is changed in the case of nitrite favouring attack of the ambident nucleophile via its nitrogen atom.



Inhibition of the reaction by the dye *10* and independent NMR-measurements support the view that the hydrophobic naphthalenes *8* and *10* but not the smaller benzylbromide *12* are complexed by *7*. The authors explain their results through the action of an entropic effect: The gathering of anions in the vicinity of the host due to electrostatic attraction should boost S_N2 attack and thus accounts for the preponderance of nitro-

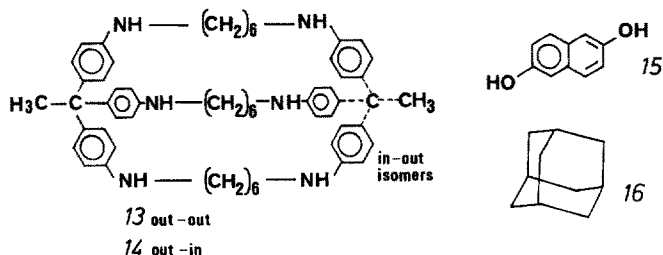
Table 3. Pseudo first order rate constants k_c and product ratio for substitution reactions of alkyl halides with nitrite ion in 50% aqueous dioxane, 30 °C; $[\text{NO}_2^-] = 0.42 \text{ M}$; ²⁶⁾

substrate	additive (concentration, mM)	$k_c \cdot 10^3 \text{ [s}^{-1}\text{]}$	product ratio R-ONO/R-NO ₂
8	—	0.7	0.50:1
8	7(43)	2.6	0.37:1
8	7(43) 10(46)	0.6	0.53:1
8	11(430)	1.1	20:1
8	N ⁺ (CH ₃) ₄ (430)	—	6.7:1
12	—	1.2	0.34:1
12	7(43)	1.2	0.34:1

product formation. The rate increase does not parallel the change in product ratio which means that several S_N2 and S_N1 processes in solution as well as in the association complex may proceed simultaneously. Since no data are given on the individual contributions to the overall process the given explanation seems somewhat superficial.

One may question, moreover, whether true catalysis is involved, or the rate augmentation rather emerges from a shift in the equilibrium constant (see Section B), visualizing the large host concentrations necessary to observe the rate effect. In the light of the inconclusive measures taken to exclude influences of micellation (from the product distribution data one would assume aggregation of the host to take place in contrast to N(CH₃)₄ salt) and the little detailed definition of the rate processes compared, the utility of these results to the improvement of molecular catalysts appears limited.

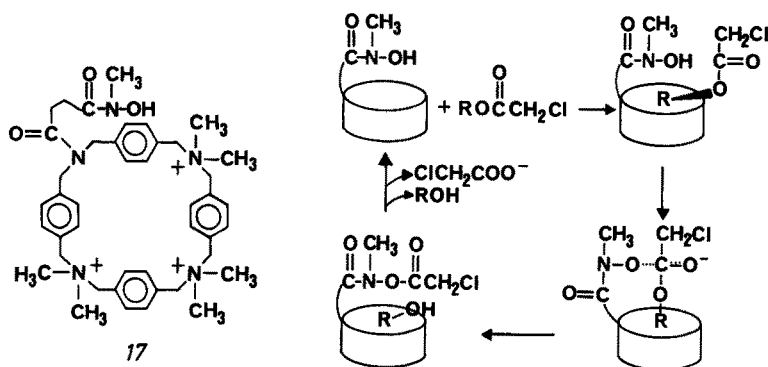
This improvement can be expected from the development of more sophisticated host structures. A recent publication of Vögtle et al. ²⁹⁾ documents this trend. They were able to synthesize the macrobicyclic heterocyclophanes **13** and **14**, which relate to each other in an "in-out" isomerism. The uptake of naphthalene derivatives like **15** was evidenced by proton NMR spectroscopy. In contrast to **14**, host **13** is capable of binding aliphatic guest molecules like adamantane **16**. This is readily conceivable on the basis of the steric argument that in **14** the endo methyl group occupies part of the cavity space necessary for inclusion binding of the quasi spherical guest **16** and thus hampers complex formation. The gross size of the cavity suffices for adamantane inclusion as deduced from the positive binding by host **13**.



A strange observation was reported ²⁹⁾ on the catalytic H/D exchange of **15** in acidic D₂O solution of **13** and **14**: Although either of these hosts form complexes with this guest, only **13** displays catalytic H/D exchange. Since no quantitative data were given the question whether this observation bears on differences in complex structure, ammonium salt acidities or indicates an unexpected change in mechanism must remain unanswered at present.

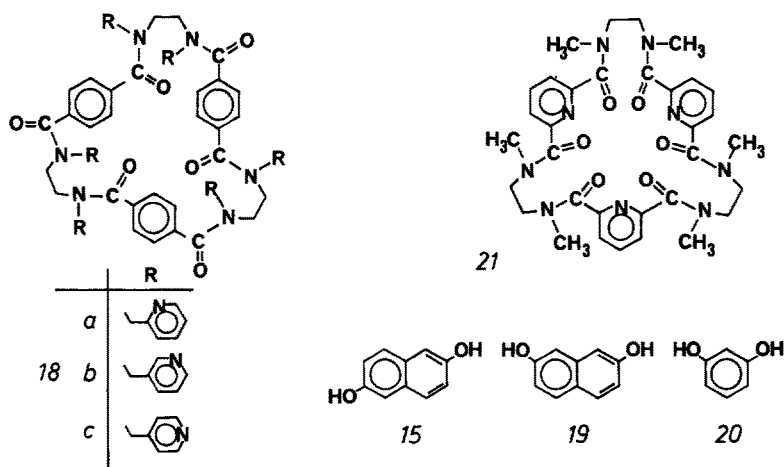
D.II Functionalized Cyclophanes

The synthetic strategy of building azacyclophanes lends itself to easy modification of the parent macrocycle through attachment of substituents capable of executing chemical catalysis mechanisms. Most frequently functions suitable for ester cleavage have been introduced. Following this route the supplementation of the quaternary ammonium cyclophane **1** with a hydroxamate function leads to the molecular catalyst **17** ³⁰⁾ with greatly improved catalytic power (see Table 2). Again the kinetics of cleavage of the activated esters **3** and **4** and others can be analyzed in terms of a rapid host-guest association followed by the intramolecular attack by hydroxamate anions to produce a tetrahedral intermediate. Contrary to the mechanism operative with host **1** the breakdown of this tetrahedral intermediate appears to be rate limiting in this case as is indicated by a Broensted β value of -0.6 in a plot of k_2 versus the pK_a of the leaving phenol. The covalent acyl-host intermediate hydrolyses fast enough to permit true catalysis (i.e. turnover) to be observed. Model **17** provides an illustrative example of the limitations of simple molecular catalysts. While it may seem straightforward to accelerate the rate determining step in a given uncatalyzed reaction by use of molecular catalysts with dedicated functionality, these enzyme models in general fall short of reaching very high acceleration factors, because another elementary step in the multistep reaction sequence takes over and thereby limits the speed of the overall process.



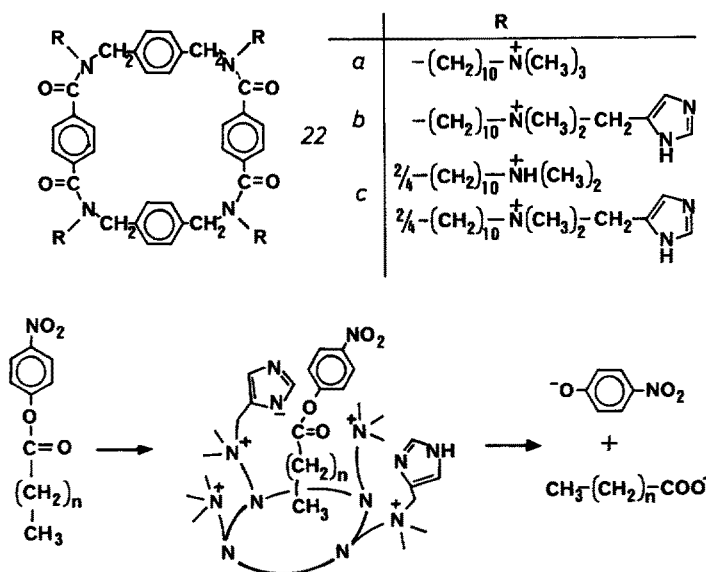
The well known ability of aromatic nitrogen bases to catalyze H/D exchange of phenols ³¹⁾ laid the basis for their use in cyclophane host-guest systems ³²⁾. The introduction of pyridinium side chains into a 30-membered azacyclophane ring **18** not only renders the molecule soluble in aqueous acid but also enables the deuteration of

aromatic diols **15**, **19** and **20** which is not observed with simple cyclophanes like **7** and proceeds more rapidly than with the pyridinium macrocycle **21**.



Again catalysis brought about by **18** appears to result from the joint action of substrate complexation as evidenced by ¹H-NMR shifts (which is not observed with **21**) and chemical steps conductable by the pyridinium substituents in **18** but not available to **7**.

The azacyclophane **18** is built according to the same general pattern which has been successfully applied in the construction of esterolytic octopus-like molecular catalysts³³). The design features and catalytic properties of functionalized octopus cyclophanes **22** and related structures have been reviewed in depth recently³⁴).



Suffice it to state that in contrast to **22a** the imidazolyl-substituted cyclophanes **22b** and **22c** indeed catalyze the hydrolysis of aliphatic carboxylic activated esters, **22c** being a little more effective. The efficiency as represented by the ratio of pseudo first order rate constants of the catalyzed versus the uncatalyzed reaction $k_{\text{cat}}/k_{\text{un}}$ displays a sharp maximum with the ester of tetradecanoic acid ($k_{\text{cat}}/k_{\text{un}}$ [**22c**] ~ 100), whereas almost no rate acceleration was found with esters of short chain acids. This and accessory results from spin label and fluorescence measurements together with the rate dependence on pH-value support the view that substrate and catalyst arrange each other in a distinct manner. The aliphatic chain of the substrate is supposed to be wrapped by the “octopus arms” of the cyclophane, causing its coiled structure to unfold and placing the ester group to be cleaved in juxtaposition to the nucleophilic imidazole moiety. The acylimidazole intermediately formed through attack of a presumably anionic imidazole decomposes at a higher rate and thus establishes a catalytic cycle. In model **22** features of micelles and molecular catalysts are successfully combined, but the purposely built-in hydrophobicity necessary for substrate binding shows up in a strong tendency to self aggregation, which limits the applicability in practice.

E Macrotricyclic Ammonium Cage Compounds

E.I Conceptual Design and Host-Guest Interactions

Recognising the fact that about 70% of all enzymes act on phosphate esters and carboxylates i.e. negatively charged substrates, one may imagine another application of molecular catalysts bearing ammonium groups which mimics this frequently occurring facet of the biocatalysts: the binding of anionic species in aqueous solution. Clearly this task requires an extension of the systems which primarily rely on hydrophobic interactions to effect substrate binding and a novel conceptual design of suitable host structures must be developed. The target structures of course should possess the general enzymic features which have proved profitable in cyclophane enzyme models. As a corollary an anion host must provide a molecular cavity which is shielded from the outside. The cavity should be rimmed by densely packed lipophilic walls to constitute a hydrophobic microenvironment like in the interior of enzymes and for maximising dispersion interactions. Since the transfer of heavily solvated anions from water into the lipophilic pocket of an host is energetically very unfavourable host-anion binding can only be expected if strong and far reaching favourable interactions outmatch the loss in hydration. By analogy to the enzymes, which in addition to forces inherent in their protein nature³⁵⁾ make utmost use of positive charges located on the side chains of arginine, lysine and histidine³⁶⁾ to bind and orient their anionic substrates, electrostatic interactions could serve to bring about complex formation in artificial anion hosts, too. The positive charges, however, must be placed in a fixed spatial relationship to each other in order to insure that ion pairing with the anionic guest will indeed result in a well definable complex structure. This can only be guaranteed by a fairly rigid molecular framework which in turn aids in the steric discrimination between different guests.

A putatively opposing requirement is the necessity to establish fast guest exchange in order to obviate rate limitations in prospected catalytic reactions due to slow association — dissociation processes. This can most easily be achieved in very flexible host molecules, but rigid structures which are not subject to major conformational reorientation on complexing the guest species may meet this requirement as well.

In contrast to host molecules for binding cations examples for anion hosts are still very scarce³⁷⁾. One simple reason becomes immediately obvious on comparison of the molecular dimensions of the guest species (Table 4).

Table 4. Van der Waals radii of selected cations and anions³⁸⁾

radius r [pm]		radius r [pm]	
Na ⁺	97	Cl ⁻	181
K ⁺	133	Br ⁻	195
Cs ⁺	167	I ⁻	217
Ag ⁺	113	BF ₄ ⁻	280
Mg ²⁺	78	ClO ₄ ⁻	300
N(CH ₃) ₄ ⁺	330	Picrate ⁻	510

Thus, host molecules which are to take up anions into a cavity must be considerably larger than their cation binding counterparts and may easily attain molecular masses exceeding 1000 D. Consequently a symmetrical host structure would be helpful for monitoring the synthesis with the ordinary instrumental tools of organic chemistry.

The synopsis of the requirements and boundary conditions culminated in the design of macrotricyclic quaternary ammonium salts 23, 24, 25. The synthetic strategy furnishing these tetrahedral structures has been elaborated by Lehn³⁹⁾ and is depicted in Fig. 1.

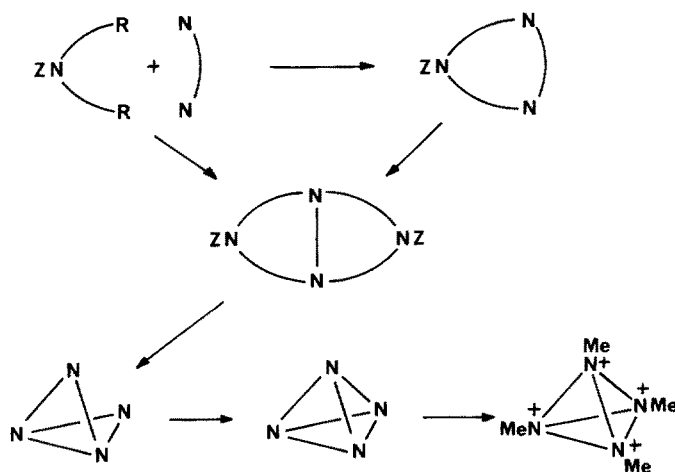


Fig. 1. Strategy for the synthesis of the tricyclic ammonium salts 23, 24 and 25

This route involves three successive cyclisations under high dilution conditions which limits the scale and yield of the overall synthesis severely. The parent macrotricyclic tertiary amines were obtained in 2–5% overall yield^{39,40)} and were quaternized under selected conditions giving the target structures 23–25⁴¹⁾ uncontaminated by in-out isomers.

Visualizing the symmetrical architecture and the high ratio of hydrophilic (N^+R_4) to lipophilic (CH_2) moieties one must presume that these compounds are not susceptible to micellation. This was confirmed through the measurement of ionic conductivities. Even the macrotricyclic 25 (as fluoride) supposedly most amenable to aggregation followed Kohlrausch square root law (equivalent conductivity vs concentration^{1/2}) up to 0.04 M without showing any curvature or break in slope of the plot. Together with results from substrate binding and kinetic experiments (see below) it appears safe to conclude that the tetrahedral ammonium salts 23–25 are strong electrolytes and form molecularly dispersed solutions in water. Solubility, however, markedly depends on the counter anion. Chaotropic anions like perchlorate, hexafluorophosphate or tetraphenylborate precipitate these compounds from aqueous solution, which can eventually be used for their gravimetric determination.

First indications that 24 and 25 indeed served the purpose they were designed for — the inclusion complexation of anions in aqueous solution — were given by their ¹H-NMR spectra (Fig. 2): On addition of iodide to solutions of 24 or 25 in D₂O the resonances of the α , β and γ , (δ) methylene groups shift to lower field without apparent line broadening or splitting but opposing the direction of shift experienced by the exomethyl groups. The dependence of shift on iodide concentration (Fig. 2) obviously suggests an 1:1 complex formation with guest exchange occurring beyond the fast exchange limit of the spectrometer. Similar shifts could be observed with other anions, too. The absolute magnitude parallels the size of the anion in the halide series, but hydrophilic oxoanions though rather large only showed a very weak effect. The tetrahedral macrocycles themselves display big differences: whereas the ¹H-NMR signals of 23 did not respond to any alteration of the type or concentration of counterions the resonances of 24 generally were influenced to a greater extent than those of the large macrocycle 25. The shifts, however, vanished on addition of acetone and were unobservable in methanol.

These NMR observations are consistently explained assuming a unique type of ion pairing: The penetration of an anionic guest into the partially compressed molecular cavity of the macrotricycles. Owing to hydrophobic interactions the alkylene chains connecting the nitrogen atoms in 24 and 25 will tend to make closest contacts to each other, thus reducing the effective diameter of the cavity. The introduction of the anion causes a breathing motion of the host, observable as a change in chemical shift which affects the bridge methylene signals and the exomethyl resonance in a differential manner. A conformational change of the host is unobservable if the structure is not compressed in the uncomplexed state due to increased repulsion of the positive charges and more hydrophilic bridges as in the smallest macrotricyclic 23 or the use of a solvent with a less pronounced solvent structure (like aqueous acetone or methanol). Moreover, if the tetrahedral symmetry of the guest allows an arrangement within the cavity with minimal reorganisation of the host structure as the inspection of CPK models suggests in the case of oxoanions, the observable effect as well may be vanishingly small.

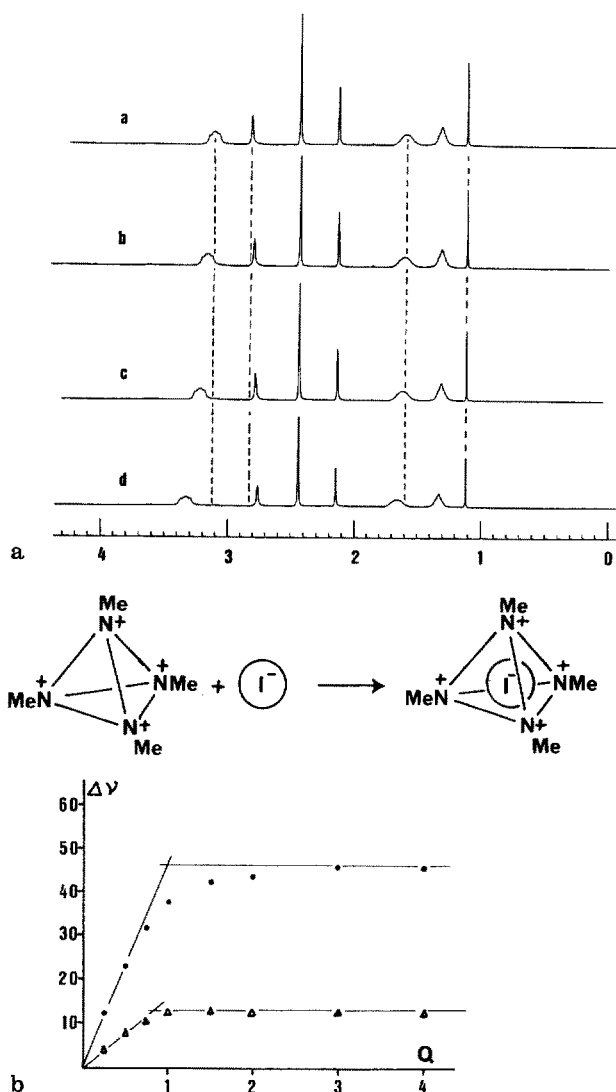


Fig. 2a and b. 200 MHz ¹H-NMR spectra of 24 (mesitylene-sulfonate salt) in the presence of increasing amounts of I⁻ ion; molar ratio I⁻/24 = Q: a = 0; b = 0.25; c = 0.5; d = 2.0, internal standard: tert.butanol; **b** Plot of the changes in chemical shift versus molar ratio Q; ● = N-CH₂ protons; △ = N-CH₃ protons

Direct proof of true inclusion complexation was provided by an X-ray crystal structure determination of the iodide complex of 24 (Fig. 3)⁴²⁾. One out of four iodide counterions occupies the central cavity formed by the host. Nearly identical I—N interatomic distances and N—I—N angles which very closely approach the tetrahedral standard indicate an almost perfect tetrahedral arrangement of the positive charges located on nitrogen around the encapsulated anion. From the notion that the torsional angles in the methylene bridges generally exceed 160° thus maximizing the chain length, and the closest contacts of the encapsulated iodide ion to the alkylene carbon atoms correspond to the sum of their van der Waals radii one must conclude that the guest fits very snugly into the molecular cavity. The bridges are even distorted a little by slight outward bending giving the complex a more spherical shape. This

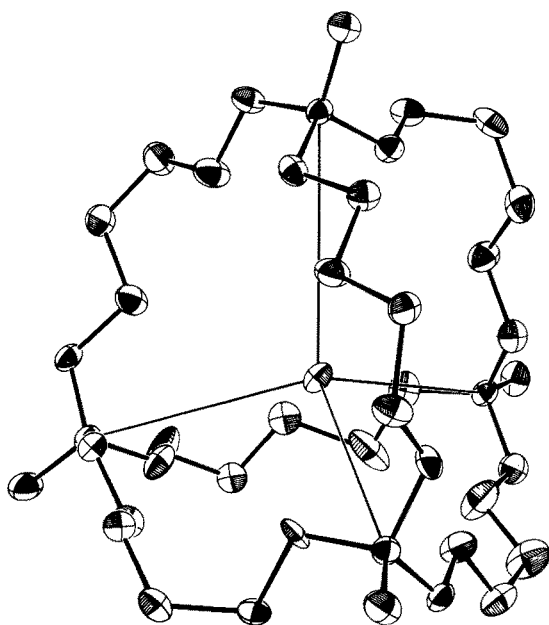


Fig. 3. X-ray-crystal structure of the iodide complex of 24⁴²⁾

finding lends further support to the speculation on the origin of NMR chemical shift changes on complexation.

For the determination of the guest binding specificity and for the elucidation of the factors governing anion complexation the quantitative determination of dissociation constants was necessary. Since no single method sufficed to yield the desired data on the whole range of guest substrates, spectrophotometry, pH-titration and potentiometry with ion selective electrodes either directly or in competition experiments served to collect the constants given in Tables 5, 6, 7⁴³⁾. Host 23, which is the smallest and most hydrophilic macrotricyclic in this series, did not form complexes with anionic guests exceeding the size of bromide.

Table 5. Dissociation constants ($-\log K_D = pK_D$) of 1:1 complexes of anionic guests with host 24 in water at 298 K (supporting electrolyte 0.1 M sodium- or tetraethylammonium toluenesulfonate, methods: A = potentiometry, B = pH titration, C = photometry)⁴³⁾

anion	pK_D	method	anion	pK_D	method
Cl^-	1.7	A	HPO_4^{2-}	2.5	A
Br^-	3.0	A	$\text{p-O}_2\text{NC}_6\text{H}_4\text{OPO}_3^{2-}$	2.1	A
I^-	2.7	A	Glucose-1-phosphate ²⁻	2.2	A
HCOO^-	1.3	B	Glucose-6-phosphate ²⁻	2.2	A
CH_3COO^-	1.9	B	Adenosin-5'-phosphate (AMP) ²⁻	2.0	A
HCO_3^-	1.8	B	Adenosin-5'-triphosphate (ATP) ⁴⁻	2.5	A
CO_3^{2-}	2.4	A	NAD^-	2.1	A
H_2PO_4^-	2.1	A	$\text{p-O}_2\text{NC}_6\text{H}_4\text{O}^-$	<0.7	A

Table 6. Dissociation constants (pK_D) of halide complexes with **24** in 95 % CH_3OH (conditions as cited in Table 5) ⁴³⁾

halide	pK_D	$K_D(\text{H}_2\text{O})/K_D(\text{CH}_3\text{OH})$
Cl^-	3.27	37
Br^-	4.71	50
I^-	4.96	180

Table 7. Dissociation constants (pK_D) of 1:1 complexes of anionic guests with host **25** in water at 299 K, (1 M tris fluoride pH 8.6, $\mu = 0.22$, abbreviations as in Table 5) ⁴³⁾

anion	pK_D	method	anion	pK_D	method
p-nitrophenolate ⁻	2.3	C	benzoate ⁻	0.4	C
2,4-dinitrophenolate ⁻	2.4	C	phthalate ²⁻	0.9	C
Br^-	2.0	C	HPO_4^{2-}	0.3	C
Br^-	2.0	A ^{a)}	iodoacetate ⁻	2.0	C
N_3^-	1.9	C	Adenosine-5-phosphate ²⁻	1.0	C
I^-	2.5	C	Adenosine-5-triphosphate ⁴⁻	1.4	C
SCN^-	2.9	C	3,5-diiodotyrosine ²⁻	1.1	C
HAsO_4^{2-}	<0.2	C	N-acetyltryptophan ⁻	<0.7	C

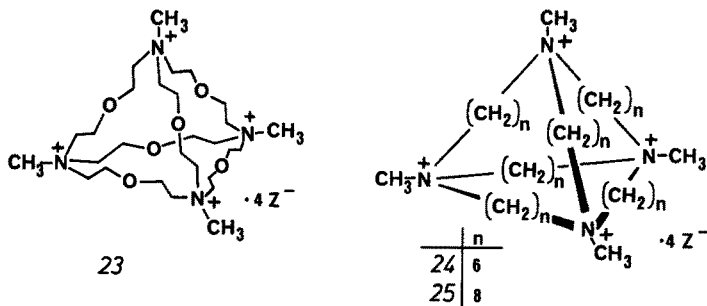
^{a)} supporting electrolyte: 0.55 M sodium glucuronate

These data reveal some important aspects of the inclusion phenomenon displayed by the anion hosts **24** and **25**: Many small and heavily hydrated anions can be bound in water with stability constants exceeding those with simple cyclodextrins ⁴⁴⁾ by factors of 20–150. The specificity of binding, however, is rather poor. The stability pattern does not follow the hydration enthalpies of the anions as is most obviously realized in the halide series. Though bromide ion possesses an intermediate enthalpy of hydration ⁴⁵⁾ it forms the most stable inclusion complex with **24**.

The situation changes to a monotonous sequence of stabilities on going to the less solvating solvent 95 % aqueous methanol. From the consideration of solvent transfer coefficients of the anions only ⁴⁶⁾ one would expect the chloride complex to experience the biggest increase in the stability constant, just the opposite being the case. In addition to solvation, which undoubtedly plays a prominent role, other factors related to the guest size in comparison with the actual dimensions of the molecular cavity i.e. the conformation of the host in a given solvent appear to influence the complex equilibria (vide supra). If the guest becomes too large to penetrate into the cavity complex formation will not be observed. It will suffice, however, if only the negatively charged moiety of a substrate, the entire structure of which is too big for inclusion, can be encapsulated.

Steric repulsion barriers in this case are not very stringent as is shown by the glucose phosphates. Electrostatic interactions seemingly dominate complex formation with the smaller host **24** to a greater extent than with **25**, the dissociation constants with small "hard" anions are typically smaller by a power of ten with **24**, but doubling the charge in homologous anions decreases K_D by a factor of 2.5 in either case. The larger tricyclic host **25** in turn is much more amenable to the polarizability of the guest

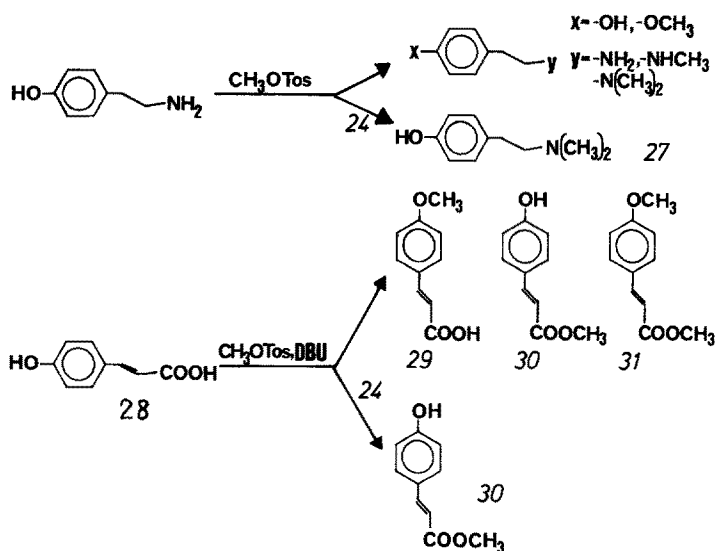
anion. This indicates that 25 is flexible enough to adjust its conformation to the incoming guest in order to make use of the short range dispersion forces. One might have expected that the quadrupolar coulomb field of the ammonium hosts should stabilize tetrahedral anions most which possess an exactly complementary charge distribution. Opposite to this idea the macrotricyclic anion hosts behave as if their molecular cavities were to a first approximation spherical.



E.II Rate Effects Shown by Macrotricyclic Quaternary Ammonium Salts

From the energetic point of view the formation of inclusion complexes between hosts and guests means a stabilisation of the ground state which in principle should show up as an altered reactivity of the guest molecule. In the simplest case substrate reactivity of the particular kind under consideration is totally lost in the noncovalent complex. Consequently the rate of the reaction in question will drop reflecting the fraction of unbound substrate that still can undergo the spontaneous process. Inhibition will only depend on the amount of host relative to the dissociation constant of the host-guest complex. Systems of this type afford a dynamic protection of the substrate i.e. protection that is based on a readily reversible equilibrium. However, as with other protecting groups, this is not a catalytic process but the host compound is required in reagent quantity. A useful application has been highlighted by A. G. M. Barrett et al.⁴⁷⁾ who took crown ethers for selective protection of primary ammonium functions in polyamines against acylation.

The idea that inclusion of an anionic function into the molecular cavity of a macrotricyclic ammonium salt might protect this moiety and probably its vicinity against reagent attack by simple steric repulsion was tested in the alkylation of tyramine 26 and p-coumaric acid 28. These bifunctional compounds offer the opportunity to detect protective action by product ratios emerging from competitive reagent attack on the same substrate. Whereas the reaction of 26 with methyl tosylate and base in ethanol yields on mixture of O- and N-methylated products, addition of host 24 changes the picture completely: Now only N-methylated products are formed, so that clean dimethylation at nitrogen can be effected with excess reagent. This result is consistent with the assumption of a noncovalent complex formation involving the anionic phenolate moiety and the tricyclic host molecule which prevents reagent attack at this substructure. The host is too small to cover the entire substrate so that the aminoethyl side chain might rather stick out into bulk solution and thus be amenable to alkylation.



Coumaric acid **28** presents a more ambitious problem because differential protection of two competing anionic sites is to be observed⁴⁸). In the absence of **24** any possible esterification and etherification product is formed but adding a slight excess of host **24** switches the reaction paths to the exclusive production of the ester. The absolute reaction rate drops considerably indicating that host-guest complexation effects both reaction centers of the substrate. Nevertheless the differences in their reactivities are stressed by virtue of this dynamic protection preferentially at the phenolate thus enabling the enhancement of reaction selectivity.

The total abolition of reactivity of the guest by inclusion complexation represents an extreme case. In practice one should be able to find examples in which the substrate in the host-guest complex shows a more or less weakened reactivity or no change at all. Even rate augmentations in truly catalytic reaction cycles may be observed. The situation is best discussed with the aid of reaction diagrams (Fig. 4).

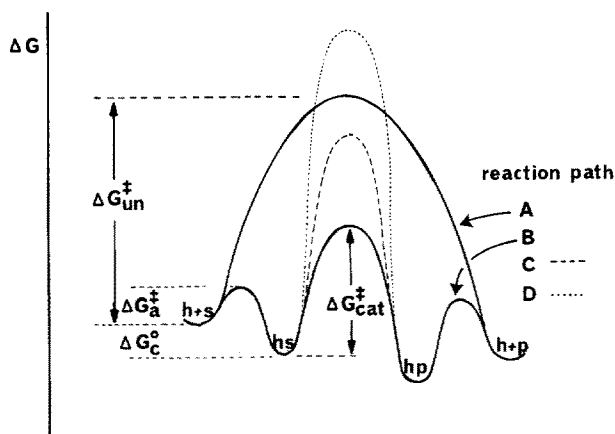
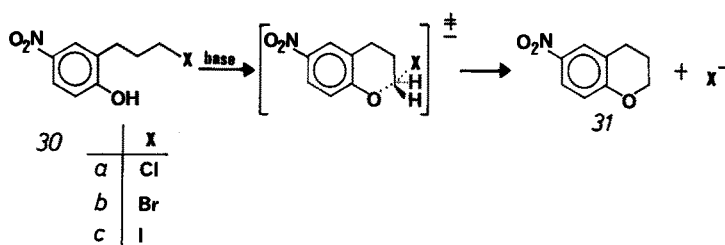


Fig. 4. Reaction diagram of a monomolecular reaction of substrate *s* in the absence and presence of a complex forming host molecule *h*

In terms of transition state theory the rate of an uncatalysed monomolecular reaction (chosen for the sake of simplicity of argument) of substrate *s* is governed by a free enthalpy barrier (path A, Fig. 4) ΔG_{un}^\ddagger which determines the "concentration" of molecules in the transition state. On addition of an host molecule *h* an alternative reaction pathway is provided which initially leads to the rapid formation (low barrier) ΔG_a^\ddagger of a corresponding host-guest complex *hs*. This complex lies in a minimum of free energy (ΔG_c^0) which translates as the association constant. If the stabilization (loss in free energy) experienced by the substrate ΔG_c^0 just matches the stabilisation of the transition state by the host ($\Delta G_{un}^\ddagger = \Delta G_{cat}^\ddagger$) no rate effect would be observable (path C). But if the energetic stabilisation of the TS exceeds or underscores the stabilisation of the substrates (paths B or D), rate augmentation or inhibition, respectively, results. Dynamic protection by steric repulsion of the attack of reagents thus may be imagined to emanate from an extremely high free energy of activation caused by the very unfavourable activation entropy of a productive encounter of the reaction partners in the confines of the molecular cavity.

Since it is the difference in the energetic interaction of ground state and transition state with the host molecule which becomes apparent as a change in reaction rate one can envisage the types of reactions which should be prone to catalysis or inhibition by the macrotricyclic ammonium salts. The influences of activation entropy are very hard to predict because there is no means of estimating the steric restrictions within the complex. If the molecular cavity is large enough to host both reaction partners in a bimolecular reaction prior to their rate limiting chemical conversion step, the entropic advantage of transforming a bimolecular into an intramolecular reaction can boost the overall rate, too. Enthalpic contributions to the activation barriers can be assigned much more readily. From the study of anion complexation it was concluded that the complex stabilities with the quaternary ammonium hosts **24** and **25** increased the more negatively charged and the more polarizable the guest was. Thus reactions running through highly delocalized anionic transition states with a greater nominal charge than the ground state are expected to experience an accelerating effect. On the contrary reactions involving monomolecular bond dissociation to produce an ion pair or even a cation in the rate determining step should be inhibited. These predictions can only hold if the substrate(s) are actually bound by the tricyclic host. The cyclisations of 3-(*o*-hydroxyphenyl)propylhalides **30** offered the opportunity to check these conceptual ideas on monomolecular aliphatic substitutions.



Similar reactions have been studied by Illuminati⁴⁹). The gross transition state structure of the uncatalyzed process did not vary with the leaving group as judged from the nearly identical activation entropies. It most likely should be described by

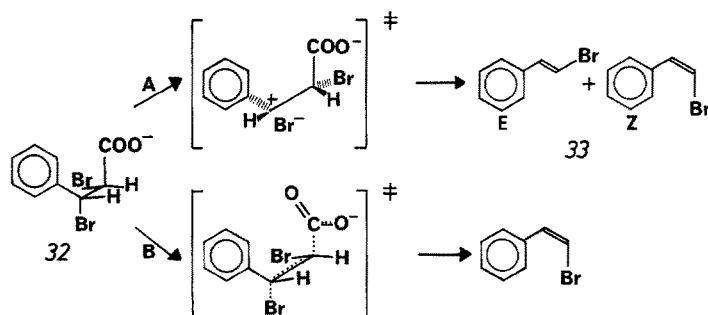
Table 8. Kinetic and activation parameters for the cyclisations of *30a–c* in the absence (un) and presence (cat) of tricyclic host 25. 24 °C, carbonate buffer pH 10.6 ⁴⁸⁾

substrate	$k_{\text{cat}}/k_{\text{un}}$	K_{M} [mM]	ΔH^\ddagger [KJ · mol ⁻¹]		ΔS^\ddagger [J · K ⁻¹ · mol ⁻¹]	
			un	cat	un	cat
<i>30a</i>	0.53	1.25	98.1	108.9	+14.7	+45.2
<i>30b</i>	0.86		90.3		+15.0	
<i>30c</i>	2.9	1.52	92.5	72.5	+18.0	−39.8

an intramolecular S_N2-type structure. The smaller tricycle 24 did not affect the cyclisation rate at all but the larger ammonium host 25 displayed differential rate effects depending on the leaving substituent (Table 8) ⁴⁸⁾. Whereas cyclisation of *30a* and *30b* was inhibited in the presence of 25, the iodo compound *30c* experienced a moderate rate enhancement. Clean first order kinetics were maintained which eased the elucidation of the factors causing this unexpected result.

Thus the activation parameters of the reactions of *30* in the presence of host 25 strongly suggest different transition state structures for *30a* and *30c*, respectively. The iodo compound *30c* experiences a considerable diminution (~20 KJ) of its enthalpic barrier by virtue of the interaction with host 25, but this favourable effect on rate is counteracted appreciably by the concomitant loss in activation entropy. This result is consistent with the expectations advanced on the grounds discussed above. The chloro derivative *30a* in contrast does not fit readily into this picture. In particular the enhancement of the activation enthalpy suggests that a different substitution mechanism might be operating in the complex. This could be caused by a peculiar structure of the host-guest complex that is not available to *30c* and shows up as an increased though unexpected complex stability (see Table 8). The bromo compound *30b* just barely displayed a rate effect which impaired the determination of the activation parameters.

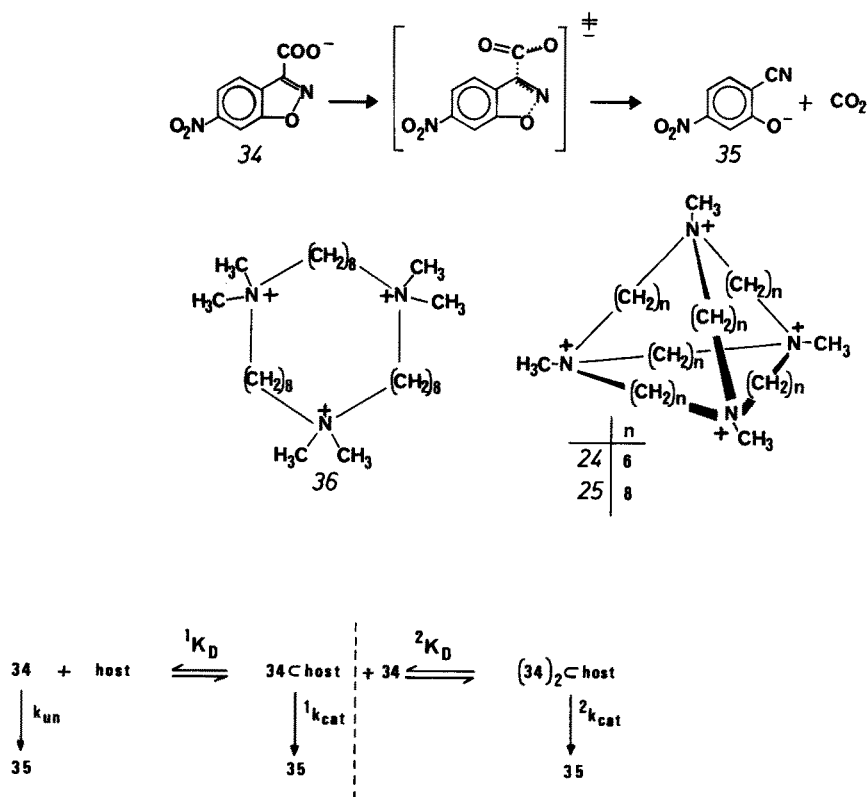
Delocalized highly polarizable anionic transition states occur in certain elimination reactions, too. The breakdown of erythro-dibromophenylpropanoic acid 32 provides an example which can serve to test the influence of the tetrahedral ammonium hosts upon two alternative competing reaction pathways. The investigations of Grovenstein ⁵⁰⁾ and Cristol ⁵¹⁾ revealed that 32 may either undergo rate limiting dissociation of the benzylic carbon-bromine bond which ultimately leads to the formation of



isomeric bromostyrenes **33** in a ratio of their thermodynamic stabilities (*E/Z* 9:1) (path A). Alternatively **32** may fragment in a concerted process yielding the less stable *Z*-bromostyrene, exclusively (path B). The product ratio of geometric isomers thus reflects the relative proportion of substrate processed by either pathway.

In aqueous methanol the substrate **32** spontaneously breaks down to give an *E/Z* ratio of 1.64. The presence of 0.04 M host **25** does not only speed up the consumption of **32** by 36% but also leads to an isomer ratio *E/Z* of 0.48⁵²⁾, with the thermodynamically less stable *Z*-**33** now predominating. Obviously host **25** specifically accelerates path B which runs through the more delocalized anionic transition state. This result is in support of the rational developed to understand the molecular catalysis of the quaternary ammonium host **25** and it illustrates a genuine enzyme-like feature: From an alternative of reaction modes one has been selected thereby establishing reaction specificity.

In an attempt to extract information on the mode of host-guest association from kinetics the decarboxylation of 6-nitrobenzoxazole-3-carboxylate **34** in the presence of quaternary ammonium hosts was investigated⁵³⁾. This reaction has been shown⁵⁴⁾ to follow clean first order kinetics the absolute rate being extremely dependent on the solvent. Addition of an ammonium host **36**, **24** or **25**



Scheme 1. Reaction scheme for the kinetic analysis of the decarboxylation of **34** in the presence of host compounds

Table 9. Kinetic parameters of the decarboxylation of **34** in water at 25 °C in the presence of hosts **36**, **24**, and **25** at $[\text{host}] \gg [34]$, $\text{FM}_{\text{rel}} = \text{normalized figure of merit: } k_{\text{un}} \cdot K_{\text{D}}/k_{\text{cat}}^{53)}$

host	$^1k_{\text{cat}} [\text{s}^{-1}]$	$^1K_{\text{D}} [M]$	$^1k_{\text{cat}}/k_{\text{un}}$	$^1k_{\text{cat}}/^1K_{\text{D}} [\text{l} \cdot \text{mol}^{-1} \cdot \text{s}^{-1}]$	FM_{rel}
36	$1.15 \cdot 10^{-4}$	0.46	31	$2.5 \cdot 10^{-4}$	2.2
24				$1.35 \cdot 10^{-4}$	1.3
25	$3.97 \cdot 10^{-4}$	0.037	110	$1.07 \cdot 10^{-2}$	100

to an aqueous solution of **34** ($[\text{host}] \gg [34]$) enhances the decarboxylation rate in any case but **36** and **25** only give saturation type kinetics on increasing the host concentration. Analysis of the rate effects according to Scheme 1 yields the constants given in Table 9.

These data reveal that the larger tricyclic host **25** is by far the most efficient catalyst in this series. Although the catalytic effect at saturation $k_{\text{cat}}/k_{\text{un}}$ compares favourably to other host-guest systems (e.g. β -cyclodextrin = 3.5)⁵⁷⁾ it is only moderately higher than with the monocycle of the same ring size **36** and falls short of the values expected on the basis of the solvent effect on rate. The dependence of ground state binding on the structure of the molecular catalyst is much more pronounced. Replacing the three dimensional cavity of **25** by the “two dimensional” pocket of the monocycle **36** lowers the complex stability by a factor of 12. Host-guest association with **24** which cannot take up aromatic molecules into its cavity is too weak to be quantified by the kinetic method. In synopsis with the surprising finding that the rate effect exhibited by **25** in this reaction does not depend on temperature, i.e. catalysis emerges solely from a change in activation entropy rather than from an enthalpic stabilisation of the transition state in the host-guest complex, one may conclude that in the catalysed process the carboxylate moiety undergoing the actual chemical conversion is not included into the molecular cavity but feels much the same molecular environment as in the uncatalysed reaction. Host-guest association in this case is mediated through hydrophobic contacts of the nitroaromatic portion of **34** penetrating into the molecular cavity of the host.

Catalysis then is apparently brought about by removing the “high energy” water structure lined up around the hydrophobic moiety of **34**. Thus the — in terms of its entropy requirement — costly rearrangement of the solvent structure on approaching the transition state is largely avoided and a greater activation entropy and consequently an augmentation in rate can be realized. Again this system demonstrates close analogy to the biocatalysts: Catalysis is caused by virtue of favourable interactions of non-reacting parts of the substrate with the catalyst which removes an unfavourable component from the rate limiting activation process.

Analogy can be driven farther still. The catalytic power of **25** in the decarboxylation process suffices to analyze the rate effects using “catalytic” quantities of the host ($[25] \ll [34]$). Under these conditions sigmoidal kinetics are observed (Fig. 5) which fit to a Hill equation taking 1.4 as an apparent Hill coefficient⁵³⁾. This suggests a cooperativity phenomenon to take place and requires the extension of Scheme 1a to 1b with involvement of a 1:2 host-guest complex to accommodate the experimental facts. The question whether the positive cooperativity observed is due to better binding of the second guest molecule or rather originates from a higher turnover number

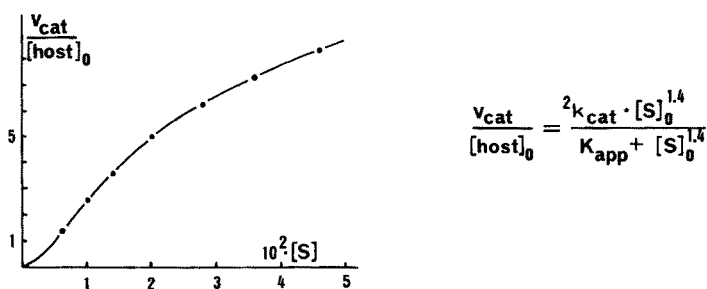
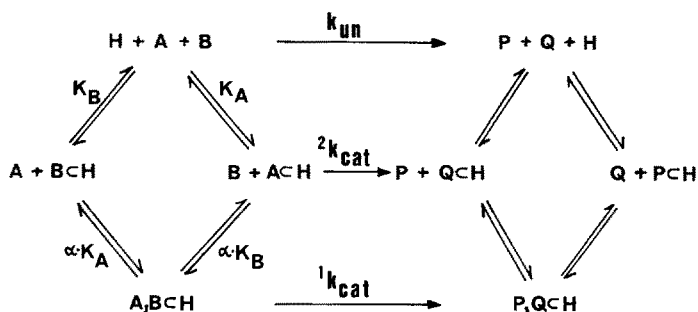


Fig. 5. Dependence of initial rates v_{cat} of the decarboxylation of **34** on substrate concentration under the experimental condition $[\text{host}] \ll [\text{S}]$ ⁵³⁾

in the 1:2 complex can be answered by the kinetic analysis. It turns out that cooperativity emerges from an increased stability of the complex hosting two guest molecules ($^1K_D = 0.037$; $^2K_D = 0.015$) which is counteracted marginally by a decrease in k_{cat} ($^1k_{\text{cat}} = 4 \cdot 10^{-4} \text{ s}^{-1}$; $^2k_{\text{cat}} = 3.3 \cdot 10^{-4} \text{ s}^{-1}$). One can rationalize this result with the aid of space filling CPK models recognizing the mismatch of host and guest structure. The flat plate like substrate cannot fill up the nearly spherical cavity of **25**. On penetration of the hydrophobic moiety into the possibly collapsed molecular pocket of the host a void is opened which eases the uptake of a second guest molecule in the same fashion. The hydrophilic portions suffering the chemical conversion extend through different faces of the tetrahedral cage into bulk solution. In this way no interaction between these groups is possible as documented by the nearly identical turnover numbers in the 1:1 and 1:2 complexes. NMR-measurements do support this picture although taken alone they do not suffice for a meaningful evaluation. This example illustrates that even kinetic cooperativity which defines an important aspect of enzyme regulation can be mimicked by simple artificial models, too.

Bimolecular reactions may gain a huge rate enhancement if a host molecule manages to gather both reaction partners in a rapid equilibrium fashion in a ternary complex prior to the rate limiting step. Theoretical estimations of this entropy effect assess the maximum magnitude of its rate acceleration factor to 10^8 ⁵⁵⁾. Although in ground state complexation studies the formation of 2:1 (ternary) complexes involving two guest anions and the macrotricyclic ammonium host has never been observed, the results emerging from the decarboxylation of **34** evidenced the possibility of their existence at least if the guests were partially hydrophobic. The evaluation of the most informative monomolecular rate constant k_{cat} for the rate limiting process within the ternary host-guest complex and the order of guest association may advantageously follow the strategies developed from steady state enzyme kinetics. This requires, however, a certain minimum catalytic activity of the molecular catalyst and may in practice frequently collide with experimental boundary conditions imposed by the reaction under consideration (rate detectability, rate magnitude, solubility etc. . . .). Part of the relevant information on the kinetics of Scheme 2 is easily extracted simply by introduction of pseudo first order conditions which saturate the host with respect to one reaction partner. This reduces the complexity of the kinetics considerably but an answer to the relevant question whether the reaction involves the formation of a kinetically competent ternary complex or rather prefers a direct conversion pathway

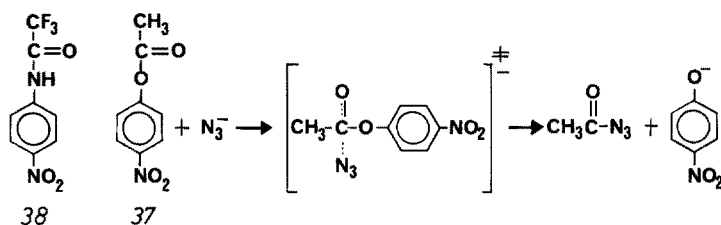


Scheme 2. General reaction scheme for the kinetic analysis of bimolecular reactions between substrates A and B as catalyzed by host H

($^2k_{\text{cat}}$, in the terminology of enzyme kinetics this would be a Theorell-Chance mechanism) cannot be found.

Instead the analysis brings up a second order rate constant k_{cat} characterising the attack of B on A \subset H (if A was the reaction partner used in excess to define pseudo first order conditions and to saturate the host H, see Scheme 2), which may be identical to $^2k_{\text{cat}}$ but alternatively may also represent $^1k_{\text{cat}}/\alpha K_B$. The comparison of k_{cat} and k_{un} reveals the change in reactivity experienced by guest A towards B on binding to the host molecule.

Inspired by the pioneering work of Tabushi (Chapter D) the effect of the macrocyclic quaternary ammonium hosts **24** and **25** on the hydrolysis of the activated carbonyl derivatives **37** and **38** was studied. In contrast to the polyammonium cyclophane **1** which gave a maximum rate enhancement $k_{\text{cat}}/k_{\text{un}}$ of 2.6 with **4** and β -cyclodextrin which yielded an enhancement factor of 16 with **38**⁶⁵⁾, neither **24** nor **25** displayed a significant rate effect in hydrolysis of **37** or **38**. This surprising finding could simply mean that substrate binding by the host is so weak ($K_{\text{ass}} < 15 \text{ l} \cdot \text{mol}^{-1}$, if $k_{\text{cat}}/k_{\text{un}} = 1.5$) that catalysis escaped the detection under the experimental conditions. Therefore another second order reaction of **37** was investigated in which the binding of one reaction partner to the tricyclic hosts had been unambiguously proven. The cleavage of **37** by azide experienced an inhibition in the presence of **24** and **25**. This is readily understandable with the aid of CPK models in the case of the smaller tricyclic host **24**. Here the formation for the transition state composed of the two reaction partners and the host would require to overcome considerable steric barriers. Thereby the free energy of activation is increased for this process and the reaction rate drops accordingly. The same argument does not hold for the larger host **25**, because model inspection suggests that transition state formation should hardly be



affected sterically. The inhibition with 25 rather points to a lack of stabilization of the transition state by 25 relative to the ground state host-guest complex. As a rational one can assume that the attack of azide onto 37 leads to a transition state in which the charge is largely localized on an oxygen atom. Since anion binding in 25 increases with the polarizability ("softness") of the guest (see Chapter EI) the transfer of charge from a more (N_3^-) to a less delocalized state on activation is a disfavoured process and should show up a decreased reaction rate within the host-guest complex i.e. inhibition. In order to observe catalysis with 24 or 25 one must look for reactions running through more delocalized transition states than their ground states. One of the sterically least demanding processes of this type is the nucleophilic aliphatic substitution of methyl-iodide by azide. In fact this reaction showed a marked rate augmentation in methanol/ H_2O in the presence of 25 which followed saturation type kinetics ⁵²⁾ (Fig. 6). The evaluation of the catalytic rate constant was hampered by experimental difficulties but a minimum enhancement factor $k_{\text{cat}}/k_{\text{un}}$ of at least 200 in 50 % aqueous methanol could be estimated. Clean first order dependence in methyl iodide was observed in the catalysed reaction and no indication of saturation behaviour with this substrate was detected in the attainable concentration range (<0.1 M).

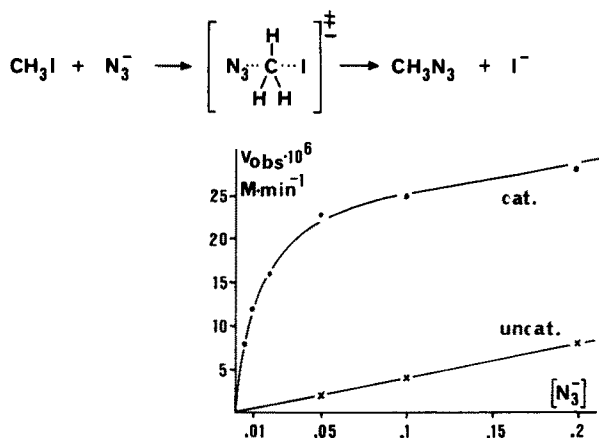


Fig. 6. Nucleophilic substitution of methyl iodide by azide. Dependence of initial rates on nucleophile concentration in the absence (uncat.) and presence (cat.) of 25 (0.01 M). $[\text{CH}_3\text{I}] = 0.01$ M

These results confirm that the macrocyclic host 25 can indeed tune the reactivity of azide depending on the reaction type: it boosts reaction rates if soft anionic transition states are involved but retards those reactions that require the localisation of charge on "hard" centers in the course of activation.

To put this working hypothesis on a more quantitative basis aromatic nucleophilic substitutions with azide as a nucleophile were tested for catalytic effects with 24 and 25. The corresponding transition states are even more delocalized than their aliphatic counterparts and thus higher rate augmentations should be expected. All or part of this favourable effect, however, can be annihilated due to an unfavourable activation entropy because the formation of the large transition state may suffer from the severe steric restrictions in the cavity of the host. As a corollary it was no surprise to find that the smaller tricyclic host 24 inhibited the substitution of 39 with azide in aqueous methanol ⁵²⁾. The same reaction experienced a big rate acceleration in the

presence of the larger host 25⁵²⁾. An extended study revealed⁵⁶⁾ that azide substitutions of the other halonitrobenzenes 40–43 as well were catalyzed by 25 (Table 10). The enhancement factors increase with the size of the halogen substituent though from steric considerations one would expect the opposite to happen.

Obviously steric requirements cannot be the dominant rate determining factors. The apparent increased reactivity of azide in these reactions may be compared to the similar effect observable on its transfer to aprotic solvents which was attributed to desolvation phenomena^{46, 58)}. Solvent transfer coefficients, however, show that the nucleophile is destabilized in these cases whereas its inclusion into the molecular cage of the host clearly exerts a stabilisation (free energy loss) of the guest. Nevertheless this penetration involves desolvation in the sense that the original solvent shell must largely be replaced by the host structure. The host thus constitutes a “microsolvent”⁵⁷⁾ that has to have an even higher solvating power towards the transition state under consideration in order to bring about rate enhancements. The increase in the rate enhancement factors with the size of the halogen substituent thus reflects the better interaction of the host structure with the more extended charge distribution of the transition states. The finding that the anionic substrate 43 shows the biggest rate enhancement in this series adds further support to the idea of transition state “solvation” by the host being the responsible factor for rate acceleration. Anion binding to 25 in the ground state had taught that doubling the charge of the guest increases host-guest complex stability. Consequently, the formation of a transition state of higher nominal charge than the ground state should receive an extra stabilisation in the cavity of the host that reduces the free energy barrier between these states and thus speeds up the reaction rate.

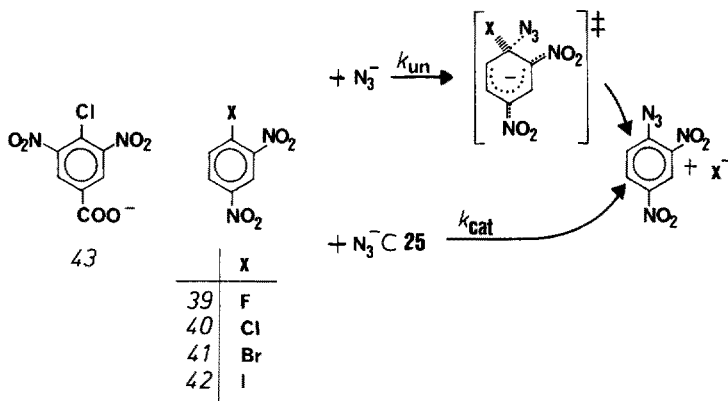


Table 10. Kinetic parameters of aromatic nucleophilic substitutions of 39–43 by azide in the absence and presence of host 25 in 25% CH₃OH/H₂O at 25 °C⁵⁶⁾

substrate	k_{un} [l · mol ⁻¹ · s ⁻¹]	k_{cat} [l · mol ⁻¹ · s ⁻¹]	k_{cat}/k_{un}	$k_{un} \cdot K_D/k_{cat}$ [M] FM
39	$4.0 \cdot 10^{-2}$	1.9	48	$1.4 \cdot 10^{-4}$
40	$7.9 \cdot 10^{-5}$	$1.0 \cdot 10^{-2}$	131	$4.4 \cdot 10^{-5}$
41	$1.2 \cdot 10^{-4}$	$1.5 \cdot 10^{-2}$	122	$4.8 \cdot 10^{-5}$
42	$9.2 \cdot 10^{-5}$	$2.1 \cdot 10^{-2}$	227	$2.5 \cdot 10^{-5}$
43	$9.3 \cdot 10^{-4}$	0.62	670	$7.0 \cdot 10^{-6}$

Table 10 contains a column that gives a measure of the efficiency (Fig. of merit FM) of 25 in the catalysis of these substitution reactions. It translates as the concentration of catalyst required to double the uncatalyzed reaction rate. Obviously the quaternary ammonium host 25 is by several orders of magnitude more active in the catalysis of these reactions than common micelles forming surfactants, which characteristically display catalysis only above their critical micelle concentration.

If desolvation of the anionic nucleophile is to be the prominent factor in the molecular catalysis one would expect the most heavily solvated guest to display the largest rate enhancement factors at saturation in a given type of reaction. Heavy solvation of the anion may, however, impair host-guest complex formation so that the complete kinetic analysis with evaluation of every rate- or complex stability constant might not be possible. This turned out to be the case when the rate effects of different anionic nucleophiles in aromatic nucleophilic substitutions were studied ⁵⁹). The catalysis by the polyammonium host molecule 25 in most of these reactions could only be characterized by a Fig. of merit ($FM = k_{un} \cdot K_D/k_{cat}$) but not by individual rate constants. In the case of nitrite nucleophile, however, the favourable situation was met that the role of this anion in aromatic nucleophilic substitutions had been thoroughly investigated ⁶⁰) and host-guest complexation happened under the experimental conditions of catalytic rate constant determination.

The data of Table 11 reveal that the reaction of 39 with NO_2^- shows similar features in the catalysis by ammonium hosts as the one using azide: Whereas the smaller tetrahedral host 24 displays no rate effect the larger host 25 gives pronounced catalysis. Even the macromonocycle 36 corresponding to one face of the tricycle 25 shows some rate augmentation. But covering the "two dimensional" cavity of 36 by a hydrophobic cap containing one additional positive charge to construct the three dimensional cavity of host 25 boosts the efficiency of the catalyst 70 fold. Again this supports the idea that the segregation of the guest anion from bulk solution through inclusion complex formation is vital to the efficiency of the catalysis.

Table 11. Kinetic parameters of aromatic nucleophilic substitutions with nitrite ion in 25% CH_3OH/H_2O at 25 °C; $K_D(NO_2^- \text{ c } 25) = 0.031 \text{ M}$ ⁵⁹)

substrate	catalyst	$k_{un} [\text{mol}^{-1} \text{ s}^{-1}]$	$k_{cat} [\text{mol}^{-1} \text{ s}^{-1}]$	k_{cat}/k_{un}	$k_{un} \cdot K_D/k_{cat} [M]$
39	36	$7.7 \cdot 10^{-5}$			$1.0 \cdot 10^{-2}$
39	24	$7.7 \cdot 10^{-5}$	no significant catalysis		
39	25	$7.7 \cdot 10^{-5}$	$1.72 \cdot 10^{-2}$	223	$1.39 \cdot 10^{-4}$
40	25	$3.2 \cdot 10^{-6}$	$1.9 \cdot 10^{-3}$	590	$5.2 \cdot 10^{-5}$
43	25	$1.7 \cdot 10^{-4}$	0.167	950	$3.3 \cdot 10^{-5}$

The comparison of rate enhancement factors of 25 with azide (Table 10) and nitrite, respectively, (Table 11) discloses, that nitrite experiences the larger effects but follows the same pattern with respect to the organic substrates as azide. The determination of the activation parameters of the reaction between 43 and NO_2^- revealed that the rate advantage of the catalyzed (by 25; $\Delta H^\ddagger = 41.4 \pm 3 \text{ KJ/mol}$; $\Delta S^\ddagger = -121 \pm 8 \text{ J/K/mol}$) versus the uncatalyzed reaction ($\Delta H^\ddagger = 61.9 \pm 3 \text{ KJ/mol}$; $\Delta S^\ddagger = -109.2 \pm 8 \text{ J/K/mol}$) is entirely due to the diminution of the enthalpic barrier. This documents the strong stabilisation of the transition state mediated presumably

Table 12. Kinetic parameters of the reaction of **40** with nucleophiles, uncatalyzed or catalyzed by **25** in 25% CH₃OH/H₂O at 25 °C ⁵⁹⁾

nucleophile	k_{un} [mol ⁻¹ s ⁻¹]	k_{cat}/K_D [mol ⁻² s ⁻¹]	$k_{un} \cdot K_D/k_{cat}$ [M] FM
OH ⁻	$1.4 \cdot 10^{-4}$	$3.6 \cdot 10^{-2}$	$3.8 \cdot 10^{-3}$
p ⁻ -OC ₆ H ₄ COO ⁻	$3.6 \cdot 10^{-4}$	38.1	$9.5 \cdot 10^{-6}$
NO ₂ ⁻	$3.2 \cdot 10^{-6}$	$6.1 \cdot 10^{-2}$	$5.2 \cdot 10^{-5}$
N ₃ ⁻	$7.9 \cdot 10^{-5}$	1.8	$4.4 \cdot 10^{-5}$
⁻ SCH ₂ COO ⁻	4.1	7140	$5.7 \cdot 10^{-4}$
⁻ SCH ₂ CH ₂ OH	2.5	2240	$1.1 \cdot 10^{-3}$
SO ₃ ²⁻	$7.0 \cdot 10^{-2}$	16.1	$4.3 \cdot 10^{-3}$

by electrostatic and dispersion forces of the host. Activation entropy counteracts this decrease in the potential energy barrier to a minor extend.

Host **25** exhibits considerable kinetic selectivity with respect to the type of the nucleophile in aromatic nucleophilic substitutions. The figures of merit (FM, Table 12), which determin the selectivity of the catalysis in nucleophilic attack on the substrate **40** in competition of the nucleophiles with each other, may be used as a guideline to separate the nucleophiles into two groups: Apart from OH⁻ which constitutes a special case presumably due to its unusual solvation properties, the first group is composed of oxygen- and nitrogen nucleophiles and is characterized by a strong susceptibility to catalysis by **25** (low FM). The other group contains the sulfur nucleophiles and exhibits FM-values at least a power of ten higher than those of the first group, indicating a greatly decreased catalytic efficiency. The experimental data do not suffice to split the FM values into the contributions of ground state binding of the nucleophile (K_D) and the activation process (k_{cat}). Thus the roots of the observed selectivity cannot be rigorously explored though in view of the anion binding studies and the rate effects analyzed a fair guess would assign this effect to k_{cat} rather than to K_D .

From the rate studies the macrotricyclic quaternary ammonium host **25** emerges as an efficient though very simple enzyme model: It is a water soluble compound of well defined structure and size which possesses one molecular cavity (active site). Substrate binding occurs there in a specific fashion and may initiate catalysis in certain reactions. The rate effects demonstrate reaction — as well as substrate specificity and originate in principal from entropic *and* enthalpic diminution of the rate limiting free enthalpy barrier. Even kinetic positive cooperativity can be observed.

Based on its success in mimicking a variety of essential facets of biocatalysis and on the magnitude of rate enhancements achieved host **25** at present compares favourably to artificial enzyme models of alternative structure.

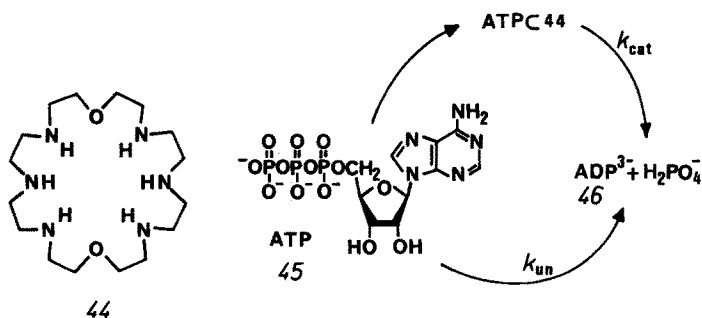
F Miscellaneous Polyammonium Catalysts

F.I Azacrown Ethers

Although the synthesis and host-guest chemistry of azacrown ethers is well developed ⁶¹⁾ their exploitation as molecular catalysts has been comparatively scarce. A

particularly interesting example has been communicated by Lehn et al.⁶²⁾ who studied the hydrolysis of adenosinetriphosphate (ATP) as catalyzed by various macrocyclic polyammonium compounds. This reaction owes much of its attraction to the analogy to biological systems because it relates to fundamental processes like photosynthesis, oxidative phosphorylation, muscle action, active transport etc. Polyammonium macrocycles had been demonstrated to bind adenosine nucleotides in water⁶³⁾ and although the structure of the complexes remained unexplored the search for potential effects on the reactivity of these ubiquitous nucleotides appears logical.

Indeed, most of the polyammonium compounds studied⁶²⁾ exhibited more or less pronounced catalysis of the hydrolytic cleavage of ATP. The most efficient compound in this series was **44** showing a pH-dependent rate enhancement factor $k_{\text{obs}}/k_{\text{un}}$ exceeding 570 at pH 8.5. Based on the notion that catalysis correlates to the sum of all complex species present (which may differ with respect to their protonation state) and the observation of kinetic saturation one must conclude the host-guest complexation is a prerequisite to catalysis. However, this condition is certainly insufficient since some macrocycles which form rather stable complexes with ATP only show very poor catalytic activity. There appears to be no obvious correlation between the host structure and the rate enhancement observed, which makes it hard to arrive at a plausible explanation of the rate augmentation. The course of the hydrolysis could unambiguously be shown to follow a stepwise sequence furnishing at first ADP which subsequently breaks down to AMP and orthophosphate. Making use of the ³¹P-NMR method to monitor the reaction an intermediate — possibly a phosphoramidate species — could be identified at neutral pH, which might offer a clue to the catalytic action. Nucleophilic catalysis by an unprotonated amino function of the macrocyclic host could in fact explain the formation of this phosphoramidate intermediate and in addition would account for the rate increase since these intermediates can hydrolyze at faster rates at a given pH-value than the parent phosphoric anhydrides. From the other two factors suggested by the authors to be involved in catalysis — general acid- and electrostatic catalysis, respectively — the latter one seems to exert a less likely contribution, because it is hard to visualize an extra electrostatic stabilisation of the rate determining transition state within the host-guest complex that has not already been realized on complex formation and thus cannot contribute to the diminution of the activation energy at saturation.



The understanding of the origin of catalysis in these reactions suffers severely from the lack of information about the structure of the host-guest complexes so that any explanatory attempt remains highly speculative at present.

F.II Steroid Based Catalysts

Molecular catalyses need not necessarily rely on macrocyclic host compounds. The relevant feature — host-guest complexation — may as well be shown by substances, which in addition to providing rigid hydrophobic surfaces suitable for association to lipophilic substrates are equipped with some catalytically active functionality. A compound of this type is the steroid based imidazole 47⁶⁴⁾, which was designed to catalyze the hydrolysis of hydrophobic activated esters. The idea influencing the construction was the anticipation that hydrophobic substructures should bind to the steroid surface in a fashion to bring the nucleophilic imidazole and the ester function of the substrate into close proximity. A comparison of the rate constants and the enhancement factors obtainable only after very sophisticated analysis of the kinetics revealed that this hypothesis holds in fact. As a corollary the more hydrophobic ester is hydrolyzed faster with either catalyst 47 or 48, but the greater efficiency of 47 leaves little doubt that in the catalytic action with this compound both steroidal hemispheres must cooperate to bind the substrate. The most plausible host-guest structure would then require the plate like aromatic substrate to be "sandwiched" between the steroid ring systems thus maximizing hydrophobic contact. These molecular catalysts, however, suffer from their very limited water solubility which complicates the kinetic analysis but the prospected introduction of supplementary ammonium functions replacing the keto groups should ease this restriction and further aid in the catalysis.

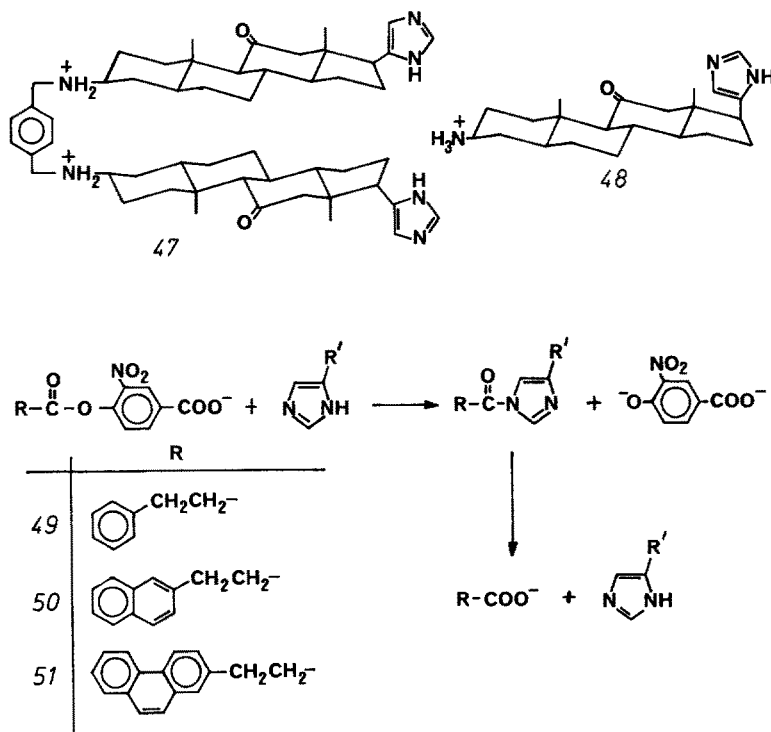


Table 13. Rate enhancement factors of the hydrolysis of 49–51 as catalyzed by 47 and 48 relative to the catalysis by unsubstituted imidazole. (recalculated from the data given in Ref. ⁶³)

	49	50	51
47	4.3	68	200
48	0.8	1.2	3.2

G Conclusion

Polyammonium salts are particularly well suited to the construction of host-guest systems possessing catalytic activity (molecular catalysts). In addition to the ease and variability in the build up of molecular frameworks inherent in this class of compounds the hydrophilicity of the charged group represents their most prominent aspect. Thus water solubility of host can be retained although very hydrophobic moieties have to be incorporated into its structure in order to effect substrate binding. The range of water soluble host systems span from heterocyclophanes, azacrown ethers, macrocyclic cage compounds to dimeric steroids. Hydrolytic reactions of carboxylic- or phosphoryl derivatives, decarboxylations as well as nucleophilic aliphatic- and aromatic substitutions are the only reaction types known so far to be amenable to catalysis by polyammonium hosts. The rate enhancement factors in these truly catalytic reactions generally amount to 10–100 with a few cases reaching a factor of 1000 or more. Compared to the natural enzymes this still appears to be quite modest, but as simple as these nonproteinogenic molecular catalysts are they in fact mimic qualitatively many of the essential features of the biocatalysts successfully. Moreover they bear the potential of rational redesign in order to improve their catalytic properties. Thus it seems likely that the present first generation of polyammonium catalysts will evolve to more sophisticated systems including several binding- or catalytically active moieties. This synthetically demanding path to modular catalysts rather than the development of completely novel host structures appears to be the more promising approach to the enhancement of selectivity in chemical systems, which in turn is the underlying motivation to design artificial polyammonium molecular catalysts.

H References

1. a) Jencks, W. P.: Binding Energy, Specificity, and Enzymic Catalysis: The Circe Effect, in: *Adv. Enzymol.* (ed. Meister, A.) 43, 219 (1975);
b) Lipscomb, W. N.: *Acc. Chem. Res.* 15, 232 (1982)
2. a) Somogyi, B., Welch, G. R., Damjanovich, S.: *Biochim. Biophys. Acta* 768, 81 (1984);
b) Stackhouse, J., Nambiar, K. P., Burbaum, J. J., Stauffer, D. M., Benner, S. A.: *J. Am. Chem. Soc.* 107, 2757 (1985)
3. Dixon, M., Webb, E. C.: *Enzymes*, 3rd Ed.; p. 56, Longman, London 1979
4. Schulz, G. E., Schirmer, R. H.: *Principles of Protein Structure*, Springer Verlag, New York 1979

5. a) Breslow, R.: *Science* **218**, 532 (1982);
b) Breslow, R.: *Acc. Chem. Res.* **13**, 170 (1980)
6. Bender, M. L., Bergeron, R. J., Komiyama, M.: *The Bioorganic Chemistry of Enzymatic Catalysis*, Chapter 1, John Wiley, New York 1984
7. Borsook, H., Schott, H. F.: *J. Biol. Chem.* **92**, 535 (1931)
8. Ise, N., Okubo, T., Kunugi, S.: *Acc. Chem. Res.* **15**, 171 (1982)
9. Fendler, J. H.: *Pure Appl. Chem.* **54**, 1809 (1982)
10. Bunton, C. A.: Reactions in micelles and similar self-organized aggregates, in: *The Chemistry of Enzyme Action* (ed. Page, M. I.) p. 461, Elsevier, Amsterdam 1984
11. a) Hopkins, A., Williams, A.: *J. Chem. Soc. Perkin Trans. II*, **1983**, 891;
b) Murakami, Y., Nakano, A., Yoshimatsu, A., Uchitomi, K., Matsuda, Y.: *J. Am. Chem. Soc.* **106**, 3613 (1984)
12. Tanford, C.: *The Hydrophobic Effect: Formation of Micelles and Biological Membranes*, 2nd Ed., Wiley, New York 1980
13. Komiyama, M., Bender, M. L.: Cyclodextrins as enzyme models, in: *The Chemistry of Enzyme Action* (ed. Page, M. I.) p. 505, Elsevier, Amsterdam 1984
14. Knowles, J. R., Boger, J.: *J. Am. Chem. Soc.* **101**, 7631 (1979)
15. a) Odashima, K., Koga, K., Itai, A., Iitaka, Y.: *ibid.* **102**, 2504 (1980);
b) Diedrich, F., Griebel, D.: *ibid.* **106**, 8024 (1984); *ibid.* **106**, 8037 (1984)
16. a) Dietrich, B., Fyles, D. L., Fyles, T. M., Lehn, J.-M.: *Helv. Chim. Acta* **62**, 2763 (1979);
b) Dietrich, B., Hosseini, M. W., Lehn, J.-M., Session, R. B.: *ibid.* **66**, 1262 (1983)
17. Jencks, W. P.: *Catalysis in Chemistry and Enzymology*, Chapter 2, 3, McGraw-Hill, New York 1969
18. Snell, E. E., DiMari, S. J.: Schiff base intermediates in enzyme catalysis, in: *The Enzymes*, Vol. II (ed. Boyer, P.) 3rd Ed., p. 335, Academic Press, New York 1970
19. Tabushi, I., Kimura, Y., Yamamura, K.: *J. Am. Chem. Soc.* **100**, 1304 (1978)
20. Tabushi, I., Kimura, Y., Yamamura, K.: *ibid.* **103**, 6486 (1981)
21. Fersht, A. R.: *Pure Appl. Chem.* **54**, 1819 (1982)
22. Fersht, A. R.: *Enzyme Structure and Mechanism*, p. 95, 261, Freeman, San Francisco 1977
23. Knowles, J. R., Alberly, W. J.: *Acc. Chem. Res.* **10**, 105 (1977)
24. Rosenberry, T. L.: *Adv. Enzymol.* **43**, 103 (1975)
25. Stoops, J. K., Horgan, D. J., Runnegar, M. T. C., de Jersey, J., Webb, E. C., Zerner, B.: *Biochemistry* **8**, 2026 (1969)
26. Schneider, H. J., Busch, R.: *Angew. Chem.* **96**, 910 (1984); *Angew. Chem. Int. Ed. Engl.* **23**, 911 (1984)
27. a) Tabushi, I., Yamamura, K., Fujita, K., Kawakubo, H.: *J. Am. Chem. Soc.* **101**, 1019 (1979);
b) Tabushi, I.: New insights into the host-guest solvent interaction of some inclusion complexes. Reaction path control in cyclodextrin inclusion as a lyase model: Solvolysis of β -bomethylnaphthalene, in *Advances in Solution Chemistry*, (ed. Bertini, I., Lunazzi, L., Dei, A.) p. 221, Plenum, New York 1981
28. Mock, W. L., Irra, T. A., Wepsiec, J. P., Manimaran, T. L.: *J. Org. Chem.* **48**, 3619 (1983)
29. Vögtle, F., Franke, J.: *Angew. Chem.* **97**, 224 (1985); *Angew. Chem. Int. Ed. Engl.* **24**, 219 (1985)
30. Tabushi, K., Kimura, Y., Yamamura, K.: Facilitated formation of tetrahedral intermediate in esterase action by a water soluble heterocyclophane in: *Chemical Approaches to Understanding Enzyme Catalysis*, (ed. Green B. S., Ashani, Y., Chipman, D.) p. 328, Elsevier, Amsterdam 1982
31. Kirby, G. W., Ogunkoya, L.: *J. Chem. Soc.* **1965**, 6914
32. Vögtle, F., Müller, W. M.: *Angew. Chem.* **96**, 711 (1984); *Angew. Chem. Int. Ed. Engl.* **23**, 712 (1984)
33. Murakami, Y., Nakano, A., Akiyoshi, K., Fukuya, K.: *J. Chem. Soc. Perkin Trans. I*, **1981**, 2800
34. Murakami, Y.: *Top. Curr. Chem.* **115**, 107 (1983)
35. Hol, W. G. J., van Duijnen, P. T., Berendsen, H. J. C.: *Nature* **273**, 443 (1978)
36. a) Cotton, F. A., LaCour, T., Hazen, E. E. Jr., Legg, M. L.: *Biochim. Biophys. Acta* **481**, 1 (1977);
b) Osherhoff, N., Brautigan, D. L., Margoliash, E.: *Proc. Nat. Acad. Sci. USA*, **77**, 4439 (1980);
c) Anderson, D. G., Hammes, G. G., Walz, F. G.: *Biochemistry* **7**, 1637 (1968)
37. Pierre, J.-L., Baret, P.: *Bull. Soc. Chim. France* **1983**, II, 367
38. Stern, K. H., Amis, E. S.: *Chem. Rev.* **59**, 1 (1959)

39. a) Lehn, J.-M., Graf, E.: *J. Am. Chem. Soc.* **97**, 5022 (1975);
b) Graf, E., Lehn, J.-M.: *Helv. Chim. Acta* **64**, 1040 (1981)
40. Schmidtchen, F. P.: *Chem. Ber.* **113**, 864 (1980)
41. Schmidtchen, F. P.: *Angew. Chem.* **89**, 751 (1977); *Angew. Chem. Int. Ed. Engl.* **16**, 720 (1977)
42. Schmidtchen, F. P., Müller, G.: *J. Chem. Soc. Chem. Commun.* **1984**, 1115
43. Schmidtchen, F. P.: *Chem. Ber.* **114**, 597 (1981)
44. Rohrbach, R. P., Rodriguez, L. J., Eyring, E. M., Wojcik, J. F.: *J. Phys. Chem.* **81**, 944 (1977)
45. Conway, B. E.: Thermodynamic and transport behavior of electrolytes, in: *Physical Chemistry* (ed. Eyring, H., Henderson, D., Jost, W.) p. 63, Academic Press, New York 1970
46. Parker, A. J.: *Chem. Rev.* **69**, 1 (1969)
47. Barrett, A. G. M., Lana, J. C. A., Tograie, S.: *J. Chem. Soc. Chem. Commun.* **1980**, 300
48. Schmidtchen, F. P.: Macrotricyclic ammonium salts: enzyme like activity, in: *Chemical Approaches to Understanding Enzyme Catalysis*, (ed. Green, B. S., Ashani, Y., Chipman, D.) p. 315, Elsevier, Amsterdam 1982
49. Illuminati, G., Mandolini, L., Masci, B.: *J. Am. Chem. Soc.* **97**, 4960 (1975)
50. Grovenstein, E., Lee, D. E.: *ibid.* **75**, 2639 (1953)
51. Cristol, S. J., Norris, W. P.: *ibid.* **75**, 2645 (1953)
52. Schmidtchen, F. P.: *Angew. Chem.* **93**, 469 (1981); *Angew. Chem. Int. Ed. Engl.* **20**, 466 (1981)
53. Schmidtchen, F. P.: *J. Chem. Soc. Perkin Trans. II*, in the press
54. Kemp, D. S., Paul, K. G.: *J. Am. Chem. Soc.* **97**, 7305 (1975); *ibid.* **97**, 7312 (1975)
55. Page, M. I.: *Angew. Chem.* **89**, 456 (1977); *Angew. Chem. Int. Ed. Engl.* **16**, 449 (1977)
56. Schmidtchen, F. P.: *Chem. Ber.* **117**, 725 (1984)
57. Straub, T. S., Bender, M. L.: *J. Am. Chem. Soc.* **94**, 8875 (1972)
58. cf. Bunton, C. A., Moffatt, J. R., Rodenas, E.: *ibid.* **104**, 2653 (1982)
59. Schmidtchen, F. P.: *Chem. Ber.* **117**, 1287 (1984)
60. a) Broxton, T. J., Muir, D. M., Parker, A. J.: *J. Org. Chem.* **40**, 3230 (1975);
b) Broxton, T. J.: *Aust. J. Chem.* **34**, 2313 (1981)
61. a) Gokel, G. W., Dishong, D. M., Schultz, R. A., Gatto, V. J.: *Synthesis*, **1982**, 997;
b) Kaden, Th. A.: *Top. Curr. Chem.* **121**, 157 (1984)
62. Hosseini, M. W., Lehn, J.-M., Mertes, M. P.: *Helv. Chim. Acta* **66**, 2454 (1983)
63. Kimura, E., Kodama, M., Yatsunami, T.: *J. Am. Chem. Soc.* **104**, 3182 (1982)
64. Guthrie, J. P., Cullimore, P. A., McDonald, R. S., O'Leary, S.: *Can. J. Chem.* **60**, 747 (1982)
65. Komiyama, M., Bender, M. L.: *J. Am. Chem. Soc.* **99**, 8021 (1977)

Complexation of Organic Molecules in Water Solution

Joachim Franke and Fritz Vögtle

Institut für Organische Chemie und Biochemie der Universität Bonn
Gerhard-Domagk-Straße 1, D-5300 Bonn 1, FRG

Table of Contents

1 Introduction: How to Complex Organic Molecules?.	136
2 The Cyclodextrins: Models for Synthetic Host Cavities.	136
3 Physicochemical Methods for the Investigation of This Type of Complexation	139
3.1 Nature of the Host/Guest Interactions	139
3.2 X-ray Analyses	140
3.3 Fluorimetric Investigations	140
3.4 NMR-Spectroscopic Studies	144
3.5 Further Methods of Investigation of the Complexes.	146
4 Complexation of Charged Guests	147
4.1 Anionic Guests	148
4.2 Cationic Guests	150
5 Complexation of Uncharged Guest Molecules	152
6 Conclusions and Outlook	166
7 References	168

1 Introduction: How to Complex Organic Molecules?

A relative young topic in organic chemistry, but facing increasing interest, deals with the complexation of organic molecules (as guests) inside cavities, niches or pockets of larger synthetic molecules (as hosts). This field has become widely known as Host/Guest Complex Chemistry ¹⁾.

The sophisticated goal of this research area is to mimick enzymes in their capability to bind substrates fast, selectively and reversibly, and to catalyse chemical reactions. In addition to that, knowledge is searched also with regard to the mechanisms of the action of odourants and tasting substances and drugs in general. Through investigations, using host and guest substances, molecular binding and recognition processes ²⁾ underlying such physiological effects most probably can be understood in detail. Studies in this direction should also give more insight into weak, but multiple intermolecular interactions similar to those that are often responsible for the binding of substrates and ligands to proteins and enzymes in biological systems. The fundamentals of these weak inter- and intramolecular interactions are not sufficiently understood as yet.

Particularly, water-soluble host cavities are thought to mimick the above mentioned biochemical interactions because water is the common medium in physiological processes.

In this progress report besides remarks on the complexation of cationic and anionic guests, special emphasis will be drawn to the encapsulation of uncharged organic guest molecules by large cavities formed by synthetic macrocyclic hosts. In preference, this allows the study of non-ionic weak multiple intermolecular interactions.

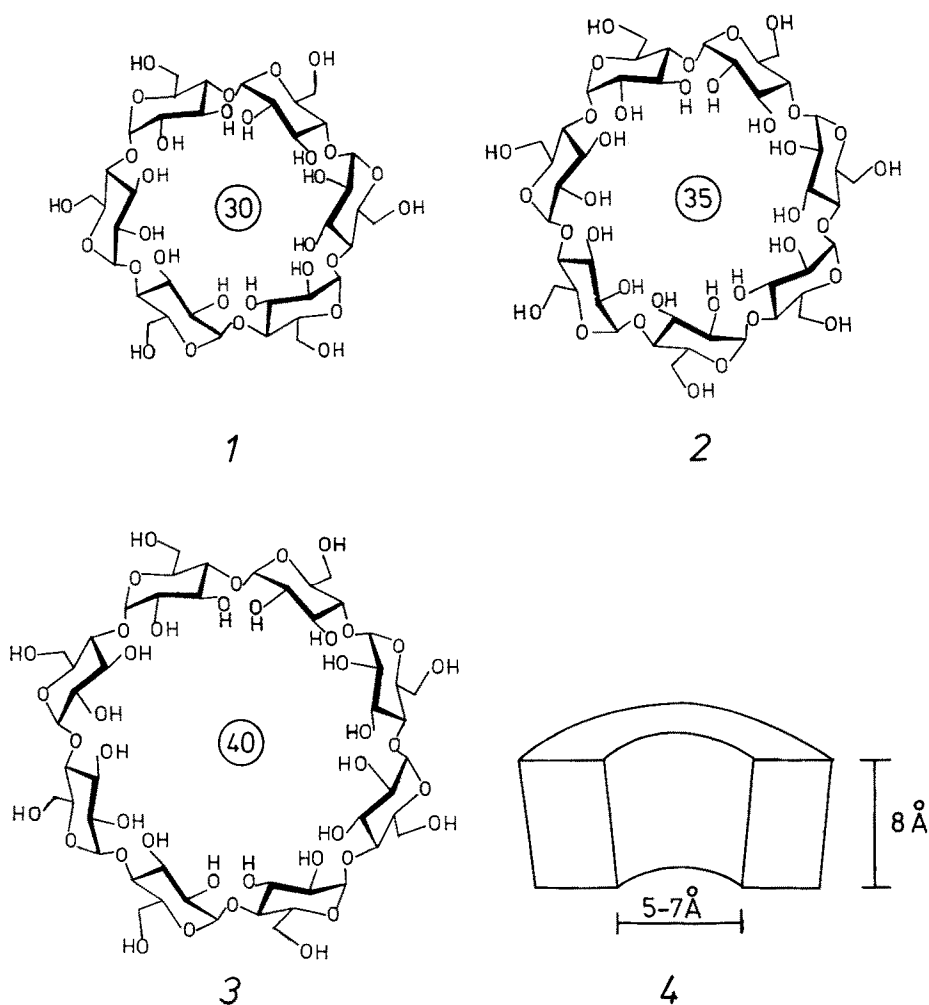
2 The Cyclodextrins: Models for Synthetic Host Cavities

The cyclodextrins were the first compounds that have been studied with regard to their complexing and catalytic — in other words enzyme mimicking — properties. The enzymatic catabolism of starch mainly yields α -, β -, and γ -cyclodextrin (CyD, 1–3). Those are macrocyclic oligosaccharides, in which six (α), seven (β) and eight (γ) α -D-glucopyranose units, respectively, are connected by 1,4-glycosidic bonds.

It is known from crystal structure and spectroscopic analyses that the cyclodextrins in the solid state as well as in solution exist in an approx. round, conical shape (4) with a height of the wall of approx. 8 Å and an inner cavity diameter varying between 5 (α -) and 7.5 Å (γ -CyD). The cyclodextrins are water-soluble due to their high number of hydroxylic groups they contain and which all lie on the outside of the molecule. In contrast to that, the cavity of the cyclodextrins is surrounded by CH- and glycosidic C—O bonds and therefore is hydrophobic inside.

Since the work of Cramer, Saenger and others in the 50th's, a high number of molecular inclusion compounds of cyclodextrins has been discovered and characterized. The guests to be included range from inorganic ions to polar organic compounds like acids and amines and even to lipophilic guest molecules. These studies were the subject of numerous reviews and monographs ³⁾. An overview with regard to the correspondence of cavity size and guest volume is given in Table 1 ⁴⁾.

The cyclodextrins most often form 1:1 complexes. It has been proved for all three



cyclodextrin hosts in numerous examples that the guest is located inside the conical cavity. By this molecular inclusion the selection of spacially fitting guest molecules by the different cyclodextrin cavities is explained as well as the discrimination of potential guests that are too large or too small in size.

The cyclodextrins are not only useful to simulate receptor binding sites, but are also versatile enzyme models ⁵⁾. A large number of reactions is known that are catalyzed by natural and modified cyclodextrins. Thereby the educts are enclosed into the cavity and, after that, often converted to the products faster and more selectively and sometimes under asymmetric induction ⁶⁾. The products are then liberated through decomplexation or in the course of a following reaction. To give an example: the hydrolyses of para-nitrophenol esters are accelerated in the presence of β -cyclodextrin by a factor of up to 750,000 ⁷⁾.

The capacity of complex formation of the cyclodextrins is of practical importance ^{3d)}: In the pharmaceutical and plant protection industry sensitive drugs and

Table 1. Overview showing the correspondence of the cavity size of cyclodextrins and the size of the guests

Cyclodextrin	Number of glucose units	Number of ring members (atoms)	Inner cavity diameter [Å]	Examples of enclosed guests
α -	6	30	~ 5	benzene, phenol, nitrophenol
β -	7	35	~ 6	naphthalene, 1,8-ANS
γ -	8	40	~ 7.5	anthracene, crown ethers, 1,8-ANS

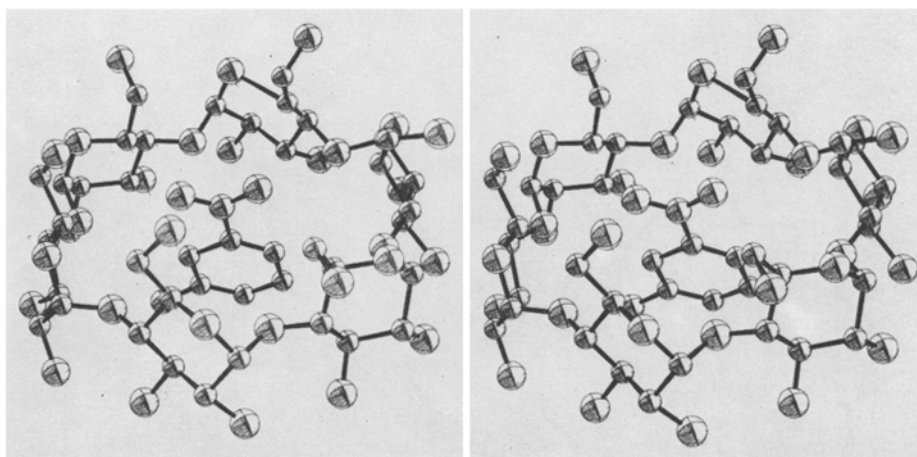


Fig. 1. Inclusion of *m*-nitrophenol in α -cyclodextrin (stereo view)

other substances are stabilized against air and moisture by molecular inclusion using the cyclodextrins or their derivatives. The solubility of substrates which are only weak soluble in water in general can be increased by inclusion into cyclodextrins. Cyclodextrins in a polymeric form or bound to a macromolecular material are applied to gel inclusion chromatography and affinity chromatography.

The low selectivity of the formation of cyclodextrin inclusion complexes with guests of similar volume but of different shape or charge is explained by the existence of several binding types: hydrophobic and van der Waals interactions as well as hydrogen bonds.

Synthetic hosts and their complexation behaviour can contribute not only to the understanding of these binding types, but also will be useful to quantify the different binding modes. One of the aims of the design, synthesis and study of new synthetic hosts also is to end up with tailor-shaped host cavities that are highly selective for special guests of biological or industrial importance, e.g.: toxic substrates, side products of industrial processes, drug metabolites with negative side effects, isomeric substances which can only be separated with difficulties by other methods. In addition to this, optically active host cavities exhibiting high enantiodifferentiation are acknowledged to be valuable synthetic goals.

3 Physicochemical Methods for Investigation of This Type of Complexation

3.1 Nature of the Host/Guest Interactions

It is appropriate first to discuss the intermolecular host/guest interactions in water solution. Usually several attractive forces are effective at the same time to a different extent depending on the nature of host and guest.

These forces essentially are the following:

- a) hydrophobic interactions,
- b) strain energy of the "empty" cavity,
- c) electrostatic interactions,
- d) hydrogen bridges,
- e) van der Waals interactions,
- f) charge transfer interactions.

If the guests are uncharged and not or only sparingly soluble in water, hydrophobic interactions are the important forces which lead to an inclusion inside the cavities of water-soluble host molecules^{3c,8-10}). The guest molecules then must get rid of their own hydration shell and also have to displace the water molecules out of the host cavity. In such a way, a hydrophobic micro environment for the guest is formed, which facilitates the complex formation. This phenomenon is known as the hydrophobic effect¹¹) and plays an important role in biochemistry. The water molecules which have been set free during this process of molecular encapsulation, are accepted by the environment, whereby they win degrees of freedom. This increase of entropy also facilitates the formation of the complex.

Saenger¹²) has noted that the water molecules located in the hydrophobic host cavity, cannot necessarily apply the optimum number of hydrogen bridges that could be thought of and therefore are in a state of activation^{10,13}). Their ejection into the environment through a gain of potential energy leads to an additional entropy decrease. This seems to explain partly the unspecific, that means guest-independent, part of the inclusion potential.

Small hosts, which in their "empty" unpolar cavity only contain water, can be considered to exist in a strained ring conformation. The uptake of a guest in this case leads to a decrease in strain and to a more stable arrangement of the ring system and consequently to an entropy gain¹⁴). These effects of course strongly depend on the size and shape of the substrate molecules. In the case of positive or negative charged hosts depending on the polarizability and charge of the guest, ion-ion-, ion-dipole- and dipole-dipole interactions can occur¹⁵), which is in contrast e.g. to the neutral cyclodextrins. This can lead to a discrimination of uncharged and non-polarizable guests by these hosts. If hydrogen bridges can be formed through favourable geometric arrangement of functional groups an additional complex stabilization results¹⁶).

If there is no functional group available at the guest, the complexation will be explained by van der Waals interactions^{13,17}). In a few cases, charge transfer interactions are discussed, but nowhere the final proof was made¹⁸).

Which of the effects mentioned above or of additional stabilization effects in a certain complex formation predominates, often is difficult to figure out. Attempts of

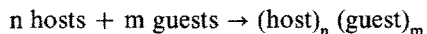
quantification by theoretical model calculations have faced difficulties but have only partly been successful^{3b,18)}.

Today the most important factor seems to be the steric fit, in other words, the optimal size fit of the convex guest inside the concave binding site of the host. In such a way, a guest selection according to the size and shape of the guest molecules is possible. Most often several of the above mentioned binding forces will be effective to a different extent. The biochemical principle of multiple recognition¹⁹⁾, in e.g. enzyme substrate binding, is mimicked here successfully.

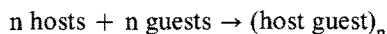
3.2 X-ray Analyses

A possibility to prove the molecular inclusion of the guest in the host cavity, at least in the crystalline state, is given by X-ray analysis²⁰⁾. There are different fundamental types of host/guest structures that have to be distinguished:

a) The crystal lattice inclusion compounds of the clathrate type²¹⁾ in which the guest molecules are located in cavities of the crystal lattice of the host:



b) If the host compound contains a cavity of any type, in which a guest can be included and bound through coordinative bonds, as has been discussed above, then the aggregate is named a cavitate and the host a cavitand²²⁾:



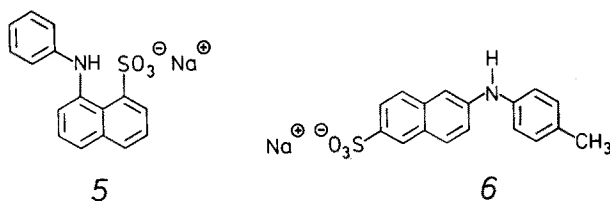
This molecular inclusion complex now crystallizes as a unity in a known crystal lattice.

The X-ray analysis all at once also reveals the conformation of the host and the orientation and conformation of the guest in the cavity. Limiting factors are that it is now always possible to grow crystals of sufficient quality and, on the other hand, the results without uncertainties cannot be translated to the different conditions in solution. The orientation of the guest in the crystal lattice of the host can be completely different compared to that in (water) solution. Dynamic effects like complex formation and dissociation processes also should be taken into account.

Despite this, X-ray analyses were very helpful in the discovery of host/guest inclusion compounds and certainly they are in most cases also instructive for the conditions in solution.

3.3 Fluorimetric Investigations

Fluorescence spectroscopy is one of the most frequently applied methods for the detection of the binding of organic guest molecules at proteins²³⁾, cyclodextrins^{3c,24)} and synthetic hosts^{18b,20b)}. The properties of hydrophobic fluorescence indicators like sodium-1,8-anilinonaphthalene sulfonate (1,8-ANS, 5) or sodium-6-*p*-toluidinyl-2-naphthalene sulfonate (TNS, 6) are used thereby, which in hydrophobic organic solvents or complexed in unpolar host cavities in water exhibit notable increases in fluorescence and blue wavelength shifts.



If 1,8-ANS as a substrate is added to a solution of a host compound in water, the guests will be enclosed in the cavity of the host and the complex formation is recognized by an increase of the fluorescence intensity. Open chained reference compounds do not show this behaviour. In the following example the fluorescence spectra of pure 1,8-ANS in water and of a water solution of the host compound 34, which is described below in more detail, and of the complex of ANS with this host are shown at the excitation wavelength 375 nm ^{18b)}:

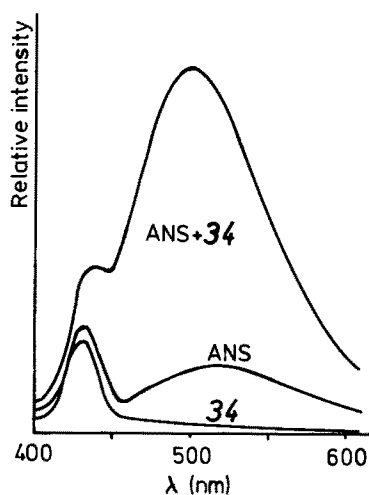


Fig. 2. Fluorescence spectra of pure 1,8-ANS (5) and host compound 34 and the complex of 1,8-ANS and 34 in water solution (excitation wavelength 375 nm)

Measurements of the relative intensities at different host (or also guest) concentrations allow to determine the complex constant as is explained in the following ^{3c, e, 25, 26)}:

The association of the host H with the guest A (1,8-ANS) to yield the 1 : 1 complex HA :



can be described by a complex constant K_A

$$K_A = \frac{[\text{HA}]}{[\text{H}][\text{A}]} \quad (2)$$

If c_H is the total concentration of host and c_A the total concentration of guest, then using

$$c_H = [H] + [HA] \quad (3)$$

and

$$c_A = [A] + [HA] \quad (4)$$

equation (1) is transformed to obtain

$$K_A = \frac{[HA]}{(c_H - [HA])(c_A - [HA])} \quad (5)$$

With the assumption that always $c_H \gg c_A$ and therefore $c_H \gg [HA]$, equation (5) simplifies to

$$K_A = \frac{[HA]}{c_H(c_A - [HA])} \quad (6)$$

It follows from Lambert-Beer's relationship that the difference ΔF in the fluorescence intensity at an appropriate complex concentration $[HA]$ to the zero point, which is the fluorescence of the fluorescence indicator in the absence of host, is proportional to the actual complex concentration:

$$\Delta F = \varepsilon_0 \cdot [HA] \quad (7)$$

ε_0 is the molar extinction coefficient. If equation (7) is solved with respect to $[HA]$ and equation (6) is applied, the Benesi-Hildebrand equation²⁵⁾ (8) is obtained:

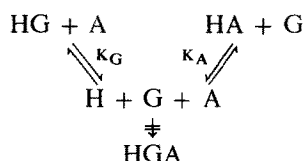
$$\frac{c_A}{\Delta F} = \frac{1}{\varepsilon_0 \cdot K_A} \cdot \frac{1}{c_H} + \frac{1}{\varepsilon_0} \quad (8)$$

If the host concentration c_H is varied at a fixed guest concentration c_A and the estimated relative fluorescence increase ΔF is plotted in the form of $c_A/\Delta F$ against $\frac{1}{c_H}$, then through least square fit the complex constant K_A is obtained.

A prerequisite to apply equation (8) besides $c_H \gg c_A$ (see above) is the formation of 1:1 complexes. In contrast, 2:1 and nonstoichiometric and other associates can be excluded through a nonlinear arrangement of the values measured according to equation (8). An additional indication for 1:1 inclusion stoichiometry is the appearance of two isosbestic points in the fluorescence spectra^{3d, 27)}.

By an extension of this method the complex constants K_G of other non-fluorescing guests G can be calculated^{3d, e, 27)}:

If we assume that no ternary complexes $[HAG]$ are formed, K_G can be determined from competitive complex formation:



If to the solution of an excess amount of guest G and host H the fluorescence indicator A is added under consideration of Eq. (9):

$$c_G \gg c_H \gg c_A \quad (9)$$

A competes with G to be complexed by H. If the relative fluorescence intensity is measured as a function of the actual concentration of H by using equation (8) a fictitious complex constant \overline{K}_A is obtained which corresponds to K_A through the following relationship:

$$\overline{K}_A = K_A \cdot \frac{(c_H - [\text{HG}])}{c_H} = \frac{[\text{HA}] \cdot (c_H - [\text{HG}])}{c_H^2 \cdot (c_A - [\text{HA}])} \quad (10)$$

The complex constant K_G wanted is given by:

$$K_G = \frac{[\text{HG}]}{[\text{H}][\text{G}]} \quad (11)$$

Furthermore the following relationships are effective:

$$c_G = [\text{G}] + [\text{HG}] \quad \text{and} \quad c_H = [\text{H}] + [\text{HG}] + [\text{HA}] \quad (12)$$

By use of equation (9) we can set

$$[\text{G}] \approx c_G \quad (13)$$

and

$$[\text{H}] \approx c_H - [\text{HG}] \quad (14)$$

Inserting (13) and (14) into equation (11) yields K_G with

$$K_G = \frac{[\text{HG}]}{c_G \cdot (c_H - [\text{HG}])} \quad (15)$$

If (6) is solved to yield $[\text{HA}]$ and equation (15) to yield $[\text{HG}]$ and these introduced into equation (10), we obtain:

$$K_G = \frac{\frac{K_A}{\overline{K}_A} - 1}{c_G} \quad (16)$$

In principle, the complex constant K_G of any guest can at least be estimated: First K_A is determined and then by the same procedure in the presence of a competing guest G the complex constant \bar{K}_A is obtained.

A list of complex constants of hosts which are described below, is given at the end of this section (Table 2).

From

$$\Delta G^0 = -RT \ln K \quad (17)$$

the free complex binding enthalpy ΔG^0 can be calculated and from the temperature dependence of the complex constant the complex binding enthalpy ΔH^0 ,

$$\frac{d \ln K}{d 1/T} = \frac{-\Delta H^0}{R} \quad (18)$$

and from

$$\Delta G^0 = \Delta H^0 - T \Delta S^0 \quad (19)$$

the entropy.

Apart from fluorescence spectroscopic methods, UV measurements have been applied to investigate the complex formation and to determine the complex constants^{3d,e,27)}. The essential prerequisite for these procedures is a noticeable, preferably bathochromic shift and an increase in intensity of the absorption wavelengths of the host or guest in the course of the complexation.

If at a given wavelength, where in contrast to the complex neither guest nor host show appreciable absorptions, in Eq. (8) ΔF is replaced by the difference of absorption ΔAbs , then the complex constant can be determined as described above.

It has to be pointed out that the temptation might be high to consider the molecular complexes of host and fluorescence (or UV-) probe as an inclusion compound, but that this method lastly does not allow a precise differentiation between an additional complex at the outer periphery of the host molecule and between an inclusion complex, whereby the guest is located inside the cavity^{20b,28-30)}. Such a differentiation, as is described in the following section, can be achieved by the 1H -NMR method, which gives more precise evidence as to the spacial arrangement of host and guest.

3.4 NMR-Spectroscopic Studies

Significant shifts of host and guest signals can be observed by 1H - and ^{13}C -NMR spectroscopic investigations of inclusion compounds³¹⁾. On account of the relatively simple and rapid procedure the 1H -NMR method has established an important and reliable method to gain insight into molecular encapsulation^{32-36,40)}.

In contrast to the uncomplexed guest, 1H -NMR signals of the guest inside the cavity and then often of the host too, are significantly shifted upfield. This, as a rule, is due to the short spacial distances between the two components (host and guest) in the molecular complex. The guest is affected by the anisotropy effects of aromatic units or by field effects of ionic centers of the host^{30,34)}. As these effects with increasing

distance quickly decrease, the protons dependent on their orientation show differing chemical shifts. Estimations and comparisons with theoretical calculations³⁷⁾ for different orientations of the guest inside the host cavity often lead to rather precise evidence as to the geometry of the complex³⁵⁾. This in addition shows that the guest inside the host has a special and not a random arrangement. These observations as well as the fact that there are no shifts if cavity containing hosts are replaced by open chained reference substances bearing no cavities, can be taken as good arguments to exclude aggregations of the guest at the outside periphery of the host as far as possible.

Diederich has noticed that in some host compounds (e.g. 63, 64) without addition of guests through aggregation of the host molecules among each other concentration dependent shifts of NMR signals may be observed³⁸⁾. Only below the critical micelle concentration (CMC) when the molecules are separated from each other in solution, an investigation of the complexation by fluorescence measurements as well as by NMR spectroscopy is justified.

Apart from only some few cases, in which the exchange of free and complexed guests is slow enough on the NMR time scale in order to observe different signals in each case, usually coalescence is found. This has been used in temperature dependent dynamic NMR spectroscopy, e.g. by Cram, to determine activation entropies³⁹⁾.

At the coalescence point the degree of the observed chemical shift of a proton $\Delta\delta$ is proportional to the percentage of the complexed guest [HG] compared to the total concentration c_G ^{31b)}. The complex constant therefore can be determined quantitatively, using the following relationship:

$$\Delta\delta = \Delta\delta_{\max} \cdot \frac{[HG]}{c_G} \quad (20)$$

where $\Delta\delta_{\max}$ corresponds to the maximum of the shift of the same proton at complete complexation.

If one dissolves equation (20) to yield [HG] and inserts it into equation (6) [here: $HA \triangleq HG$, $c_A \triangleq c_G$], after rearranging, one obtains:

$$\frac{1}{\Delta\delta} = \frac{1}{K \cdot \Delta\delta_{\max}} \cdot \frac{1}{c_H} + \frac{1}{\Delta\delta_{\max}} \quad (21)$$

If the shift of one and the same proton at several different host concentrations c_H is measured and plotted as $\frac{1}{\Delta\delta}$ against $\frac{1}{c_H}$, from the slope and axial section the complex formation constant searched for is obtained. The advantage of this method compared with the fluorescence method lies in the possibility of measuring the constant for each guest directly and not using the detour of the competitive inhibition. On the other hand, in the case of small amounts and low solubilities the results are not very exact.

3.5 Further Methods of Investigation of the Complexes

As fluorimetric, UV and NMR measurements are the most often used methods to determine the formation of the complexes and to measure the complex constants, further methods of investigation here only briefly shall be discussed:

Through solid/liquid-^{41,42)} and liquid/liquid³⁰⁾ extraction with the solution of the host, complexes with guests which are not soluble in this phase, can be obtained. Considering the maximal solubility of the free guest in the medium used, the complex constant can be calculated through determination of the complex concentration, e.g. using NMR or UV measurements⁴³⁾.

If the host catalyzes reactions involving the guest, kinetic data can be applied. As an example, Murakami et al.⁴⁴⁾ have used the hydrolysis of p-nitrophenol esters, and Tabushi et al.⁴⁵⁾ have used temperature jump methods for the determination of kinetic and thermodynamic constants of complex formation.

In the case of acidic or basic hosts or guests, the pH titration can be used as a very simple procedure⁴⁶⁾.

Further methods like circular dichroism, electron spin resonance, polarography, calorimetry, diffusion across semipermeable membranes and surface strain measurements were only used in the case of the cyclodextrins as yet; they are described in more detail in the monographs cited above^{3b, e)}.

Table 2. Complex Constants for the Below Described Host and Guest Compounds

Host	Guest	pK of the host/guest complex	Method of determination	Ref.
2	5	1.8	fluorimetric	20 b)
2	6	3.2	fluorimetric	76)
8	9	2.4	titrimetric	54)
10	5	2.6	fluorimetric	55)
11	5	3.2	fluorimetric	56)
10	13	3.1	UV-Vis	45)
10	14	3.1	UV-Vis	45)
17	oxalate	3.7–4.7	titrimetric	59)
17	tartrate	2.5–2.9	titrimetric	59)
17	malonate	3.3–3.9	titrimetric	59)
17	citrate	4.7–7.6	titrimetric	59)
17	AMP	3.4	titrimetric	59)
17	ADP	6.5	titrimetric	59)
17	ATP	8.9	titrimetric	59)
18	glutarate	4.4	titrimetric	19 b)
19	ATP	11.0	titrimetric	60)
20	CH ₃ NH ₃ ⁺	2.9	unpublished	61)
20	NH ₃ ⁺ —CH ₂ —CH ₂ —NH ₃ ⁺	3.2	unpublished	61)
21	22	2.7	NMR	36)
21	23	> 5	NMR	36)
24	5	2.35	fluorimetric	62)
30	5	2.8	fluorimetric	64)
34	5	3.8	fluorimetric	34)
37	5	4.0	fluorimetric	69)
38	5	4.7	fluorimetric	69)

Table 2. (continued)

Host	Guest	pK of the host/guest complex	Method of determination	Ref.
40	5	5.7	fluorimetric	69)
34	6	5.0	fluorimetric	70)
38	6	4.5	fluorimetric	70)
34	36	3.5	fluorimetric	70)
38	36	2.4	fluorimetric	70)
40	36	3.6	fluorimetric	70)
47	5	5.2	fluorimetric	30)
47	49	3.2	NMR	30)
47	50	3.2	NMR	30)
47	51	3.0	NMR	30)
47	52	2.9	NMR	30)
47	53	3.1	NMR	30)
47	54	1.0	NMR	72)
47	55	1.4	NMR	74)
47	56	0.5	NMR	74)
45	5	4.2	fluorimetric	75)
46	5	3.0	fluorimetric	75)
63	6	3.6	fluorimetric	38)
63	36	3.1	fluorimetric	38)
64	65	7.2	unpublished	77)
64	66	6.1	unpublished	77)
64	67	6.0	unpublished	77)
64	51	4.2	unpublished	77)
64	68	4.3	unpublished	77)
64	35	3.3	unpublished	77)
64	5	6.5	fluorimetric	77)
64	6	6.7	fluorimetric	77)
64	69	2.2	unpublished	77)
102	67	6.6	difference of solubility	82)
102	51	4.1	difference of solubility	82)
104	5	4.6	fluorimetric	83)
105	5	4.0	fluorimetric	83)

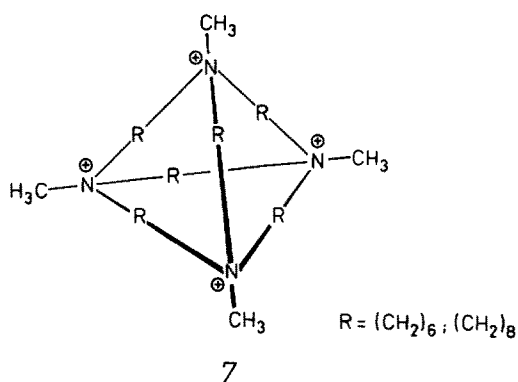
4 Complexation of Charged Guests

Crown compounds not only complex metal and ammonium cations inside their many-membered ring, they are also able to complex uncharged organic guest compounds *outside* their cavity, very often with an arrangement of guests above and below the crystalline state. This field has been reviewed recently⁴⁷⁾; we therefore will not deal with this type of complexation here.

There are much less examples of the complexation of charged *organic guest* ions *inside* the cavity of a host molecule in water solution. This on one hand could be due to the fact that the solvation of potential guests in water competes with the complexation through macrocyclic hosts. As a result, a low tendency of molecular inclusion is usually observed. In addition to that, many organic ion "receptors" are sparingly water-soluble, which means that many investigations have to be carried out in lipophilic solvents. As an example we note Cram's cavitands⁴⁸⁾, the cryptands of Lehn⁴⁹⁾ and Sutherland⁵⁰⁾ and the calixarenes described by Gutsche⁵¹⁾.

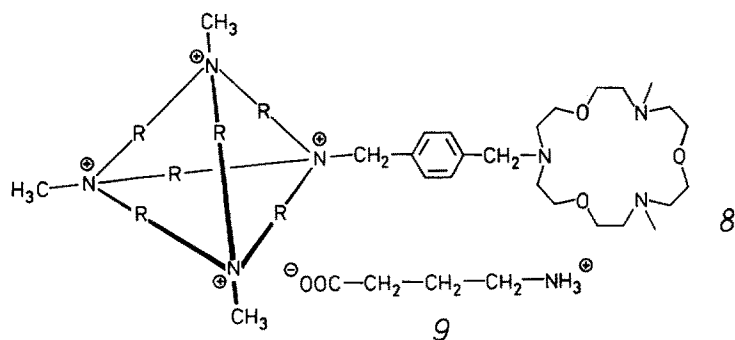
4.1 Anionic Guests

After work done by Simmons dealing with catapinands and of Lehn with the soccer ball type cryptand, Schmidtchen described macrotricyclic tetraammonium salts **7**, which allow to complex inorganic anions as well as acetate, and more interestingly, biochemical relevant guests like AMP, ATP and NAD⁵²⁾.

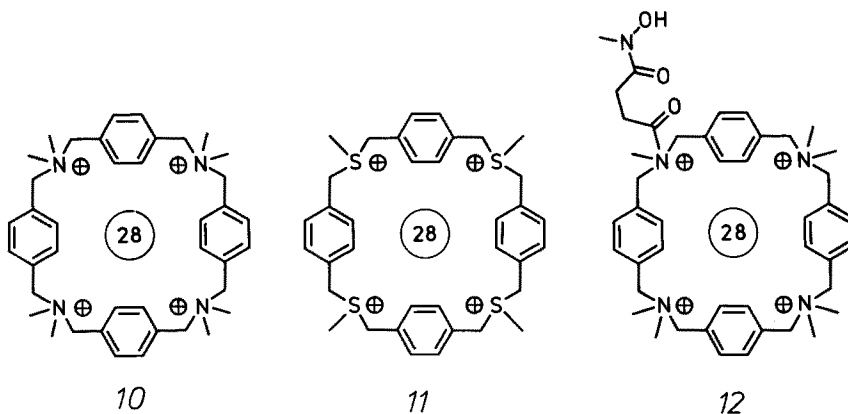


The guests are transferred into the cavity through desolvation and are bound there preferably through strong electrostatic interactions. The anionic guests which can be regarded as naked inside the cage, lead to a remarkable acceleration of nucleophilic substitutions at activated aromatic substrates with the guest (anion activation). In addition to that, a stabilization of the transition state by the host is postulated⁵³⁾.

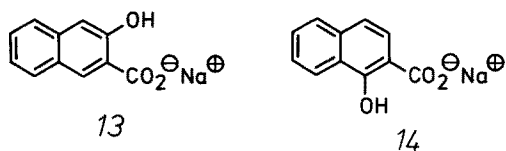
By a combination of the cage structure **7** with an azacrown compound as cation receptor, Schmidtchen obtained the ditopic host **8**, which complexes ω -amino acids⁵⁴⁾. The highest complex constant as yet ($pK = 2.4$) has been obtained for the neurotransmitter 4-aminobutyric acid (GABA, **9**), a guest molecule, which is just fitting in size.



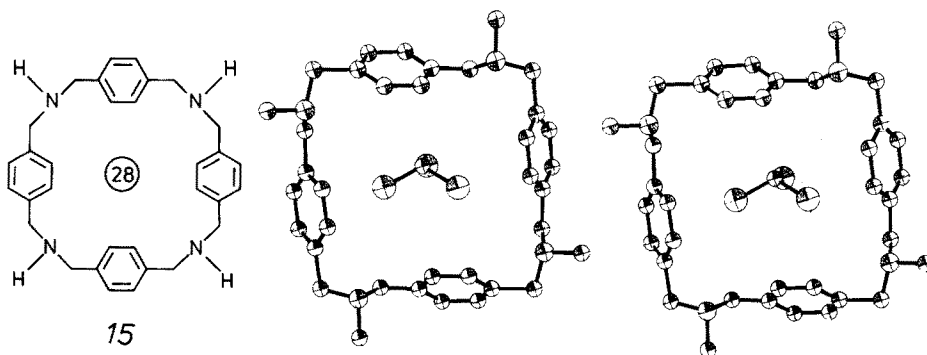
Tabushi et al. described the water soluble paracyclophanes **10–12**, but at that time a direct proof, e.g. through NMR highfield shift, of the formation of concrete inclusion complexes has not been achieved^{20b)}.



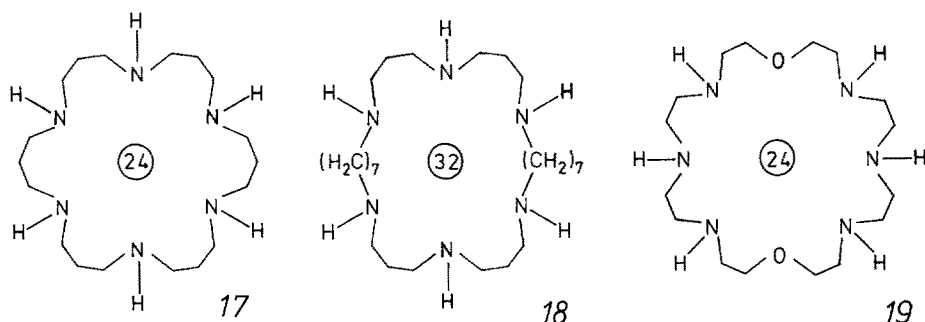
Nevertheless, using the 1,8-ANS (5) method, with ANS as a guest, fluorescence increases with *10*⁵⁵⁾ and *11*⁵⁶⁾ and therefrom complex formation constants have been obtained, which are remarkably higher than that of the cyclodextrins and of open chained reference host compounds. The complex constants of *10* towards the hydroxynaphthalene carboxylates *13* and *14* as guests have also been determined⁴⁵⁾. The authors suppose the intermediate formation of inclusion complexes also because of the capability of *10* and especially *12* to accelerate the hydrolysis of chloroacetic acid phenolates in water solution. The increase of the hydrolysis rate is explained by the activation of the complexed esters.



The inclusion capacity of this class of compounds has also been proved through the existence of stable *crystalline* complexes of the free amine *15* with dioxane⁵⁷⁾ and chloroform⁵⁸⁾. The stereo formula *16* shows the 1:1 inclusion of chloroform with *15*.



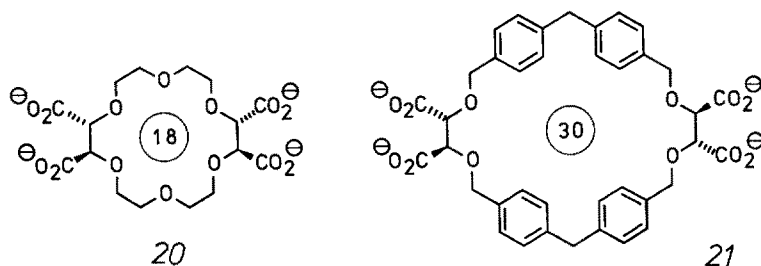
The 24- to 32-membered azacrown compounds described by Lehn et al. proved to be effective host substances for organic guest ions in water solution⁵⁹⁾. For example the fully protonated macrocycle **17** complexes di- and tricarboxylates like oxalate, tartrate, malonate and citrate and also the phosphates AMP, ATP and ADP⁵⁹⁾ utilizing ion pair and hydrogen bridge interactions. The macrocyclic ligand **18** in its protonated form shows a remarkable guest selectivity towards open chained dicarboxylic acids of different size^{19b)}. The highest complex constant is observed with glutarate as a guest. Each carboxylic group of the guest is bound to a tris(ammonium) unit of the host whereby the alkyl chains can be oriented parallel and strain-free.



The host **19** is a strong complexing agent for ADP as a guest in water solution⁶⁰⁾. The 1 : 1 stoichiometry of the host : guest aggregate was proved by ³¹P-NMR spectroscopy (pK = 11.0). The capability of **19** to accelerate the ATP hydrolysis by a factor of 10³ is explained by an initial host/guest complexation followed by intramolecular hydrolysis.

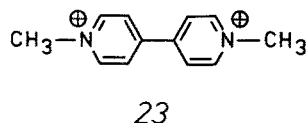
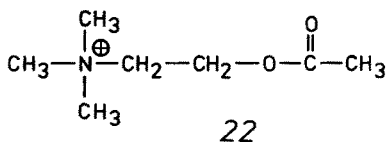
4.2 Cationic Guests

By introducing two chiral (*R,R*)-tartrate units into the well known [18]crown-6 skeleton, Lehn et al. obtained the achiral host **20**, which is able to complex small primary ammonium salts like methylammonium and ethylenediammonium through hydrogen bridges and electrostatic interactions⁶¹⁾.

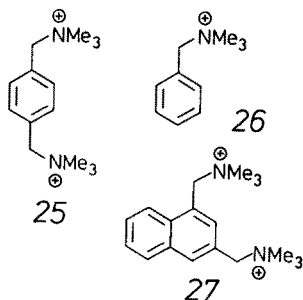
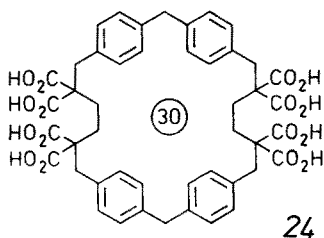


The water soluble chiral 30-membered macrocycle **21** has been designed making use of the lipophilic and stiffening diphenyl-methane spacer unit³⁶⁾. It is a good host for a series of ammonium ions. The formation of molecular inclusion compounds

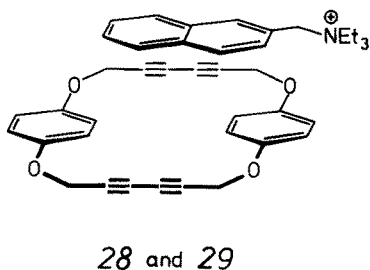
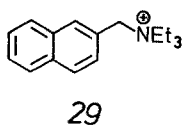
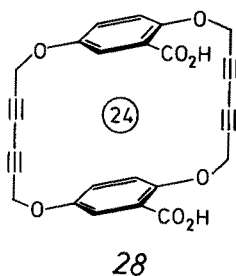
of **21** as well as the 1:1 stoichiometry of the complexes were proved through NMR highfield shifts of the complexed guests. The strong complexation of acetylcholine (**22**) ($pK = 2.7$) and of methylviologen (**23**) ($pK \geq 5$) appears to be of special interest. Hydrophobic effects as well as electrostatic interactions should be responsible for the stability of these complexes.



Recently, Vögtle and Merz have described the first *carbocyclic* large cavity **24**⁶². The diphenylmethane unit and eight carboxylic acid groups allow the complexation of quaternary ammonium salts in the host's cavity as was shown by significant up-field shifts of several guest protons. A guest fitting well into the cavity of **24** is 1,4-xylylene-bis(trimethylammonium)iodide (**25**).



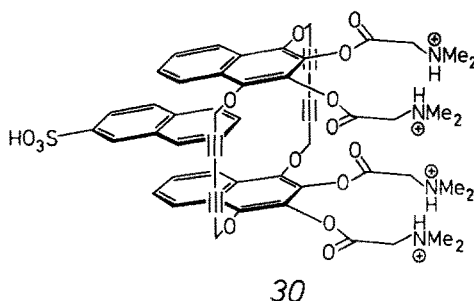
In $D_2O/NaOD$ solution after addition of **24** *all* guest protons of **25** are upfield shifted. In contrast to **25**, the guests **26** and **27** seem to fit spacially less well into the cavity. Also there seems to be a discrimination between singly and doubly charged cations, when **25** and **26** are compared. The good complexation ($pK = 2.35$) with **5** as the guest is remarkable, if it is taken into account that different to the crown complexes of primary, secondary and tertiary ammonium salts, hydrogen bridges here seem not to be responsible for the binding. The main influence here should stem



from electrostatic forces, as the hydrophobic effect alone seems not to be sufficient to enclose uncharged hydrocarbons like e.g. naphthalene.

Whitlock et al. have investigated cyclophanes containing several spacing acetylenic bridges with regard to their conformational and inclusion behaviour. With the cavitand **28** and the guest **29** in the NMR spectrum highfield shifts are observed, but the authors refer this to a classical aggregation and not to an inclusion complex⁶³⁾.

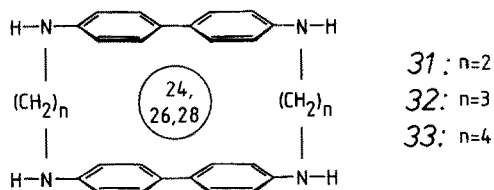
In contrast to this, the improved host structure **30** in the complexed state exists in the *syn*-conformation and is able to complex 2,7-naphthalene sulfonic acid. This was also shown by NMR studies in D₂O/DCI. With 1,8-ANS a complex constant of $pK = 2.8$ was determined⁶⁴⁾.



5 Complexation of Uncharged Guest Molecules

The roots of this research area can be followed back to investigations of Stetter and Roos', which were done in the early 50's at Bonn university⁶⁵⁾. Their correct experimental observations only some years ago have underwent a somewhat different and more precise interpretation in the light of X-ray analysis, but the consequent development of their type of macrocyclic hosts brought the breakthrough in this field.

In the framework of studies on macroheterocyclic ring systems of the cyclophane type, Stetter and Roos synthesized the macrocyclic tetraamines **32** and **33**, which after recrystallization from dioxane or benzene retain solvent in stoichiometric amounts in the solid state. Particularly, **33** binds dioxane so strongly that even in vacuo during 30 hours at 150 °C it cannot be removed.



From space filling molecular model considerations the authors followed that because of the fit of the guest into the host's cavity a new complex type with the guest inside the hosts's cavity would be most probable. This seemed plausible at that time,

because reference host compounds with shorter alkyl chains like **31** and having smaller ring size yielded no addition compounds in the course of recrystallization⁶⁵⁾.

Only as late as 1982 the true nature of this type of adduct has been precisely cleared up. In the course of work dealing with spaced large cavities in our group⁶⁶⁾ we resynthesized Stetter's complexes and put forward the question of clarification by X-ray analysis if these adducts were clathrates or inclusion complexes. Because of difficulties in the X-ray analysis of the benzene adduct it took several years until it was found that the benzene is not located inside a cavity of the host molecule, but is situated in crystal lattice cavities in between several host molecules⁶⁷⁾.

In the meantime³⁴⁾ Koga had taken up Stetter's adduct philosophy also: By replacing the benzidine by diaminodiphenylmethane units he obtained the 30-membered macrocyclic tetraamine **34**.

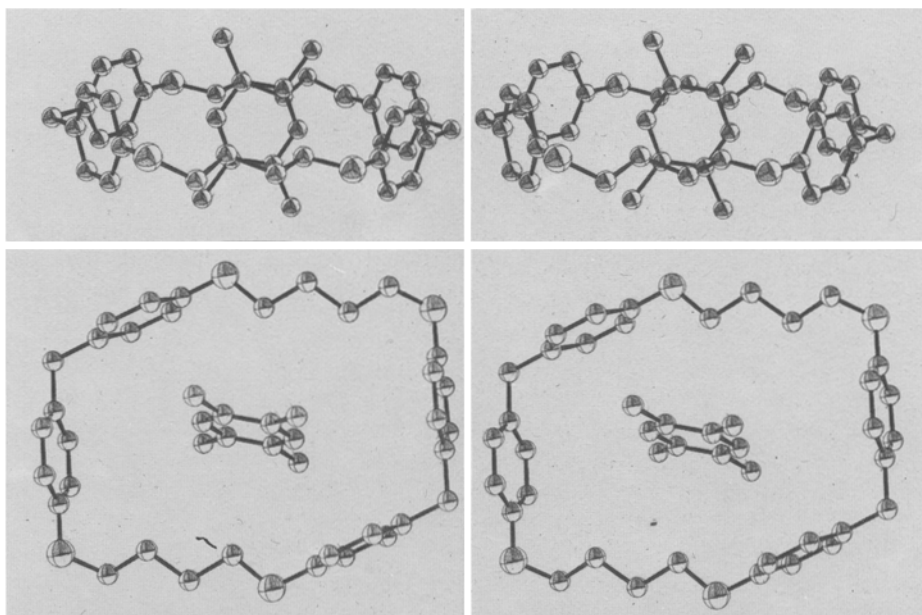
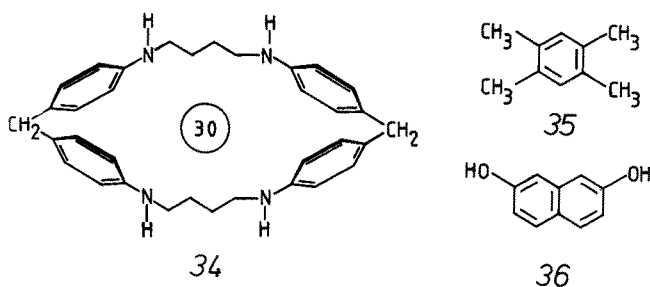


Fig. 3. Inclusion of durene in host **34** (stereo view)

This macrocycle, which is soluble in water at a pH lower than 2, with 1,8-ANS (5) shows a strong increase of the fluorescence which hints to an inclusion of the guest (ANS) in the host cavity. The complex constant determined in this way ($pK = 3.8$) even is remarkably higher than that of β -cyclodextrin (1.8). The host **34** with a row of uncharged aromatic hydrocarbons like naphthalene, xylene, durene (**35**) forms stable, crystalline inclusion complexes. The stereo picture shown in Fig. 3 is drawn according to the results of an X-ray analysis of the $34 \cdot 4 \text{H}_2\text{O} \cdot 4 \text{HCl} \cdot \text{durene}$ complex. Obviously, for the first time here the complete encapsulation of an unpolar guest in a synthetic host has been proved. The guest completely fills the cavity and is situated around its center.

In the ^1H -NMR spectrum another guest, 2,7-naphthalenediol (**36**), in the presence of the host **34** in $\text{D}_2\text{O}/\text{DCl}$ exhibits strong upfield shifts. Anisotropy effects of the aromatic rings and electrostatic effects of the ammonium centers are considered to be responsible. From the fact that the different protons of **36** are differently shifted after the guests enclosure, a preferred orientation of the guest in the host cavity has to be concluded and statistical or random geometries can be excluded³⁵). A comparison of the upfield shifts observed with those calculated for reasonable geometries leads to the conclusion that the pseudoaxial orientation of the guest is favoured compared to the axial or equatorial orientation.

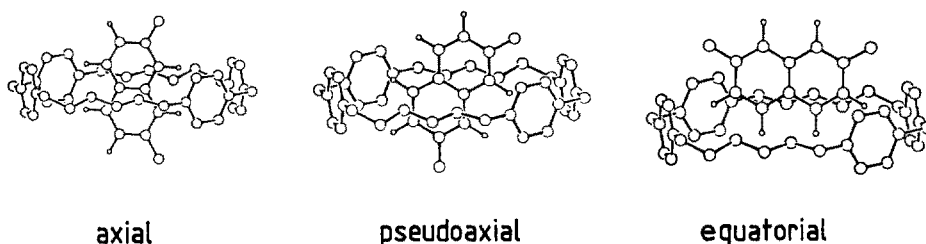
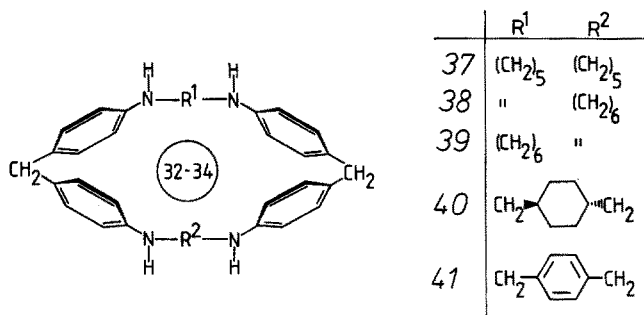


Fig. 4. Possible orientations of 2,7-naphthalene diol in host **34**

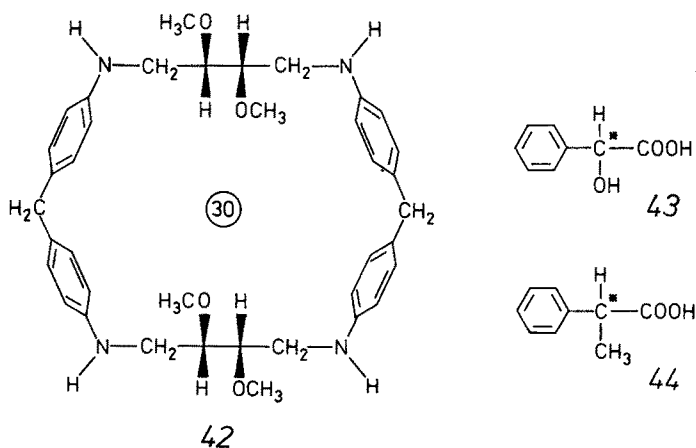
A recent X-ray analysis of the $34 \cdot 4 \text{HCl} \cdot \text{naphthalene}$ complex impressively proves the preference of this supposed orientation. In contrast to this result, the same guest, if complexed by the host **37**, two ring members larger in size, is enclosed in



an equatorial orientation [68]. From the fact that these complexes have been obtained in water solution, it follows that hydrophobic interactions are strongly contributing to this type of complexation, whereas polar forces seem not to play a dominant role here.

The cavity size of this type of hosts was modified by Koga et al. by changing the bridge lengths as well as the hydrophobic character of the bridges (37, 38, 40, 41). The complex formation ability was studied by use of 1,8-ANS as a probe⁶⁹. The complex stability increased in the row $34 < 37 < 38 \ll 40$, whereas with the host 41 or through replacement of the diphenylmethane unit by a dicyclohexylmethane unit only low complex stabilities were obtained. The enlargement of the hydrophobic cavity using cyclöhexane units is responsible for the fact that 40 exhibits by far the highest complex constant values, a 80fold increase compared with 34. A decrease of the hydrophobic character of the host as exhibited by 41 gives rise to a low inclusion capability. The diphenylmethane units seem to be rather essential as they serve as spacers for the cavity and also favour the "face orientation" with the benzene rings turned perpendicular to the macrocyclic ring, which leads to a deeper cavity. The quantitative results show that by variation of the cavity the host can be tailor-shaped for specific guests like e.g. 5.

In reverse, the hosts exhibit selectivities towards different guests. The compounds 34, 38 and 40 were studied with regard to their complexing capability towards naphthalendi- and monosulfonic acids and 36 by qualitative ¹H-NMR- and quantitative fluorescence measurements⁷⁰. As a result, 34 shows selectivity towards β -substituted and 38 and 40 towards α -substituted naphthalenes. This can be reduced to the pseudo-axial orientation of the guests in the smaller cavity of 34 and to the equatorial orientation in larger cavity of 38 and 40. In addition to that, 40 forms the most stable complexes with all guests studied. It is remarkable that the hosts investigated do complex monosulfonic acids or benzene derivatives weaker and aliphatic guests not at all. These observations can be interpreted in terms of the precisely fitting diameters of the cavity as well as the electrostatic interaction to be necessary prerequisites for a strong binding between host and guest. It fulfills the biochemical principle of multiple recogni-

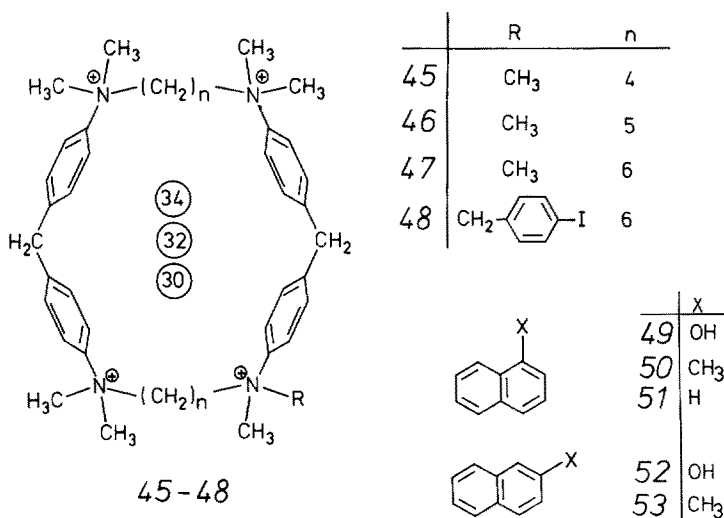


tion in enzyme/substrate complexes that one single of these factors alone is not sufficient but both have to be present simultaneously.

In modifying the successful "mother host" 34, Koga et al. have synthesized the first synthetic water soluble host 42 with a chiral cavity by using L-tartaric acid units ⁷¹). The complexation of chiral aromatic carboxylic acids like 43 and 44 by the enantiomeric pure host has been proved by ¹H-NMR spectroscopy in acidic water solution yielding strong upfield shifts of guest protons.

The different shifts observed for the (*R*)- and (*S*)-guests are especially remarkable. They can be interpreted to be due to diastereomeric host/guest complexes with different stabilities and inclusion geometries.

The success that has been achieved with hosts of the type 34 seems to have inspired other investigators to synthesize similar structured hosts. The octamethyl derivative of 39 (45), however, has the advantage that it can be dissolved in neutral water solution ⁷²).

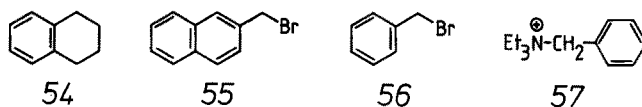


Proof for the inclusion capacity of the host 45 is obtained by upfield shifted protons of the naphthalene guest 51. These are explained in terms of the influence of the anisotropy effects of the aromatic rings of the host 47. Fluorescence spectroscopy and NMR signal shift titrations of the guests 5 and 49-53 give proof of the inclusion capacity of the host 45. A strong decrease of the complexation energy with increasing amounts of organic solvent (alcohols) in water is observed. The mechanism of the binding of hydrophobic substrates in lipophilic cavities seems to be similar to the mechanism of the dissolution of hydrocarbons in water.

Immobilization of the azacyclophane 47 by absorption on silica gel allows chromatographic applications ⁷³). Substrates like naphthalene sulfonic acids which are complexed particularly well by 47, are retained stronger compared to unprepared silicagel (methanol as eluent). This corresponds to a decrease of the *R_F* value. A smaller decrease is shown by carboxylic acids. Aliphatic acids and phenols did not show strong influences, but variations of the eluent (methanol/water or methanol/ammonia

instead of pure methanol) leads to a stronger binding of these guest compounds, too. These findings may open new possibilities of separation of natural products or synthetic substrates.

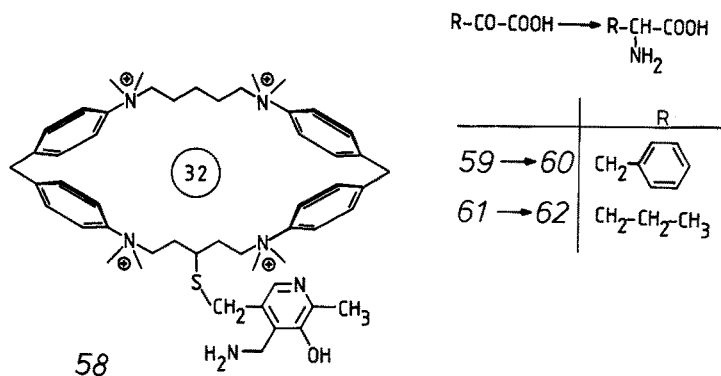
Attempts to catalyze the chlorination of hydrocarbons by fixing of a halogen transferring iodophenyl group to the azacyclophane host ring, e.g. 48, were unsuccessful due to the instability and low solubility of the host ⁷²). On the other hand, 47 is capable to complex tetralene (54) in water solution with the low complex constant of $pK = 1$ and to affect with chlorotetralines a passive protection against hydrolysis.



An acceleration by a factor of 20 compared with the uncatalyzed reaction was observed in the reaction of 2-bromomethylnaphthalene (55) with sodium nitrite in the presence of the host 47 ⁷⁴). Also the product ratio $[\text{RONO}]/[\text{RNO}_2]$ changing from 0.5:1 to 0.16:1 alters with the ambident nucleophile. The phase transfer catalyst 57 affects an opposite steering of the product formation and no increase of the reaction speed. These facts suggest a complexation step which is preceding the main reaction. The product steering can consequently be explained by a crowding of nitrite ions at the positively charged centers of 47, which increase the number of $\text{S}_{\text{N}}2$ attacks and in such a way leads to an attack at nitrogen instead of oxygen. Substrates like 5 which are bound stronger to 47 inhibit the catalysis and such guests that are not complexed well like 56 are either not accelerated or substituted with another product distribution.

Complex formation towards 1,8-ANS and 2,7-naphthalene diol (36) has been studied also for the macrocycles 45 and 46, which are homologous to 47 ⁷⁵). By affixing a pyridoxamine side chain to 46, the host 58 was obtained. The catalytic activity in the transamination of phenylpyruvate (59) to phenylalanine (60) and of α -ketovaleric acid (61) to norvaline (62) was studied using this host.

A 31-fold acceleration of the reaction $59 \rightarrow 60$ compared with simple pyridoxamines and a twofold acceleration compared with the cyclodextrin analogous compound was stated. In the transamination of 61 and 62 a sixfold (threefold resp.) acceleration

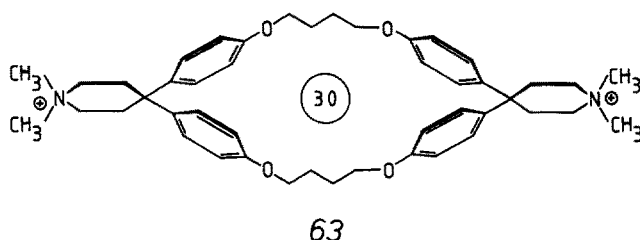


of the reaction was observed. The chirality of the products as induced by cyclodextrins could not yet be observed in the case of the racemic host 58.

Diederich has modified Koga's concept in that he located the positive ammonium centers as a part of the many-membered ring to the periphery of the macrocycle, but retaining the diphenylmethane spacer units. The hydrophobic cavity now inside is no longer disturbed by positive charges and as a consequence so to say enlarged. On the other hand, increased micelle formation and aggregation of the host molecules was observed by shifts of the host protons, without guest being present, in the ^1H -NMR spectrum depending on the concentration of the host.

Only at concentrations below the critical micelle concentration (CMC) a molecularly dispersed solution can be taken for granted, and only then complexation studies should be carried out.

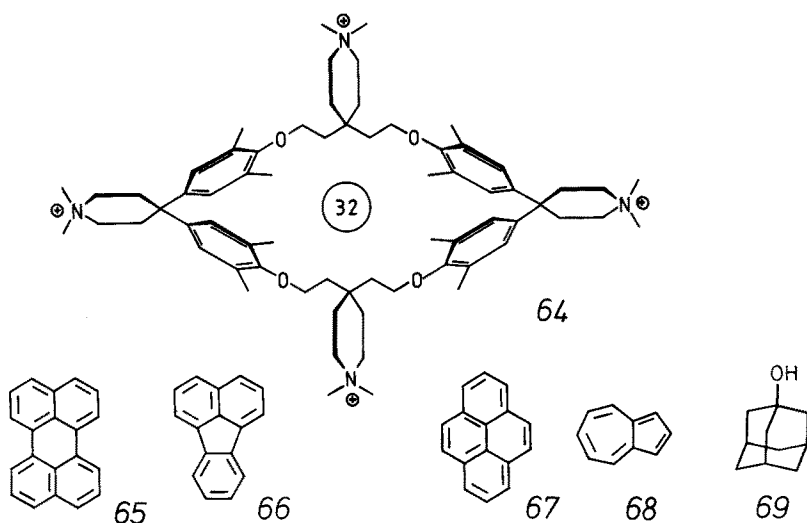
In this way using the host compound 63 below the CMC value = 2.5×10^{-4} the complexation of TNS (6) was determined by fluorescence spectroscopy³⁸⁾. The complex constant is of the same order of magnitude as the one of β -cyclodextrin⁷⁶⁾. With 2,7-naphthalene diol (36) as the guest no significant ^1H -NMR highfield shifts could be obtained. The complex constant of 36 nevertheless was determined using the competitive inhibition of TNS.



These results led to an improved host structure 64, the application of which because of the higher CMC value of 7.9×10^{-3} was remarkably enlarged. Through solid/liquid- and liquid/liquid extraction 1:1 complexes of 64 even with such arenes could be obtained, which are extremely low soluble in water like perylene (65), fluoroanthrene (66), pyrene (67), naphthalene (51), but also azulene (68), and durene (35).

The highest binding constant with $\text{pK} = 7.2$ was found for the complex with perylene, whereas the stability towards smaller arenes decreased as expected⁷⁷⁾. The much weaker complexation of 69 by the host 64 in methanol and the missing of inclusion in DMSO most probably mean that hydrophobic interactions are decisive here for the host/guest binding. In addition to that, 64 also bind polar substituted aromatic guest compounds like 1,8-ANS (5) strongly and aliphatic compounds like 1-adamantanol (69) much weaker.

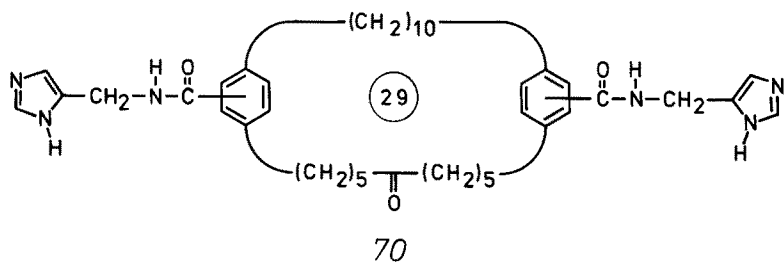
^1H -NMR investigations of the complexes in water solution have shown that all aromatic guest molecules are located in a specific plane of the cavity which links the spiro carbon atoms of the diphenylmethane units and is perpendicular to the medium molecular plane of 64⁷⁸⁾. In the case of polar guests besides the hydrophobic interactions ion pair bonds with the piperidinium rings in the aliphatic bridges are effective in addition.



For the first time, with the synthetic host 64 the transport of arenes in a U-shaped tube from a lipophilic phase across a water phase in a second lipophilic phase in the direction of the gradient of the concentration was observed. It was shown by competitive inhibition of the host that the host/guest complexation in the water phase is responsible for the transport observed. A high transport selectivity was also stated, which is in accord with the complex constants determined.

Recently, a series of new host structures has been evaluated, especially of those types, which do not contain diphenylmethane as the spacer unit. Many of them are suitable hosts in water solution.

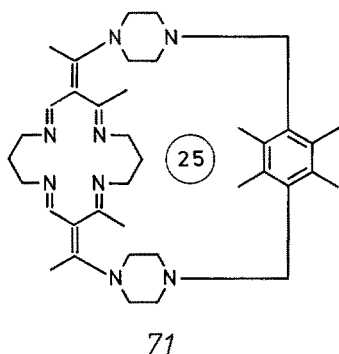
Murakami et al. have synthesized numerous substituted [20]- and [10.10]paracyclophanes like 70^{44d)}. Because of low solubility and a high tendency of aggregation, a complexation with clear stoichiometry and geometry has not been achieved. Nevertheless, a remarkable acceleration of the hydrolysis of *p*-nitrophenol esters has been observed, which is explained in terms of the formation of inclusion complexes between host and substrate.



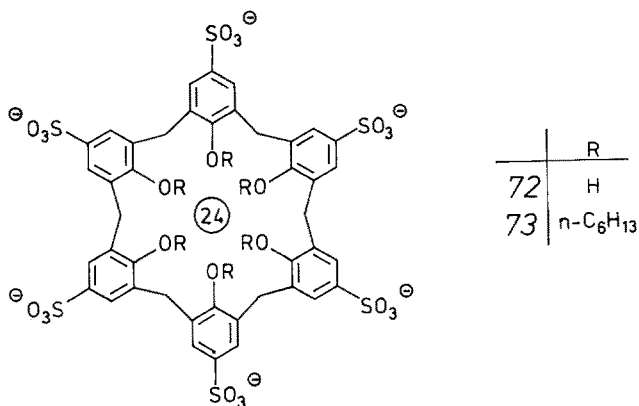
Busch et al.³²⁾ on their search for a cytochrome P450 model useful for the selective oxidation of alkanes investigated the macrobicyclic nickel(II) complex 71 with respect to its inclusion capacity for aliphatic alcohols and phenols. A shift of the host protons in the course of the guest addition (e.g. 1-butanol, phenol) in D_2O the formation of in-

clusion complexes has been stated by ^{13}C -NMR spectroscopy. Semiquantitative determinations of the formation constant by NMR shifts during titration yielded values around $\text{p}K = 1$ for several alcohols.

For the corresponding iron(II)- and cobalt(II) complexes the reversible binding of oxygen has been detected. The aim of these investigations is to develop novel catalysts for oxidations in the course of which in a first reaction step oxygen is coordinated by the metal ion and the substrate is enclosed by the hydrophobic cavity.

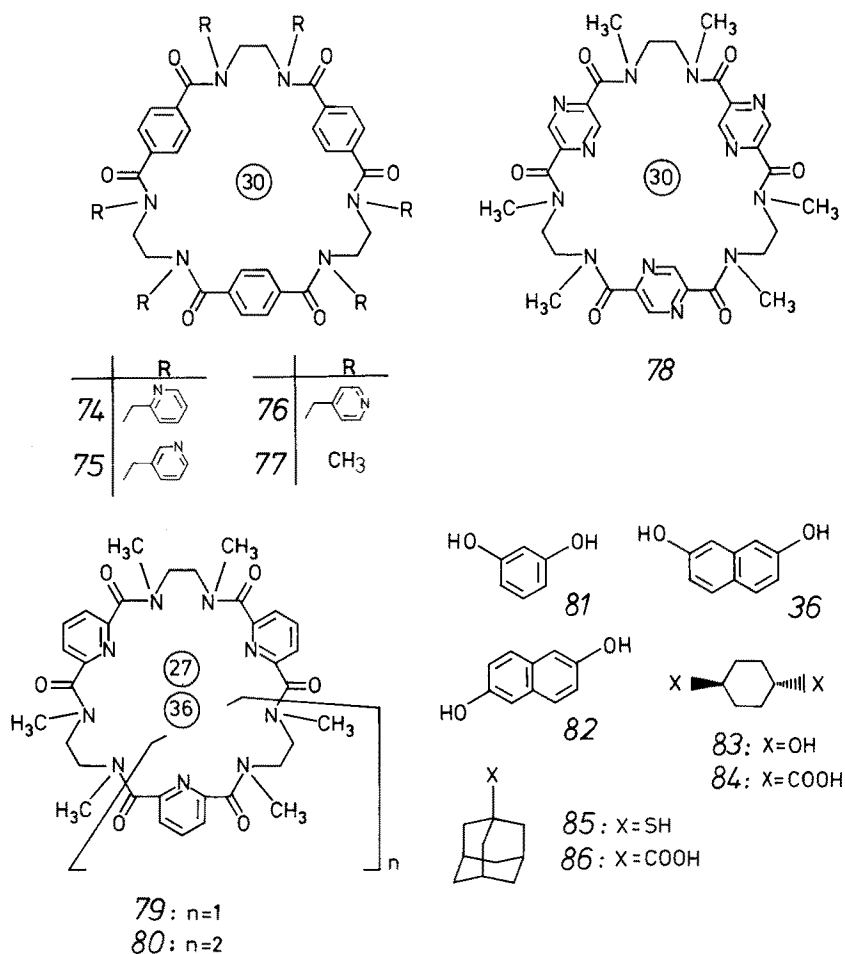


The calixarenes⁵¹⁾ have a flexible or rigid cavity, resp., which can be shaped to some extent. Some inclusion compounds in the solid state have been described, but the low solubility in water did not allow applications in respect to an enzyme mimick as yet. Host/guest interactions in solution according to studies of Gutsche et al. seem to occur in some cases, but are weak. Shinkai and coworkers⁷⁹⁾ seem recently to have overcome parts of these problems by incorporation of sulfonic acid groups in this skeleton (72 and 73).



From fluorescence and absorption spectroscopic studies the authors conclude that 72 and 73 are able to uptake naphthalene but not pyrene in their cavity.

Recently, Vögtle et al. have developed a large family of new hosts 74–80 and 87–101, which are based mainly on an oligolactam skeleton. This facilitates water solubility and lends some peptide analogy to these hosts. The inclusion properties for phenols



like resorcinol (81), 2,6- and 2,7-naphthalene diol (82, 36) have been investigated using the ^1H -NMR upfield shifts of guest and host protons^{80, 81}.

In the series of the hexalactam macrocycles 74-78 particularly those hosts with α -, β - and γ -pyridylmethylene side arms (74-76) and especially 75 even more pronounced upfield shifts in acidic water solution are observed than with the hosts 77 and 78. This can be referred to the different spatial distances of the six pyridine nitrogen atoms from the formal identical cavities of 74-77. Hydrogen bridges between the OH groups of the naphthalene diols and the nitrogen atoms of the pyridine rings can also be made responsible for it. A further quality of the hosts 74-76 is their capability not only to complex aromatic, but also aliphatic guests like cyclohexane and adamantane derivatives in acidic water solution, as has been proved by ^1H -NMR upfield shifts.

The host macrocycles 79 and 80 contain 27 and 36 ring members resp., compared to the 30-membered macrocyclic hosts 74-78. Having a somewhat smaller and larger cavity resp., they did not exhibit strong host properties, which stresses the need of a distinct cavity size for a given guest.

For the first time, in the presence of the synthetic hosts 74–76, a rapid H/D exchange of the 1,5- (1,8-) protons of 2,6- (2,7-) naphthalene diol as well as the two protons of resorcinol has been observed. This catalysis is referred to the combination of the fitting cavity size and the attacked pyridine rings. In accord with this interpretation, open chained reference substances containing either several amide bonds or pyridino side chains or both together, do not comparably accelerate the deuterium exchange of the same guests ⁸¹⁾.

Hosts with varying lactam and amine structures (87–101) with ring member numbers of 30–48 have been synthesized and tested with respect to their host properties ⁸¹⁾.

In Table 3 some examples are given illustrating the upfield shifts of the aromatic guest protons in the ¹H-NMR spectra, the guest being 2,7-naphthalene diol (36).

With the 30- and 32-membered hosts 89 and 91 and the guest 36 strong intermolecular isotropy effects are observed, whereas the *o*-terphenyl macrocycle 96 seems to be too small for the guest 36 but seems to be exactly fitting for the smaller resorcinol 81.

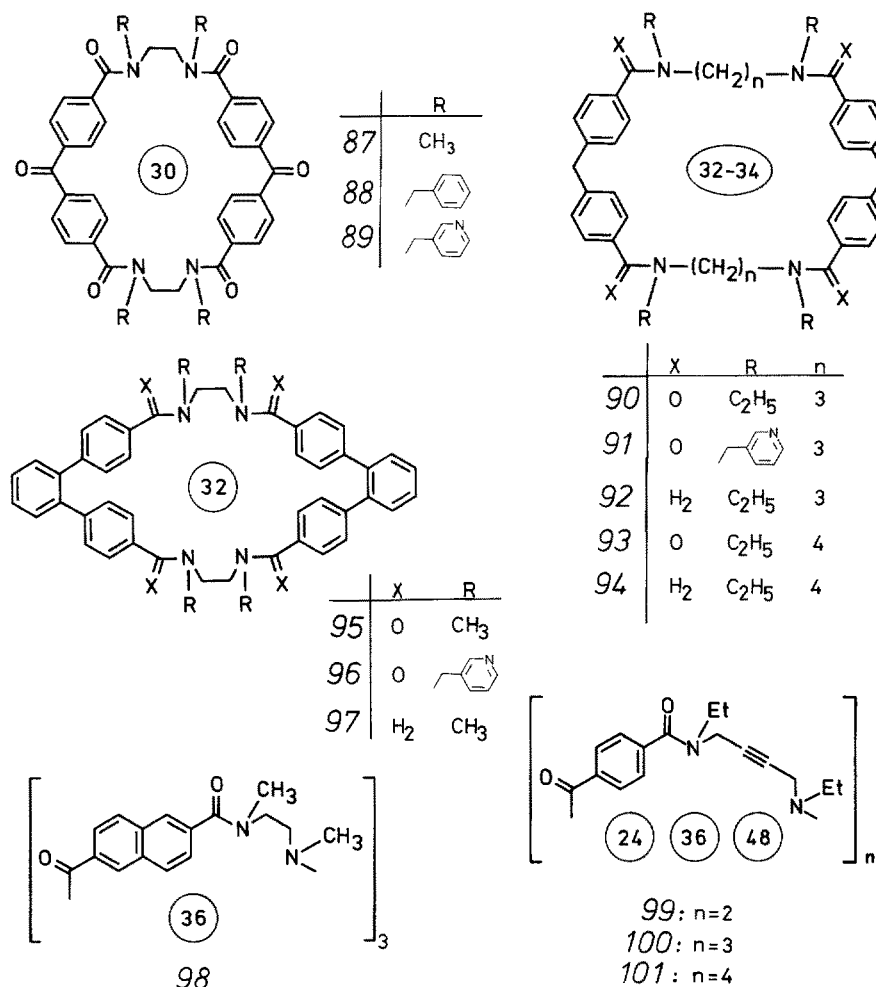
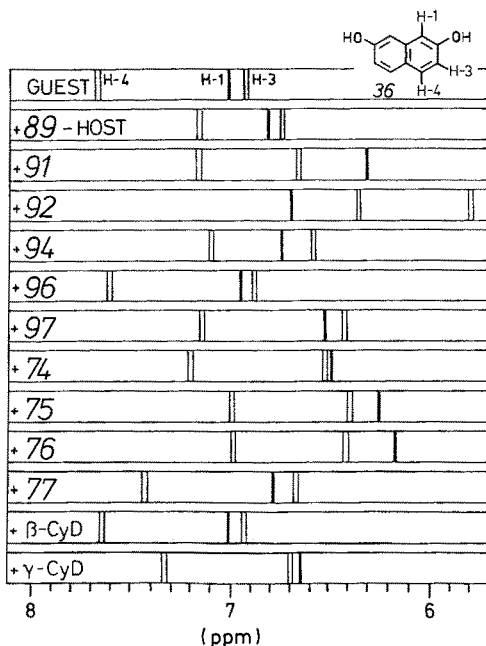


Table 3. Upfield shifts of the proton signals of the guest 2,7-naphthalene (36) in the presence of diverse guests

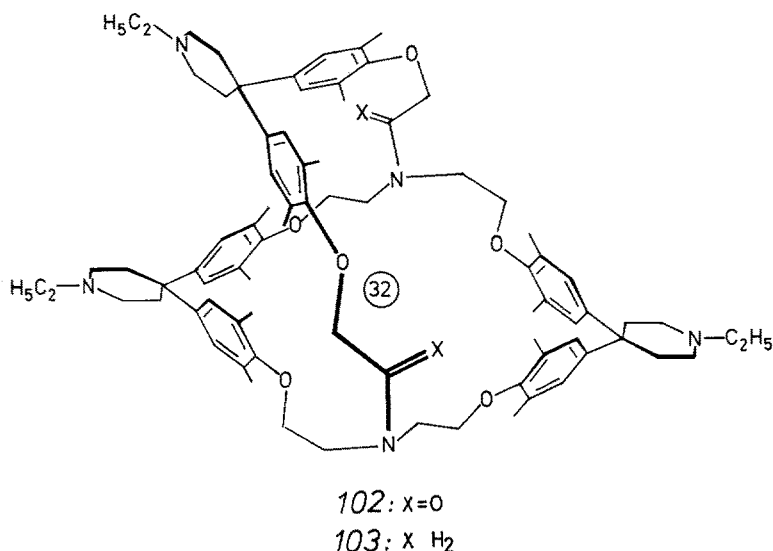
If as in the hosts 92, 94 and 97 the amine nitrogens are placed in the benzylic position in contrast to their aryl position in Koga's hosts, e.g. 34, then the complexation behaviour is no longer disturbed.

The many-membered acetylenic macrocycles 99–101 do not show upfield shifts under similar conditions.

Besides several phenols aliphatic alcohols and thiols like 83 and 85 are complexed particularly by the *o*-terphenyl hosts 95–97. As in the case of the macrocycles 74–76 the pyridyl substituted hosts 89, 91 and 96 accelerate the H/D exchange of the 2,7-naphthalene diol guest 36. It is interesting in this connection that with the 35-membered β-cyclodextrin host and 36 as a guest no upfield shifts are obtained, which is in striking contrast to the 40-membered γ-cyclodextrin and the same guest ⁸¹).

Recently, novel host structures have been designed, which strongly differ from the hitherto known macromonocycles. Diederich and Dick synthesized the macrobicyclic hosts 102 and 103 and studied their capability to complex neutral arenes like pyrene (67) and naphthalene (51) in water solution ⁸²).

In weak acidic solution 102 contains an extended unpolar cavity because the ammonium centers which increase the solubility are located as an appendage outside the periphery of the host skeleton. The guests 67 as well as 51 and 98 by solid/liquid extraction can be dissolved in water. The complex constants (pK = 6.6 for 107/67; 4.1 for 107/51) can be evaluated using the concentration of the guests in this solution and by taking into account the maximal solubility of the guest in host-free water. In the ¹H-NMR spectra the signals of the complexed arene guest are strongly upfield shifted.



An orientation of the guests in the plane of *102*, which connects the three spiro carbons is proposed. The exchange between host and guest is slow on the NMR time scale; the signals of the free and complexed pyrene guest appear separately.

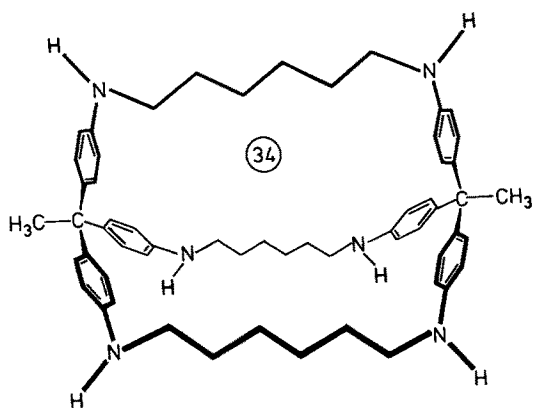
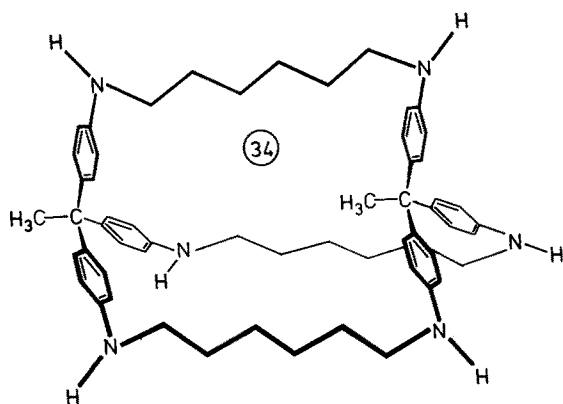
Switching from host *102* to *103*, in weak acidic solution the nitrogen atoms are protonated also inside the cavity, which lowers the hydrophobic character of the host and leads to a remarkable weaker complexation of arene guests. The interpretation that this weaker complexation is due to the two protonated cavity nitrogen atoms and not due to geometric factors, is supported by the observation that the complexation between *67* and the protonated host *103*, which is not soluble in methanol, is surprisingly strong.

Vögtle and Franke have described two *in/out* isomeric macrobicyclic cavities *104* and *105*, which have one and the same chemical constitution and therefore have very similar chemical properties, however, differ significantly in their effective cavity size and shape⁸³⁾:

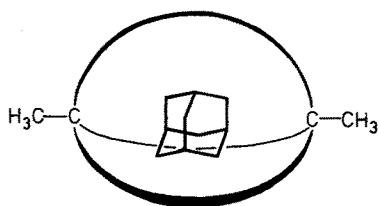
Both hosts *104* and *105* in acidic water solution are able to complex polar aromatic guest compounds like 2,7- and 2,6-naphthalene diol (*36*, *82*) as is shown by ¹H-NMR upfield shifts. In striking contrast to *34* and *105* the *out/out* isomeric host *104* catalyses the H/D exchange of the 1 H protons of the guests *36* and *82*. This can be reduced to a more favourable encapsulation of the guests in the host *104* compared with *34* and *105*, which could lead to an activation of the 1-position.

Unsubstituted aromatic hydrocarbons like naphthalene (*51*) even are complexed by both isomeric hosts, whereas the larger durene (*35*) neither by the host *104* nor by its isomer *105* is enclosed.

In addition to this, the host *104*, but not its isomer *105*, were shown to be able to encapsulate adamantane as a guest. This apparently is the first example of the molecular encapsulation of a non-functionalized aliphatic hydrocarbon in water solution by solid/liquid extraction using a synthetic host. As a consequence, aliphatic hydrocarbons will be amenable to be dissolved and complexed in water. This capacity has

*104: out/out**105: out/in*

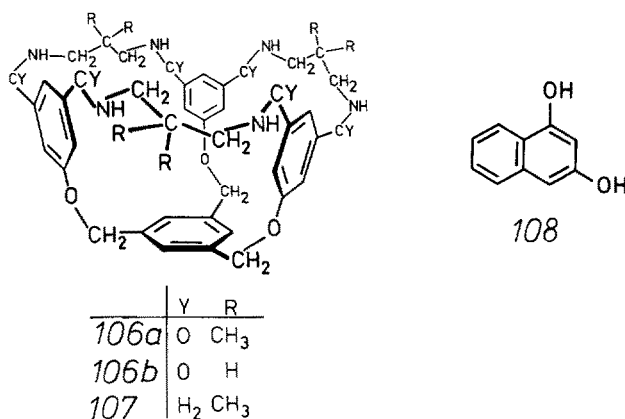
been observed only with the cyclodextrins as yet. The advantages of the new synthetic hosts are obvious in that *104* and *105* are the first examples of two isomers with similar but modified cavity size and shape, whereas in cyclodextrin chemistry only the α -, β - and γ -cyclodextrins up to now are the only representatives. The capacity of the synthetic hosts *104* and *105* to even complex aliphatic hydrocarbons like adamantane, and the significant differences in selectivity are explained in terms of the somewhat

*104*, adamantane as guest (schematic drawing)

smaller and "symmetry-disturbed" cavity of the *out/in* isomer *105*, compared to the better fitting size and shape of the more symmetric *out/out* cavity *104*, which leads to an optimum fit in the course of enclosure of the ballshaped adamantane. In good accord with this observation and explanation, adamantane thiol (*85*) also only is complexed by *104*, but not by *105*.

A further verification for the different complex forming abilities of the isomeric hosts *104* and *105* is given by the higher complex constant of *104* towards 1,8-ANS (*5*) ($pK = 4.6$) compared with $pK = 4.0$ of the *105/5* complex.

Vögtle and Wambach recently for the first time described basket-shaped host molecules of the types *106a*, *b* and *107* which apart from a 30-membered ring as the wall contain a "floor-plate", which cannot "dive" through the 30-membered basket-rim⁸⁴⁾.



¹H-NMR studies of the lactam *106a* in deuterated acetic acid with several phenols and diphenols as potential guests did not reveal significant upfield shifts. However, with 1,3-naphthalene diol (*108*), and, in particular, with resorcinol (*81*), in only few minutes a rapid H/D exchange of the guest protons in the 1-position is observed. With a large number of other phenols and naphthalene diols this H/D exchange is not observed under analogous conditions. It seems to be specific for 1,3-diols as with reference guest substances, which do not have this specific configuration of the OH groups, even after one day under analogous conditions there is no significant deuteration at all.

6 Conclusions and Outlook

As this progress report points out, a remarkable broad spectrum of synthetic hosts containing large cavities has become known up to now recently, since the breakthrough in this field around 1980.

Synthetic organic chemistry therewith has clearly demonstrated that it is capable of designing and constructing water-soluble macrocyclic and macropolycyclic host

molecules which even now can partly compete with biological receptors and enzymes with regard to some of their properties, e.g. substrate selectivity and strength of complexation. Some of the synthetic hosts already now have overcome the cyclodextrins to some extent.

Nevertheless, it can be seen from the structure of the synthetic hosts described as yet that they all contain similar structural building blocks like the diphenylmethane unit and aliphatic $(CH_2)_n$ bridges. But in principle, there is no restriction regarding these building blocks as long as they are spacer units preforming a cavity and units that allow water solubility, e.g. positive or negative charges or crown or polyethylene glycol units etc. All in all, the most simple features to end up with a synthetic receptor model for organic guest molecules in water solution include a macrocyclic ring containing 30–40 ring members and at least four positive or negative charges that allow or increase water solubility.

The future of research in this field will show that there is a lot of modification of structural building blocks with the aim of designing new host structures with varying selectivities towards specific guests and certainly the complex constants towards more interesting biological guest molecules will be increasing.

Using enantiomeric pure chiral hosts, the separation of racemic substrates hopefully will be possible soon. It seems of great advantage in this context that the guests must not necessarily bear functions, but can be hydrocarbons, heterocycles, and so on. This will also include immobilized hosts bound to resins. Then not only enantiomer separations will be possible, but affinity-type chromatography will allow more specific separations of guests which can be separated of a mixture of similar substrate molecules.

As has been shown in the cyclodextrin field, a stabilization of enclosed guest molecules (e.g. steroids, enamines, amino acids, sugars, prostaglandins, penicillins, antibiotics) against decomposition, air oxidation and moisture will be possible. Odourants and sex attractants and repellants can be more or less fixed depending on the complex constant chosen to manipulate their volatility similar to the applications of cyclodextrins. Even for cigarette filters selective adsorbents should be of value as e.g. benzpyren, nicotine, and other specific guest molecules could be filtered out with polymer bound tailor-shaped hosts. This also holds for carcinogenic and toxic substances like DDT, dioxine and other polyhalo aromatics and aliphatics which are of interest in environment, analytics and protection.

Of special interest, though somewhat farer in future, cartouches filled with polymer bound selective hosts could be used to filter out metabolites of drugs, which are responsive for side effects, from blood and serum. In such a way, a higher doping of the corresponding drugs appears possible. As a result the positive effects could be enhanced and the negative side effects depressed.

Functionalized hosts should accelerate selectivity of reactions at complexed guest molecules in analogy to the function of enzymes. One can imagine that for many synthetic problems the best suited macrocyclic hosts can be tailor-shaped to yield an optimum catalyst.

With catalytical amounts of chiral hosts hopefully enantio- and diastereoselective syntheses can be carried out. Regioselective reactions using cavity-enclosed guests have been already achieved using the cyclodextrins. This can most certainly be mimicked by synthetic hosts which are tailor-shaped to meet the specific problem.

The progress in this field as reported above already today shows that research on "receptor and enzyme mimick chemistry" in water solution has just started. It will be most interesting which of the perspectives mentioned before will be reached and which novel goals will be attractive in future.

7 References

1. Cram, D. J., Cram, J. M.: *Science* **183**, 803 (1974)
2. For an explanation and restriction of the term "keylock principle" see text books of biochemistry as well as: Chapeville, R., Haenni, A.-L.: *Chemical Recognition in Biology*. Springer Verlag, Berlin—Heidelberg—New York, 1980
3. a) Cramer, F.: „Einschlußverbindungen“, Springer Verlag, Berlin 1954;
b) Bender, M. L., Komiyama, M.: "Cyclodextrin Chemistry", Springer Verlag, Berlin 1978;
c) Cramer, F. et al.: *J. Am. Chem. Soc.* **89**, 14 (1967);
d) Saenger, W.: *Angew. Chem.* **92**, 343 (1980); *Int. Ed. Engl.* **19**, 344 (1980);
e) Szejtli, J.: "Cyclodextrins and their inclusion complexes", Akadémiai Kiadó, Budapest, 1982
4. A detailed listing is given in Ref. ^{3e)}, p. 130ff.
5. a) Tabushi, I.: *Acc. Chem. Res.* **15**, 66 (1983);
b) Breslow, R.: *Chem. Brit.* **19**, 126 (1983)
6. a) Cramer, F.: *Chem. Ber.* **86**, 1576 (1953);
b) Cramer, F., Dietsche, W.: *ibid.* **92**, 1739 (1959);
c) Cramer, F.: *Angew. Chem.* **73**, 49 (1961)
7. Breslow, R.: *Science* **218**, 532 (1982)
8. Stillings, F. H.: *ibid.* **209**, 451 (1980)
9. Nemethy, G., Scheraga, H. A.: *J. Chem. Phys.* **36**, 3401 (1962)
10. Komiyama, M., Bender, M. L.: *ibid.* **100**, 2259 (1978)
11. Tanford, C.: "The hydrophobic effect", John Wiley and Sons, New York, 1980
12. Lindner, K., Saenger, W.: *Angew. Chem.* **90**, 738 (1978); *Angew. Chem., Int. Ed. Engl.* **17**, 694 (1978)
13. Van Etten, R. L. et al.: *J. Am. Chem. Soc.* **89**, 3242, 3253 (1967)
14. a) Manor, P. C., Saenger, W.: *Nature* **237**, 392 (1972);
b) Manor, P. C., Saenger, W.: *J. Am. Chem. Soc.* **96**, 3630 (1974);
c) Saenger, W., Noltemeyer, M.: *Angew. Chem.* **86**, 594 (1974); *Angew. Chem., Int. Ed. Engl.* **13**, 552 (1974);
d) Hingerty, B., Saenger, W.: *J. Am. Chem. Soc.* **98**, 3357 (1976)
15. a) Tabushi, I. et al.: *Tetrahedron Lett.* **1976**, 3327;
b) Murakami, Y. et al.: *Bull. Chem. Soc. Jpn.* **49**, 3633 (1976);
c) Murakami, Y. et al.: *J. Chem. Soc. Perkin Trans. I*, **1979**, 1669;
d) Murakami, Y. et al.: *ibid.* **1981**, 2800;
e) Odashima, K., Koga, K.: *Heterocycles* **15**, 1151 (1981)
16. "Hydrogen Bonds" (Schuster, P., ed.): *Top. Curr. Chem.* **120**. Springer Verlag Berlin—Heidelberg—New York—Tokyo, 1984
17. a) Murakami, Y. et al.: *J. Chem. Soc., Perkin Trans. I*, **1979**, 1560;
b) Odashima, K., Koga, K.: *Cyclophanes*, Vol. II (Keehn, P. M., Rosenfeld, S. M., eds.), Academic Press, New York, 1983, p. 629ff.
18. Cramer, F.: *Angew. Chem.* **68**, 115 (1956);
b) Bergeron, R. et al.: *J. Am. Chem. Soc.* **99**, 5146 (1977);
c) Casa, B., Rava, L.: *Ric. Sci.* **36**, 733 (1966)
19. a) Harata, K.: *Bull. Chem. Soc. Jpn.* **49**, 2066 (1976);
b) Tabushi, I. et al.: *J. Am. Chem. Soc.* **100**, 916 (1978)
20. a) Kimura, E. et al.: *J. Am. Chem. Soc.* **104**, 3182 (1982);
b) Hosseini, M. W., Lehn, J. M.: *ibid.* **104**, 3525 (1982);
c) Tabushi, I. et al.: *ibid.* **99**, 7100 (1977);
d) Matsui, Y., Okimoto, A.: *Bull. Chem. Soc. Jpn.* **51**, 3030 (1978);
e) Boger, J., Knowleg, J. R.: *J. Am. Chem. Soc.* **101**, 7631 (1979)

21. Löhr, H.-G. et al.: *Angew. Chem.*, in press. Löhr, H.-G.: Ph. D. thesis, Univ. Bonn, 1983.
Worsch, D.: diploma work, Univ. Bonn, 1983
22. Weber, E., Josel, H.-P.: *J. Incl. Phenom.* 1, 79 (1984)
23. Turner, D. C., Brand, L.: *Biochemistry* 7, 338 (1968)
24. Tabushi, I.: *J. Am. Chem. Soc.* 98, 7855 (1976)
25. Benesi, H. A., Hildebrand, J. H.: *ibid.* 71, 2703 (1949)
26. Bergeron, R. J., Roberts, W. P.: *Anal. Biochem.* 90, 844 (1978)
27. Mochida, K. et al.: *Bull. Chem. Soc. Jpn.* 46, 3703 (1973)
28. Lehn, J. M. et al.: *Angew. Chem.* 85, 622 (1973); *Angew. Chem., Int. Ed. Engl.* 10, 579 (1973)
29. Jarvi, E. T., Whitlock, H. W.: *J. Am. Chem. Soc.* 104, 7196 (1982)
30. Schneider, H. J. et al.: *Angew. Chem.* 96, 907 (1984); *Angew. Chem., Int. Ed. Engl.* 23, 908 (1984)
31. Examples of older complexation studies by use of NMR spectroscopy are found in Ref. ^{3e)} and in: a) Bergeron, R. J. et al.: *J. Am. Chem. Soc.* 100, 2878 (1978); b) Granot, J.: *ibid.* 100, 1539 (1978)
32. Takeuchi, K. J., Busch, D. H.: *J. Am. Chem. Soc.* 105, 6812 (1983)
33. Jarvi, E. T., Whitlock, H. W.: *ibid.* 104, 7196 (1982)
34. Odashima, K. et al.: *ibid.* 102, 2504 (1980)
35. Odashima, K. et al.: *Tetrahedron Lett.* 21, 4347 (1980)
36. Dhaenens, M. et al.: *Chem. Commun.* 1984, 1097
37. Johnson, C. E., Jr., Bovey, F. A.: *J. Chem. Phys.* 29, 1012 (1958)
38. Diederich, F., Dick, K.: *Tetrahedron Lett.* 23, 3167 (1982)
39. a) Anthansen, T., Cram, D. J.: *Chem. Commun.* 1983, 1414;
b) Artz, S. P., Cram, D. J.: *J. Am. Chem. Soc.* 106, 2160 (1984)
40. Cram, D. J., Trueblood, K. N.: *Top. Curr. Chem.* 98, 43 (1981)
41. Diederich, F., Dick, K.: *Angew. Chem.* 95, 730 (1983); *Angew. Chem., Int. Ed. Engl.* 22, 715 (1983)
42. Diederich, F., Dick, K.: *Angew. Chem.* 96, 789 (1984); *Angew. Chem., Int. Ed. Engl.* 23, 810 (1984)
43. A development and explanation of the formulae applied for the picrate extraction method is found in: Nolte, R. M., Cram, D. J.: *J. Am. Chem. Soc.* 106, 1416 (1984); see also: Helgeson, R. C. et al.: *ibid.* 101, 4928 (1979); Koenig, K. E. et al.: *ibid.* 101, 3553 (1979)
44. a) Murakami, Y. et al.: *Chem. Lett.* 1973, 223;
b) Murakami, Y. et al.: *Bull. Chem. Soc. Jpn.* 47, 1238 (1974);
c) Murakami, Y. et al.: *ibid.* 48, 1537 (1975);
d) Murakami, Y.: *Top. Curr. Chem.* 115, 107 (1983)
45. Tabushi, I. et al.: *J. Am. Chem. Soc.* 103, 6486 (1981)
46. Dietrich, B. et al.: *Helv. Chim. Acta* 66, 1262 (1983)
47. a) Vögtle, F. et al.: *Top. Curr. Chem.* 125, 131 (1984);
b) Vögtle, F. et al.: *ibid.* 98, 107 (1981);
c) Sutherland, I. O.: *Heterocycles* 21, 235 (1984);
d) "Host Guest Complex Chemistry, Macrocycles" (Vögtle, F., Weber, E., eds.), Springer Verlag, Berlin—Heidelberg—New York—Tokyo, 1985
48. a) Cram, D. J.: *Science* 219, 1177 (1983);
b) Sirlin, C.: *Bull. Soc. Chim. Fr.* II, 1984, 5
49. a) Kotzyba-Hilbert, F. et al.: *Tetrahedron Lett.* 1980, 941;
b) Pascard, C. et al.: *Chem. Commun.* 1982, 557
50. Sutherland, I. O. in: *Cyclophanes*, Vol. II (Keehn, P. M., Rosenbaum, S. M., eds.), Academic Press, New York, 1983, p. 679 ff
51. a) Gutsche, C. D.: *Acc. Chem. Res.* 16, 161 (1983);
b) Zinke, A. et al.: *Monatsh. Chem.* 83, 1213 (1952);
c) Andreotti, G. D. et al.: *Chem. Commun.* 1979, 1005;
d) Gutsche, C. D.: Lecture at the 40th Southwest Regional ACS Meet., Lubbock, Texas, Dec. 5–7th, 1984
52. a) Schmidtchen, F. P.: *Angew. Chem.* 89, 751 (1977); *Angew. Chem., Int. Ed. Engl.* 16, 720 (1977);
b) Schmidtchen, F. P.: *Chem. Ber.* 114, 597 (1981)

53. a) Schmidtchen, F. P.: *Chem. Ber.* **117**, 725 (1984);
b) *ibid.* **117**, 1287 (1984)
54. Schmidtchen, F. P.: *Tetrahedron Lett.* **1984**, 4361
55. Tabushi, I. et al.: *J. Am. Chem. Soc.* **100**, 1304 (1978)
56. Tabushi, I. et al.: *ibid.* **98**, 5727 (1976)
57. Abbott, S. J. et al.: *Chem. Commun.* **1982**, 796
58. Tabushi, I. et al.: *J. Am. Chem. Soc.* **106**, 2621 (1984)
59. Dietrich, B. et al.: *ibid.* **103**, 1282 (1981)
60. Hosseini, M. W. et al.: *Helv. Chim. Acta* **66**, 2454 (1983)
61. Behr, J. P. et al.: *Chem. Commun.* **1976**, 621
62. Vögtle, F., Merz, T., Wirtz, H.: *Angew. Chem.* **97**, 226 (1985); *Angew. Chem. Int. Ed. Engl.* **24**, 221 (1985).
63. Jarvi, E. T., Whitlock, H. W.: *J. Am. Chem. Soc.* **102**, 657 (1980)
64. Adams, S. P., Whitlock, H. P.: *ibid.* **104**, 1602 (1982)
65. Stetter, H., Roos, E.-E.: *Chem. Ber.* **88**, 1390 (1955)
66. Vögtle, F., Rossa, L., Müller, W. M.: unpublished results
67. Hilgenfeld, R., Saenger, W.: *Angew. Chem.* **94**, 788 (1982); *Angew. Chem., Int. Ed. Engl.* **21**, 781 (1982)
68. Mori, K. et al.: *Heterocycles* **21**, 338 (1984)
69. Soga, T. et al.: *Tetrahedron Lett.* **21**, 4351 (1980)
70. Odashima, K. et al.: *ibid.* **22**, 5311 (1981)
71. Takahashi, I. et al.: *ibid.* **25**, 973 (1984)
72. Schneider, H.-J., Philippi, K.: *Chem. Ber.* **117**, 3056 (1984)
73. Schneider, H.-J. et al.: *Angew. Chem.* **96**, 909 (1984); *Angew. Chem., Int. Ed. Engl.* **23**, 908 (1984)
74. Schneider, H.-J., Busch, R.: *Angew. Chem.* **96**, 910 (1984); *Angew. Chem., Int. Ed. Engl.* **23**, 908 (1984)
75. Winkler, J. et al.: *J. Am. Chem. Soc.* **105**, 7198 (1983)
76. Kondo, J. et al.: *J. Biochem.* **79**, 393 (1976)
77. Diederich, F., Dick, K.: *J. Am. Chem. Soc.* **106**, 824 (1984)
78. Diederich, F., Griebel, D.: *ibid.* **106**, 8037 (1984)
79. Shinkai, S. et al.: *Tetrahedron Lett.* **25**, 5313 (1984)
80. Vögtle, F., Müller, W. M.: *Angew. Chem.* **96**, 711 (1984); *Angew. Chem., Int. Ed. Engl.* **23**, 712 (1984)
81. Vögtle, F. et al.: *Naturwissenschaften* **72**, 155 (1985)
82. Diederich, F., Dick, K.: *Angew. Chem.* **96**, 789 (1984); *Angew. Chem., Int. Ed. Engl.* **90**, (1984)
83. Franke, J., Vögtle, F.: *Angew. Chem.* **97**, 224 (1985); *Angew. Chem., Int. Ed. Engl.* **24**, 219 (1985).
84. Wambach, L., Vögtle, F.: *Tetrahedron Lett.* **26**, 1483 (1985)

Author Index Volumes 101–132

Contents of Vols. 50–100 see Vol. 100

Author and Subject Index Vols. 26–50 see Vol. 50

The volume numbers are printed in italics

- Alekseev, N. V., see Tandura, St. N.: *131*, 99–189 (1985).
- Anders, A.: Laser Spectroscopy of Biomolecules, *126*, 23–49 (1984).
- Asami, M., see Mukaiyama, T.: *127*, 133–167 (1985).
- Ashe, III, A. J.: The Group 5 Heterobenzenes Arsabenzene, Stibabenzene and Bismabenzene. *105*, 125–156 (1982).
- Austel, V.: Features and Problems of Practical Drug Design, *114*, 7–19 (1983).
- Balaban, A. T., Motoc, I., Bonchev, D., and Mekenyan, O.: Topological Indices for Structure-Activity Correlations, *114*, 21–55 (1983).
- Baldwin, J. E., and Perlmutter, P.: Bridged, Capped and Fenced Porphyrins. *121*, 181–220 (1984).
- Barkhash, V. A.: Contemporary Problems in Carbonium Ion Chemistry I. *116/117*, 1–265 (1984).
- Barthel, J., Gores, H.-J., Schmeer, G., and Wachter, R.: Non-Aqueous Electrolyte Solutions in Chemistry and Modern Technology. *11*, 33–144 (1983).
- Barron, L. D., and Vrbancich, J.: Natural Vibrational Raman Optical Activity. *123*, 151–182 (1984).
- Beckhaus, H.-D., see Rüchardt, Ch., *130*, 1–22 (1985).
- Bestmann, H. J., Vostrowsky, O.: Selected Topics of the Wittig Reaction in the Synthesis of Natural Products. *109*, 85–163 (1983).
- Beyer, A., Karpfen, A., and Schuster, P.: Energy Surfaces of Hydrogen-Bonded Complexes in the Vapor Phase. *120*, 1–40 (1984).
- Böhner, I. M.: Evaluation Systems in Quantitative Thin-Layer Chromatography, *126*, 95–188 (1984).
- Boekelheide, V.: Syntheses and Properties of the [2_n] Cyclophanes, *113*, 87–143 (1983).
- Bonchev, D., see Balaban, A. T., *114*, 21–55 (1983).
- Bourdin, E., see Fauchais, P.: *107*, 59–183 (1983).
- Cammann, K.: Ion-Selective Bulk Membranes as Models. *128*, 219–258 (1985).
- Charton, M., and Motoc, I.: Introduction, *114*, 1–6 (1983).
- Charton, M.: The Upsilon Steric Parameter Definition and Determination, *114*, 57–91 (1983).
- Charton, M.: Volume and Bulk Parameters, *114*, 107–118 (1983).
- Chivers, T., and Oakley, R. T.: Sulfur-Nitrogen Anions and Related Compounds. *102*, 117–147 (1982).
- Collard-Motte, J., and Janousek, Z.: Synthesis of Ynamines, *130*, 89–131 (1985).
- Consiglio, G., and Pino, P.: Asymmetrie Hydroformylation. *105*, 77–124 (1982).
- Coudert, J. F., see Fauchais, P.: *107*, 59–183 (1983).
- Cox, G. S., see Turro, N. J.: *129*, 57–97 (1985).
- Czochralska, B., Wrona, M., and Shugar, D.: Electrochemically Reduced Photoreversible Products of Pyrimidine and Purine Analogues. *130*, 133–181 (1985).
- Dhillon, R. S., see Suzuki, A.: *130*, 23–88 (1985).
- Dimroth, K.: Arylated Phenols, Aroxyl Radicals and Aryloxonium Ions Syntheses and Properties. *129*, 99–172 (1985).

- Dyke, Th. R.: Microwave and Radiofrequency Spectra of Hydrogen Bonded Complexes in the Vapor Phase. *120*, 85-113 (1984).
- Ebel, S.: Evaluation and Calibration in Quantitative Thin-Layer Chromatography. *126*, 71-94 (1984).
- Ebert, T.: Solvation and Ordered Structure in Colloidal Systems. *128*, 1-36 (1985).
- Edmondson, D. E., and Tollin, G.: Semiquinone Formation in Flavo- and Metalloflavoproteins. *108*, 109-138 (1983).
- Eliel, E. L.: Prostereoisomerism (Prochirality). *105*, 1-76 (1982).
- Endo, T.: The Role of Molecular Shape Similarity in Specific Molecular Recognition. *128*, 91-111 (1985).
- Fauchais, P., Bordin, E., Coudert, F., and MacPherson, R.: High Pressure Plasmas and Their Application to Ceramic Technology. *107*, 59-183 (1983).
- Franke, J., and Vögtle, F.: Complexation of Organic Molecules in Water Solution. *132*, 135-170 (1986).
- Fujita, T., and Iwamura, H.: Applications of Various Steric Constants to Quantitative Analysis of Structure-Activity Relationship. *114*, 119-157 (1983).
- Fujita, T., see Nishioka, T.: *128*, 61-89 (1985).
- Gärtner, A., and Weser, U.: Molecular and Functional Aspects of Superoxide Dismutases. *132*, 1-61 (1986).
- Gerson, F.: Radical Ions of Phases as Studied by ESR and ENDOR Spectroscopy. *115*, 57-105 (1983).
- Gielen, M.: Chirality, Static and Dynamic Stereochemistry of Organotin Compounds. *104*, 57-105 (1982).
- Gores, H.-J., see Barthel, J.: *111*, 33-144 (1983).
- Green, R. B.: Laser-Enhanced Ionization Spectroscopy. *126*, 1-22 (1984).
- Groeseneken, D. R., see Lontie, D. R.: *108*, 1-33 (1983).
- Gurel, O., and Gurel, D.: Types of Oscillations in Chemical Reactions. *118*, 1-73 (1983).
- Gurel, D., and Gurel, O.: Recent Developments in Chemical Oscillations. *118*, 75-117 (1983).
- Gutsche, C. D.: The Calixarenes. *123*, 1-47 (1984).
- Heilbronner, E., and Yang, Z.: The Electronic Structure of Cyclophanes as Suggested by their Photoelectron Spectra. *115*, 1-55 (1983).
- Heller, G.: A Survey of Structural Types of Borates and Polyborates. *131*, 39-98 (1985).
- Hellwinkel, D.: Penta- and Hexaorganyl Derivatives of the Main Group Elements. *109*, 1-63 (1983).
- Hess, P.: Resonant Photoacoustic Spectroscopy. *111*, 1-32 (1983).
- Heumann, K. G.: Isotopic Separation in Systems with Crown Ethers and Cryptands. *127*, 77-132 (1985).
- Hilgenfeld, R., and Saenger, W.: Structural Chemistry of Natural and Synthetic Ionophores and their Complexes with Cations. *101*, 3-82 (1982).
- Holloway, J. H., see Selig, H.: *124*, 33-90 (1984).
- Iwamura, H., see Fujita, T.: *114*, 119-157 (1983).
- Janousek, Z., see Collard-Motte, J.: *130*, 89-131 (1985).
- Jørgensen, Ch. K.: The Problems for the Two-electron Bond in Inorganic Compounds. *124*, 1-31 (1984).
- Jurczak, J., and Pietraszkiewicz, M.: High-Pressure Synthesis of Cryptands and Complexing Behaviour of Chiral Cryptands. *130*, 183-204 (1985).
- Kaden, Th. A.: Syntheses and Metal Complexes of Aza-Macrocycles with Pendant Arms having Additional Ligating Groups. *121*, 157-179 (1984).
- Karpfen, A., see Beyer, A.: *120*, 1-40 (1984).
- Káš, J., Rauch, P.: Labeled Proteins, Their Preparation and Application. *112*, 163-230 (1983).

- Keat, R.: Phosphorus(III)-Nitrogen Ring Compounds. *102*, 89–116 (1982).
- Keller, H. J., and Soos, Z. G.: Solid Charge-Transfer Complexes of Phenazines. *127*, 169–216 (1985).
- Kellogg, R. M.: Bioorganic Modelling — Stereoselective Reactions with Chiral Neutral Ligand Complexes as Model Systems for Enzyme Catalysis. *101*, 111–145 (1982).
- Kimura, E.: Macrocyclic Polyamines as Biological Cation and Anion Complexones — An Application to Calculi Dissolution. *128*, 113–141 (1985).
- Kniep, R., and Rabenau, A.: Subhalides of Tellurium. *111*, 145–192 (1983).
- Krebs, S., Wilke, J.: Angle Strained Cycloalkynes. *109*, 189–233 (1983).
- Kobayashi, Y., and Kumadaki, I.: Valence-Bond Isomer of Aromatic Compounds. *123*, 103–150 (1984).
- Koptyug, V. A.: Contemporary Problems in Carbonium Ion Chemistry III Arenium Ions — Structure and Reactivity. *122*, 1–245 (1984).
- Kosower, E. M.: Stable Pyridinyl Radicals. *112*, 117–162 (1983).
- Kumadaki, I., see Kobayashi, Y.: *123*, 103–150 (1984).
- Laarhoven, W. H., and Prinsen, W. J. C.: Carbohelicenes and Heterohelicenes. *125*, 63–129 (1984).
- Labarre, J.-F.: Up to-date Improvements in Inorganic Ring Systems as Anticancer Agents. *102*, 1–87 (1982).
- Labarre, J.-F.: Natural Polyamines-Linked Cyclophosphazenes. Attempts at the Production of More Selective Antitumorals. *129*, 173–260 (1985).
- Laitinen, R., see Steudel, R.: *102*, 177–197 (1982).
- Landini, S., see Montanari, F.: *101*, 111–145 (1982).
- Lavrent'ev, V. I., see Voronkov, M. G.: *102*, 199–236 (1982).
- Lontie, R. A., and Groeseneken, D. R.: Recent Developments with Copper Proteins. *108*, 1–33 (1983).
- Lynch, R. E.: The Metabolism of Superoxide Anion and Its Progeny in Blood Cells. *108*, 35–70 (1983).
- Matsui, Y., Nishioka, T., and Fujita, T.: Quantitative Structure-Reactivity Analysis of the Inclusion Mechanism by Cyclodextrins. *128*, 61–89 (1985).
- McPherson, R., see Fauchais, P.: *107*, 59–183 (1983).
- Majestic, V. K., see Newkome, G. R.: *106*, 79–118 (1982).
- Manabe, O., see Shinkai, S.: *121*, 67–104 (1984).
- Margaretha, P.: Preparative Organic Photochemistry. *103*, 1–89 (1982).
- Martens, J.: Asymmetric Syntheses with Amino Acids. *125*, 165–246 (1984).
- Matzanke, B. F., see Raymond, K. N.: *123*, 49–102 (1984).
- Mekenyan, O., see Balaban, A. T.: *114*, 21–55 (1983).
- Meurer, K. P., and Vögtle, F.: Helical Molecules in Organic Chemistry. *127*, 1–76 (1985).
- Montanari, F., Landini, D., and Rolla, F.: Phase-Transfer Catalyzed Reactions. *101*, 149–200 (1982).
- Motoc, I., see Charton, M.: *114*, 1–6 (1983).
- Motoc, I., see Balaban, A. T.: *114*, 21–55 (1983).
- Motoc, I.: Molecular Shape Descriptors. *114*, 93–105 (1983).
- Müller, F.: The Flavin Redox-System and Its Biological Function. *108*, 71–107 (1983).
- Müller, G., see Raymond, K. N.: *123*, 49–102 (1984).
- Müller, W. H., see Vögtle, F.: *125*, 131–164 (1984).
- Mukaiyama, T., and Asami, A.: Chiral Pyrrolidine Diamines as Efficient Ligands in Asymmetric Synthesis. *127*, 133–167 (1985).
- Murakami, Y.: Functionalized Cyclophanes as Catalysts and Enzyme Models. *115*, 103–151 (1983).
- Mutter, M., and Pillai, V. N. R.: New Perspectives in Polymer-Supported Peptide Synthesis. *106*, 119–175 (1982).
- Naemura, K., see Nakazaki, M.: *125*, 1–25 (1984).
- Nakatsuji, Y., see Okahara, M.: *128*, 37–59 (1985).
- Nakazaki, M., Yamamoto, K., and Naemura, K.: Stereochemistry of Twisted Double Bond Systems. *125*, 1–25 (1984).
- Newkome, G. R., and Majestic, V. K.: Pyridinophanes, Pyridinocrowns, and Pyridinocryptands. *106*, 79–118 (1982).

- Niedenzu, K., and Trofimenko, S.: Pyrazole Derivatives of Boron. *131*, 1–37 (1985).
 Nishide, H., see Tsuchida, E.: *132*, 63–99 (1986).
 Nishioka, T., see Matsui, Y.: *128*, 61–89 (1985).
 Oakley, R. T., see Chivers, T.: *102*, 117–147 (1982).
 Ogino, K., see Tagaki, W.: *128*, 143–174 (1985).
 Okahara, M., and Nakatsuji, Y.: Active Transport of Ions Using Synthetic Ionophores Derived from Cyclic and Noncyclic Polyoxyethylene Compounds. *128*, 37–59 (1985).
 Paczkowski, M. A., see Turro, N. J.: *129*, 57–97 (1985).
 Painter, R., and Pressman, B. C.: Dynamics Aspects of Ionophore Mediated Membrane Transport. *101*, 84–110 (1982).
 Paquette, L. A.: Recent Synthetic Developments in Polyquinane Chemistry. *119*, 1–158 (1984).
 Perlmutter, P., see Baldwin, J. E.: *121*, 181–220 (1984).
 Pietraszkiewicz, M., see Jurczak, J.: *130*, 183–204 (1985).
 Pillai, V. N. R., see Mutter, M.: *106*, 119–175 (1982).
 Pino, P., see Consiglio, G.: *105*, 77–124 (1982).
 Pommer, H., Thieme, P. C.: Industrial Applications of the Wittig Reaction. *109*, 165–188 (1983).
 Pressman, B. C., see Painter, R.: *101*, 84–110 (1982).
 Prinsen, W. J. C., see Laarhoven, W. H.: *125*, 63–129 (1984).
 Rabenau, A., see Kniep, R.: *111*, 145–192 (1983).
 Rauch, P., see Káś, J.: *112*, 163–230 (1983).
 Raymond, K. N., Müller, G., and Matzanke, B. F.: Complexation of Iron by Siderophores A Review of Their Solution and Structural Chemistry and Biological Function. *123*, 49–102 (1984).
 Recktenwald, O., see Veith, M.: *104*, 1–55 (1982).
 Reetz, M. T.: Organotitanium Reagents in Organic Synthesis. A Simple Means to Adjust Reactivity and Selectivity of Carbanions. *106*, 1–53 (1982).
 Rolla, R., see Montanari, F.: *101*, 111–145 (1982).
 Rossa, L., Vögtle, F.: Synthesis of Medio- and Macrocyclic Compounds by High Dilution Principle Techniques. *113*, 1–86 (1983).
 Rubin, M. B.: Recent Photochemistry of α -Diketones. *129*, 1–56 (1985).
 Rüchardt, Ch., and Beckhaus, H.-D.: Steric and Electronic Substituent Effects on the Carbon-Carbon Bond. *130*, 1–22 (1985).
 Rzaev, Z. M. O.: Coordination Effects in Formation and Cross-Linking Reactions of Organotin Macromolecules. *104*, 107–136 (1982).
 Saenger, W., see Hilgenfeld, R.: *101*, 3–82 (1982).
 Sandorfy, C.: Vibrational Spectra of Hydrogen Bonded Systems in the Gas Phase. *120*, 41–84 (1984).
 Schlögl, K.: Planar Chiral Molecular Structures. *125*, 27–62 (1984).
 Schmeer, G., see Barthel, J.: *111*, 33–144 (1983).
 Schmidtchen, F. P.: Molecular Catalysis by Polyammonium Receptors. *132*, 101–133 (1986).
 Schöllkopf, U.: Enantioselective Synthesis of Nonproteinogenic Amino Acids. *109*, 65–84 (1983).
 Schuster, P., see Beyer, A., see *120*, 1–40 (1984).
 Schwochau, K.: Extraction of Metals from Sea Water. *124*, 91–133 (1984).
 Shugar, D., see Czochralska, B.: *130*, 133–181 (1985).
 Selig, H., and Holloway, J. H.: Cationic and Anionic Complexes of the Noble Gases. *124*, 33–90 (1984).
 Shibata, M.: Modern Syntheses of Cobalt(III) Complexes. *110*, 1–120 (1983).
 Shinkai, S., and Manabe, O.: Photocontrol of Ion Extraction and Ion Transport by Photo-functional Crown Ethers. *121*, 67–104 (1984).
 Shubin, V. G.: Contemporary Problems in Carbonium Ion Chemistry II. *116/117*, 267–341 (1984).
 Siegel, H.: Lithium Halocarbonoids Carbanions of High Synthetic Versatility. *106*, 55–78 (1982).
 Sinta, R., see Smid, J.: *121*, 105–156 (1984).
 Smid, J., and Sinta, R.: Macrocyclic Ligands on Polymers. *121*, 105–156 (1984).
 Soos, Z. G., see Keller, H. J.: *127*, 169–216 (1985).

- Steudel, R.: Homocyclic Sulfur Molecules. *102*, 149–176 (1982).
- Steudel, R., and Laitinen, R.: Cyclic Selenium Sulfides. *102*, 177–197 (1982).
- Suzuki, A.: Some Aspects of Organic Synthesis Using Organoboranes. *112*, 67–115 (1983).
- Suzuki, A., and Dhillon, R. S.: Selective Hydroboration and Synthetic Utility of Organoboranes thus Obtained. *130*, 23–88 (1985).
- Szele, J., Zollinger, H.: Azo Coupling Reactions Structures and Mechanisms. *112*, 1–66 (1983).
- Tabushi, I., Yamamura, K.: Water Soluble Cyclophanes as Hosts and Catalysts. *113*, 145–182 (1983).
- Takagi, M., and Ueno, K.: Crown Compounds as Alkali and Alkaline Earth Metal Ion Selective Chromogenic Reagents. *121*, 39–65 (1984).
- Tagaki, W., and Ogino, K.: Micellar Models of Zinc Enzymes. *128*, 143–174 (1985).
- Takeda, Y.: The Solvent Extraction of Metal Ions by Crown Compounds. *121*, 1–38 (1984).
- Tandura, St. N., Alekseev, N. V., and Voronkov, M. G.: Molecular and Electronic Structure of Penta- and Hexacoordinate Silicon Compounds. *131*, 99–189 (1985).
- Thieme, P. C., see Pommer, H.: *109*, 165–188 (1983).
- Tollin, G., see Edmondson, D. E.: *108*, 109–138 (1983).
- Trofimenko, S., see Niedenzu, K.: *131*, 1–37 (1985).
- Tsuchida, E., and Nishide, H.: Hemoglobin Model — Artificial Oxygen Carrier Composed of Porphinatoiron Complexes. *132*, 63–99 (1986).
- Turro, N. J., Cox, G. S., and Paczkowski, M. A.: Photochemistry in Micelles. *129*, 57–97 (1985).
- Ueno, K., see Tagaki, M.: *121*, 39–65 (1984).
- Urry, D. W.: Chemical Basis of Ion Transport Specificity in Biological Membranes. *128*, 175–218 (1985).
- Veith, M., and Recktenwald, O.: Structure and Reactivity of Monomeric, Molecular Tin(II) Compounds. *104*, 1–55 (1982).
- Venugopalan, M., and Vepřek, S.: Kinetics and Catalysis in Plasma Chemistry. *107*, 1–58 (1982).
- Vepřek, S., see Venugopalan, M.: *107*, 1–58 (1983).
- Vögtle, F., see Rossa, L.: *113*, 1–86 (1983).
- Vögtle, F.: Concluding Remarks. *115*, 153–155 (1983).
- Vögtle, F., Müller, W. M., and Watson, W. H.: Stereochemistry of the Complexes of Neutral Guests with Neutral Crown Molecules. *125*, 131–164 (1984).
- Vögtle, F., see Meurer, K. P.: *127*, 1–76 (1985).
- Vögtle, F., see Franke, J.: *132*, 135–170 (1986).
- Volkman, D. G.: Ion Pair Chromatography on Reversed-Phase Layers. *126*, 51–69 (1984).
- Vostrowsky, O., see Bestmann, H. J.: *109*, 85–163 (1983).
- Voronkov, M. G., and Lavrent'ev, V. I.: Polyhedral Oligosilsequioxanes and Their Homo Derivatives. *102*, 199–236 (1982).
- Voronkov, M. G., see Tandura, St. N.: *131*, 99–189 (1985).
- Vrbancich, J., see Barron, L. D.: *123*, 151–182 (1984).
- Wachter, R., see Barthel, J.: *111*, 33–144 (1983).
- Watson, W. H., see Vögtle, F.: *125*, 131–164 (1984).
- Weser, U., see Gärtner, A.: *132*, 1–61 (1986).
- Wilke, J., see Krebs, S.: *109*, 189–233 (1983).
- Wrona, M., see Czocharlska, B.: *130*, 133–181 (1985).
- Yamamoto, K., see Nakazaki, M.: *125*, 1–25 (1984).
- Yamamura, K., see Tabushi, I.: *113*, 145–182 (1983).
- Yang, Z., see Heilbronner, E.: *115*, 1–55 (1983).
- Zollinger, H., see Szele, I.: *112*, 1–66 (1983).